Modelling forward programmed megakaryocyte culture for manufacturing process development

By

Elizabeth Anne Cheeseman

A thesis submitted to Loughborough University for the degree of

DOCTOR OF PHILOSOPHY

November 2019

Centre for Biological Engineering

Wolfson School of Mechanical, Electrical and Manufacturing Engineering

Loughborough University

Abstract

Advanced therapy medicinal products (ATMPs), which include cell and gene therapies, have the potential to revolutionise the healthcare industry through curing conditions which have previously been manageable at best. ATMP developers face challenges due to the complexity of their products since cells dynamically change, and are changed by, their environment through complex interactions. Defining the relationships between cells and their environment will allow developers to better characterise and control their processes, leading to more consistent and lower risk processes, which in turn would reduce COGs.

Here, it was hypothesised that modelling approaches could be used to define complex cell-environment interactions and produce meaningful process improvements for cell-based therapy manufacture. To test this hypothesis, two modelling approaches were applied to a clinically relevant, cell type that would face the same generic challenges a commercial, allogenic cell-based therapy (system productivity and maintaining or producing the required cell quality) – forward programmed platelet precursor cells (megakaryocytes) FOPMKs.

The first modelling approach selected was Quality by Design (QbD) due to its acceptance and promotion by regulatory bodies for the manufacture of small molecules. A Quality Target Product Profile (QTPP) was compiled for an in vitro platelet product and Critical Quality Attributes (CQAs) – extracellular marker positive expression of CD41a, CD42a and CD42b and negative expression of CD235a - were identified.

In order to reproducibly measure CQAs, substantial analytical development was undertaken to develop a novel flow cytometry assay that measured extracellular marker expression and characterise the differentiation of FOPMKs including on-target and off-target expression.

Following assay development statistical Design of Experiments (DOE), was used to link control variables to CQAs. This work showed that concentrations of medium consumables doxycycline (Dox) and thrombopoietin (TPO) correlated with increased yield and CD41a expression. Whereas seeding density and removal of Dox from culture correlated with lower cell yields and lower CD41a expression.

The second modelling approach applied was a novel, dynamic, mechanistic modelling approach which showed that cell growth was inhibited, and viable cells were converted non-viable cells as a function of cell.time mediated medium exhaustion. Firstly, the system productivity was found to be approximately $1.48 \pm 0.28 \times 10^6$ viable cells.mL^{-1} and the system limitation was a product of the number of cells present and time. Dynamic modelling confirmed this hypothesis and indicated that growth inhibition as a function of medium exhaustion was also present.

Dynamic models were also applied to pluripotent cell culture where growth inhibition was shown to be a function of cell density, and the density threshold at which the cells became growth inhibited could be increased through the addition of Rhok Inhibitor in the first 24 hours of culture.

Future work for FOPMKs should focus on identifying the root cause of the medium limitation (initial screening showed it was unlikely to be glucose, lactate or ammonium concentrations). Modelling frameworks for phenotypically unstable populations require the ability to handle higher numbers of parameters, or more efficient methods to screen and reduce the number parameters required.

Acknowledgments

First and foremost, I would like to give my sincerest thanks to my supervisors, Prof. Rob Thomas and Dr. Katie Glen for your contribution to this work. Thank you for your support, guidance, encouragement, and for sharpening my mind. Thank you for teaching me the importance of the differential of the rate. Thank you also to Dr. Adrian Stacey for your contribution to this work, mentorship and reading lists. Soon you will no longer be my supervisors and I already miss our frequent “good chats”, but I’m sure we will always be good friends. I would also like to thank and acknowledge Dr Cedric Ghevaert, Dr Thomas Moreau, Dr Amada Evans and colleagues at the Cambridge Haematology and NHS Blood Transfusion Service for deriving and providing the cell lines used in this work, for providing much help and guidance throughout this project and welcoming me into your lab.

I would also like to thank and acknowledge the Rob Thomas Research group and colleagues at the Centre for Biological Engineering, especially Jon Harriman and Dr. Rebecca Moore, who provided much assistance and guidance throughout my project and beyond. Thank you to Dr Karen Coopman for many years of mentorship, from my undergraduate degree through my PhD and to the late Prof. Chris Hewitt, without you both I would have not found the CBE. I would like to thank Prof. David Williams for your mentorship and for challenging me to think differently. Thank you also to Dr Thomas Heathman for mentoring and friendship since my undergraduate project. Your varied knowledge, from insight into the business of regenerative medicine to the best place to find ice cream in New Jersey, continues to be much appreciated.

It has been a privilege to work alongside many talented undergraduate and Masters students. I would like to acknowledge Anita Luo, Hadi Al-Afoo, Saif Kazim, and most recently Jenny Cathy Beltran-Rendon – with whom most experimental work from Section 6 was conducted

in collaboration. Thank you for your hard work, dedication and for asking questions that changed my perspective.

Thank you to my parents, Thora and Stephen Cheeseman, Stephen and Teresa Buckley, for your love, wisdom, support and for instilling in me a strong work ethic. I'd like to acknowledge and thank nan, Doris Cheeseman, for showing me how to be resilient and confident. To my new family, Flo and Roy McCall, Jill, Richard and Elsie Cregan – thank you for your love and support. Thank you also to my wider family and friends for your support and for picking me up when I was down. Without you all I would not have been where I am today, and for that I am eternally grateful.

Last, but by no means least, I would like to thank Dr Mark McCall for all your support and encouragement. Thank you for being a shoulder to cry on, cooking delicious food, telling terrible jokes, constructively challenging my thinking and encouraging me to pursue my dreams. I can't wait to be your wife and for our next great adventure together in beautiful Northern Ireland.

List of Figures

List of Abbreviations

ATMP	Advanced Therapy Medicinal Product
COGs	Cost of Goods
CQA	Critical Quality Attribute
DOE	Design of Experiments
Dox	Doxycycline
EMA	European Medicines Agency
FDA	U.S. Food and Drug Administration
FOP	Forward Programme(d)
FVS	Fixable Viability Stain
HLA	human leukocyte antigen
HSC	Haematopoietic Stem Cell
iPSC	(induced) Pluripotent Stem Cell
MK	Megakaryocyte
MoA	Mechanism of Action
MSC	Mesenchymal Stromal Cell
ODE	Ordinary differential equations
QbD	Quality by Design
QTPP	Quality Target Product Profile
SCF	Stem Cell Factor
TPO	Thrombopoietin

List of Selected Publications and Presentations

Journal Publications

A. J. Stacey, E. A. Cheeseman, K. E. Glen, R. L. L. Moore, and R. J. Thomas, "Experimentally integrated dynamic modelling for intuitive optimisation of cell based processes and manufacture," *Biochem. Eng. J.*, vol. 132, pp. 130–138, 2018.

K. E. Glen, E. A. Cheeseman, A. J. Stacey, and R. J. Thomas, "A mechanistic model of erythroblast growth inhibition providing a framework for optimisation of cell therapy manufacturing," *Biochem. Eng. J.*, vol. 133, pp. 28–38, 2018.

F. Masri, E. A. Cheeseman, and S. Ansorge, "Viral vector manufacturing: how to address current and future demands?," *Cell Gene Ther. Insights*, vol. 5, no. 5, pp. 949–970, 2019.

Conference Presentations

Cheeseman, E. A., Glen, K. E., Stacey, A. J., Beltran-Rendon, J. C., Moore, R. L. L., McCall, M. J. S, Moreau, T, Ghevaert, C, Thomas, R. J, Application of Quality by Design Tools to Upstream Processing of Platelet Precursor Cells to Enable In Vitro Manufacture of Blood Products (oral snapshot presentation). ECI Manufacture of Cell and Gene Therapies IV, San Diego, USA, 2019

Cheeseman, E. A., Glen, K. E., Moore, R. L. L., McCall, M. J. S, Stacey, A. J., Moreau, T., Ghevaert, C., Thomas, R. J, Enabling human pluripotent stem cell derived megakaryocyte manufacture for in vitro platelet production (oral presentation), Future Investigators of Regenerative Medicine Symposium, Girona, Spain, 2018

Cheeseman, E. A., Glen, K. E., Moore, R. L. L., McCall, M. J. S, Stacey, A. J., Moreau, T., Ghevaert, C., Thomas, R. J, Developing mechanistic models of human pluripotent stem cell derived megakaryocyte growth to enable in vitro platelet manufacture (oral presentation),

Biochemical Engineering Special Interest Group and Young Researchers Meeting, 2017, London, UK.

Cheeseman, E. A., Glen, K. E., Moore, R. L. L., McCall, M. J. S, Stacey, A. J., Moreau, T., Ghevaert, C., Thomas, R. J, Enabling human pluripotent stem cell derived megakaryocyte manufacture for in vitro platelet production (oral snapshot presentation), ESACT-UK, Oxford, UK, 2017

Cheeseman, E. A., Moore, R. L. L., McCall, M. J. S., Ahmed, F., Moreau, T., Ghevaert, C., Thomas, R. J., Transforming hematopoietic progenitor manufacture (oral presentation), ISCT Singapore, 2016

Contents

1. Introduction and Literature Review

1.1. Introduction

1.1.1 Research area and motivation

So far only 13 Advanced Therapy Medicinal Products (ATMPs) have been approved by the European Medicines Agency (EMA), and four of those have been withdrawn. Concurrent with the development of this research the regenerative medicine industry has undergone a sea-change, with the first genetically modified T-cell therapies (known as CAR-T therapies) KYMRIAH and YESCARTA receiving market approval in 2017. As this industry begins to move into the commercialisation phase, new challenges are emerging.

Both approved CAR-T therapies command reimbursement prices of over $100,000. The high cost of goods (COGs) are driven by the availability of vectors used in genetic modification and the expansion of the cells [1]. There are many uncertainties in the processes which drive cell expansion and genetic modification since cells are complex structures, which change dynamically in response to their environment. An additional complexity for cell therapy developers has been the lack of understanding of the mechanism of action (MOA) by which treatments are effective, and therefore critical quality attributes (CQAs) are challenging to identify [2]. The lack of CQAs is challenging for cell therapy developers since the impact of process changes on product efficacy cannot be easily measured.

Annually there are over 4.5 million platelet transfusions worldwide, currently all of which are sourced from volunteer donors. Receiving a platelet transfusion is not a risk-free process, as 10% of new HIV diagnoses in developing countries are a result of contaminated blood transfusions in the early 2000s [3] and the Serious Hazards of Transfusion (SHOT) scheme (which was established following the contaminated blood scandals of the 1980s and 90s)

showed that there were 49 infections from contaminated blood products in the decade after enhanced monitoring was introduced [4].

To overcome the reliance on volunteer donors, an approach for developing genetically modified platelet-precursor cells (forward programmed megakaryocytes) from pluripotent stem cells was developed [5]. To develop a process that produces functional platelets at a clinically relevant quantity, and a price which is cost effective for healthcare providers, process development work must be undertaken to first define and then improve expansion of these cells whilst retaining the desired cell quality.

1.2 Overview of the Field

1.2.1 Regenerative Medicine

Regenerative medicine is defined as the replacement, or regeneration of cells, tissues or organs to restore or establish normal function [6]. It has the potential to revolutionise healthcare worldwide, as it offers cures for ailments which until now have been treated using pain management and symptom control. The therapeutic application of cells, known as cell therapies or cell-based therapies, is a crucial platform technology which bridges regenerative medicine and other treatment approaches [7]. In relevant literature, the terms “Regenerative Medicine” and “Cell Therapy” are often intertwined, however in this review the terms are used as defined above.

1.2.2 Cell Therapy

The last five years have been a water-shed moment for cell therapies with the regulatory approval of three products; firstly Strimvelis in 2016, an orphan drug for ADA-SCID, followed by KYMRIAH and YESCARTA in 2017, both for oncology applications. By the first quarter of 2019, there were over 640 active clinical trials involving cell therapies [8]. Cell therapies can be broadly categorised into two fields, autologous and allogeneic. The cells from autologous treatments are derived from the patient, expanded or modified in some form and infused or transplanted into the same patient. Allogeneic, or “off-the-shelf” therapies are generally not patient specific, cells are harvested from donors and expanded to make a product which is then infused into multiple patients [9]. Some cell therapies exist which use allogeneic cells for a single patient’s treatment, such as specific T-cells or human leukocyte antigen (HLA) type matched bone marrow grafts but these are not scalable approaches to meet the demands of large patient populations without significant investment in infrastructure, as has been

achieved in cord blood transplantation [10]. In contrast Allogeneic, one to many, cell therapies are more aligned to traditional bioprocessing, including centralised manufacturing and employing economies of scale; process development challenges will focus on “scale-up”. Autologous treatments are likely to follow more bespoke manufacturing routes, including distributed manufacturing and process development will focus on “scale-out” [11].

Despite these very different challenges, commercialisation of both autologous and allogeneic cell therapies will require solutions to common problems as all regulatory-approved cell therapies must be safe, efficacious and consistent. COGs must also be low enough to enable widespread market adoption and return on investment for developers. To achieve this, process and product variability must be minimised. This challenge will be partly met by the implementation of automation, to minimise operator error and contamination risks, and by moving towards xeno-free media components, reducing inherent lot-to-lot variations [12]. However, the greatest challenge for many cell therapies is defining Critical Quality Attributes (CQA) that measure desired functional outputs and link to simple, convenient or online monitoring assays. These are used to optimise manufacturing processes [2] and ensure product purity, potency, stability safety and efficacy. In many cases the Mechanism of Action (MoA) is not fully defined, which makes developing CQA more challenging since the defining features for clinical efficacy are not known and therefore cannot be linked to assays for use in process control [13].

1.2.2.1 Hematopoietic Cell Therapies

The hematopoietic linage is relatively well characterised [14], and therefore CQAs for CT using hematopoietic cells may be easier to define. HSCs are readily available as there are multiple sources of hematopoietic cells including bone marrow [15], umbilical cord [16], peripheral

blood [17]; pluripotent sources can also be differentiated or genetically programmed to specific cell types [5]. Perhaps this contributes to hematopoietic cells being the most common cell type used in active CT clinical trials and their use in a wide range of clinical fields; such as oncology, immunology and cardiology [18]. However it should be noted there is a great deal of variation in the current clinical processes which utilise HSCs [19].

From a bioprocessing perspective, hematopoietic cells are suspension cells so their culture and harvest is less complex compared to adherent clinical cell types, for example mesenchymal stromal cell (MSC) culture requires optimisation of microcarrier attachment surface [20], cell to microcarrier ratio [21] and cell detachment from microcarriers [22]. More parameters are intrinsic to processes with greater complexity, the impact of which must be assessed to define appropriate levels of control to reduce the resulting process variability. The suspension nature of hematopoietic cells allows them to be grown in traditional biotechnology equipment, such as stirred tank reactors, without the need for additional components, such as microcarriers, which are required for adherent cell culture. This in turn permits the reuse of decades of scale-up knowledge developed. Technology transfer in this way will allow the CT industry to take advantage of systems that have been well characterised over the past century [23].

1.3 Manufacture of Platelets

1.3.1 Uses of Platelets

1.3.1.1 Clinical Need

Platelets are enucleate cells produced by fragmentation of megakaryocytes (MKs) in vivo [24] (see section 1.3.2 for further discussion). Platelets circulate in peripheral blood at a concentration of 100-450 × 10^9 L^{-1} [25] and play key roles in haemostasis, inflammation,

wound healing and innate immunity [26]. Thrombocytopenia (platelet deficiencies) may occur as a result of bone marrow failure, caused by inherited conditions or from certain cancer treatments, or following an event that requires a massive transfusion, such as a motoring accident [27]. Regardless of cause, the most effective method to treat thrombocytopenia in the short term is platelet transfusion and demand for platelet transfusions is increasing due to ageing populations [28]. Indeed from 2006-2008 platelet transfusions increased by 16.8% in the USA; the average unit price of apheresis platelets was US$535.17, and approximately 2.2 million units are transfused annually [29]. In the UK nearly 300,000 platelet units were transfused in 2012, representing a 30% increase from 2000 [30], at a cost of £192.42 per standard unit in 2015/16.

Currently platelets are sourced from volunteer donors; these units must be ABO and Rhesus-D matched, and in some circumstances patients require specifically matched donations [31]. Collected platelet samples for transfusion (with concentrations of approximately 3-4 × 10^{11} platelets per unit [32]) have a short life span of 3-7 days and must be stored at room temperature [28], which increases contamination risks from bacteria. Although rare, occurring in 1:3000 platelet units, transfusion of contaminated products often leads to death in patients who are immunosuppressed or undergoing cancer therapies. Platelet units which exceed this storage time are discarded leading to significant waste; approximately a third of platelet units are disposed of in this way [29]. In military operations, the short-shelf life can lead to platelet units being exhausted quickly resulting in transfusions of whole blood. Military personnel who received platelet transfusions had a 20% lower mortality risk compared to those receiving whole blood [33].

Despite their widespread use, platelet transfusions are not risk-free. Platelet transfusions can transmit blood-borne pathogens such as HIV, hepatitis C and CMV. Blood donors are screened for conditions, and those at risk are prevented from donating. Through screening, transmission of these pathogens has greatly decreased, but it is impossible to eliminate this risk whilst relying on donors. Immunological reactions can occur in patients such as Graft vs. Host Disease (GvHD), alloimmunisation and transfusion-related acute lung injury (TRALI). These are prevented by donor screening for antibodies, irradiation and leucocyte reduction [34].

The in vitro manufacture of platelets for transfusions has the potential to alleviate the current reliance on blood donors, and therefore overcome supply and logistical challenges currently associated with platelet sourcing. Furthermore, the risk of pathogen transmission from donor to patient will be eliminated along with donor-to-donor variability, leading to a more consistent platelet transfusion product. Since platelets are enucleate, the final platelet product can be irradiated prior to transfusion, which gives a significant safety advantage as potentially oncogenic cell fractions arising in the production process will be eliminated [35].

1.3.1.2 Human Platelet Lysate

Fetal Bovine Serum (FBS) is commonly used in the production of CTs as a source of growth and attachment factors, proteins and nutrients to support proliferation of cells. Despite the regulators consent for its use in the manufacture of regulated CTs [36], FBS is a source of process variability [37]. It is at risk of contamination by prions or other known and unknown adventitious pathogens and may illicit immune reaction from patients [38]. Furthermore as the CT industry comes to fruition the supply of FBS will become more constricted, indeed currently only three countries produce over 90% of the FBS demand [38]. This limited supply

will cause costs to escalate. Human platelet lysate (hPL) has been proposed as a xenofree alternative to FBS supplementation. It has been shown to reduce variability and promote higher proliferation in MSC cultures [39].

Fully defined, serum-free media has advantages over both HPL and FBS. This includes minimal lot-to-lot variations, lower risk of contamination from pathogens and potentially fewer supply chain issues [38]. However, serum is a complex milieu of beneficial components. PDGF-BB, TGF- β1 and bFGF are growth factors found in hPL which were shown to have the largest impact on MSC proliferation when removed. A cocktail of these growth factors, at equal concentrations as found in hPL, were used to supplement basal media and did not promote MSC proliferation [40].

To manufacture platelet lysate currently, whole blood is collected from donors, and is screened according to regulatory procedures for pathogens. Plasma and red blood cells are separated from platelets using multiple centrifugation steps. Using approximately 450 mL of whole blood, a standard platelet unit is produced of approximately 50 mL with a concentration of 1.2×10^6 μL^{-1} platelets [41]. This solution then undergoes freeze-thaw cycles in order to lyse the platelet solution. MSC cultures are supplemented with approximately 10% (v/v) hPL [42]. 50 mL of clinical grade hPL can be brought for approximately £92.50. In vitro platelets can produce anywhere between 5 and 2,000 platelets per MK [43].Assuming in vitro megakaryocytes produced 100 platelets per cell , then 600 million MKs are required for one 50ml unit of hPL, to supplement 500 mL of basal media. In vitro culture of platelets for the production of hPL has the potential to overcome supply and biohazard burdens associated with the harvest of platelets from donors, whilst retaining the culture benefits of hPL.

1.3.2 Platelet and Megakaryocyte Biology

As discussed in section 1.2.2, defining CQAs that link to in vivo function is essential to manufacturing CT products as this enables control strategies to be implemented to optimise final products. This section reviews platelet and megakaryocyte biology which will be crucial to informing product specifications.

The hematopoietic linage is relatively well defined, as mentioned in Section 1.2.2.1, although the exact hierarchy of the linage is still debated [44]. The process of megakaryocyte differentiation from hematopoietic stem cells, megakaryopoiesis, and platelet biogenesis is shown in Figure 1-1. The development can be divided in four main stages [45], [46]. Firstly, HSCs proliferate within the bone marrow, maintaining their multipotency. The second stage is megakaryocyte differentiation, where the cells become committed to first the Megakaryocyte–erythroid lineage and then megakaryocytes only. Cells in this stage have the highest nucleus to cytoplasm ratio and contain elevated levels of RNA and α-granules [47].

In the third stage endomitosis occurs, which is the duplication of the cell's nucleus, without the cell splitting. The extent to which this occurs in a single cell is known as its ploidy, and is transcribed as copies of the chromosomes, for example 2N is two copies of the chromosomes and is therefore the equivalent to one complete nucleus. Mature MKs are polyploidy and are up to 128N. During this stage cytoplasm also matures and expands and cells can reach 50-100 µm in diameter.

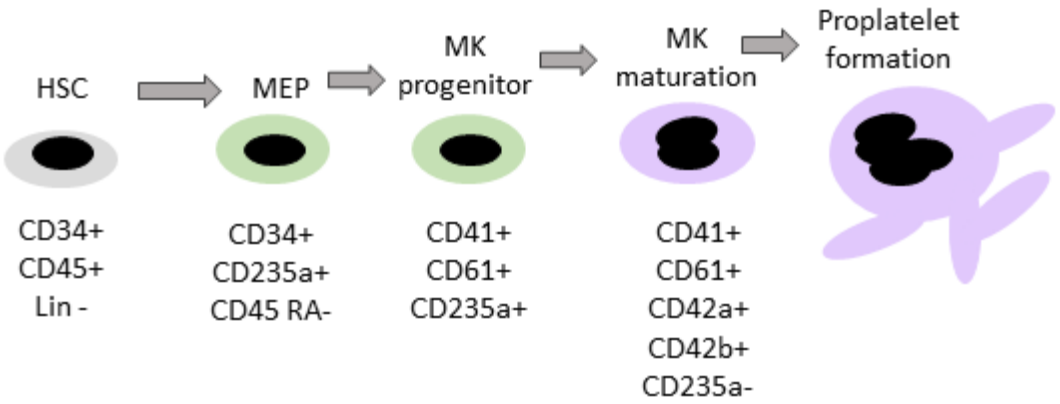

Figure 1-1: Summary of megakaryopoeisis and platelet production in vivo.

The final stage of maturity is platelet biogenesis where MKs undergo cytoskeletal reorganisation [48] extend and protrude blood vessels, and pro-platelets are sheared off. There is evidence to suggest that this is not the final stage of platelet maturity, as they continue to mature as they circulate in peripheral blood [49] and platelets can also be formed from a more global fragmentation of the cytoplasm [50].

1.3.3 Potential Cell Sources

MKs are the least represented cell type in the bone marrow, making a proportion of less than 0.01% of total nucleated cells. Due to their lack of availability, studies have been conducted which successfully produced MKs from CD34+ HSCs. These were sourced from umbilical cord blood (CB) [43], mobilised peripheral blood (mPB) [51], and bone marrow [45]. Although high platelet yields were achieved from each MK, the yield of MKs per HSC was often low or variable, producing anywhere between 0.04 MKs per input cell to 1,580. Usually either FBS or human serum was required (as discussed in Section 1.3.1.2 the use of serum should be avoided where possible), and/or a complex mixture of growth factors was required. GMP grade growth factors are costly which will weigh heavily on future COGs. Each extra component added must be validated and increases process complexity [52], therefore the number of different growth factors should be minimised where possible. Furthermore, all

sources listed must be routinely collected from donors which has implications on supply and biosafety hazards.

Some studies have identified embryonic stem cells (ESCs) and induced pluripotent stem cells (iPSCs) as a way of overcoming supply issues faced by using HSCs [53]. Gaur et al. (2006) differentiated ESCs to produce functional and platelet producing MKs, but again the culture yielded only 0.1 MK per input ESC. Other groups have increased the yield of MKs [54], but these culture systems required co-culturing with feeder cells, which is not desirable for commercial manufacture. A more recent approach reported utilising iPSCs, does not use feeder cells, and is cultured in serum-free medium, however in this case only 12 mature MKs are produced per input iPSC [55].

To overcome the culture limitations, a novel process has been devised which can produce large numbers of MKs from iPSCs. Using a process known as “forward programming” (FOP) where exogenous transcription factors GATA1, FLI1 and TAL1 are introduced to iPSCs using a lentiviral vector. This method produces over 200,000 MKs per iPSC cell input over 90 days. Furthermore cells are cultured in serum-free conditions using only recombinant Stem Cell Factor (SCF) and Thrombopoietin (TPO) [5].

1.3.4 Manufacturing Challenges - Platelets Production for Transfusion

A process flow diagram for the production of platelet transfusions from FOPMKs is shown in Figure 1-2, and the challenges at each stage are briefly considered in order to assess where improvements should be investigated.

Either embryonic stem cells (ESCs) or induced pluripotent stem cells (iPSCs) can be used as the source material in FOPMK production. Both cell types are pluripotent, i.e. they have the potential to differentiate into cells from all three germlines and cells are able to theoretically

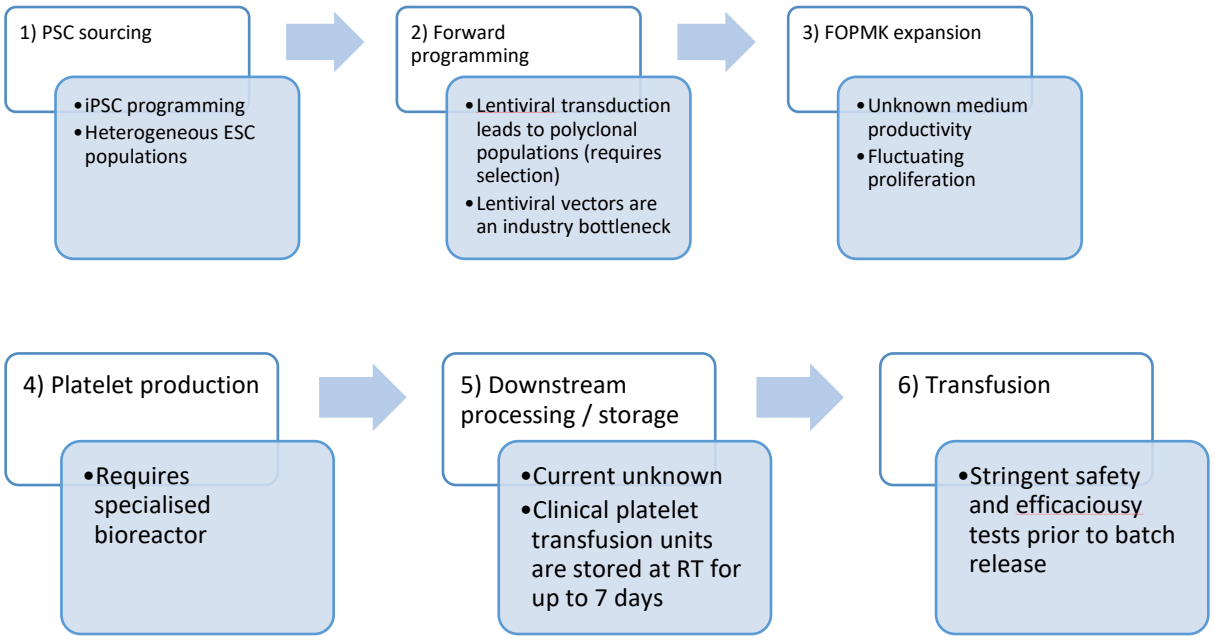

Figure 1-2: Process flow diagram depicting the stages required for platelet production from iPSCs using a forward programming process.

produce an unlimited number of cells. However, since iPSCs are somatic cells genetically reprogrammed using a small number of genes to resemble ESCs [56], they pose fewer ethical issues as ESC production requires the destruction of human embryos [57].

The pluripotent cell of choice is then forward programmed using lentiviral vectors with transcription factors GATA1, FLI1 and TAL1 as noted in Section 1.3.3. This process was developed across 2 generations. The first process utilised a cocktail of lentiviral vectors to produce a polyclonal population. The transduction process had an efficiency of approximately 60%, and by day 15 >95% of the cells expressed CD41a. The first generation FOPMKs could then be expanded for around 90 days. Indeed, some cultures expanded until day 132 [5]. However, since one iPSC was reported to generate 200,000 FOPMKs over 90 days, this is equivalent to a doubling time of approximately 5 days. The equivalent proliferation rate was low compared to many human cells, for example the doubling time of MSCs is approximately

24-48 hours [39], and is as low as 12 hours for HSC [58]. In the second generation of the FOPMK production process, a TET-ON promoter was incorporated in a genetic cassette containing the three transcription factors, followed by colony selection, produced a mono-clonal population. The inclusion of the TET-ON promoter allowed the modified iPSCs to be cultured (theoretically) indefinitely as pluripotent cells, with forward programming triggerable by the addition of a chemical trigger, doxycycline. The promoter therefore reduced the reliance on viral vectors.

During the expansion of FOPMKs, proplatelet particles can be constantly seen forming in culture, but to produce larger numbers of platelets the MKs must be differentiated using co-culture with feeder cells. Some groups have investigated platelet production using silk bioreactors [59], which is preferable for clinical platelet production as feeder cultures pose contamination risks. Platelet Biogenesis, a spin-out company from Harvard University, also claims to have developed a platform to produce a high number of functional platelets from megakaryocytes [60], but their technology is confidential currently.

Since stages 1-3 (will be common for all products using FOPMKs (for example platelet transfusion units and HPL production); these are examined in further detail below.

1.3.4.1 iPSC Generation

There are many ways in which variation can occur within iPSC cultures, the effect of which on the FOPMK culture and subsequent platelet production is not yet known. A study of genetic integrity of 66 iPSC lines showed that approximately 20% of lines displayed genetic abnormalities which may affect their differentiation potential [61]. The variation between iPSC cell source and donor variability has also been investigated, and it was concluded that the variation between donors outweighed the variation between initial somatic cell type.

Here the authors cite “DNA-methylation, gene-expression, miRNA, and splicing differences” which may all lead to ultimately different iPSC characteristics [62], but again the ultimate effect on iPSC function or characteristics is yet to be verified. It should be noted that genetic abnormalities may be indicative of tumorgenicity in vivo [63]. If these abnormalities are in clinically relevant cells differentiated cells, this may pose a risk to patient safety. Since platelets for transfusion are enucleate, transfusion units can be irradiated, as mentioned in section 1.3.2, and therefore tumorgenicity arising from iPSC genetic variations is less concerning for platelet production.

It has been shown that automating iPSC generation, can reduce genetic abnormalities and produce more consistent lines [64]. However, the CQAs used to characterise and select iPSC lines are still being debated, and therefore if the wrong criteria of selection are used this could still lead to producing inferior quality iPSC lines, albeit lines which are more consistent.

1.3.4.2 Forward Programming

Production of FOPMKs using somatic cells as the initial cell type requires two rounds of transduction. Firstly, to produce iPSCs and secondly to transform pluripotent cells to MKs. Throughout the past three decades there has been significant research into gene therapy, where gene therapy is the introduction of genetic material into cells to correct and treat disease [65]. This research has led to great advances in genetic programming which ultimately led to advances which make forward programming possible since the goal of gene therapy is to produce stable and safe genetic expression in the target tissue [66]. The first generation of adenovirus and retroviral vectors produced promising preclinical results. However the phase one clinical trials for ornithine transcarbmaylase (OTC) deficiency led to the death of 18 year old Jessie Gelsinger [67], and the use of retroviral vectors to treat X-linked severe combined

immunodeficiency (SCID) led to leukaemia [68]. These tragic incidents sparked research into safer transduction methods such as the lentiviral vectors, used in FOPMK production, and gamma retroviral vectors [69], [70]. The development of these safer vectors has also enabled revolutionary cancer treatments using genetically modified T-cells [71].

As discussed in Section 1.3.4.1, donor to donor variation transduction processes can lead to variation between iPSC lines, although it is not clear what effect these variations have on overall iPSC function. Since the forward programming process for FOPMK production is similar to iPSC generation the same principles could also be applied to both and therefore could be assumed that automation will enable more consistent FOPMK production. Viral transduction leads to the generation of polyclonal populations [72] with a distribution of integration of the factors into the genome. Coupled with heterogeneous pluripotent cell populations, this random transduction led to a transduction efficiency of 60% of iPSCs as reported in Section 1.3.3.

1.3.4.3 Expansion of FOPMKs

Despite the challenges, the current protocols have so far produced FOPMKs and functional platelets which have been effective in mouse models; yet the expansion of FOPMKs in culture is not yet well characterised. The effect of variation in iPSC generation and forward programming is not easily measurable until the expansion of FOPMKs is more fully understood. Furthermore, once the efficiency of the MK expansion is known, this will determine the required production rate of platelets from FOPMKs; and in large-scale allogeneic treatments such as platelet transfusions, where more than 100,000 doses per year will be required, it is estimated that the medium will make up to 58% of the COGs [73].

Current process inconsistencies could in part be due to a lack of understanding of what the cells require. Cell cultures grow and develop in response to the complex composition of the cell culture media. However, the environment is not constant but is changed dynamically by the cells. Some of these changes are qualitatively generic across different cell types, such as utilisation of a carbon source for energy. However others, such as release of cell specific cytokine profiles, and sensitivity in feedback, will be highly specific to individual phenotypes. FOPMK expansion, and indeed CT manufacture in general, requires a detailed understanding of such media modification and feedback loops both to control quality of product and maximise economic product yield. Appropriate models of these dynamic characteristics will allow optimisation and risk reduction. Section 1.4 reviews methods for modelling cell culture processes.

Commercial platelet manufacture will also require process transfer to scalable technologies. Currently expansion of FOPMKs takes place in static culture, i.e. in T-flask or plates. At small scale, these culture platforms do not offer online monitoring of key process parameters, such as dissolved oxygen (DO) concentration and pH. Despite being suspension cells, FOPMKs settle to the bottom of the flask if left unmixed. When the volume of medium in the culture flask is less than 4mm it can be assumed that the DO concentration at the bottom of the flask is equal to the concentration at the gas interface which is approximately atmospheric or 20% [74]. However, this assumption does not hold at larger volumes or flask stacks, where mass transfer may become limiting and will lead to heterogeneous cultures. Heterogeneity will lead to inefficient use of media by limiting the maximum number of cells supported and producing variations in cell populations [12].

Conventional stirred tank systems are widely used in the culture of CHO cells for biologics production. These systems incorporate on-line monitoring and control which promotes homogenous culture environments. To meet the required lot sizes for platelet production stirred tank reactors will be required.

1.4 Quantifying cell culture productivity limits and population dynamics

Cells are complex, dynamic structures which exhibit variation from each other. When considering methods to quantify population dynamics it is essential to consider the required model output since the closer a model becomes to reality, the more complex it becomes. A more complex model requires more a detailed background understanding of the observed cell culture system for model construction, more computational power for model execution and more analytical insight, which require more resources.

There are many ways in which models of cell cultures have been defined. However, these definitions are not standardised within the literature. In order to provide a common level of understanding for analysis common definitions are outlined in Table 1-1, along with examples of where they have been applied to cell culture. Furthermore these definitions are not always straight-forward to apply and models can combine elements from apparently contradictory stances; for example a pseudo-stochastic and deterministic model was developed by Nielsen et al. to describe in vitro haematopoiesis [75].

Table 1-1: Different modelling approaches and examples of their application to cell based therapy or cell growth.

Approach	**Definition**	**Examples**	**Also known as**
Empirical	Relationships derived from observations of the system. This approach produces correlative equations which do not necessarily reflect underlying mechanisms. Different statistical methods can be used to develop empirical models such as factorial design of experiments (DOE) and response surface methodology (RSM) for linear relationships and artificial neural networks (ANN) for non-linear relationships.	Design of Experiments (DOE) [13] Response surface methodologies (RSM) [76] Neural networks [77], [78]	
Mechanistic	Model structure attempts to explicitly quantify behaviour by understanding underlying phenomena.	[79]–[82]	
Deterministic	Randomness does not influence the outcome of a system.	[81], [82]	
Stochastic	Outcome which is based on a probability distribution and cannot be predicted absolutely.		
Segregated	The segregation of a culture into individual units.	Agent based models (ABM) or individual based models (IBM) (cultures segregated into individual cells).	Corpuscular [83]
Non-segregated	Approach assumes that the culture is “lumped” together as a single population with identical behaviour.		
Structured	Approach assumes cells are composed of different chemical, biochemical or physical components which can vary from each other and/or overtime.	Metabolic flux analysis [84]	
Unstructured	Assumes constant cell composition of individual or populations of cells.	[80]	Macroscopic [85]

Top-down	Using observations at a whole system level to develop understanding of fundamental molecular networks.	[86]	
Bottom-up	Developing an understanding of fundamental molecular component interactions (e.g. genome) from independent experimental data to inform system characteristics.	[87]	
Population Balance Model (PBM)	PBMs characterises cells as they change dynamically relative to a state variable which is a continuum [88].	[89]	

When developing quantitative models, the simplest model that delivers the required level of insight should be chosen. This fundamental principle of developing parsimonious models is known as “Occam’s Razor” [90]. For a cell therapy production system, a model closest to reality would incorporate mechanistic, deterministic, stochastic, segregated and structured elements. However, this complexity would be challenging to practically achieve. A simpler model may deliver the level of understanding required and under Occam’s Razor would be preferred.

Two modelling approaches have been selected to test their applicability and utility in defining cell population dynamics. The first, statistical DOE is empirical and stochastic. The second is a novel, dynamic, mechanistic modelling platform which treats cells as whole homogenous populations (or can split cells into distinct populations). The two approaches are outlined in more detail below in Sections 1.4.1 and 1.4.2. A model platform which split cells into further sub-components was not selected since this would have required significantly more resource. Rather than attempt to fully characterise cell populations, these two approaches were chosen as they readily accessible for proof of concept studies to determine the utility of quantifying cell population dynamics to develop more robust manufacturing processes for cell therapies.

1.1.1. Quality by Design

Quality by Design (QbD) is a risk-based approach to product and process development, endorsed by regulatory bodies for the development of pharmaceutical products. Its objectives include the development of meaningful product quality specifications that are linked to clinical mechanism of action, reduce product variability and enhance post regulatory approval change management [91].

The QbD process is outlined in **Error! Reference source not found.**; initially the Target Product P rofile (TPP – also referred to as Quality Target Profile) defines the attributes of the product that are required to achieve the desired clinical outcomes. From the QTPP, measurable Critical Quality Attributes (CQAs) can be identified which are "a physical, chemical, biological, or microbiological property or characteristic that should be within an appropriate limit, range, or distribution to ensure the desired product quality" [92]. A systematic risk assessment which links control variables to CQAs is undertaken using available qualitative and quantitative knowledge. Variables are ranked based on criticality, occurrence and detectability [93] which is important to reduce variables to a manageable number for onwards experimentation. Appropriate experimentation is then used to link prioritised control variables to CQAs to

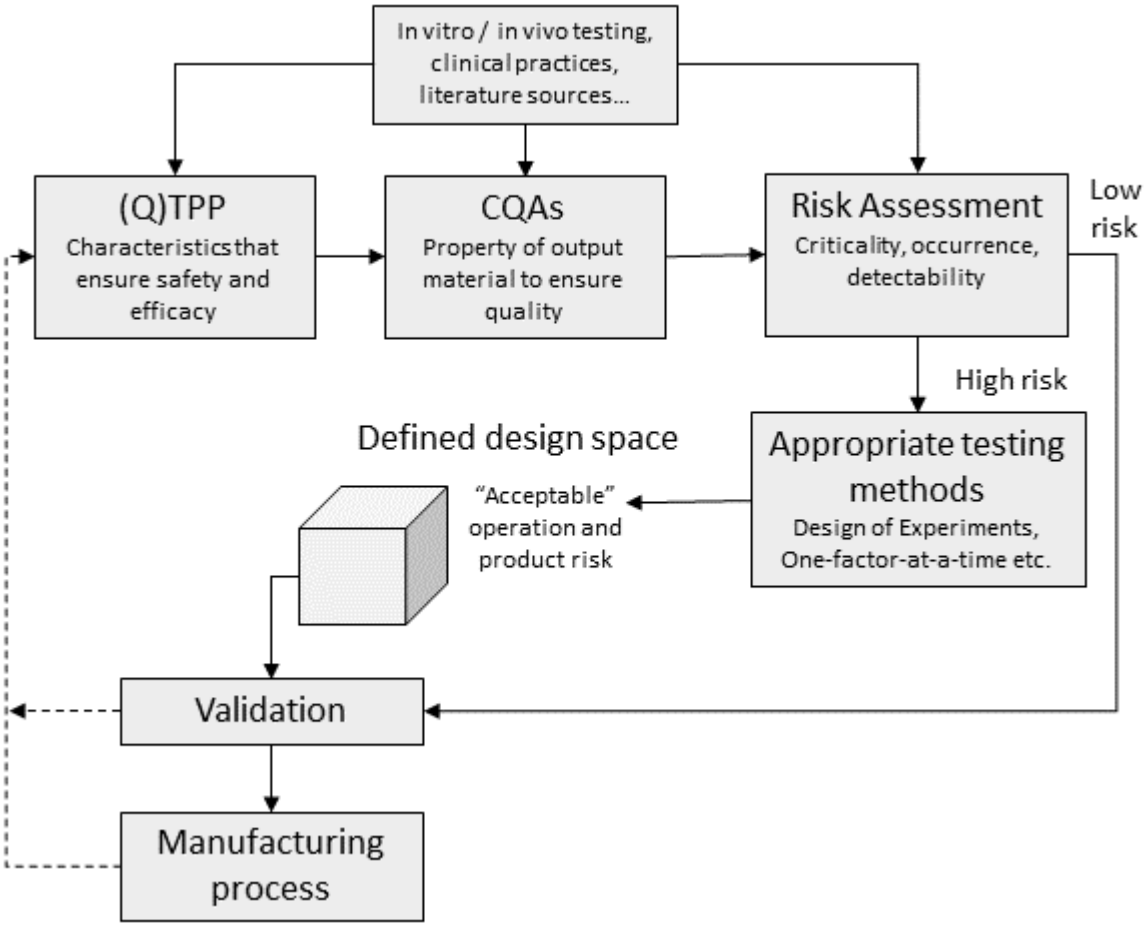

Figure 1-3: Schematic diagram of the QbD process. The focus of QbD is to design quality into a product through understanding how variation in input and processes impact final product outcome. QbD can be iterative process, as more knowledge is built it can be used to redefine earlier parts of the process.

define the process design space. Once this has been validated a manufacturing process can be implemented. The information gained can be recycled back into the start of the QbD process to inform process refinement.

1.4.1 Design of Experiments

Factorial design of experiments (DOE) is a structured methodology facilitating the investigation of multiple conditions on process outcomes. DOE has been used to characterise elements of CT processes, including determining effect of metabolites on net growth rate during the exponential growth rate [58], and understanding effects such as time since previous passage and freeze rate on the quality of hESC during cryopreservation [13]. It is an efficient methodology as it allows multiple process variables to be analysed in a single experimental set-up which can be easily analysed in a range of commercial software packages. When properly designed to include randomisation and replication these stochastic models allow an estimate of the variation in a system and empirical, correlative equations can be obtained which link all tested process variables to process outcome [94].

Factors chosen for investigation should be selected based on a mechanistic rationale of effect on process outcome, but the complex nature of cell therapy production could lead to the empirically defined relationships failing across the longer time courses required for cell therapy manufacture as that the control variables lead to an evolving environment over time. Although these multiple arising subsidiary variables will be a function of the selected control variables at any given time, they are likely to generate a complexity of relationship between the initial control variables and the response variables that will not be well represented by the linear or simple curvilinear equations to which DOE is most suited.

1.4.2 Mechanistic modelling

The simplest type of mechanistic modelling is unstructured, unsegregated and deterministic. These types of models have been applied to bacterial and mammalian cultures to enhance control and productivity of such systems [76], [79], [80], [95]. Models have been as simple as developing a Monod type approach which characterised the response of HSCs to growth factors [96]. Such modelling techniques have also been applied to PSC cultures. Yeo et al [82]. developed ODE kinetic models by dividing a culture into two homogeneous subpopulations - pluripotent or differentiated - in stirred suspension reactors. The conversion rate of pluripotent into differentiated cells was modelled as driven by the accumulation of inhibitory molecules. ODE models have also been used to describe the transition of cells across four differentiation states based on gene expression where gene expression was dependent of the use of different differentiation protocols [97]. A further example is the application of ODE models to describe the nutrient and oxygen depletion of PSC fed-batch cultures and following development of perfusion cultures[98]. ODE models have also been applied to HSC cultures and used to successfully predict growth limitations [99].

The above approaches show the applicability of ODE, mechanistic modelling and its potential utility. However, there is a high barrier to entry in terms of the mathematic and programming knowledge required for the development and implementation of these types of models. Our group has developed a flexible platform [100] which allows users to describe cell populations behaviours using a series of Di-graphs, and can test these hypothesises through fitting ordinary differential equation based models to experimental data using a least squares method. Proof of concept studies have shown that this mechanistic modelling methodology can be applied to describe growth inhibition in euthyroid lineage cells [81]. This work aims to

test the broader applicability of the modelling paradigm to more complex cell / environment interactions.

1.5 Conclusion

This introduction outlines the relevant background information, including current state and major challenges, for the regenerative medicine and cell therapy industries. The production of platelets for transfusion from pluripotent stem cells exemplify the challenges of cell expansion for cell therapies including high cell yields required, high COGs and undefined system productivity limits. Different methods for quantitative models are described and two methods are presented for further investigation as potential methods for defining cell and environment interactions in order to first define and then improve system productivity. The first is established statistical modelling through DOE and the second a novel mechanistic modelling paradigm. Both were tested in detail throughout Sections 4, 5 and 6. Finally, detailed background for the analytic technique flow cytometry was presented, which was the analytical technology selected for cell characterisation. Flow cytometry allows single cell measurements to be taken from a heterogenous population of cells, but assay development must be meticulous and an in-depth understanding is required of cell attributes to be measured, flow cytometry equipment used and fluorochrome selection to develop robust and reliable assays. Selection of measured cell attributes and subsequent flow cytometry analysis is presented in Section 3.

1.5.1 Aims and objectives

This research aims to address some of the issues discussed above by using forward programmed megakaryocytes as a manufacturing case study. Specifically, the work will focus on defining bioprocesses for upstream manufacture of FOPMKs, whilst simultaneously

evaluating the methodologies applied for deficiencies and potential improvements considering the characteristics of the system. The focus will further be on the productivity of the culture system with respect to use of upstream input resource, mainly cell culture medium and processing time, and quality of output cells
for the useful application of modelling tools to characterise cell expansion systems to define and improve system productivity.

The objectives of the project were to:

- Identify candidate CQAs for Megakaryocytes, and develop robust assays to monitor CQAs, to provide a sound basis for quality assessment in process development.
- Identify process characteristics that inform the selection of a process development methodology; provide a narrative analysis of the transfer of the exemplar process between laboratories and the insights that can be used for planning detailed process design.
- Apply both the industry standard and relatively generic Design of Experiments approach, and an ODE based mechanistic framework, to characterise FOPMK production. Compare and review the advantages and disadvantages of the approaches and where methodological opportunities exist for improvement to characterise megakaryocyte expansion and linkage of process variables to CQAs.
- Given the applied methodologies discuss the current state of potential FOPMK and platelet manufacture, process improvement opportunities identified in this work, and where future focus is required to make manufactured platelets a reality.

2. Materials and Methods

2.1. Introduction

‘The research aims of this work are to investigate, identify and define the behavioural characteristics of FOPMKs in culture to the level required to achieve the overarching goal: definition of a manufacturing strategy aligned with market demands. The aim of this section is to outline the materials and methods used throughout the work. However, because this work process development focused, individual experiments will require different methodologies to test the impact of processing on product outcomes. In these instances, a basal protocol is specified, and deviations from the protocol detailed in the relevant chapters.

2.2. Non-inducible FOPMK Culture

2.2.1. Derivation

FOPMKs were provided by Cedric Gheavart, Hematology department, University of Cambridge. Cells were derived by our collaborators as described by Moreau et al. [5]. Briefly, iPSC lines are transduced with three different batches of lentiviral vectors containing transcription factors GATA1, FIL1 and TAL1 to produce self-replicating FOPMKs which can be sustained for approximately 90 days in culture.

Three independently derived iPSC lines were used: BOB (formal line name A1ATD1) and BOBc were derived from the same donor [101], with the BOBc line being corrected for the A1AT gene [102]. FFDK originated from a different donor [103].

2.2.2. Culture

For static culture FOPMKs were cultured in ultra-low attachment tissue plastic ware (Corning, UK). Unless otherwise stated the culture medium used was Cellgenix SCGM (Cellgenix, Germany) which was supplemented with 20 $ng.mL^{-1}$ TPO and 50 $ng.mL^{-1}$ SCF (both R&D

Systems, UK). Initially cells were seeded at 5×10^5 cells.mL^{-1} and medium supply was defined by regular time intervals where every 3 days the culture volume was doubled by the addition of fresh medium with double concentrated growth factors. When viable cell seeding densities exceeded 1.5×10^6 cells.mL^{-1}, cultures were reseeded at 5×10^5 cells.mL^{-1}. Every 10 days a complete medium exchange was performed. Cells were placed into an incubator at 37°C, 100% humidity and 5% CO_2.

For stirred suspension culture spinner flasks were used. For spinner flask cultures the glass surfaces of two Integra Cellspin 100 mL spinner flasks (diam. T = 70mm, SLS, UK) with a magnetic, vertical stirrer bar (diam. D = 20mm) were siliconised with Sigmacoat (Sigma-Aldrich, UK) according to manufacturer instructions. Following inoculation the culture was agitated constantly at a low at a rate of 20 revolutions per minute (RPM). Medical grade tubing was used to assemble a syringe pump (PHD/Ultra, Havard Apparatus, UK) for drip feeding medium into the spinner flasks. The spinner flasks were also modified to allow a sample point and gas air filter to be assembled. The system was placed into the incubator at 37°C, 100% humidity and 5% CO_2. Each spinner flask was positioned on one magnetic stirrer (Bellennium Compact Five Position Magnetic Stirrers, BellCo, USA).

2.3. Inducible FOPMK culture

2.3.1. Derivation

Inducible FOPMKs were provided by Cedric Gheavart, Hematology department, University of Cambridge. Briefly, the iPSC line BOBc were targeted with a TET-ON system, which incorporated a tetracycline-responsive promoter, GFP, GATA1, TAL1 and FLI1. Post transduction, cells which are stable homozygous clones, were cultured as PSCs. When required, the genetic cassette was activated by adding doxycycline hyclate (Dox – a

tetracycline derivative) to the culture medium, which induced forward programming. The derivation of this inducible system is not currently published.

2.3.2. Culture

2.3.2.1. PSC culture

Based on information from our collaborators the following culture methods were employed: Prior to induction iPSC were cultured in medium called AE6 which contained DMEM/F12 (Gibco, UK) supplemented with 0.05% w/v Sodium Bicarbonate (Gibco, UK), 64.1 $mg.L^{-1}$ L-Ascorbic acid 2-phosphate sesquimagnesium salt hydrate (LAA) (Sigma-Aldrich, UK), Insulin-Transferrin-Selenium (Gibco, UK) and sterile filtered. On the day of use medium was supplemented with 15 $ng.mL^{-1}$ FGF2 and 15 $ng.mL^{-1}$ Activin-A (Biotechne, UK) and was exchanged daily. Upon passaging, cell cultures were washed with PBS and were then treated with 0.5 mM EDTA incubated for 7 minutes in a humidified incubator at 37˚C. Cells were seeded at 10,000 $cells.cm^{-2}$ (5×10^4 $cells.mL^{-1}$) in medium containing 10 µM ROCK inhibitor Y27632 (Miltenyi biotech, Germany). Tissue culture plastic was coated with 5 $\mu g.mL^{-1}$ Vitronectin for a least one hour prior to use, according to the manufacturer's instructions.

2.3.2.2. Forward Programming

Prior to forward programming, iPSCs were passaged using TryPLE (Gibco, UK) and were incubated for 7 mins in a humidified incubator at 37˚C. TrypLE was quenched using sterile AE6 medium. Unless otherwise stated, cells were seeded at 12,500 $cells.cm^{-2}$ in 0.2 $mL.cm^{-2}$ PSC supplemented medium with ROCK inhibitor. Twenty-four hours later (referred to as Day 0) PSC medium was aspirated and replaced with 0.2 $mL.cm^{-2}$ of mesoderm medium – which contained, unless otherwise stated, AE6 supplemented with 20 $ng.mL^{-1}$ FGF2 and 10 $ng.mL^{-1}$ BMP4 (Biotechne, UK) and 1 $\mu g.mL^{-1}$ Dox (Sigma-Aldrich, UK). At two days post Dox addition

(day 2) mesoderm medium was aspirated and replaced with MK programming medium which contained, unless otherwise stated, Cellgenix SCGM (Cellgenix, Germany) supplemented with 1 µg.mL^{-1} Dox, 100 ng.mL^{-1} TPO and 25 ng.mL^{-1} SCF.

At four days after Dox addition (Day 4) the culture volume was doubled through addition of fresh MK programming medium with double concentrated growth factors (2 µg.mL^{-1} Dox, 200 ng.mL^{-1} TPO and 50 ng.mL^{-1} SCF) so the total volume of medium was 0.4 mL.cm^{-2}. At Day 6 and Day 8 50% of the culture volume was removed and cells were collected by centrifugation at 120g for 8 mins, slow acceleration and slow brake. Spent medium was aspirated and replaced with fresh MK programming medium with double concentrated growth factors. At Day 10 cultures were passaged. Medium supernatant containing suspended cells were collected and cells were washed with PBS, and incubated with for 7 mins in a humidified incubator at 37˚C. TrypLE was quenched using sterile Celgenix medium and passaged cells were mixed with spent medium containing suspended cells and were centrifuged at 120g, for 8 mins, slow brake and slow acceleration. Supernatant was aspirated and cells were suspended in MK expansion medium – Cellgenix SCGM supplemented with 20 ng.mL^{-1} TPO and 25 ng.mL^{-1} SCF - at 5 × 10^5 cells.mL^{-1} in ULA tissue culture plastic.

2.3.2.3. MK culture

From Day 13 onwards medium supply was defined by regular time intervals where every 3 days the culture volume was doubled by the addition of fresh medium with double concentrated growth factors. When viable cell seeding densities exceeded 1 × 10^6 cells.mL^{-1}, cultures were reseeded at 5 × 10^5 cells.mL^{-1}. Every 10 days a complete medium exchange was performed.

2.4. Other cell culture processes

2.4.1. Cryopreservation

Cells were cryopreserved at 1-10 million cells.mL^{-1} using sterile filtered medium containing RPMI 1640 (Life Technologies, UK) 10% Anhydrous DMSO (Sigma Aldrich, UK) and 4% human serum albumin (Irvine Scientific, USA). Cells were frozen using a CoolCell™ FTS30 Freezing container (Biocision, USA) placed at -80°C for 24 hours and transferred to vapour phase of liquid nitrogen for long term storage.

2.4.2. Thaw

Two centrifuge tubes containing medium were prepared for thaw, one containing 50 ng.mL^{-1} SCF and 20 ng.mL^{-1} TPO and the second containing no growth factors. These were warmed in a water bath for 15 min. The required vial was removed from the vapour phase of a cryostore and thawed for 2 min in a water bath whilst gently agitating the vial. Using a 1000 µL pipette tip cells and cyro-medium solution were removed from the vial and gently added to a tube labelled “SCGM no added growth factor”.

Using the same 1000 µL pipette tip, 1 mL of medium containing no added growth factors was added to a vial to wash. The medium was gently mixed twice in the vial and added to remaining cell/medium solution containing no growth factors. The tube was centrifuged for 8 min, 120g, slow acceleration and slow brake.

Supernatant was aspirated and the tube was gently tapped to suspend the cell pellet. The target seeding density post-thaw was 7.5 × 10^5 cells.mL^{-1} and the volume of the medium containing growth factors was added accordingly. This was mixed twice prior to adding to tissue culture vessel. The vessel was gently tilted to ensure base was covered.

2.5. Cell counting methods

Since FOPMKs are suspension cells, samples were taken by mixing vessels (either tissue culture plate, T-flasks or spinner flasks) thoroughly, aspirating and releasing a least half the culture medium three times with sterile pipette tips or stripettes.

Viable cell counts were assessed in several ways discussed below. The specific expansion rate of cells was calculated as follows:

$$\mu = \frac{ln\left(\rho_{viable\ t2}/\rho_{viable\ t1}\right)}{\Delta t} \quad (2\text{-}1)$$

Where μ is the specific expansion rate (h^{-1}), and $\rho_{viable\ t1}$ and $\rho_{viable\ t2}$ are the viable cell densities ($cells.mL^{-1}$) at the end and beginning of a culture period respectively, and Δt is the culture period (h). The specific expansion rate can be used to calculate the doubling time (t_d):

$$t_d = \frac{\ln(2)}{\mu} \quad (2\text{-}2)$$

The number of population doublings (PDs) over a given time period (Δt) was calculated as follows:

$$PDs = \frac{ln\left(\rho_{viable\ t2}/\rho_{viable\ t1}\right)}{ln(2)} \quad (2\text{-}3)$$

2.5.1. NucleoCounter® 3000

When using a NucleoCounter® NC-3000™ (Chemometec, Allerod, Denmark) 76 µL of cell and medium solution was taken from a well-mixed vessel. Four µL of solution containing 30 $\mu g.mL^{-1}$ acridine orange (Sigma-Aldrich, Dorset, UK) and 100 $\mu g.mL^{-1}$ DAPI (Thermo Fisher Scientific, Loughborough, UK) dissolved in distilled water was added to cell and medium solution. 32 µL of cell/medium/stain mix was added to a single chamber in an A2 slide for analysis or 11 µL added to a single chamber in an A8 slide.

2.5.2. Flow cytometry

The BD FACS CANTO II (BD Biosciences, San Jose, USA) was used for cell counts obtained through flow cytometry (see Section 2.6.2 for equipment details). 75 µL of cell and medium solution was taken from a well-mixed vessel and 150 µL flow buffer (see Section 2.6.1) was added to a 96 well plate for analysis. Data was acquired using the high throughput system (HTS) using the following settings in Table 2-1 and the PMT voltage settings shown in Table 2-2.

Table 2-1: HTS settings for cell counting acquisition

Parameter	Value
Sample volume flow rate	1.5 µL.s^{-1}
Sample volume	150 µL
Mixing volume	100 µL
Mixing speed	100 µL.s^{-1}
Number of mixes	5
Wash volume	200 µL

Table 2-2: Parameters and PMT voltages used for cell count protocols

Marker/ attribute	Fluorochrome	Laser	PMT - filter	Voltage
Viability	DAPI (Invitrogen, UK)	Violet	B – 450/40	165
Cell size	FFS	Blue	N/A	125
Granularity	SSC	Blue	F	350

Cell densities were calculated using the following equations:

$$\rho_{total} = \frac{1000 \times \frac{v_c + v_d}{v_c}}{v_s} \times \left(E_{singlets} + 2E_{doublets}\right) \quad (2\text{-}4)$$

$$\rho_{viable} = \frac{1000 \times \frac{v_c + v_d}{v_c}}{v_{sample}} \times \left[\left(E_{singlets} \times P_{sNDP}\right) + \left(2E_{doublets} \times P_{dNDP}\right)\right] \quad (2\text{-}5)$$

Where:

- ρ_{total} is the total cell density (cells.mL^{-1}),
- v_c is the volume of cell and medium sample, in this case 75 µL,
- v_d is the volume of diluent flow buffer and DAPI solution, in this case 150 µL,
- v_s is the volume of sample analysed, in this case 150 µL,
- $E_{singlets}$ is the number of events which are single cells as defined by the forward and side scatter profiles,
- $E_{doublets}$ is the number of events which are doublet cells as defined by the forward and side scatter profiles,
- P_{sNDP} and P_{dNDP} are the proportion of cells which are non DAPI permeable in the singlet and doublet cell populations respectively

After acquisition FACS files were exported to FACS Analysis software FlowJo® for analysis. The gating strategy to define the events required for the inputs required for equations (2-4) and (2-5) is shown in Figure 2-1 as an example of two samples with high and low viability. First, debris was excluded using FSC-SSC plots, followed by selection of singlet and doublet cell populations using a histogram of forward scatter width. Figure 2-1 far right shows the resulting gated populations.

Debris were excluded and the remaining events were categorised as “MKs”. Cells were then gated based on a histogram of forward scatter width and back gated to the position of the cells on SS/FS plots. The exclusion of DAPI was the criterion for cell viability. It should be noted that there are many methods to determine viability, and the choice of membrane integrity is based on wide acceptance, literature citation and good correlation with FS/SS [104](see Section 3.4 for discussion of cell counting methods development).

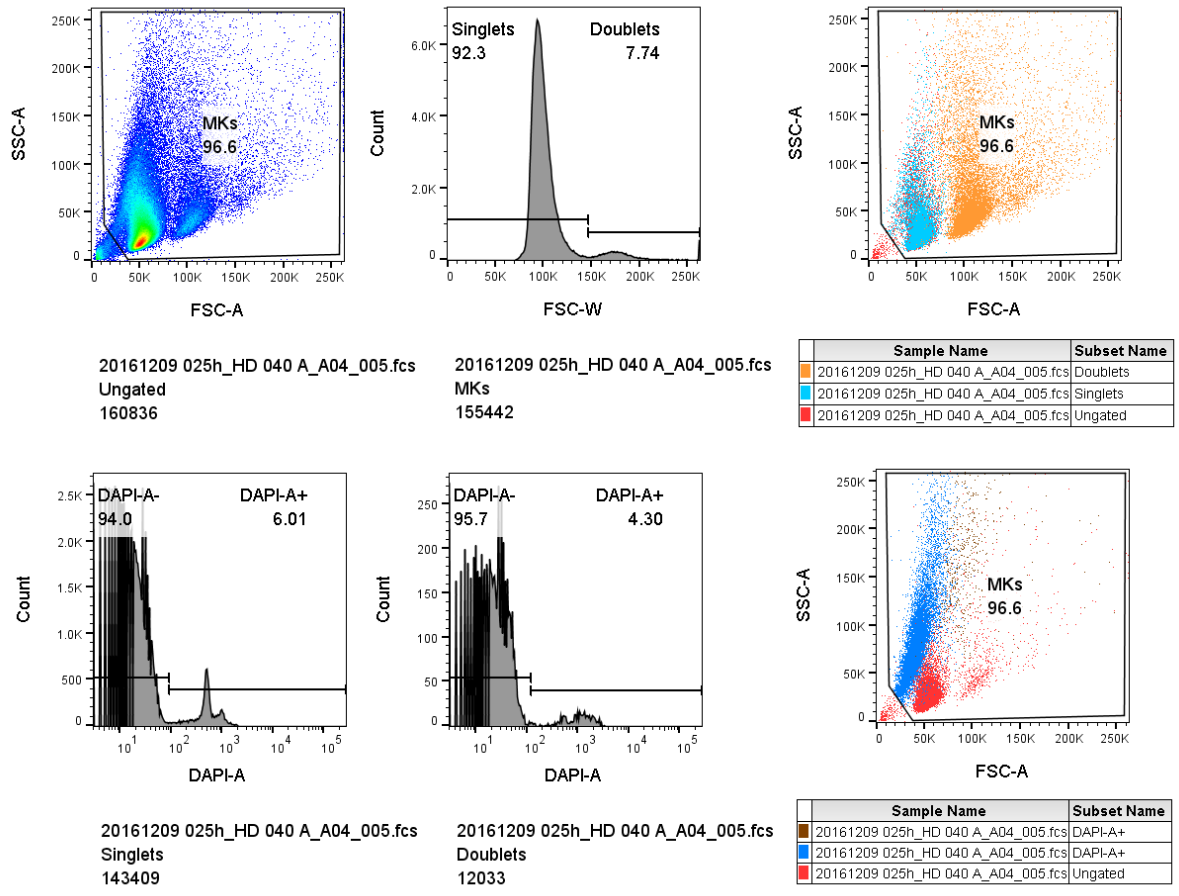

Figure 2-1: Gating stragey for cell counts. Debris was excluded first and from the remaining sample doublets and singlets were separated. DAPI positivity was determined based on unstained controls.

2.6. Flow cytometry

2.6.1. Sample preparation

The target cells of interest for this work, FOPMKs, are suspension cells and therefore sample preparation does not require enzymatic or mechanical treatment to achieve a cell suspension. When analysing tissue samples or adherent cell populations it is critical that any pre-treatment steps do not impact the attributes being measured, or at least the impact is understood and managed, as this could lead to false conclusions. Cell clumping was minimised as these larger clumps could cause blockages within the cytometer, cause interference with fluorochrome binding and distort output data (for example showing a large single event with higher marker expression, when the event is two adjoined cells).

Necrosis induced through sample preparation causes excessive debris and the release of components that could interact with the cells and/or fluorochromes, which could also skew data outputs. This is especially important when cell counting assays are required. To preserve cells in the required state and minimise clumping, a flow cytometry buffer was employed that contained dissociation reagents and protein in a salt solution with the correct osmolality. In this case the flow cytometry buffer used contained 1% Bovine Serum Albumin, 1 mM EDTA and 2 mM HEPES dissolved in PBS (all Sigma-Aldrich, UK), stored at 4^{o}C and added to a collection tube or 96-well plates. Non-viable cells often have increased non-specific binding which could lead to falsely high expression levels in target cell populations. Methods for identifying non-viable cell populations are discussed in Section 3.4, and where possible viability probes (DAPI or fixable viability stain – FVS) have been included in flow cytometry experiments.

In order to measure cell ploidy level cells were fixed using a 4% formaldehyde solution and incubated for 10 minutes at room temperature and washed prior to staining. After staining (see Section 2.6.3 for details), cells were permeabilised using Perm Wash Solution (BD Biosciences, Oxford, UK).

2.6.2. Flow cytometry equipment

During acquisition samples were collected either from collection tubes attached to the sample injection tube (SIT) or from the 96 well plates using the high through-put system (HTS) which connects to the SIT. Target particles suspended in buffer solutions were forced through the flow cell, where the laser interacted with the sample, at a flow rate designated by the user.

The flow cytometer used for this work was the BD FACS Canto II (BD Biosciences, USA) with the 4-2-2 configuration, meaning it was possible to run assays with up to eight fluorochromes. Three lasers emitted light: Coherent Sapphire solid state blue laser (488 nm), JDS Uniphase HeNe air cooled red laser (633 nm) and Point Source™ iFLEX™2000-P-1-405-0.65-30-NP violet laser (405 nm) [105]. The filters and mirrors are summarised in Table 2-3.

The photomultiplier tubes (PMTs) collected the side scattered light and fluorescence from the articles measured in the flow cell. The forward scatter was collected by a photodiode, and the light was directed to the collection optics. The 4-2-2 configuration used for this work contains three collection arrays. Light from the blue laser is collected in the octagon array containing five PMTs and the light from the violet and red lasers are collected in trigon arrays.

Once the light arrived at an array a longpass (LP) mirror (filter) transmitted the highest wavelengths through into the first PMT, and reflect lower wave lengths to the next PMT. The filter in front of the next PMT which transmited the next highest wavelengths, and reflected the lower wavelength further round the array etc.. The PMTs produced a signal proportional

to the amount of light detected which was then converted to electronic signals. The magnitude of these signals was determined by the PMT voltage set.

Table 2-3: Details of the lasers and collection arrays in the BD FACS Canto II used for this work adapted from the BD FACS Canto Reference Manual [105]

Laser	PMT	LP Mirror/Filter	BP Mirror or LP Mirror	Common fluorochromes
Blue	A	735	780/60	PE-Cy7
	B	655	670	PerCP-Cy5.5, PerCP, PE-Cy5
	C	610	-	
	D	556	585/42	PE
	E	502	530/30	FITC, AlexaFlur 488
	F	-	488/10	SSC
	G	-	-	
	H	-	-	
Red	A	735	780/60	APC-Cy7
	B	685	-	-
	C	-	660/20	APC, Alexa Fluor 647
Violet	A	502	510/50	AmCyan, BV510, BV500
	B	-	450/40	DAPI, Pacific Blue, BV421
	C	-	-	

2.6.3. Staining and sample acquisition protocol

When using FOPMKs, cell counts were performed (see Section 2.5) and then at least 1×10^5 - 1×10^6 cells were used for phenotype analysis where practically possible suspended in 100 or 150 µL of flow cytometry buffer (see Section 2.6.1) or cell culture medium. The appropriate volume of antibody volume was added to the cell / buffer suspension (volumes were determined by either manufacturers recommendation or using antibody titrations - see Section 3.3.2) and were protected from light and incubated at RT for 30 minutes in 2 mL Eppendorf tubes (Fisher Scientific, Loughborough, UK).

After 30 minutes 1.5 mL of flow cytometry buffer was added to Eppendorf tubes containing stained cells. Tubes were centrifuged for eight minutes at 120g, with low acceleration and low brake. Supernatant was aspirated and cells were suspended either in 300 µL or 500 µL of

flow cytometry buffer containing 1 µg.mL^{-1} DAPI solution and transferred to either non-tissue culture treated 96 well plates for use with the high throughput system (HTS) or collection tubes for use with the sample injection tube (SIT). When using the HTS the following parameters were used for collection:

Table 2-4: Parameter used for sample acquisition with the HTS system

Parameter	Value
Sample volume flow rate	2.0 µL.s^{-1}
Sample volume	200 µL
Mixing volume	100 µL
Mixing speed	100 µL.s^{-1}
Number of mixes	5
Wash volume	200 µL

When using the SIT the sample flow rate selected was “medium” and in both cases the number of events set to record was a minimum of 30,000 of the target population, where possible, or the maximum number of events.

2.6.4. Optic capture settings

Optic capture settings and corresponded PMT voltages are described in Section 3.3.

2.6.5. Calculating compensation

Either cells or compensation beads were used to calculate appropriate compensation values, depending on which particle gave the highest signal. Particles were stained for 30 mins then washed with flow cytometry buffer and centrifuged at 120g for 8 minutes when using cells or 500g, 5 mins when using beads. Particles were resuspended in 300 µLof flow buffer for sample acquisition. Assay development and comparison of compensation methods is discussed further in Section 3.3.

2.6.6. Gating strategy

Where possible, biological controls were used to set gates; for example where there were large and obvious separations between populations. This method was used in conjunction with isotype controls to check for non-specific binding, “fluorescence minus one”(FMO) controls to check for errors caused by incorrect compensation and unstained cells to check for auto-fluorescence issues.

2.6.7. Antibody reagents

The antibodies used throughout this thesis are listed below in Table 2-5.

Table 2-5: List of antibody reagents

Marker	Flurochrome	Supplier	Cat number	Lot number	Isotype control
CD235a	PE	BD Biosciences	555570	4283906	mouse IgG2b
CD235a	PE-Cy7	BD Biosciences	563666, 563667	7319640	mouse IgG2b
CD34	PerCP-Vio700	Miltenyi	130-097-951	5161107547	mouse IgG2aκ
CD41a	APC	BD Biosciences	559777	7215863	mouse IgG1
CD41a	BV510	BD Biosciences	563250	7164967	mouse IgG1
CD41a	FITC	BD Biosciences	555466	6112532	mouse IgG1
CD41a	PE	BD Biosciences	555467	3162697	mouse IgG1
CD42a	FITC	BD Biosciences	558818	5323668	mouse IgG1
CD42a	PE	BD Biosciences	558819	5204818	mouse IgG1
CD42a	BV421	BD Biosciences	565444	7145668	mouse IgG1
CD42b	BB700	BD Biosciences	742219	7212833	mouse IgG1
CD42b	PE	BD Biosciences	555473	6012555	mouse IgG1
CD49b	Alexa Fluor 647	BD Biosciences	564314	5295626	mouse IgG2a
CD49b	PE	BD Biosciences	555669	715950	mouse IgG2a
CXCR4	APC	BD Biosciences	555976	7151568	mouse IgG2b
Ki-67	PE	BD Biosciences	51-36525X	77187	mouse IgG1
NANOG	PE	BD Biosciences	560483	8087675	mouse IgG1
Oct3/4	PerCP-Cy5.5	BD Biosciences	560794	8100700	mouse IgG1
TRA-1-81	Alexa Fluor 647	BD Biosciences	560793	7283709	mouse IgGM

2.7. Nutrient and metabolite analysis

To assess the metabolic activity of cell during culture, 0.6 mL of culture volume was removed from cultures. Samples were taken from each culture vessel (static tissue plastic or spinner flask), and centrifuged at 500g for 5 mins. Medium supernatant was collected and stored initially at -18°C and then transferred to -80°C for long term storage. Multiple medium samples were thawed, randomised and analysed for glucose, lactate, ammonia and lactate dehydrogenase (LDH) using the Cedex Bio-HT metabolite analyser (Roche, Germany).

2.7.1. Cedex Bio-HT

The Cedex is an automated, high-throughput analyser. Its technology is based on enzymatic assays with photometric and potentiometric analysis, principles of which have remained unchanged since mid-20th century [106]. The system requires minimal manipulation by users which contributes to the low CV data presented in its brochures.

2.7.1.1. Glucose

In the presence of hexokinase (HK) Glucose was phosphorylated by ATP to glucose-6-phosphate (G-6-P). Glucose-6-phosphate was oxidized by NADH in presence of glucose-6-phosphat dehydrogenase (G-6-PDH). The rate of NADPH formation was measured UV-photometrically and was directly proportional to the glucose concentration.

$$Glucose + ATP \xrightarrow{HK} G-6-P + ADP$$

$$G-6-P + NADP^{+} \xrightarrow{G-6-PDH} Gluconate-6-P + NADPH + H^{+}$$

2.7.1.2. Lactate

In the presence of lactate oxidase (LOD), lactate was oxidised to pyruvate and peroxide. In the presence of peroxidase (POD), a coloured dye was produced and the photometrically measured absorbance was proportional to the L-lactate concentration.

$$L - lactate \ + O_2 \xrightarrow{LOD} Pyruvate + H_2\ O_2$$

$$H_2O_2 + H\ donor + 4 - AAP \xrightarrow{POD} H_2O + Chromogen$$

2.7.1.3. Ammonium

In the presence of glutamate dehydrogenase (GLDH), ammonium reacted with 2-oxoglutarate and NADPH in a reductive amination to form L-glutamate and NADP+. The decrease of NADPH was directly proportional to the ammonia concentration and is measured photometrically at 340 nm.

$$NH_4{}^+ + 2 - oxoglutarate + NADPH \xrightarrow{GLDH} L - glutamate + NADP^+ + H_2O$$

2.7.1.4. LDH

The oxidation of L-lactate to pyruvate by NAD was catalysed by Lactate dehydrogenase (LDH). The initial rate of NADH formation was directly proportional to the catalytic LDH activity and was measured photometrically.

$$L - lactate + \ NAD^+ \xrightarrow{LDH} Pyruvate + NADH + H^+$$

2.8. Statistical Analysis

2.8.1. Design of experiments

All DOE experiments conducted were 2-level factorial designs analysed with backwards stepwise elimination analysis (α = 0.1 for removal), which retained hierarchy using statistical

analysis software Minitab version 17. The factors used, their respective levels and whether a mid-point was included is specified in relevant sections.

2.8.2. ANOVA

To determine statistically significant differences, one-way ANOVA was applied using statistical analysis software, Minitab ($\alpha = 0.05$).

2.9. Mechanistic modelling framework

The modelling paradigm used to construct mechanistic models is described in detail by Stacey et al. [100]. Briefly, a parsimonious framework was built using a set of ordinary differential equation modelling building blocks that represented common cell culture dynamics and was designed to avoid mathematical pathologies. Cell culture behaviour hypothesises were developed using a set of di-graphs and the framework fitted model parameters using a least square method based on user-inputted model parameter estimates and ranges.

3. QTPP and assay development for a Quality by Design approach to in vitro platelet manufacture

3.1. Introduction

This section focuses on the identification of CQAs that indicate the potential for FOPMKs to produce the required number of functional platelets. Where inducible pluripotent stem cells are being expanded, pluripotency markers will be used to indicate potential for differentiation, with the absence of any MK markers on pluripotent cells, the assumption was made that pluripotency acts as a surrogate measure for forward programming potential.

In this chapter a Quality Target Product Profile (QTPP) for an in vitro derived platelet product was developed followed by the identification of CQAs which relate to the cell phenotype. In addition to cell quality, yield is also identified as an important attribute to measure. Therefore, assays to measure cell quality (using phenotype) and yield (using cell counting methods) are developed and compared.

To draw meaningful conclusions from experiments and adequately test the presence of CQAs, assays which test cell culture attributes must be reliable and repeatable and the limitations of these tests must be understood. In this work, most assays are used to measure either cell number or phenotype. The technology tool used most for phenotype analysis is flow cytometry because it allows for single cell analysis and is a well-established technology for process development, manufacture and clinical applications. For cell counting automated methods are preferred since they are rapid, eliminate or greatly reduce operator variation and are therefore more easily validated and repeatable. The automated cell counting platform the Nucleocount-3000 and flow cytometry were used in this work.

3.1.1. Chapter objectives

- Develop a QTPP for an in vitro manufactured platelet product and the CQAs required to deliver the QTPP

- Rationally determine a set of in process CQAs that megakaryocyte progenitors require to enable delivery of the QTPP
- Develop robust and repeatable assays to determine cell culture characteristics that are relevant for measuring cell properties relevant to manufacturing outputs including:
    - Phenotype analysis
    - Cell counting (using NC-3000 and flow cytometry)

3.2. Development of a Quality Target Product Profile

Using a template provided by the Cell and Gene Therapy Catapult, Table 3-1 shows the developed QTPP. The attributes for the product was based on platelet transfusion units sourced from volunteer donors as this is the current clinical standard.

Table 3-1: Quality Target Product Profile (QTPP) of in vitro derived platelets for intravenous transfusion developed using guidelines produced by the Cell and Gene Therapy Catapult.

Overview		
Primary Indication and Usage	Platelet transfusions are the most immediate way to treat thrombocytopenia (low platelet blood counts). Platelets produced from "forward programmed" megakaryocytes would be used as an alternative platelet transfusion unit where suitable donor platelets are not available.	
Description of proposed drug substance	Functional, in vitro derived platelets suitable for transfusion.	
Description of proposed drug product	A single platelet transfusion which has 3-5× 10^{11} platelets in 180-300 mL (average 210 mL) [107].	
Mechanism of Action	Prophylactic platelet transfusions are administered to thrombocytopenia patients who have a platelet blood count of less than 1 × 10^{11} platelets/L in order to prevent bleeding [108]. The platelet infusion increases the concentrations of blood platelet to normal levels which prevents bleeding.	
Description of raw and starting materials	Dox inducible FOP-iPSCs, DMEM/F12, Celgenix SCGM , FGF2, Activin-A, BMP-4, SCF, TPO, Doxycycline hyclate	
QTPP element	**Target**	**Justification**
Dosage form	Cell suspension [108].	Donor derived platelet transfusion units are delivered in a cell suspension [108].
Formulation (excipients)	Cell suspension in 210 mL of saline-adenine-glucose-mannitol [109].	Current NHS platelet transfusion units are stored in blood plasma derived from donors when donating blood platelets. However, using donated plasma does not overcome the supply chain and biosafety advantages of in vitro derived platelets for transfusion. Saline-adenine-glucose-mannitol solutions have been used as storage substitutes for platelet units [109] and is regularly used for red blood cell storage for up to 45 days[110].
Strength / Potency	3-6 ×10^{11} platelets per transfusion unit [107], [108].	This is the average range for current clinical platelet transfusion units [107], [108].
Container Closure System	Storage requires n-butyryl tri-n-hexyl citrate (BTHC) or tri- (ethylhexyl)-	This is the clinical standard for donor derived platelet transfusion units [111].

	trimellitate–plasticized polyvinyl chloride (PVC) bags [111].	
Route of Administration	Intravenous infusion.	Intravenous infusion is the current clinical practice for donor derived platelet transfusion units.
Storage and Stability (including in-use stability)	Transfusion units are stored at 20°C - 24°C under constant horizontal agitation and can be stored for up to 7 days in the UK [111].	This is the established clinical protocol for platelet transfusion unit storage [111].
Release strategy	Stage 1 (immediately after platelet production and irradiation, prior to storage): Sterility testing Marker expression [112]: CD42a+, CD42b+, Calcein-AM positive, CD62P- Stage 2 (after 7 days storage): Swirl testing	CD42a, CD42b are markers are essential for von Willebrand factor adhesion and therefore platelet functionality [113]. CD62P is a measure of platelet activation, which should not be present in platelet transfusion units. [114]. Swirl tests are routinely conducted is hospitals by holding a platelet transfusion unit to the light, and gently agitating to observe the scattering of light. If transfusion units do not scatter the light, this indicates they should be discarded as platelets have become activated [115].

3.2.1. Identification of Critical Quality Attributes

Currently there is no straightforward in vitro test to prove conclusively the functionality of platelets or conclusive predictors that megakaryocytes will produce functional platelets. To prove the derivation of function platelets from FOPMKs, Moreau et al used mouse models to should that FOP-derived platelets incorporated in mouse thrombus [116] which would be impracticable for a batch release criteria, and is not useful as an assay to test the platelet production potential of a MK. Lack of CQAs is a known issue for cell-based therapies and are

caused by lack of biological understanding and consequently lack of available process analytical technologies due to the complexity of such products [117], [118].

Functional platelets must be able to respond to Von Willebrand factor in order to initiate adhesion to damaged blood vessels and subsequent aggregation and therefore initiate clotting [119]. The glycoprotein IIb/IIIa (CD41a/CD61) and Ib-IX-V (CD42a/CD42b) respond to Von Willerand factor and therefore its presence on MKs (for subsequent platelet production) would be required to produce function platelets [113]. Therefore, in the absence of a direct assay to measure the potential of a MK to produce functional platelets expression levels of CD41a, CD42a, CD42b were measured.

If it were possible to use early differentiation markers as accurate predictor of end stage outputs this could lead to cost savings through early identification in a manufacturing setting of conditions that were going to lead to outputs that were outside the acceptable end product specification. Monitoring changes in early stage differentiation markers (CD34 and CD235a in this case) could enable the application of resources to keep a process “on-track” to achieve the right end stage yields and purities modifying the process control variables to bring the process back on the right trajectory. Therefore, the expression of CD34 and CD235a will be tracked throughout differentiation to monitor the progression of forward programming as an early indicator of cell phenotype trajectory.

When culturing iPSCs prior to induction the above markers will not be expressed. The technology is newly developed and so specific markers to measure the programming potential of Dox-inducible iPSCs. In the absence of these specific markers, pluripotency markers Oct3/4 [56], NANOG [56], TRA-1-81 [64] were measured. A flow cytometry assay is developed in Section 3.3.2.5 to measure these markers.

3.3. Flow cytometry

Flow cytometry passes through a linear fluid stream and uses light to measure the properties of those cells. These properties can be either intrinsic such as size and granularity, or extrinsic, measured by targeting markers with fluorescent particles. Each particle that passes through a light stream is recorded as an "event" and has the values of the different output signals recorded. In this way, it is possible to gain high throughput single cell analysis. This section details the development of flow cytometry assays to measure the CQAs identified in Section 3.2.1.

3.3.1. Optic capture settings

There are many established methods for selecting flow cytometry optic capture settings. This section shows the outcomes of using different methods to create optical settings for flow cytometry assays to ascertain FOPMK characteristics and describes advantages and disadvantages for each method.

3.3.1.1. Setting PMT voltages using the first log decade

For MEP (Panel 1) and MK maturity (Panel 2), shown in Table 3-2 and Table 3-3 respectively, PMT voltages were selected by setting the negative populations in the first log decade. This method was used historically to determine correct PMT voltages, ensuring that the autofluorescence of the target particles was low compared to the signal (as shown in Figure 3-1 and Figure 3-2). This is adequate in some situations (for example when using fluorochromes with shorter wavelength emissions and when there is large separation between positive and negative populations as this overcomes the large variance caused by signal noise) but is not universally optimal [120]. Single stained cells were used to calculate

the compensation matrix for the MEP and MK maturity panels, shown in Table 3-3 and Table 3-4.

Table 3-2: Megakaryocyte Erythroid Progenitor (MEP) – Panel 1

Marker/ attribute	**Fluorochrome**	**Relative Brightness**	**Laser**	**PMT - filter**	**Voltage**
Viability	DAPI	Data not available	Violet	B – 450/40	165
CD235a	PE	Bright	Blue	D – 575/26	270
CD42a	FITC	Moderate	Blue	E – 530/30	280
CD41a	APC	Bright	Red	C – 660/20	425
Cell size	FFS	N/A	Blue	N/A	125
Granularity	SSC	N/A	Blue	F	350

Table 3-3: MK maturity panel – Panel 2

Marker/ attribute	**Fluorochrome**	**Relative Brightness**	**Laser**	**PMT - filter**	**PMT voltage**
Viability	DAPI	Data not available	Violet	B – 450/40	170
CD42b	PE	Bright	Blue	D – 575/26	290
CD42a	FITC	Moderate	Blue	E – 530/30	280
CXCR4	APC	Bright	Red	C – 660/20	370
Cell size	FFS	N/A	Blue	N/A	125
Granularity	SSC	N/A	Blue	F	350

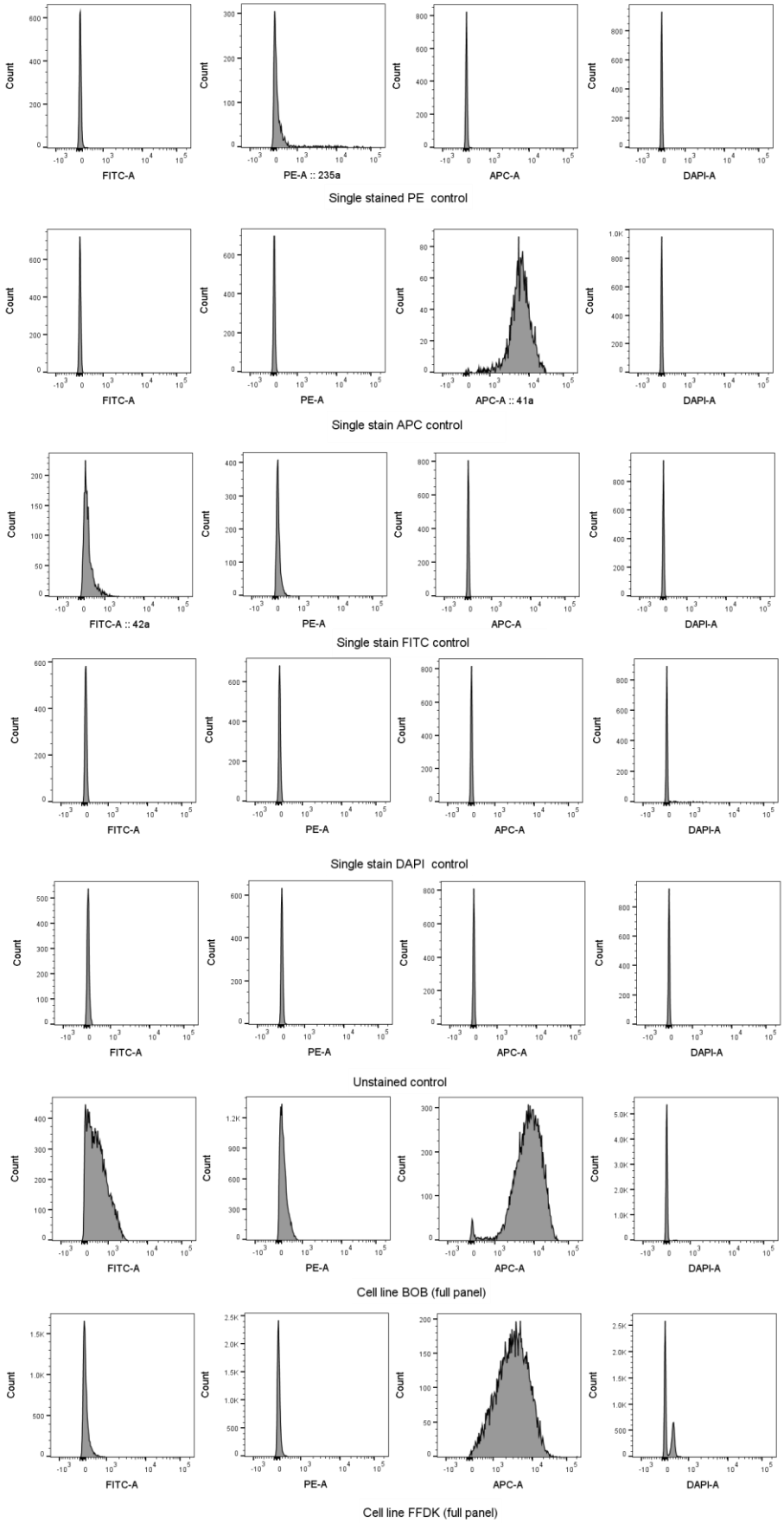

Figure 3-1: Single stained single FOPMK cells in the MEP panel used to calculate compensation matrix and 2 cell lines stained with all antibodies as an example.

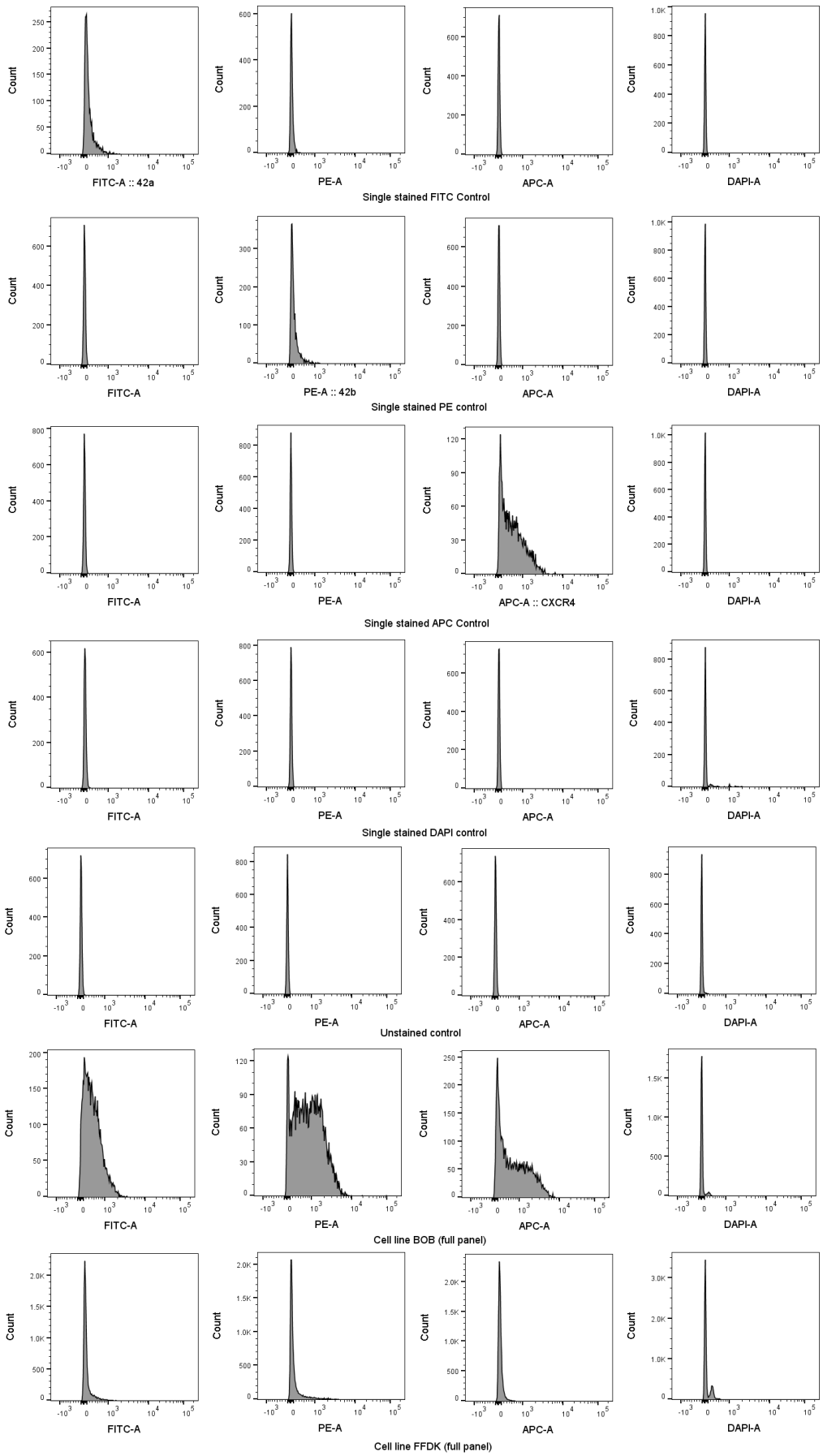

Figure 3-2: Single stained single FOPMK cells in the MK maturity panel used to calculate compensation matrix and 2 cell lines stained with all antibodies as an example.

Table 3-4: Compensation matrix for MEP panel (Panel 1)

Fluorochrome	-% fluorochrome	Compensation
APC	FITC	1.92
DAPI	FITC	0.72
FITC	PE	0.00
APC	PE	1.11
DAPI	PE	0.00
FITC	APC	0.00
PE	APC	0.00
DAPI	APC	0.00
FITC	DAPI	4.59
PE	DAPI	7.93
APC	DAPI	1.30

Table 3-5: Compensation matrix for MK maturity panel (Panel 2)

Fluorochrome	-% fluorochrome	Compensation
APC	FITC	3.04
DAPI	FITC	0.86
FITC	PE	6.98
APC	PE	4.14
DAPI	PE	0.00
FITC	APC	0.00
PE	APC	0.00
DAPI	APC	0.00
FITC	DAPI	8.43
PE	DAPI	5.84
APC	DAPI	4.91

Figure 3-1 and Figure 3-2 show the single colour stains, an unstained control and examples of full colour analysis. In the single colour stains the lack of overlap into the other channels from the fluorochromes shows qualitatively that only a small amount of compensation will be required to remove overlap. This is reflected in the compensation matrices shown in Table 3-4 and Table 3-5.

The two example samples show that the difference between cultures that highly express measured attributes and those that express low levels of these attributes can be distinguished using this method. However, the major disadvantage of setting PMT voltages qualitatively by

placing the unstained sample in the first log decade is that low expression cannot be easily distinguished from negative expression, leading to poor resolution sensitivity.

3.3.1.2. Using calibration beads to define PMT voltages

Resolution sensitivity, the ability to resolve dimly fluorescent populations at the lower end of the scales, can be defined using the percentage robust coefficient of variation (%rCV) of dim particles, where the %rCV is more statistically resilient to data outliers than %CV [121]. Using flow cytometry calibration beads, such as SPHERO™ 8 peak beads, the optimum voltage for adequate separation for dimly fluorescent particles can be determined. This is achieved by [120]:

- increasing the PMT voltage at set intervals
- selecting the second peak
- calculating the %rCV
- Plotting the PMT voltage against %rCV
- finding the point of inflection

The results are a combination of instrument settings and fluorochrome properties, and accurate results depend on appropriate storage of SPHERO™ bead reagent. Figure 3-3 shows examples of 2 fluorochromes, APC and APC Cy-7. It shows the increased resolution with increasing PMT voltage and highlights the difference between fluorochromes since the second APC peak can be resolved at 500 V whereas the APC-Cy7 second peak is still not resolved at 700 V.

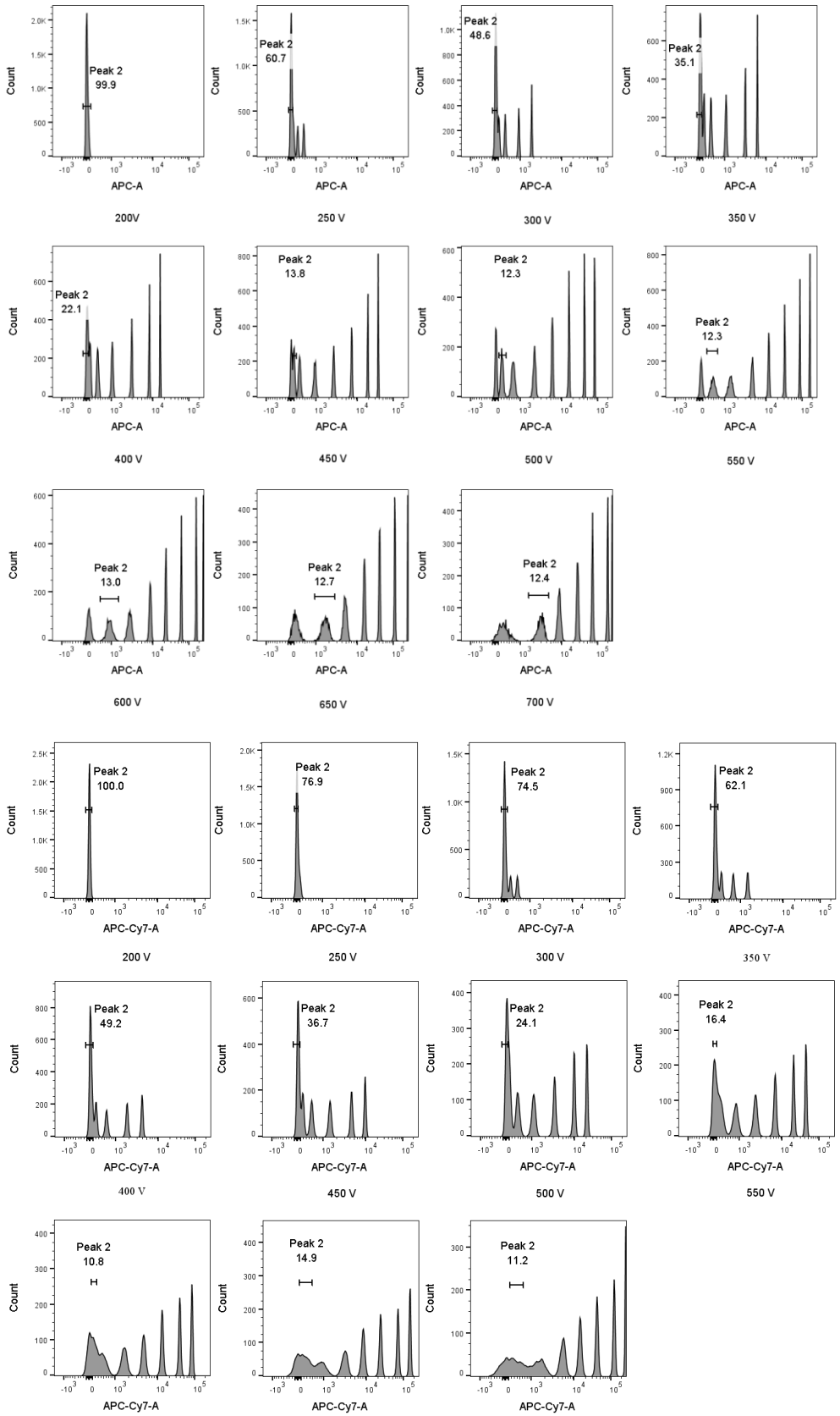

Figure 3-3: Histograms show increasing voltage for APC and APC-Cy7 fluorochromes on SPHERO™ beads allows resolution of fluorescent populations of varying brightness. Using a PMT voltage of 700 it was still not possible to separate the second peak form the dim peak in the APC-Cy7 channel.

A comparison of all fluorochrome channels is shown in Figure 3-4. Each fluorochrome should theoretically have a smooth asymptotic curve similar to Pacific Orange and Blue. However, PE-Cy7 demonstrated a linear relationship between %rCV and PMT voltage up to 600 V then a step change. At this point the second peak could be resolved for the first time, causing a sharp reduction in %rCV.

(A)

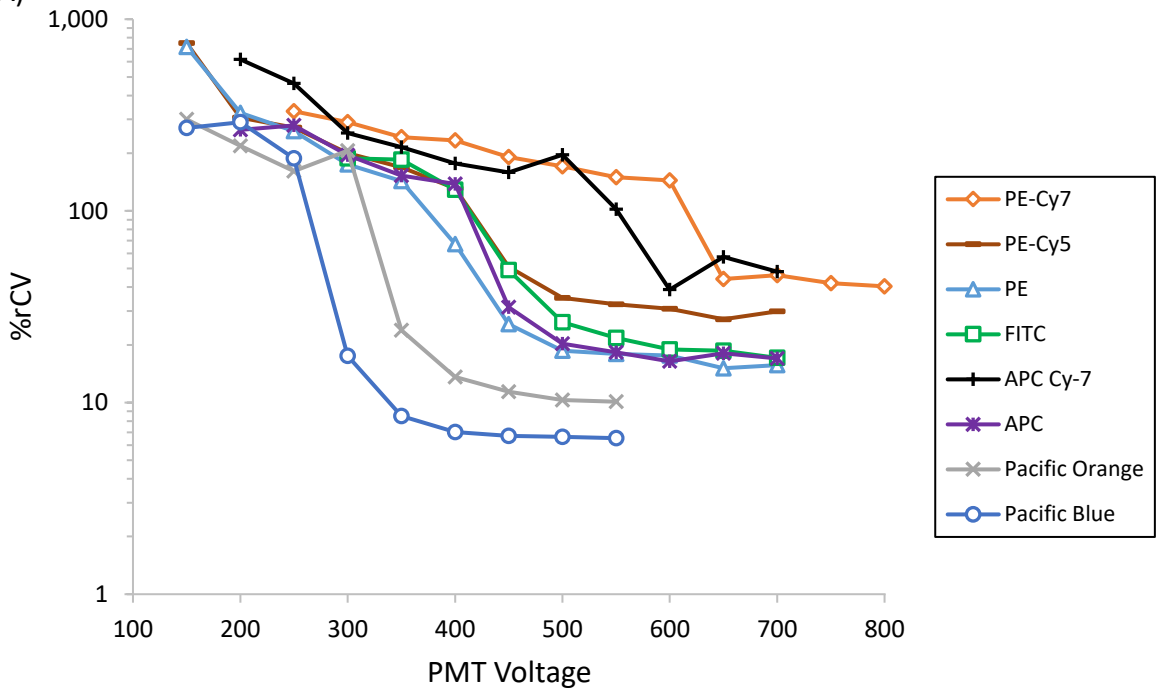

(B)

Laser	PMT	Fluorochrome	Optimal PMT voltage range	Relative brightness
Blue	A	PE-Cy7	650-700	Bright
	B	PE-Cy5	500-550	Very bright
	D	PE	500-550	Bright
	E	FITC	500-550	Moderate
Red	A	APC Cy-7	Not determined	Dim
	C	APC	500-550	Bright
Violet	A	Pacific Orange	400-450	Dim
	B	Pacific Blue	350-400	Moderate

Figure 3-4: Characterising the sensitivity of each channel of the BD FACS CANTO. Plotting %rCV and PMT voltage was used to determine the optimal voltage for resolving dimly fluorescent populations by identifying the inflection point. (A) shows %rCV of the second peak of SPHERO™ beads and PMT voltage (B) Inflection points identified to determine optimal range with fluorochrome attributes.

A disadvantage of this method is that not every fluorochrome is associated with a calibration bead, particularly newer, more stable and mostly brighter fluorochromes. For example, both BD Horizon™ BB515 and FITC are excited by the blue laser and detected using PMT E, yet BB515 is considered a “very bright” fluorochrome and FITC only “moderately” bright, therefore BB515 would require a lower voltage to detect lowly expressed markers (equivalent to a dim particle since fewer fluorochromes are attached).

3.3.1.3. Using BD Cytometer Setup and Tracking (CS&T) software to define PMT voltages

BD Cytometer Setup and Tracking (CS&T) software tracks the cytometer performance by tracking the voltages required to separate dimly fluorescent particles on specialist CS&T beads, and sets the value based on 10 times above the electronic noise of the instrument. These suggested values can also be used as a starting point and can then be reduced to bring the fluorescence within the linear cytometer range. However, the issue of fluorochrome specificity does not apply because the dim bead population is set to the auto fluorescence of lymphocytes when being excited by that laser channel. However, this could result in bright fluorochromes fluorescing higher than the readable scale. This highlights the importance of choosing the correct brightness of fluorochrome to match the expression of the target antigen.

For long term FOPMK cultures CD235a was mostly negative and CD42b expression correlates with CD42a, so a third panel was developed which to include CD41a, CD42a and CXCR4. To obtain the PMT voltages, the CS&T suggested PMT voltages were used as a starting value. Voltages were then decreased to bring the values within the linear detection range. The resulting single stained samples and fluorochromes are shown in Figure 3-5.

The need for compensation is shown in Figure 3-5 (A) when considering the single stained FITC control spill over into the PE channel as the median PE fluorescence shifts from 394 to

2480 despite there being no PE present in the sample. In contrast, there is little spill over from other fluorochromes into the APC channel. The median value for the single stained APC population is 1890 compared to 120 when using FITC and PE stained controls. The calculated compensation values are shown in Table 3-7.

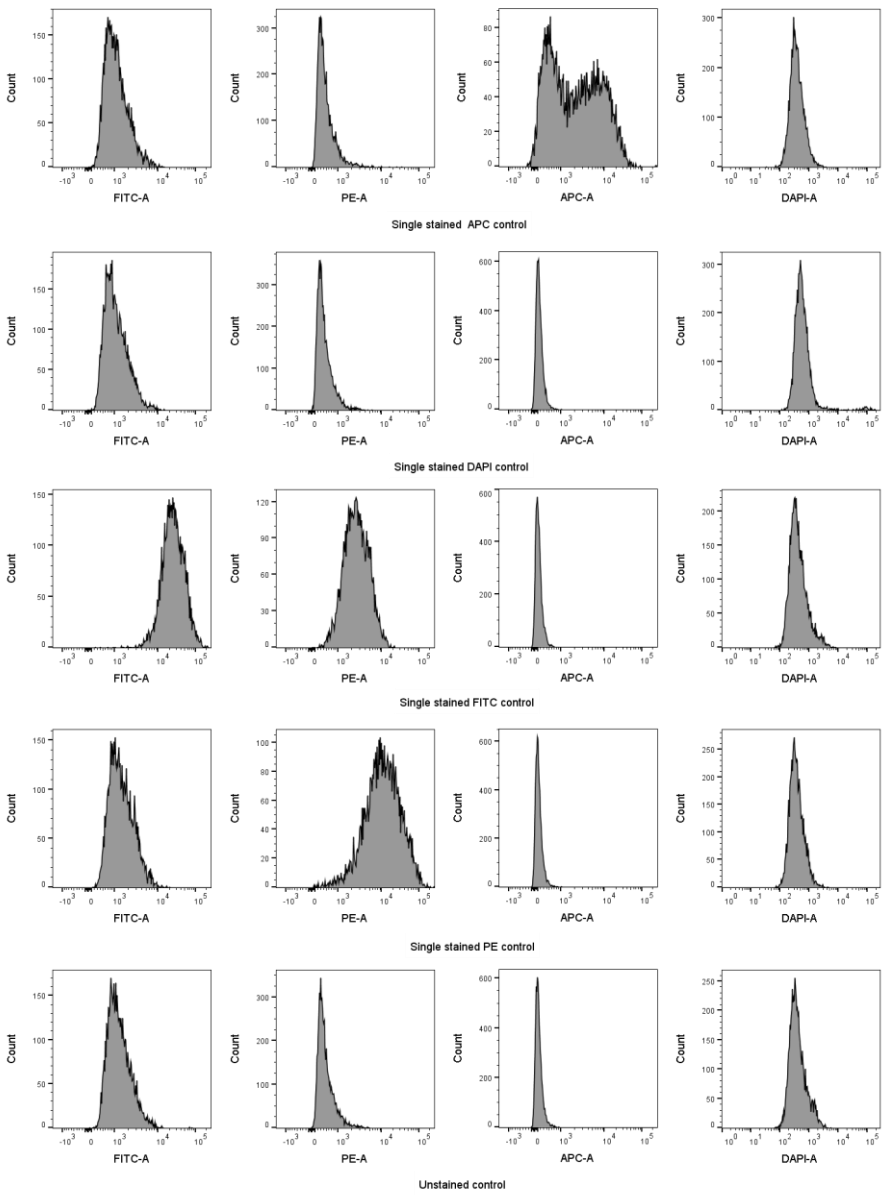

Figure 3-5: Panel 3 utalised condensed panel to capture MK phenotypic changes in a single assay. PMT voltages were set by using the CS&T values. Here single cells stained with a single fluorochromes were used for compensation.

Table 3-6: Fluorochrome details and PMT settings for Panel 3.

Marker / attribute	Fluorochrome / light scatter	Relative Brightness	Laser	PMT - filter	PMT voltage
Viability	DAPI	Data not available	Violet	A – 525/50	350
CD42a	PE	Bright	Blue	D – 575/26	470
CD41a	FITC	Moderate	Blue	E – 530/30	533
CXCR4	APC	Bright	Red	C – 660/20	580
Cell size	FFS	N/A	Blue	N/A	180
Granularity	SSC	N/A	Blue	F	400

Table 3-7: Compensation values for Panel 3 - a condensed version of MEP and MK maturity panels

Fluorochrome	-% fluorochrome	Compensation value
PE	FITC	9.00
APC	FITC	0.00
DAPI	FITC	0.01
FITC	PE	1.94
APC	PE	0.06
DAPI	PE	0.04
FITC	APC	0.00
PE	APC	0.00
DAPI	APC	0.00
FITC	DAPI	2.39
PE	DAPI	1.10
APC	DAPI	0.35

Both the Panel 1 and Panel 3 measure CD41a and CD42a expression with different fluorochromes and used different methods of PMT voltage settings. Figure 3-6 compares the results from these assays using cells from equivalent culture. The FS/SS voltages for the MEP assay were set lower than required to ensure population shifts in size and granularity were adequately captured, however this lead to a loss of resolution around the target population, hence the voltages were increased which resulted in better resolution of the target population (Figure 3-6 A).

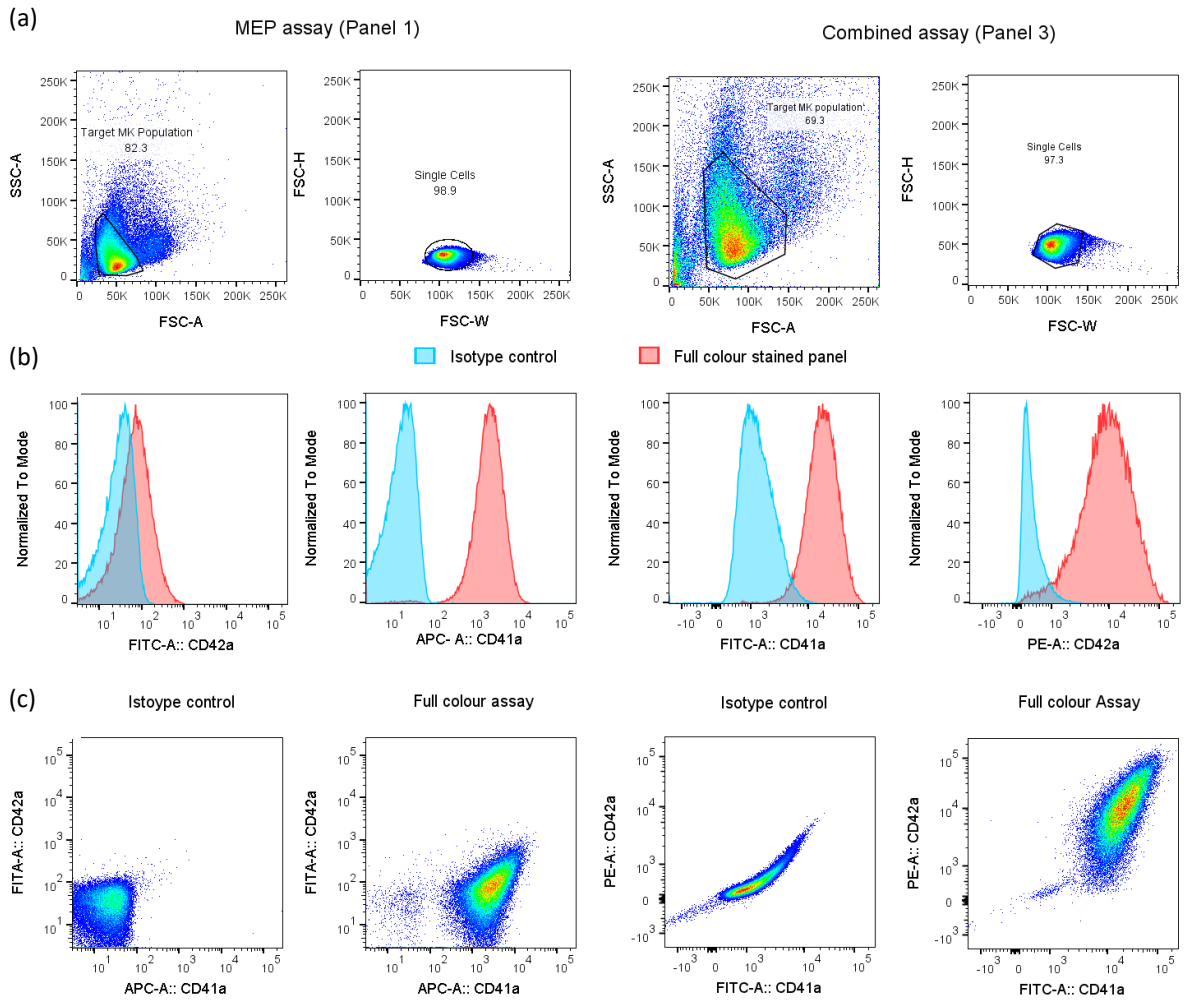

Figure 3-6: Comparison between of the same cell sample analysed with MEP assay (panel 1) and combined assay (panel 3) shows the effect of fluorochrome selection and PMT voltage setting on perceived marker expression. (a) FS/SS voltages determined the separation between populations of a different size/granularity. (b) Use of a PE-CD42a provided better separation than a FITC-CD42a conjugated antibody, and APC-CD41a provides better separation than FITC-CD41a conjugates. (c) Isotype control for MEP panel showed adequate compensation and low background signal whereas the isotype control for the combined panel shows that there was either a positive correlation between non-specific binding for CD42a/41a, compensation issues, or changing autofluorescence.

CD42a expression changes throughout 1st generation, non-Dox inducible FOPMK culture and typically decreases past 90 days post FOPMK derivation from iPSCs when monitored using a FITC-conjugated antibody [5]. The culture represented in Figure 3-6 is late stage (day 127) and the expression level shown in Figure 3-6 b on FITC (which is a moderately bright fluorochrome) is in line with this, particularly considering the low PMT voltage used – the SI between positive and negative population was 1.46 calculated using equation (1-1). When using PE, which is a

relatively bright fluorochrome when excited with the blue laser, a higher separation is achieved with a corresponding SI of 29.3.

The isotype control shown in Figure 3-6 for the MEP panel shows low background fluorescence and no obvious trends between the APC and FITC overlap, whereas there was a trend with increasing FITC and PE background signal. This could be attributed to inadequate compensation, for example, by misplacing the control gates used to calculate compensation. It could also have been a true increase in non-specific binding between the two antibody conjugates, particularly as they are co-expressed. Where possible, co-expressed antibodies should be measured using fluorochromes which are excited by different lasers to reduce compensation issues. The increased FITC and PE background signal may have been caused by changing autofluorescence of the populations also. This could have been tested by running an unstained sample alongside the full stained panel and the isotype control.

3.3.1.4. Use of Application settings and target boxes for setting PMT voltages

The methods described thus far for setting PMT voltage settings do not account for variation of the cytometer over time. BD CS&T software checks performance to ensure reproducible performance day to day and variations in performance can be adjusted by creating and applying "Application Settings".

CS&T software measures five critical performance metrics [122]:

- Robust standard deviation of electronic noise (rSD_{EN})
- Relative detection efficiency for each detector (Qr)
- Relative optical background (Br)
- Robust coefficient of variation for each setup bead (rCV)
- Linearity maximum channel (the maximum acceptable signal level for good linearity)

The CS&T tracking uses dim (equivalent autofluorescence to lymphocytes), medium and bright standard beads to characterise the flow cytometer. Part of this characterisation is defining PMT voltages that place the dim beads outside 10 times the rSD_{EN}, therefore ensuring these measurements are not dominated by electronic noise or optical background. To set Application Settings, the rSD_{EN} for each channel were obtained from a current CS&T report and the values multiplied by 2.5 to obtain target values (Table 3-8). The 2x rSD_{EN} values became the target rSD for the unstained FOPMK target cell population. Target rSD_{EN} were not specific to which fluorochrome is being used in each PMT channel – it depended upon the properties of that PMT channel.

With Application Settings, it is critical to ensure that the stained population remains within the linear range of the detector, so the measured fluorescence must not exceed the maximum value for that channel. Since the measured fluorescence is both dependent on the fluorochrome brightness and the marker expression level it was possible that the Application Settings would have required adjustment once marker expression through different stages of forward programming was acquired.

Table 3-8: Exported CS&T report values from 14th March 2017, including 2.5 times the rSDEN and resulting PMT voltage settings

Laser	Detector	Example Parameter	Linearity Min Channel	Linearity Max Channel	Electronic Noise Robust SD	2.5 rSD_{EN}	Set PMT voltage
Blue	FSC	FSC	N/A	N/A	N/A		
Blue	F	SSC	N/A	N/A	N/A		
Blue	E	FITC	86	240270	25.8	64.5	400
Blue	D	PE	79	241702	22.8	57	400
Blue	B	PerCP	93	239414	23.8	59.5	400
Blue	A	PE-Cy7	230	237197	25.9	64.75	550
Red	C	APC	46	238645	20.5	51.25	550
Red	A	APC-Cy7	47	239047	20.5	51.25	550
Violet	B	DAPI	76	245676	20.4	51	300
Violet	A	BV510	59	244454	18.8	47	300

Robust standard deviations in each channel were recorded by increasing the PMT voltage by 50 V increments, as shown in Figure 3-7. The voltage required to distinguish the signal from the electronic noise (the inflection point) was negatively correlated with the channel capture wavelength; i.e. the DAPI channel which captures wavelengths close to 440 nm required the lowest PMT to achieve the target rSD, whereas the APC-Cy7 channel which captures wavelengths close to 680 nm required the highest PMT voltage to achieve the target rSD. This indicates that higher noise levels correlate with lower frequency channels so bright fluorochromes should be used or these channels should be used when a dump channel is required.

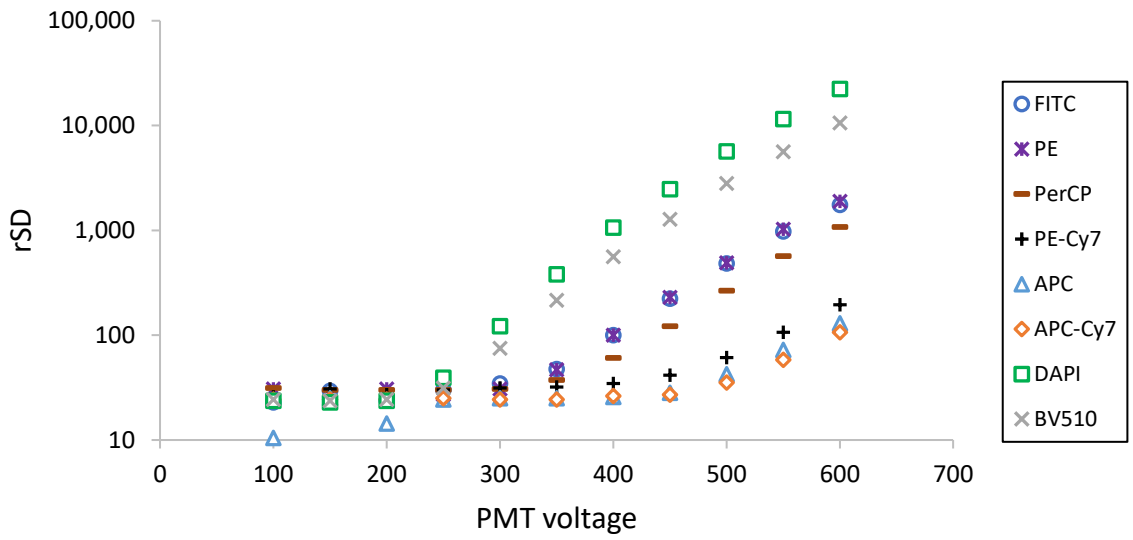

Figure 3-7: Establishment of Application Settings for an 8 colour FOPMK assay; rSD did not increase until a PMT voltage threshold was achieved, PMT voltages which placed unstained populations in the required 2.5 time rSD_{EN} are above this inflection point. Legend shows example parameters for the flow cytometer used for this work.

3.3.2. Comparison of methods for setting optical capture settings

Section 2.6.4 describes four methods for setting PMT voltages which are summarised in Table 3-9. Since each method produces a slightly different recommended PMT voltage setting understanding the advantages and disadvantages of each method is key to determining which method to use.

Setting the PMT voltage based on minimising autofluorescence produces low background signal, but does not always lead to good separation since the positive target populations may be within the background noise and not easily distinguishable (see MEP panel in Figure 3-6b), and although was widely employed for use with analogue cytometers this method is now largely outdated [120]. Using SPHERO™ beads to set PMT voltages minimises the effect of background noise but relies on the specific fluorochrome conjugates, and is therefore limited in its uses. Furthermore, this method produced comparatively high recommended PMT voltages (Table 3-9) which could lead to positively stained populations falling outside of the cytometer linear detection range.

CS&T reports recommend settings based on placing the rSD of the fluorescence values for dim 10 times the rSD_{EN} [122], which ensures minimal interaction with background noise and is not fluorochrome specific, but is PMT specific. However, the CS&T recommended settings fluctuate day to day (albeit by small amounts). This is dependent on cytometer maintenance, laser fluctuations, and environmental conditions, such as room temperature and humidity. The use of Application Settings can mitigate fluctuations and can ensure comparability between cytometers. However, performance is monitored only daily, and can shift throughout the day. How intra-daily performance fluctuations affect data is unknown, but can be monitored by using SPHERO™ or CS&T beads intermittently throughout the day.

Table 3-9: Comparison of the different methods for setting PMT voltages / optical capture settings

Laser	Detector	Example Parameter	PMT voltage (V)			
			Method 1	Method 2	Method 3	Method 4
Blue	E	FITC	280	500	535	400
Blue	D	PE	270	500	509	400
Blue	B	PerCP		500	552	400
Blue	A	PE-Cy7		650	622	550
Red	C	APC	425	500	584	550
Red	A	APC-Cy7		Not determined	518	550
Violet	B	DAPI	165	400	404	300
Violet	A	BV510		350	478	300

Using the established best practises described throughout Section 2.6, fluorochromes were selected for phenotypic markers with the aim to comprehensively characterise 1st generation, non-Dox inducible FOPMKs in a single panel (Panel 4) shown in Table 3-10. Application Settings were used to determine PMT voltages and beads were used to calculate the compensation in each channel (shown in Table 3-11). Antibody titrations were performed to find the optimum concentration where there were amenable cell populations as shown in Figure 3-8. Antibody titrations could not be performed where they were markers which were not expressed (CXCR4 and CD49b).

Table 3-10: Comprehensive panel for 1st generation FOPMK charectorisation or latter stage of 2nd generation Dox-inducible FOPMKs (Panel 4)

Marker/attribute	Fluorochrome	Relative Brightness	Laser	PMT - filter	PMT voltages
FSC					220
SSC					385
CD42a	BV421	Very Bright	Violet	B – 450/40	400
CD41a	BV510	Moderate	Violet	A – 525/50	449
CD49b	PE	Bright	Blue	D – 575/26	549
CD42b	BB700	Very Bright	Blue	B – 695/40	500
CD235a	PE-Cy 7	Bright	Blue	A – 780/60	544
CXCR4	APC	Bright	Red	C – 660/20	305
Viability	Fixable viability dye 780	No data available	Red	A – 780/60	357

Table 3-11: Calculated compensation values used for Panel 4 (outlined in Table 3-10).

Fluorochrome	-% Fluorochrome	Spectral Overlap
BB700	PE	21.00
PE-Cy7	PE	5.45
APC	PE	0.03
FVS780	PE	0.01
BV421	PE	0.01
BV510	PE	0.01
PE	BB700	1.07
PE-Cy7	BB700	59.78
APC	BB700	4.63
FVS780	BB700	21.11
BV421	BB700	0.00
BV510	BB700	0.11
PE	PE-Cy7	0.31
BB700	PE-Cy7	2.00
APC	PE-Cy7	0.01
FVS780	PE-Cy7	9.38
BV421	PE-Cy7	0.04
BV510	PE-Cy7	0.04
PE	APC	0.00
BB700	APC	0.67
PE-Cy7	APC	0.25
FVS780	APC	13.17
BV421	APC	0.01
BV510	APC	0.01
PE	FVS780	1.41
BB700	FVS780	1.85
PE-Cy7	FVS780	4.33
APC	FVS780	0.76
BV421	FVS780	3.04
BV510	FVS780	3.15
PE	BV421	0.00
BB700	BV421	0.00
PE-Cy7	BV421	0.00
APC	BV421	0.00
FVS780	BV421	0.00
BV510	BV421	9.22
PE	BV510	0.09
BB700	BV510	0.06
PE-Cy7	BV510	0.02
APC	BV510	0.02
FVS780	BV510	0.00

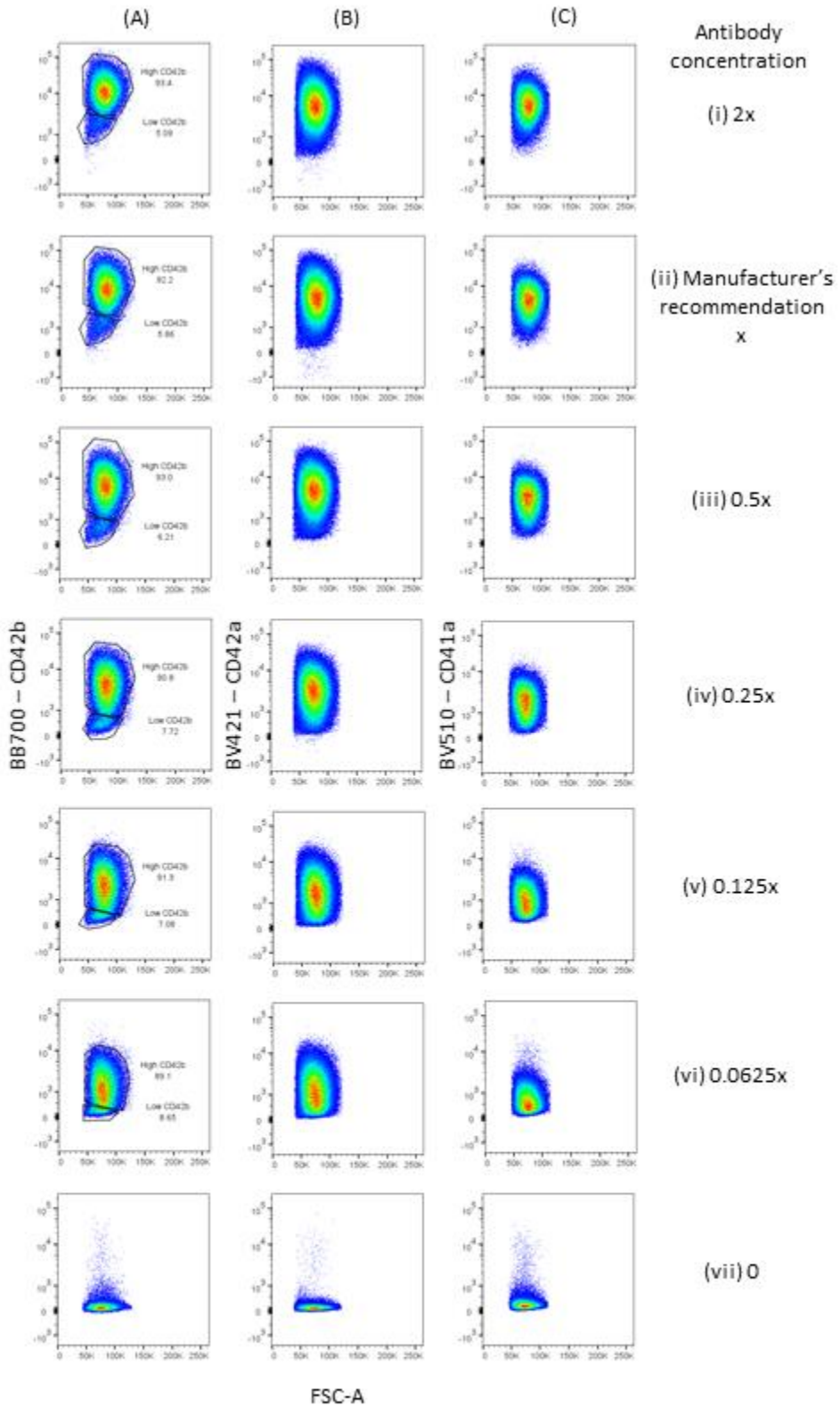

Figure 3-8: Antibody titrations of (A) CD42b, (B) CD42a and (C) CD41a. Antibody concentrations were varied with respect to the manufacturer's recommended concentration (i – vii). There were two populations of CD42b expression, one positive and one negative, making it possible to calculate the optimal SI. However, there was only one population of CD42a and CD41a therefore the recommended concentrations were used.

Antibody titrations were performed for CD41a, CD42a and CD42b as shown in Figure 3-8. The only marker that had two populations of expression was CD42b, so this was the only marker for which the SI could be calculated. Therefore, for CD41a and CD42a the recommended concentration was used for assays. Across all markers increased antibody concentrations increased fluorescence but higher concentrations can lead to non-specific binding, which is reflected in the Sensitivity Index (SI) calculation as shown in Figure 3-9. SI is a measure of measurement sensitivity as it indicates the separation between positive and negative populations. It is calculated using Equation 3-1 [123]:

$$SI = \frac{median\ signal - median\ background}{(84th\ percentile\ median\ background - median\ background)/0.995} \quad 3\text{-}1$$

The maximum SI achieved was at an antibody concentration of 5 µg.mL^{-1}, and at higher and lower concentrations similar suboptimal population separations were achieved.

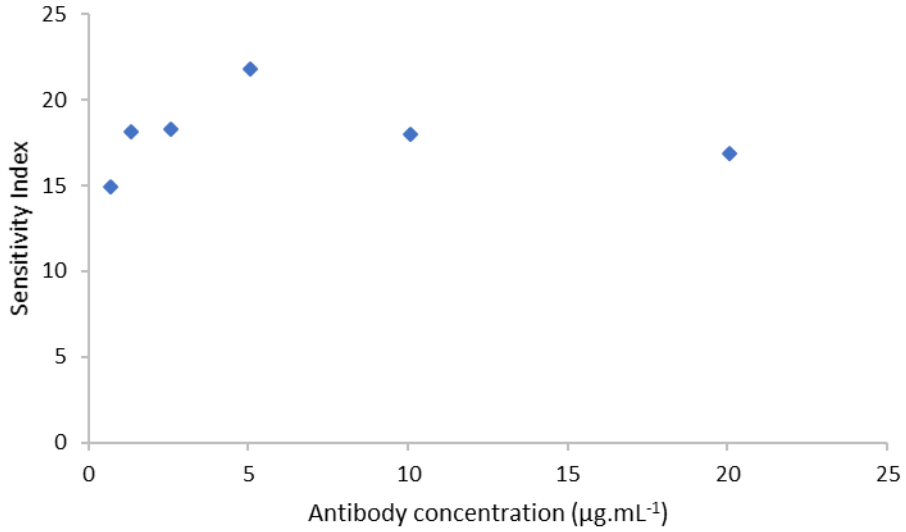

Figure 3-9: SI index for CD42b concentrations showed the optimal concentration was 5 µg.mL^{-1} which was half of the manufacture's recommended concentration.

3.3.2.1. Adjustment of panels to overcome issues associated with green fluorescent protein

The use of green fluorescent protein (GFP) in flow cytometry panels can be challenging. GFP is associated with the expression of the forward programming factors and therefore its expression level is set. It cannot be titrated, as with antibody concentration for example. The following section describes assays developed either to incorporate its expression in the panel (thus gaining more information about the expression level of the forward programming genetic cassette) or exclude it to reduce issues of spectral overlap with other fluorochromes.

3.3.2.2. Reduced colour panel for 2nd generation forward programming

The use of Panel 4 for early stage (prior to day 10) 2nd generation Dox-inducible FOPMKs was challenging since there was large overlap into the violet A channel, which was being used to measure BV510 – CD41a, by GFP as shown in Figure 3-10. Therefore, a smaller panel was developed which did not use the FITC and BV510 channels and utilised only essential FOPMK markers CD41a, CD42a and CD235a as an early indicator of lineage trajectory. The PMT voltages were set using Application Settings as detailed in Section 3.3.1.4. The compensation matrix (Table 3-13) was calculated using a combination of single stained capture beads for phenotypic markers, cells stained with viability stain and unstained cells.

Table 3-12: Fluorochrome details and optical settings for Panel 5 which was reduced colours, without GFP or BV510 channels, for characterising inducible FOPMKs

Marker/attribute	Fluorochrome	Relative Brightness	Laser	PMT - filter	PMT voltages
FSC					180
SSC					380
CD235a	PE-Cy7	Bright	Blue	A – 780/60	549
CD41a	APC	Bright	Red	C – 660/20	525
Viability	FVS780	No data available	Red	A – 780/60	544
CD42a	BV421	Very bright	Violet	B – 450/40	306

Table 3-13: Compensation matrix for Panel 5 described in Table 3-12.

Fluorochrome	-% Fluorochrome	Spectral Overlap
APC	PE-Cy7	0.02
APC-Cy7	PE-Cy7	9.64
BV421	PE-Cy7	0.04
PE-Cy7	APC	0.19
APC-Cy7	APC	9.79
BV421	APC	0.01
PE-Cy7	APC-Cy7	3.48
APC	APC-Cy7	0.62
BV421	APC-Cy7	0.26
PE-Cy7	BV421	0.00
APC	BV421	0.00
APC-Cy7	BV421	0.00

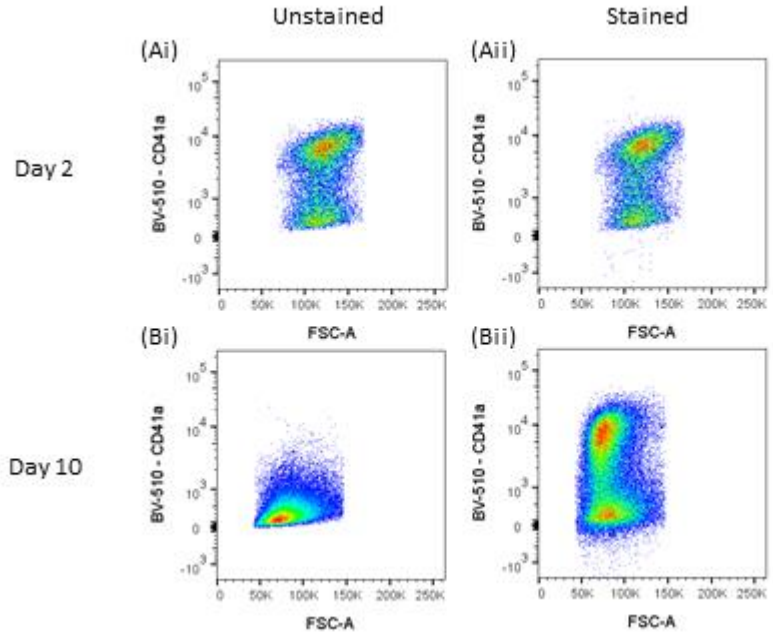

Figure 3-10: Spectral overlap from GFP into the 525/50 channel skewed BV510-CD41a measurement. skewed-CD41a which was used to capture-CD41a which was used to capture BV510 florescence. fluorescence. (A) Unstained samples showed GFP expression in the BV510 channel. (B) Stained samples show CD41a expression on the background GFP expression. (i) Cells at Day 2 post Dox addition expressed high levels of GFP and low levels of CD41a expression, which can only be discerned from comparing stained and unstained cells. (ii) There is still a high level of background GFP fluoorescence at Day 10. Flow cytometry assays for Dox-inducible FOPMKs should not include the BV510 fluorochrome.

3.3.2.3. Early stage forward programming comprehensive panel

To increase the information gained from FOPMK cultures, including GFP expression, which was linked to the expression of the forward programming genetic cassette, and CD34 as a marker of early haematopoietic lineage trajectory, the panel was expanded to include more fluorochromes. As in Panel 5, Application Settings (Section 3.3.1.4) were used to set PMT voltages, but due to the high fluorescence of GFP the voltages of the FITC channel was decreased. In order to keep the compensation values low (and minimise noise introduced through high compensation values), the voltages of other channels were decreased also. This reduced sensitivity but allowed GFP and more parameters to be measured than in Panel 5. This highlights the importance of the balance between numbers of parameters measured, noise, sensitivity and resource required for implementation is for process development assays.

Table 3-14: Fluorochrome details and optical settings for characterising early stage inducible FOPMK panel (Panel 6).

Marker/attribute	Fluorochrome	Relative Brightness	Laser	PMT - filter	PMT voltages
FSC					180
SSC					380
GFP		No data available	Blue	E – 530/30	390
CD41a	PE	Bright	Blue	D – 575/26	304
CD34	PerCP-Vio700	Moderate	Blue	B – 695/40	320
CD235a	PE-Cy7	Bright	Blue	A – 780/60	346
TRA-1-81	APC	Bright	Red	C – 660/20	346
Viability	FVS780	No data available	Red	A – 780/60	318
CD42a	BV421	Very bright	Violet	B – 450/40	240

Table 3-15: Compensation settings for Panel 6 (assay described in Table 3-14).

Fluorochrome channel	-% Fluorochrome	Spectral Overlap
PE	GFP	2.48
PerCP-Vio700	GFP	0.17
PE-Cy7	GFP	0.02
APC	GFP	0.00
FVS780	GFP	0.00
BV421	GFP	0.05
GFP	PE	5.33
PerCP-Vio700	PE	13.29
PE-Cy7	PE	1.47
APC	PE	0.00
FVS780	PE	0.07
BV421	PE	0.06
GFP	PerCP-Vio700	0.04
PE	PerCP-Vio700	0.04
PE-Cy7	PerCP-Vio700	31.11
APC	PerCP-Vio700	1.01
FVS780	PerCP-Vio700	3.06
BV421	PerCP-Vio700	0.00
GFP	PE-Cy7	0.91
PE	PE-Cy7	1.30
PerCP-Vio700	PE-Cy7	5.20
APC	PE-Cy7	0.00
FVS780	PE-Cy7	4.37
BV421	PE-Cy7	0.00
GFP	APC	0.05
PE	APC	0.05
PerCP-Vio700	APC	1.20
PE-Cy7	APC	0.14
FVS780	APC	6.67
BV421	APC	0.07
GFP	FVS780	0.00
PE	FVS780	0.00
PerCP-Vio700	FVS780	0.00
PE-Cy7	FVS780	11.50
APC	FVS780	0.86
BV421	FVS780	0.00
GFP	BV421	0.03
PE	BV421	0.00
PerCP-Vio700	BV421	0.01
PE-Cy7	BV421	0.00
APC	BV421	0.00

3.3.2.4. Snapshot panel for early stage FOP

To increase resolution for early- (<day 10) to mid-stage (<day 18) Dox-inducible FOPMKs, a reduced colour panel was devised that included GFP, CD34, CD235a and CD41a – Panel 7. Optical capture settings are shown in Table 3-16 and were again developed using Application Settings. Compared to Panel 6 (Table 3-14), the PMT voltages were higher due to the lower number of parameters, which increases sensitivity. Compensation was calculated using single stain beads, cells stained with DAPI and unstained cells.

Table 3-16: Fluorochrome details and optical capture settings for reduced panel to characterise early stage FOPMKs produced by the inducible iBOBc line (Panel 7).

Marker/attribute	Fluorochrome	Relative Brightness	Laser	PMT - filter	PMT voltages
FSC					230
SSC					420
GFP		No data available	Blue	E – 530/30	502
CD235a	PE	Bright	Blue	D – 575/26	379
CD34	PerCP-Vio700	Moderate	Blue	B – 695/40	418
CD41a	APC	Bright	Red	C – 660/20	530
Viability	DAPI	No data available	Violet	B – 450/40	280

Table 3-17: Compensation matrix for Panel 7 shown in Table 3-16.

Fluorochrome	-% Fluorochrome	Spectral Overlap
PerCP	FITC	0.00
APC	FITC	0.00
DAPI	FITC	4.61
FITC	PE	6.30
PerCP	PE	19.08
APC	PE	0.25
DAPI	PE	0.01
FITC	PerCP	0.03
PE	PerCP	0.00
APC	PerCP	3.36
BV421	PerCP	0.00
FITC	APC	0.00
PE	APC	0.00
PerCP	APC	0.30
DAPI	APC	0.00
FITC	DAPI	10.04
PE	DAPI	1.38
PerCP	DAPI	0.74
APC	DAPI	0.2820135

3.3.2.5. iPSC Panel development

Pluripotency markers NANOG, Oct 3/4 and TRA-1-81 were selected to measure the pluripotency of iPSC cells during expansion prior to forward programming via induction of the FOP genetic cassette with Dox. Optical capture settings were defined using Application Settings and are shown in Table 3-18. The compensation matrix was calculated using stained capture beads, viability stained cells and unstained cells and is shown in Table 3-9.

Table 3-18: Fluorochrome details and optical capture settings for iPSC phenotype monitoring (Panel 8).

Marker/attribute	**Fluorochrome**	**Relative Brightness**	**Laser**	**PMT - filter**	**PMT voltages**
FSC					140
SSC					350
NANOG	PE	Bright	Blue	D – 575/26	430
Oct 3/4	PerCP	Dim	Blue	B – 695/40	470
TRA-1-81	APC	Bright	Red	C – 660/20	502
Viability	FVS780	No data available	Red	A – 780/60	450

Table 3-19: Compensation settings for Panel 8 (assay described in Table 3-18).

Fluorochrome	-% Fluorochrome	Spectral Overlap
PerCP	PE	17.60
APC	PE	0.02
APC-Cy7	PE	0.00
PE	PerCP	0.00
APC	PerCP	1.79
FVS780	PerCP	2.09
PE	APC	0.01
PerCP	APC	1.32
FVS780	APC	5.31
PE	FVS780	0.00
PerCP	FVS780	0.32
APC	FVS780	1.02

3.3.2.6. iPSC antibody titrations

Antibody titrations were performed with all pluripotency markers to determine the optimal concentration of antibody stain to use. Figure 3-11 (A) shows each antibody stained with decreasing concentration relative to the manufacturer's recommended concentration, with both positive and negative populations. The positive and negative populations are gated and were used to calculate the SI using Equation 3-1 and are shown for each stain concentration in Figure 3-11 (A). Both APC-TRA-1-81 and PE-NANOG had the highest separation at the manufcturers concentration, whereas there was better separation between populations for PerCP-Oct3/4 at 25% of the manufacturer's recommended concentration. The difference in SI highlights the importance of antibody titrations for high sensitivity assays.

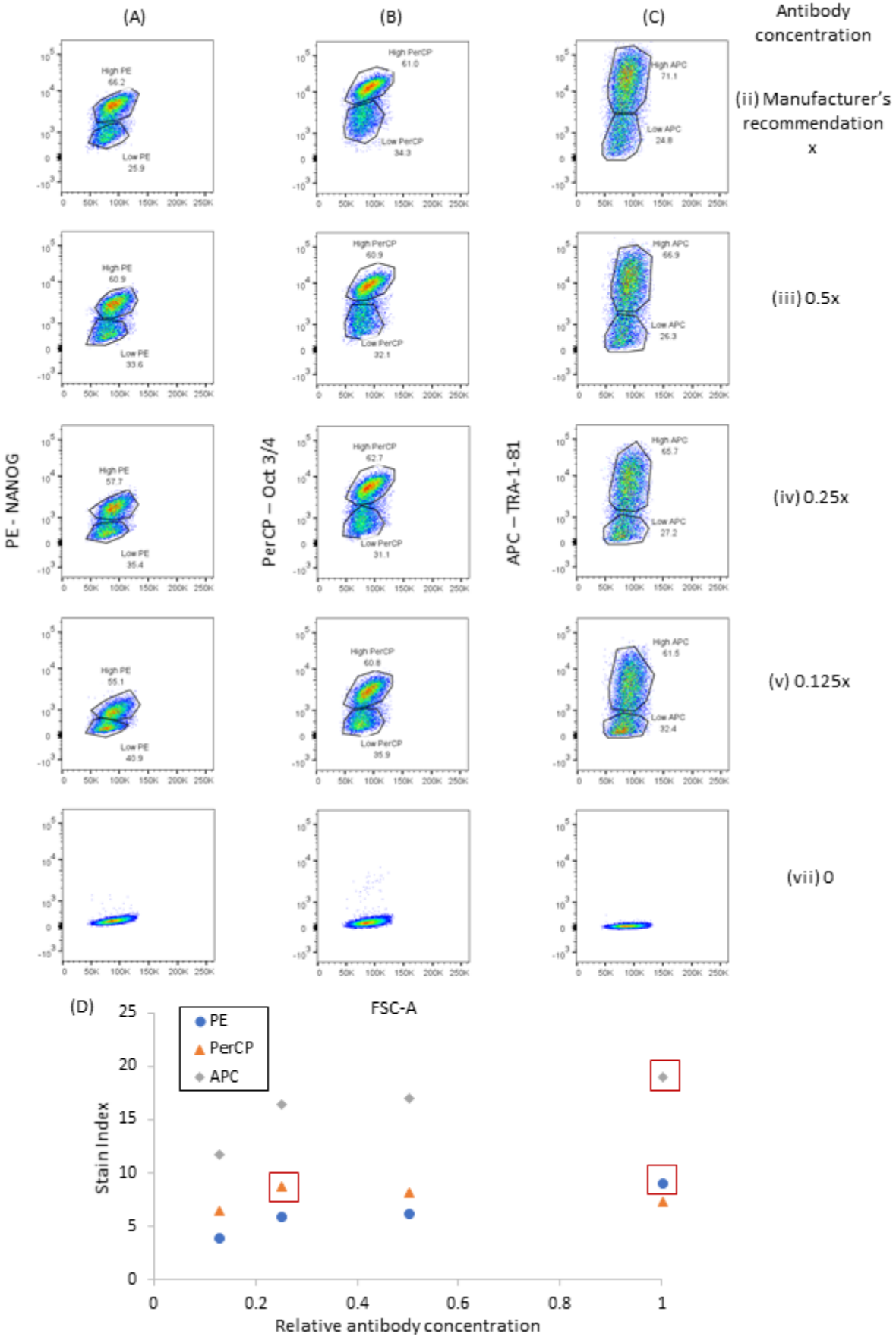
(A)
(B)
(C)
Antibody concentration
(ii) Manufacturer's recommendation x
(iii) 0.5x
(iv) 0.25x
(v) 0.125x
(vii) 0
PE - NANOG
PerCP – Oct 3/4
APC – TRA-1-81
High PE 66.2
Low PE 25.9
High PerCP 61.0
Low PerCP 34.3
High APC 71.1
Low APC 24.8
High PE 60.9
Low PE 33.6
High PerCP 60.9
Low PerCP 32.1
High APC 66.9
Low APC 26.3
High PE 57.7
Low PE 35.4
High PerCP 62.7
Low PerCP 31.1
High APC 65.7
Low APC 27.2
High PE 55.1
Low PE 40.9
High PerCP 60.8
Low PerCP 35.9
High APC 61.5
Low APC 32.4
(D)
FSC-A
PE
PerCP
APC
Stain Index
Relative antibody concentration
0
5
10
15
20
25
0
0.2
0.4
0.6
0.8
1

Figure 3-11: Antibody titrations for antibodies used in iPSC Panel 7; (A) NANOG, (B) OCT 3/4 and (C) TRA-1-81. Antibody concentrations were varied with respect to the manufacturer's recommended concentration (i – vii) There were two populations of relatively high and low expression for each marker, which allowed stain indices to be calculated. (D) Stain index for each of the antibodies and the optimal for each stain highlighted with a red box.

3.4. Cell counting characteristics of the culture system

Ideal cell counting methods are accurate, consistent, precise and able to distinguish between cell populations that are viable and non-viable. An in-depth review of methods for measuring viability is beyond the scope of this chapter, but can was reviewed by Cook and Mitchell [124]. It is assumed here that a cell with an integral membrane is viable and is capable of replication. Membrane integrity is commonly determined by cells' ability to exclude nuclear stains such as DAPI. Other characteristics associated with programmed cell death, apoptosis, are decreased cell size and increased granularity [125]. Figure 3-12 shows three different FOPMK cultures in varying cell states relating to cell size, granularity of proportion of cells permeable to DAPI. In (a), minimal cells are present in the high SS / (high granularity) population and greater than 97% of the population negative for DAPI. The same culture expanded for five days without a medium exchange is shown in (b). Here the cells are shown shifted to lower FS, showing a decreased size, and became more granular.

The proportion of DAPI positive cells concurrently increased to more than 50% which shows that the cells are likely to be undergoing apoptosis [126]. In both (a) and (b) the singlet cell population had a larger proportion of DAPI+ cells compared to the doublet population, and in (a) 31% of cells are doublets, whereas in (b) only 16% of cells are doublets, which indicates a relationship between cell viability and the number of doublets in culture.

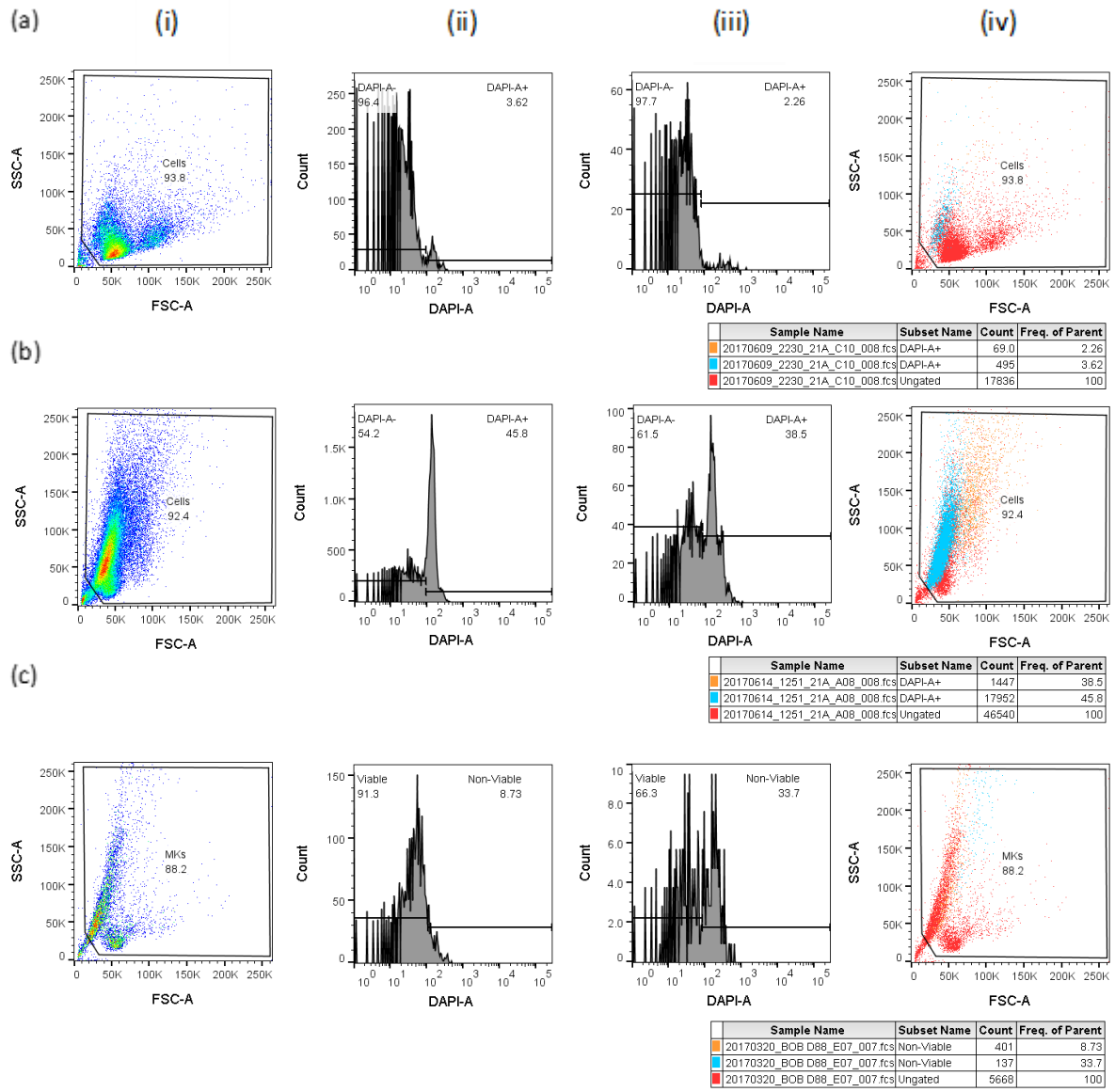

Figure 3-12: Flow cytometry data showing FOPMK cultures in different states. (a) Cells in this state were larger in size and less granular with a lower proportion of DAPI permeable cells. (b) Culture with a higher proportion of DAPI permeable cells were smaller size and more granular. (c) Culture contains a high proportion of cells with high granularity but this population did not appear DAPI positive. (i) FS/SS profiles show cell size and granularity. (ii-iii) Histogram plots of fluorescence of single cells (ii) and doublets (ii) in the DAPI channel. (iv) DAPI positive single and doublet populations overlaid on FF/SS profiles.

In Figure 3-13 (c) there were a high proportion of cells with a high SS profile which were not DAPI positive. This culture had been expanded over a three week period, compared to five days between (a) and (b) and it is assumed that these cells were non-viable and the A-T regions within the DNA - which DAPI binds to [127] – had decayed preventing binding. If this is the case non-viable cells could be split into two categories, cells that have recently become non-viable and cells that are long term non-viable. Cromatin breakdown of long term non-viable cells has been noted in the literature previously [128]. Further data would need to be gathered in order to test this hypothesis. Since this effect could impact measurement of cell populations it could impact efforts to quantify cell culture dynamics. As a conclusion is was therefore decided that DAPI exclusion assays appeared to be useful in short term cultures for identifying viable cells, but must be treated with caution over longer time periods. To ensure that DAPI exclusion is an appropriate measure for viability, the high SS population was monitored regularly to ensure it continued to stain positive for DAPI (data not shown).

Often it is practical and beneficial to work with different pieces of cell counting equipment. Reasons for this include comparability, measurement speed and convenience. Confirming assay results through different methods gives increased confidence and comparability of results obtained through different counting methods is critical if a piece of equipment or process moves to a different manufacturing facility. Furthermore, a different number of measurements may need to be taken and the speed at which they are required might change, favouring one piece of equipment over another, or a piece of equipment might become unavailable on a certain day.

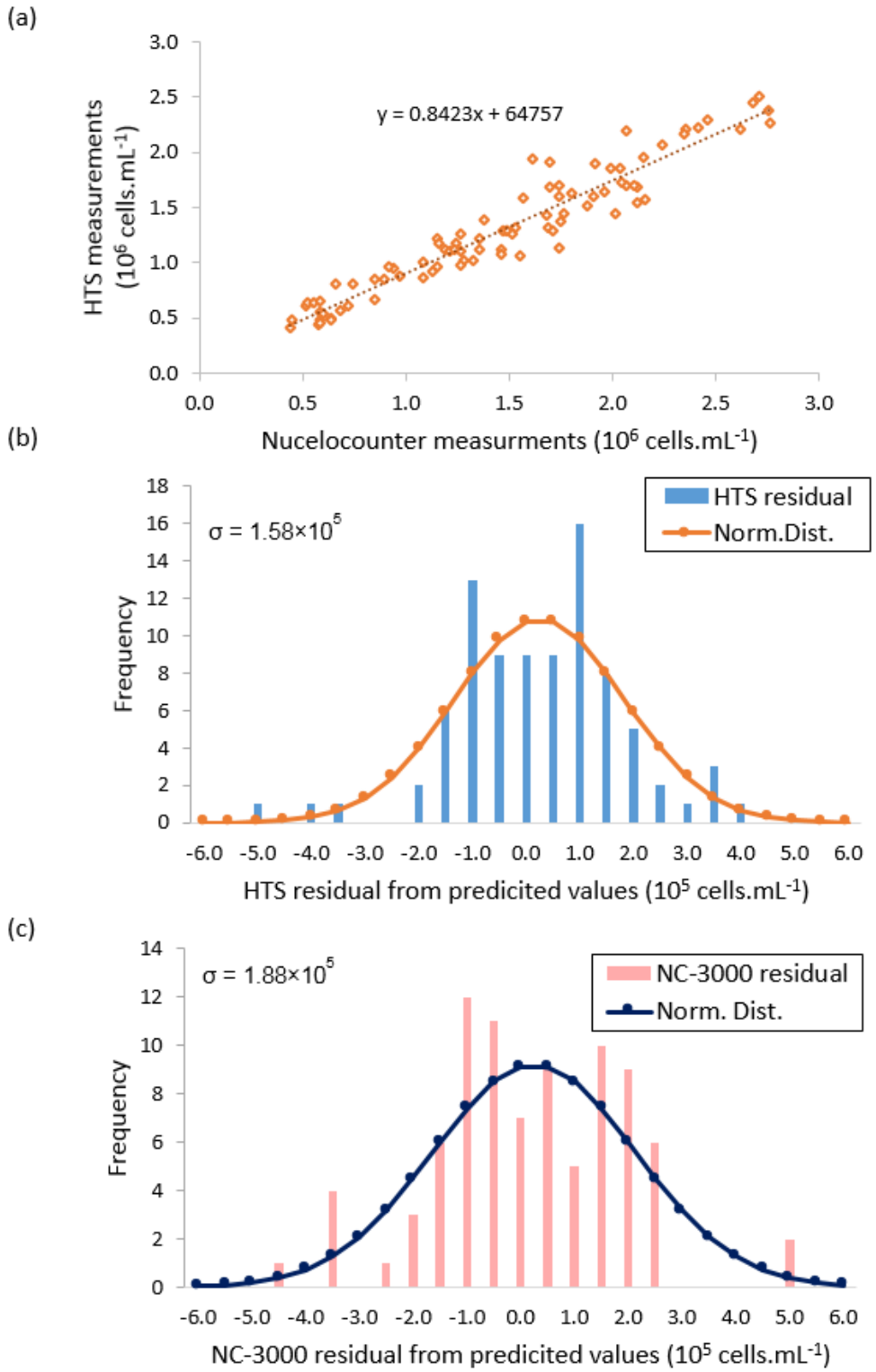

Figure 3-13: Cell counts obtained from the Nucleocounter NC300, and HTS module through the HTS (a) shows a linear relationship between HTS and NC-3000 measurements, however the measurements are offset. (b) & (c) show the distribution of cell counts taken from the mean on HTS and NC-3000 respectively and are normally distributed.

Figure 3-13 shows a comparison between cell counts taken using the HTS system on the BD FACS Canto II flow cytometer and the NC-3000. The linearity of the measurements shows that they are within the range of 5×10^5 and 2.5×10^6 cells.mL^{-1} and the distribution of the data in (b) and (c) show both counting methods have no discernible difference from the normal distribution.

The proportional offset between the HTS system and the NC-3000 could be caused by physical attributes of the equipment, for example, the Nucleocounter A2 slides might have been made smaller than the stated volume used in the assay, causing an apparent increase in the concentration of cells, or a slight off-set in the HTS aspiration lines could mean that 16% of the sample is lost each time. Since there is an absence of an absolute "truth" reference material for cell counting assays it is very difficult to determine the absolute true measurement for cell counts [129].

Although the standard deviation of the measurements from the HTS system was 1.58×10^5 compared to 1.88×10^5 cells.mL^{-1} using the Nucleocounter measurement system, the variation as a proportion to the mean was more similar; 12% and 13% respectively. This indicates that the inherent variation for each piece of equipment was very similar or that cell sampling effects were the dominant cause of the deviations from the predicted value from each measurement system.

It is not desirable to wash the cells used for cell counting protocols after staining with DAPI, as this extra processing step could add multiple failure modes. For example, through washing cells may be lost adding variability or offset and extra processing time is added which may detrimental to cell samples. Therefore, it was important to assess whether the proportion of DAPI stained cells changed with increased incubation times.

Figure 3-14 shows the counts of sample from the same cell culture with increasing time exposure to DAPI over 50 minutes. There was no increase in the proportion of non-viable cells across the time period, showing that FOPMKs suspended in a concentration of 1 µg.mL^{-1} DAPI were stable with regards to DAPI permeability over this time period. However, (b) shows an increase in the total cell concentration with time. This could have been an artefact of sampling, for example cells settling to the bottom of the flask after being mixed. Since each count took approximately 2 minutes to run, the samples were run in the same order as the time sequence,

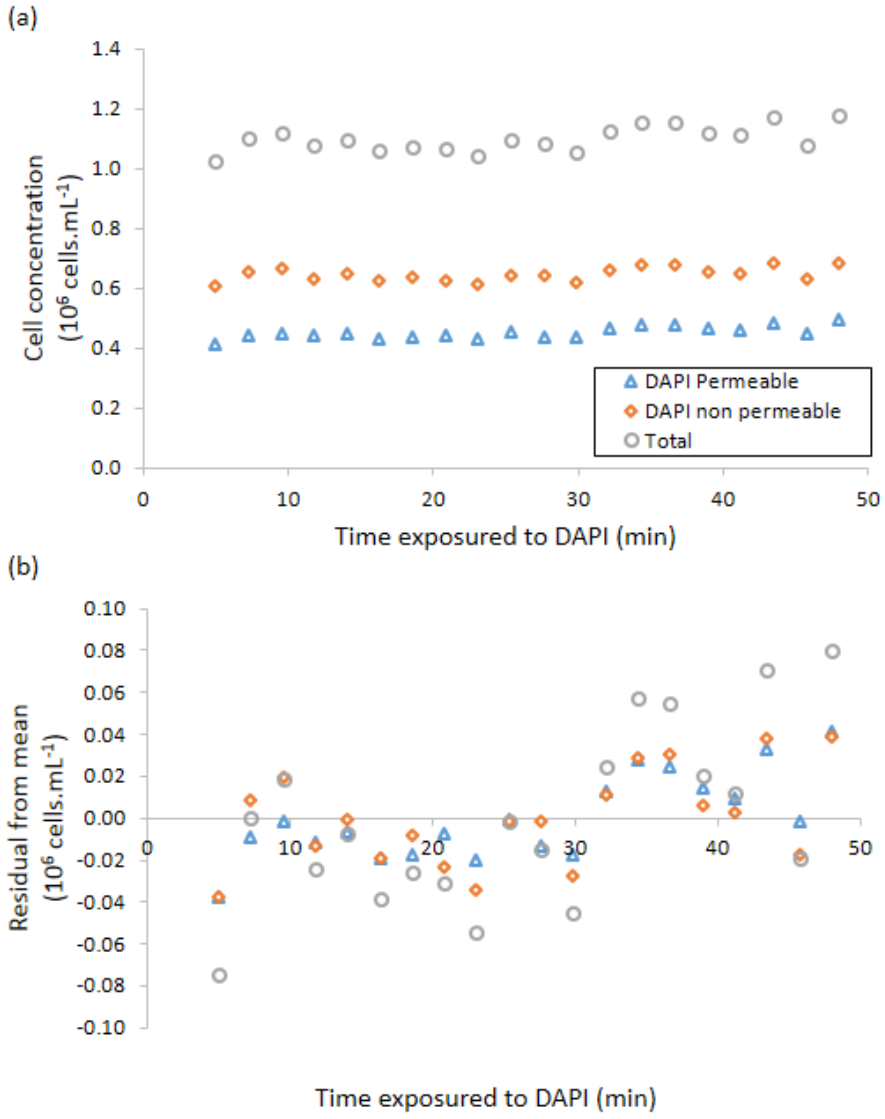

Figure 3-14: Over a 50 minute period at room temperature permeability to DAPI did not increase. (a) Cell counts of viable (DAPI non permeable), non-viable (DAPI permeable) and total (sum of viable and non-viable) cells from equivalent culture show consistent cell numbers over a 50 minute period. (b) Residuals from the mean value show an increase in total cell number with time

which governed the exposure time. Therefore, the increase in cell number with time could have been a result of the run order on the HTS system. Experiments which required large sample numbers to be run in succession had their run order tracked in future experiments to ensure the run order was not introducing bias in to the counts.

To test whether sample mixing was the cause of the decreased counts across time, FOPMKs were mixed well and placed into a 50 mL centrifuge tubes. Cells were sampled from the top of the tube carefully whilst avoiding disturbing or mixing the tube. Figure 3-15 (a) shows the cell concentration of the samples over this period. The concentration decreases by a third within the first minute, but it is not clear whether this is a real effect. The initial measurements

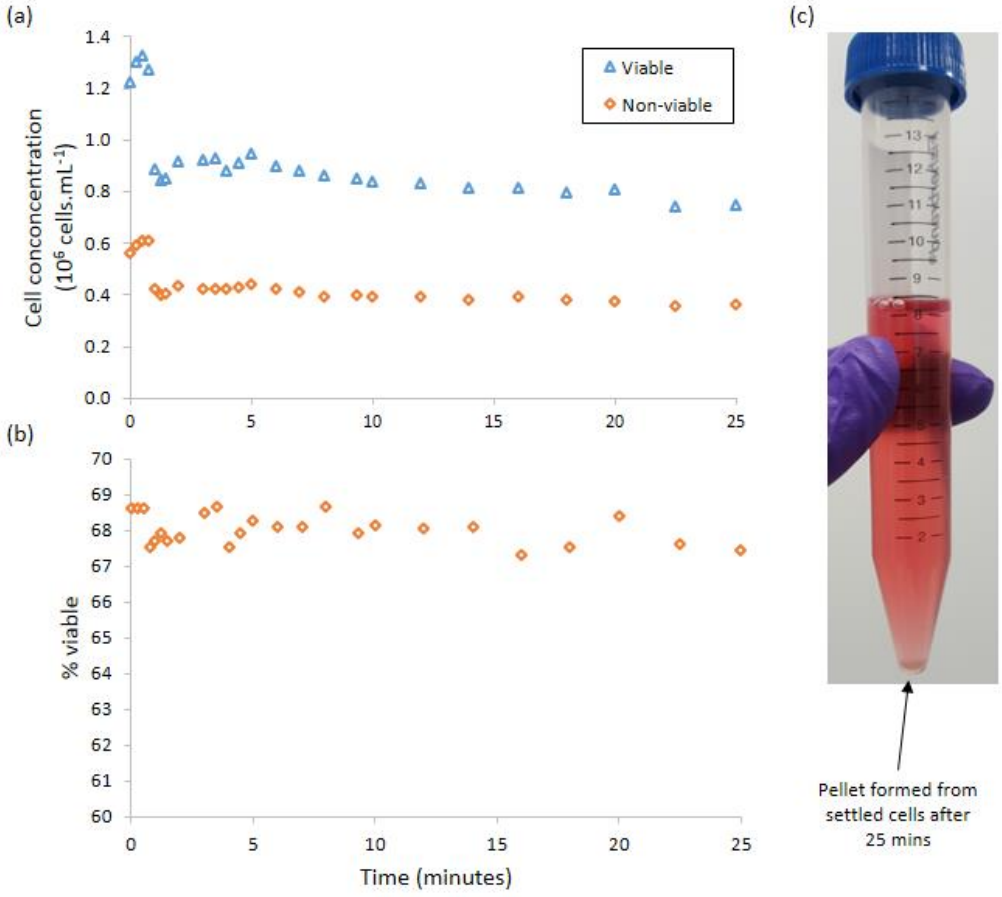

Figure 3-15: FOPMKs settle over time if cultures are not mixed. (a) Cell concentration over time shows a decrease in both viable and non-viable cells of a third during the first minute, then a steady decline over the next 24 minutes (b) the proportion of viable cells in the cell counts remains approximately consistent, therefore the settling rates of viable and non-viable populations appears to be consistent. (c) Image shows visible cell pellet at the bottom of the 15 mL centrifuge tube over the 25 min period.

were assumed to have been higher because the samples were taken close to the meniscus of the medium, where there may have been a higher concentration of cells, since it is documented that cells gather at surface boundaries [130]. If the rapid settling of cells was a true effect this could affect the main measurements of the FOPMK culture system, whereas the slower rate of settling from 1-25 minutes produced a reduction in cell number by around 16%, which over this time frame is negligible., since measurements would be taken within 2 minutes post mixing.

Viable and non-viable cells appeared to settle at the same rate as shown in Figure 3-15 (b). Therefore, any settling would not allow for selective advantage of viable and non-viable populations so measurements would likely show the true proportion of cells, even if the absolute concentration was offset. In Figure 3-15 (c) a visual cell pellet can be seen which formed after the 25-minute period. This confirms that cell settling took place but since the pellet would be less dense than a pellet produced by centrifugation, comparison is flawed and therefore it cannot be visually determined from the image whether rapid settling occurred.

Determining culture dynamics requires precise high temporal resolution cell counts and so counts that are biased within a certain time window would be problematic. Figure 3-16 shows that following a medium exchange FOPMKs temporally adhered to standard tissue culture treated plastic (STCP) within an hour post-seeding. This did not occur when using ultra-low attachment (ULA) plasticware . After 24 hours the cells recorded from both STCP and ULA were equivalent, suggesting the cells lifted off of the plastic. After 48 hours the STCP complete exchange appeared to have more cells present, this may have been caused by removing medium for cell counts in the early stage of culture whilst retaining cells, since they were

adhered to the plastic. This means that the cells have been concentrated, rather than outperforming the ULA or partial exchange STCP.

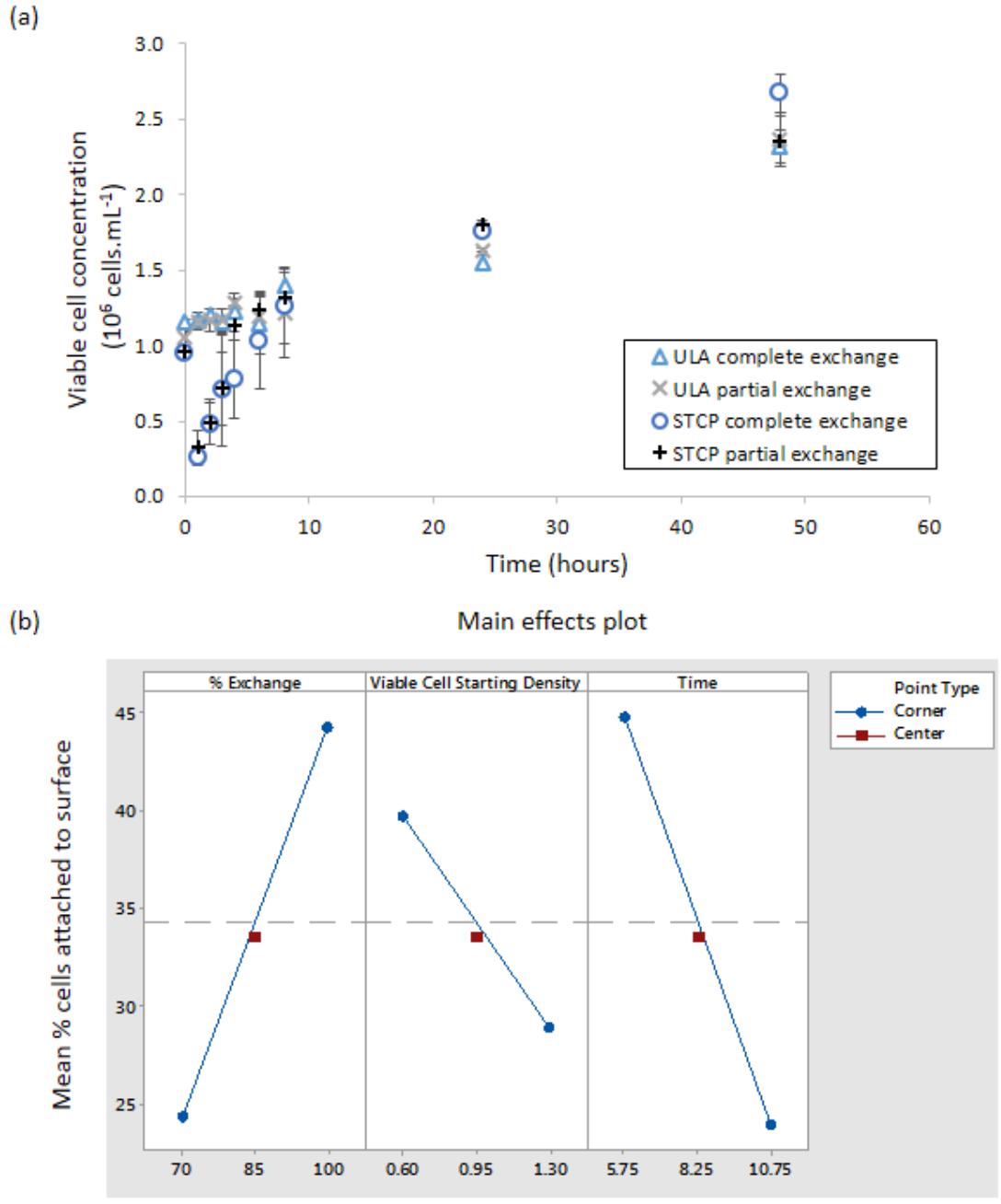

Figure 3-16: FOPMKs temporarily adhered to standard tissue culture plastic (STCP) following a medium exchange. This effect was alleviated by using ultra-low attachment (ULA) tissue culture plastic. (a) Approximately 75% of cells attached to STCP within the first hour following a medium exchange, but within 24 hours the cell counts of the cultures using ULA and STCP were equivalent. Data shows N=2 ±STD. (b) Main effects plot from statistical analysis software Minitab showing linear relationships between the proportion of medium exchanged, viable cell starting density, time in culture and the percentage of cells attached.

After four hours the cell counts from the partial exchange STCP cultures were equivalent to the ULA cultures, which suggested there was a positive effect from retaining a proportion of the cell growth medium in an exchange to prevent attachment. If spent medium affected the cells attachment properties, it was hypothesised that it was factors released by the cells into the medium causing the behaviour change. If this was correct, cell density would also determine attachment rate, since more cells would release more factor. Indeed, Figure 3-16 (b) shows that there are linear relationships between proportion of exchange, cell seeding density and time, which supports this hypothesis and explained difference in STCP cultures in (a).

From this work it appears that FOPMKs show similar growth profiles whether cultured using STCP or ULA plasticware. From the perspective of the ability to monitor growth dynamics using high temporal resolution cell counting methods, ULA prevented attachment issues that might bias counts in the 24 hour post-seeding. It has also been reported that ULA plasticware increases primary human MK viability and promotes polyploidy development [131]. Therefore, ULA tissue culture plastic should be used for culturing suspension FOPMKs.

3.4.1. Cell counting issues when using iPSCs

Two cell counts were taken from iPSC wells with target seeding densities of 1000, 5000 and 9000 cells.cm^{-2} prior to seeding wells (i.e. cell counts were taken from a pooled vessel) and immediately after cells and medium suspensions had been placed into wells. The cell counts shown in Figure 3-17 demonstrated that across all seeding densities and all wells that the post seeding counts were higher than the pre-seeding counts.

It is hypothesised that the uplift in cell number was caused by cell aggregates disassociating and becoming visible on the flow cytometer. Despite the use of TrypLE to reduce cell clumping,

doublets and the edge of a triple cell population were observed on the FSC/SSC profile (data not shown). The pre-seeding count cell count may not have been mixed as thoroughly as the post-seed count (although this seems unlikely since effort was taken to mix the cells thoroughly first). Whatever the underlying mechanism, it is difficult to find a reason to suspect cells were over counted in the post-seed count, since generally cells are more likely to be lost through liquid handling. Therefore, it is assumed that the post-seeding count was more accurate and was therefore used where possible to calculate cell losses in the first day of culture in relevant sections (see Section 6.6). Even if this were not true, consistent use of post-seeding cell counts would provide comparability between experiments.

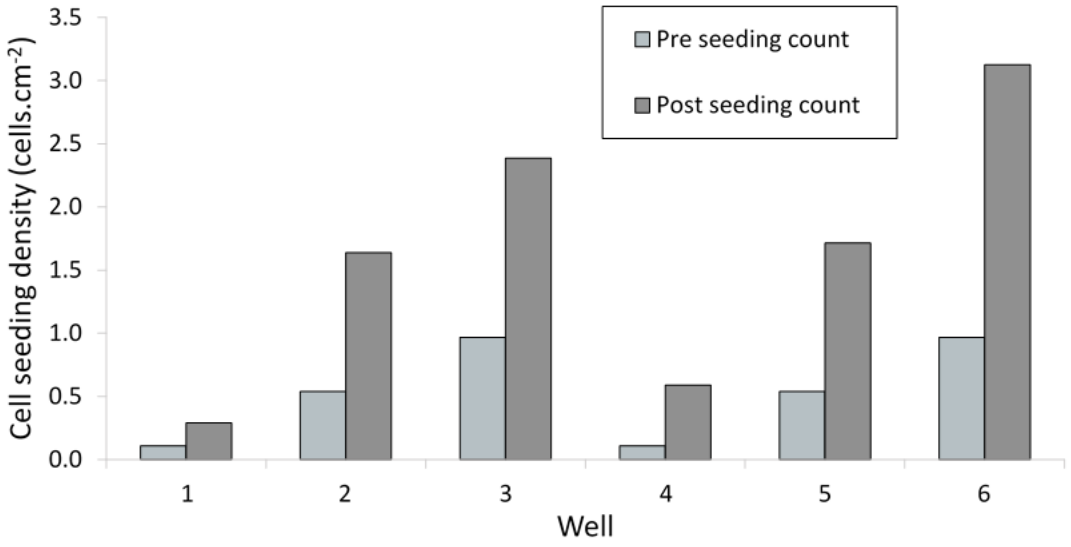

Figure 3-17: Cell counts for iPSC cells seeded at a target density of 1,000 (wells 1 and 4) 5,000, (wells 2 and 5) and 9,000 (wells 3 and 6) cells.cm-2 show that in all cases measured cell counts were higher post-seeding than pre-seeding.

3.5. Conclusions

This chapter presents a QTPP for FOPMK, in vitro derived platelet transfusion units and proposes CQAs. Corresponding assays are developed to measure CQAs quantities of FOPMKs (both 1st generation non-inducible lines and 2nd generation Dox-inducible FOPMKs) and iPSCs.

The QTPP was developed using the current clinical standard of platelet transfusion units derived from volunteer donors, with additional markers added (CD41, 42a/b, CD62P) to ensure the correct identity of platelets. These markers are not routinely monitored currently, probably because the use of apheresis for collecting platelets is a long established process that reduces the contamination of platelet units by other blood cells [132].

However, the development of a QTPP based on platelet transfusion units still presents challenges in establishing CQAs that can be used for process development in a production process that requires cells to differentiate and therefore change marker expression throughout production. A detailed literature search found no assay that could predict the ability of MKs to produce a certain number of platelets. Therefore, assays were developed to measure established lineage trajectory and platelet functional markers (CD34, CD235a, CD41a, CD42a, CD42b) in the case of FOPMKs or pluripotency markers (TRA-1-81, NANOG, Oct3/4) for iPSC expansion. Once assays become available that directly link to platelet yield and quality from FOPMKs, these should be measured also, and this would allow further tailored process improvements and corroboration of original assays However, these assays should give a good starting basis for measuring FOPMK functionality and can thus be used to make informed process risk decisions.

Different methods for setting PMT voltages for flow cytometry assays were explored. Using Application Settings to establish baseline PMT voltages required more resource to set-up

initially compared to other methods (such as first log decade or use of CS&T bead suggested values), but often produced voltages that required minimal adjustment (expect in the case of GFP in extended Panel 6, Table 3-14, due to the high fluorescence of GFP, which was challenging to accommodate on an extended panel without loss of sensitivity through reduced PMT voltages). Assay sensitivity through the enhanced separation of population was enhanced through antibody titrations. In addition to the enhanced sensitivity, assay costs were also improved in half of antibodies titrated, since the highest Sensitivity Index was achieved at lower concentrations than the manufacture's recommendation.

Cell count methods were developed using different equipments (BD FACS CANTO and NC-3000) . Both methods were found to produce cell count measurements that were normally distributed around the mean and were calibrated for comparability between assays. The permeability of viability stain, DAPI, was monitored over a period of 50 mins at room temperature and was found to be stable, which increased assay flexibility.

A cell count measurement issue was noted during the use of standard tissue culture plastic when FOPMKs temporarily attached. The attachment was dependent on proportion of medium exchange performed and cell density. To avoid cell counting issues related to cells attaching to standard tissue culture plastic, ultra-low attachment tissue culture vessels were used throughout the rest of the project.

When seeding iPSCs, a discrepancy in cell counts before and after seeding was recorded. It was assumed that the higher cell counts were more accurate, since the loss of cells through liquid handling was more plausible than the creation of cells. Regardless of the "true" count, cell counts post-seeding were used to ensure comparability between experiments.

3.5.1. Future work

The cell therapy industry has previously suffered due to a lack of meaningful CQAs. Since cell products are so complex, it is often challenging to link CQAs to MOA [118]. Once the process of platelet production from FOPMKs is more thoroughly understood and defined any noted CQAs should be recycled back into the process of QTPP definition.

Flow cytometry assay development was shown to be complex and subjective. Methods such as Application Settings have been developed to ensure greater comparability between experiments and sites, but subjectivity in set-up remains inherent. The choice of fluorochromes combinations is also highly subjective, comparisons between manufacturers and out comes on different pieces of equipment are not readily available. As the cell therapy industry matures, flow cytometry assay comparability, accuracy and sensitivity will become pressing issues and there are already programmes that are attempting to address some of these issues [133].

4. The application of mechanistic modelling tools to determine the system productivity of non- doxycycline inducible forward programmed megakaryocytes

4.1. Introduction

This chapter focuses on the production of FOPMKs from the first generation process where iPSCs were targeted with a cocktail of 3 viral vectors which individually contain transcription factors GATA1, FLI1 or TAL1 and created a semi-immortalised megakaryocyte line which proliferated in vitro for around 90 days [5]. Figure 4-1 summarises this process and was devised based on publications by Moreau [5] and Dalby [134].

The use of viral vectors is an industry bottleneck, with wait-times for GMP vectors of up to 18 months and vectors have a high COGs. Therefore, achieving acceptable process costs for in vitro platelet production will be dependent on optimising the expansion phase of FOPMKs to produce a high yield of cells per input genetically programmed iPSCs, with respect to resource consumed, which are of sufficient quality for platelet production.

In order to define how a process will affect product quantity and quality many factors must be measured, controlled or in some way considered. These are likely to have complex and interacting relationships. A qualitative description of dynamics includes the nature of processes such as growth inhibition and/or cell death, the nature of population changes, and whether these mechanistically relate to operations such as media provision and other culture system attribute. These dynamic culture characteristics are critical to determining a manufacturing strategy [135]. This chapter presents proof of concept for a methodology, using FOPMKs as a clinically relevant case study, where key process dynamics, that are critical for cell expansion, are identified through high temporal resolution cell culture experiments and quantified using ODE based, dynamic, mechanistic models.

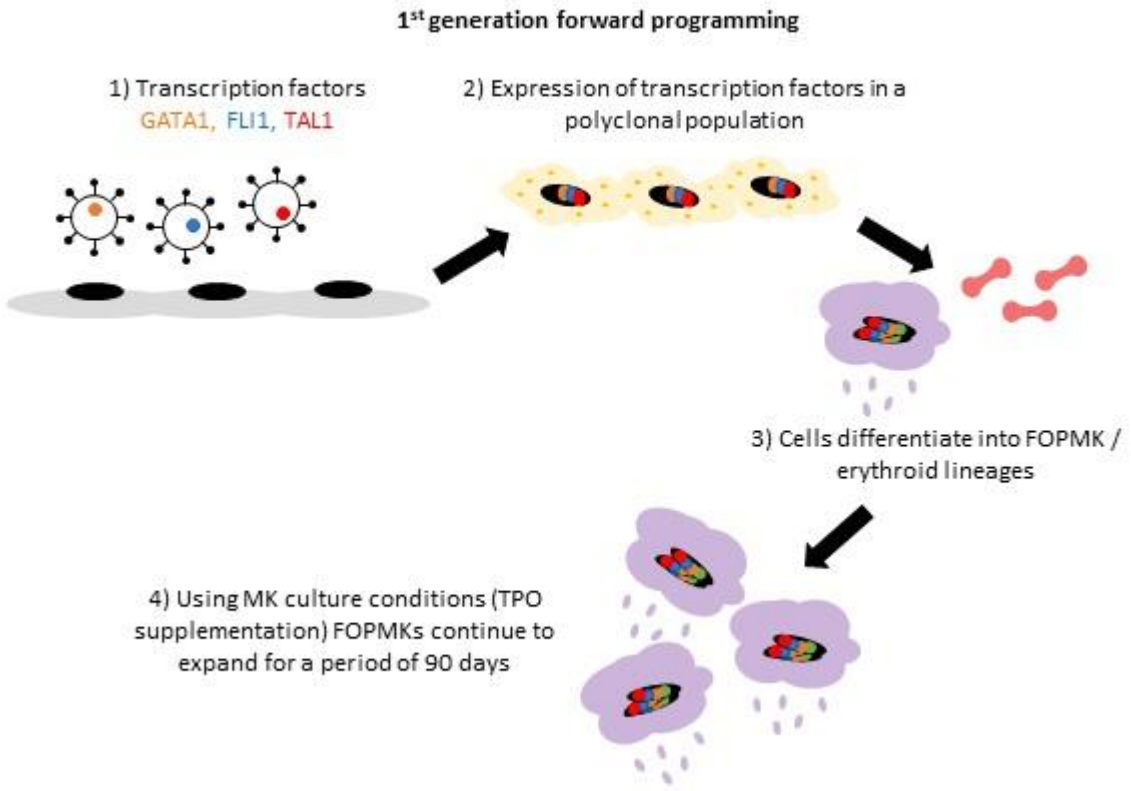

Figure 4-1: Summary of first generation FOPMK derivation and expansion. The expansion phase of FOPMKs is critical to achieving acceptable COGs for an in vitro manufactured platelet product.

4.1.1. Chapter Objectives

- Qualitatively identify culture dynamics which affect FOPMK expansion system productivity
- Identify candidate mechanisms for observed culture dynamics
- Quantify key culture dynamics using a novel mechanistic modellingframework
- Validate model applicability to scalable culture systems

4.2. Materials and methods

Cell line derivation and culture was performed as described in Section 2.3 & 2.4. Two cell lines were used for this work, BOB and FFDK; the experiments conducted with each are outlined below in Table 4-1.

Table 4-1: Table showing the cell line used in each section.

Cell line	BOB	FFDK
Section used in	4.3.1 **Error! Reference source not found.** 4.3.4 4.3.5 4.4.2 4.5.1 4.5.2 4.5.3 4.5.4 4.5.5	4.3.3 4.4.1 4.4.3 **Error! Reference source not found.** 4.6

For medium comparison in Section 4.4.3, Iscove's modified Dulbecco's medium (IMDM) base medium was used which was supplemented with:

- IMDM with GlutaMAX-I (Invitrogen, Paisley,UK)
- 1.5 % human AB serum (Sigma-Aldrich, Dorset, UK)
- 0.1% insulin (Sigma-Aldrich, Dorset, UK)
- 2% human albumin serum (Invitrogen, Paisley,UK)
- 0.4% heparin (Sigma-Aldrich, Dorset, UK)
- 100 $ng.mL^{-1}$ SCF (R&D Systems, Abingdon, UK)
- 40 $ng.mL^{-1}$ TPO (R&D Systems, Abingdon, UK)

Cell counting was performed using flow cytometry and described in Section 2.5.2. Flow cytometry sample preparation, equipment used, staining and acquisition is described in Sections 2.6.1 - 2.6.3. The flow cytometry assays and cell counting assays used are described in Section 3.3.1, and the assays used are identified in relevant sections and figure legends associated with flow cytometry data.

Design of experiments were conducted as detailed in Section 2.8.1. The number of factors, levels of factors, outputs and whether a centre point was included is detailed along with the results of the DOE outputs in the relevant sections.

4.2.1. Dynamic modelling framework

The dynamic modelling framework used here is described in detail by Stacey et al. [100] and also in Section 2.9.

4.3. Qualitative growth dynamics of the culture system

4.3.1. Initial system assessment

The standard operating procedure provided by our collaborators for medium supply was a partial medium exchange every 3-4 days [5] (see also Section 2.2.2). Using this method, Moreau et al. noted qualitatively variable net expansion rates. Therefore, this culture method was repeated to determine baseline performance which is shown in Figure 4-2. High viability cultures were maintained for the first 48 hours, after which point the number of viable cells diverged from the total number of cells. Despite medium addition, the proportion of viable cells did not recover.

4.3.2. Distinguishing between time and cell.time culture limitations

It was assumed that non-viable cells do not proliferate, and only viable cells were capable of cell growth, so non-viable cells were created by conversion from viable cells. Therefore, after 48 hours it was hypothesised there was a change in culture conditions which caused an increased conversion rate of viable cells to non-viable cells. It was unlikely that cell density caused the rapid conversion of viable to non-viable cells, since the cell number reset at 72 hours would have triggered an increase in the number of viable cells.

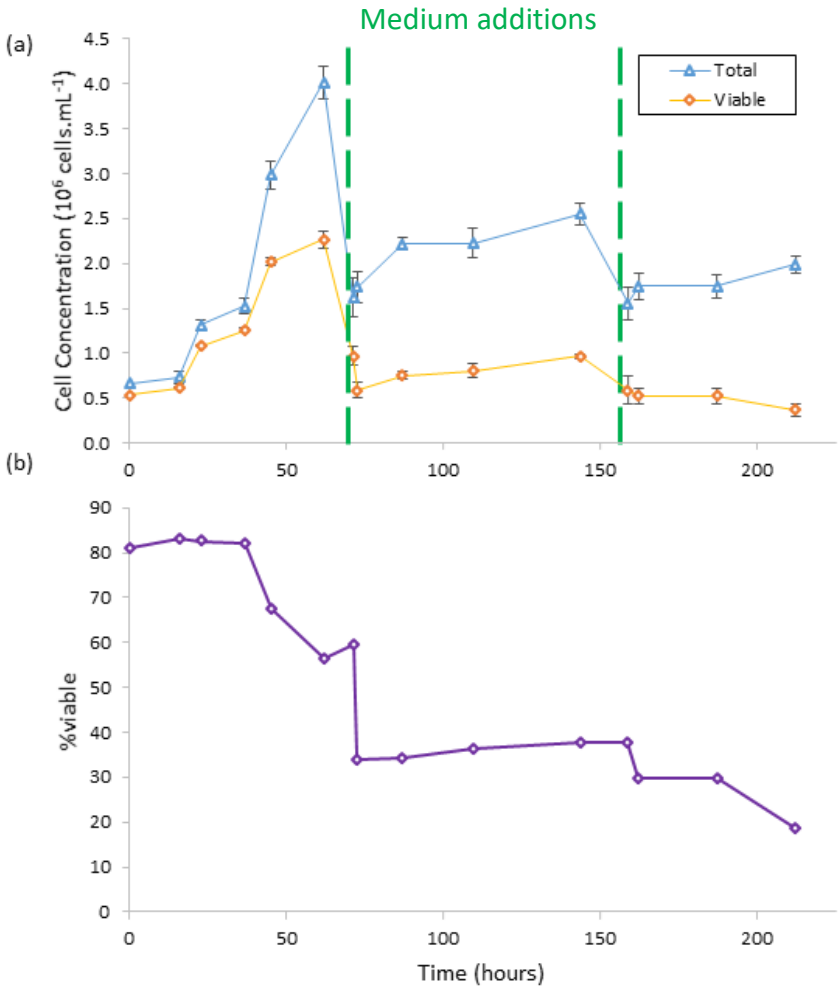

Figure 4-2: Established medium supply regime did not support consistent expansion over 200 hours. (a) Green dashed lines show a medium addition to decrease the cell seeding density to the starting density of 5×10^5 cells.mL^{-1}. Data show N=2 ±STD. (b) Average viability decreased across the culture period.

This led to the hypothesis that a component in the medium was causing the enhanced conversion. This may have either been decay of a component which was critical for maintaining cell viability or the production of a component which was toxic to cells. The production/decay rate may have either been a function of time or a cell mediated metabolism which was a function of the product of cell number and time (cell.time). To distinguish between a time or cell.time conversion rate mediator, cells were cultured using various cell seeding densities and proportions of medium exchange at zero hours. No further medium was supplied to the cultures. Figure 4-3 shows high-temporal resolution cell counts. Viable

cell concentrations increased for cell cultures seeded at higher densities until 60 hours, after which the viable cell concentration declined. The decline in concentration happened approximately 20 hours later for cultures that underwent a complete medium exchange compared to a partial medium exchange.

This shows that medium exhaustion, rather than effects related from cell density such as contact inhibition or mass transfer limits, promoted conversion to non-viable cells and that the volume productivity of the system was $1.48 \pm 0.28 \times 10^6$ viable cells.ml^{-1} (based on the high and low density, complete exchange cultures). In addition to conversion of viable to non-viable cells, the plateau in viable cell concentration at 60 to 80 hours, with a relatively small increase in total cell concentrations demonstrated that growth inhibition related to medium exhaustion was also likely to be present.

Since the conversion of viable cells occurred later in time in the lower density cultures, the promotion of conversion was likely to be linked to a cell.time mediator rather than time alone. However, the cause of growth inhibition may have been more complex. Since growth inhibition occurred in both high density and low density cultures at around the same time of 60 hours, this may have been linked to a time related inhibition, for example decay of medium components [136] [96]. Comparison between partial medium and complete medium exchanges would not distinguish between a time and cell.time mediator, because the proportion of medium remaining from a partial exchange may have decayed also. However, cell death was a higher risk to process outcome than growth inhibition, and therefore understanding the growth inhibition mechanism was of a lower priority.

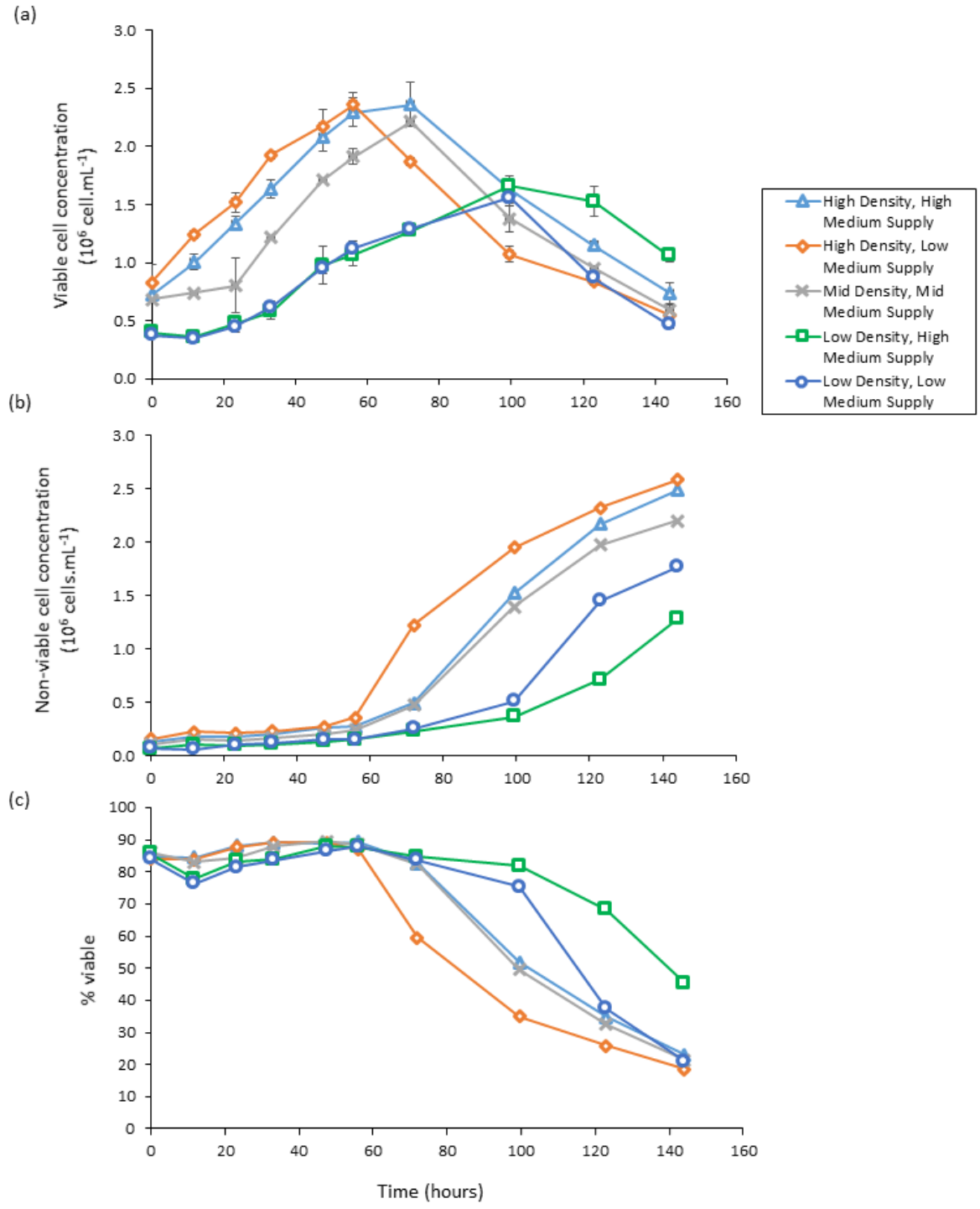

Figure 4-3: Viable FOPMKs were converted to non-viable cells due to medium exhaustion. (a) Cultures seeded at higher concentrations reached a peak concentration of viable cells earlier than cultures seeded with lower cell concentrations. Lower medium supply also led to deceasing viable cell concentrations earlier than culutres with a complete medium exchange. (b) Non-viable cell concentrations increased with concurrent decrease in viable cell concentrations, showing a conversion of viable to non-viable cells. (c) %viable cells acros time.Data shows cell line BOB, N=2 ± STD.

4.3.3. The relationship between growth rate and cell seeding density at seeding

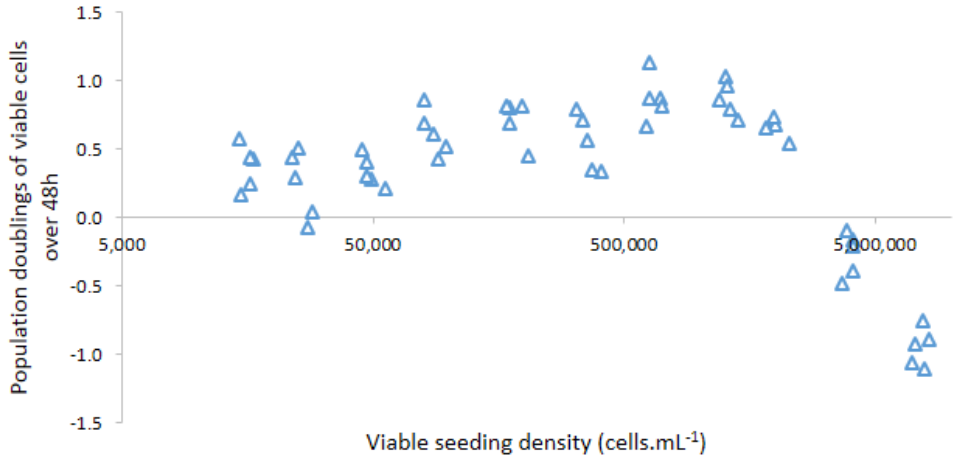

Figure 4-4: Increasing viable cell seeding density from 1.5×10^4 to 1×10^6 cells.mL^{-1} increased the number of population doublings which occurred over a 48 hour period. Cell line used was FFDK.

The relationship between growth rate promotion and cell seeding density was complex. Figure 4-4 shows the number of population doublings over a 48-hour period following a complete medium exchange increased for cultures seeded between 1.5×10^4 to 1.5×10^6 cells.mL^{-1}. It was hypothesis that the improvement in growth rate was derived from cell released factors which promoted growth; factors which would have been removed during a complete medium exchange.

In order to understand the relationship between cell seeding density and promotion of growth rate, cells were seeded at 5×10^4 and 2×10^6 viable cells.mL^{-1} and a high temporal resolution growth curve was conducted. In Figure 4-5 cultures seeded at lower cell densities had associated higher growth rates than cultures seeded at higher cell concentrations. The cultures seeded at 5×10^4 cells.mL^{-1} with a complete medium exchange had an average growth rate of 0.0151 h^{-1}, but in Figure 4-4 the equivalent cultures had an average growth rate of 0.005 h^{-1}, around a third of that observed in Figure 4-5.

The cultures used were from the same FOPMK derived cell line (FFDK) and had been cultured for around 130 days since FOPMK derivation, and therefore were assumed to be equivalent cultures. The experiment in Figure 4-4 was conducted using 96 well plates, whereas Figure 4-5 was conducted using 6 well plates; the difference in observed growth rates may be linked to different mass transfer limits of the two culture platforms, either in terms of dissolved oxygen concentration or localised concentration gradients of nutrients and metabolites formed around the cells. These limitations may also account for the lower growth rate observed at the higher culture density of 2×10^6. Since the growth rate was consistently lower over the 48 hour period this cannot be attributed to the same accumulation of factor that caused the growth inhibition and death in Figure 4-3.

Investigating the differences in mass transfer limits is of limited value to defining a manufacturing strategy which would likely rely on large-scale reactor systems, such as stirred tank vessels. However, many process development experiments are conducted using static

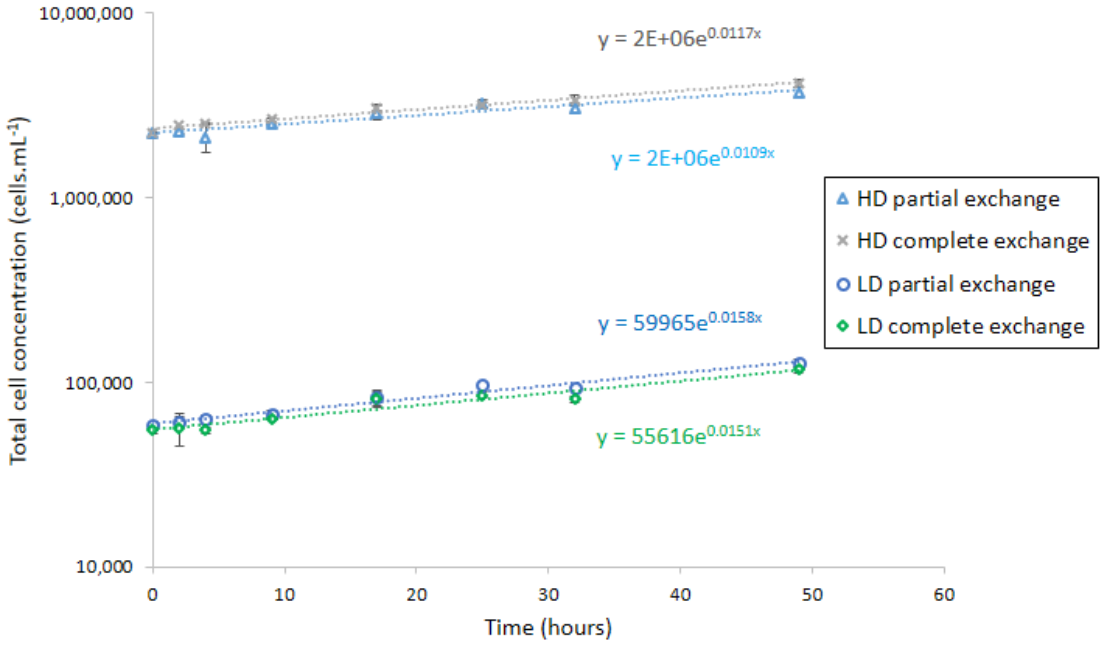

Figure 4-5: Cultures seeded at 5×10^4 had on average ~30% faster growth rates than cultures seeded at 2×10^6 viable cells.mL^{-1} over 48 hours. Growth rates between culture which had partial and complete medium exchanges had little difference in growth rates. Cell line used was FFDK, data shows N=2 ±STD.

culture platforms due to their ease of use, ability to use small cell numbers and reagents, therefore it was important to develop and understanding of the limits of the culture platforms used and how they might impact the culture dynamics.

4.3.4. Adjusted medium supply regime to control density

It was hypothesised that since medium exhaustion caused rapid cell death, increasing the medium supply would lead to sustained, stable cell growth. Compared to the growth rate fluctuations shown in Figure 4-2, the growth rate achieved was higher and more stable in Figure 4-6. The adjusted medium supply was based on addition of fresh medium to maintain cell densities between 5×10^5 and 1×10^6 cells.mL^{-1}. This density would likely be outside of mass transfer limitations, and addition of medium would negate the risk of possible effects from removing positive conditioning factors from the medium, which would occur in a complete exchange. It was assumed that growth factor decay could be mitigated by adding double concentrated growth factors as in the established SOP. Using this method, a high proportion of viable cells (Figure 4-6a) was maintained, in contrast to Figure 4-2; again showing medium supply controlled the conversion of viable to non-viable cells.

The linear increase in cumulative population doublings with time shown in Figure 4-6b shows a stable growth rate across the culture period of approximately 0.019 h^{-1} was achieved, but there was an oscillation in the residual error of the cumulative number of population doublings from the trend line across time (Figure 4-6c). This indicated that a higher growth rate than 0.019h^{-1} was achieved, but it is unclear whether this could be sustainable across the culture period.

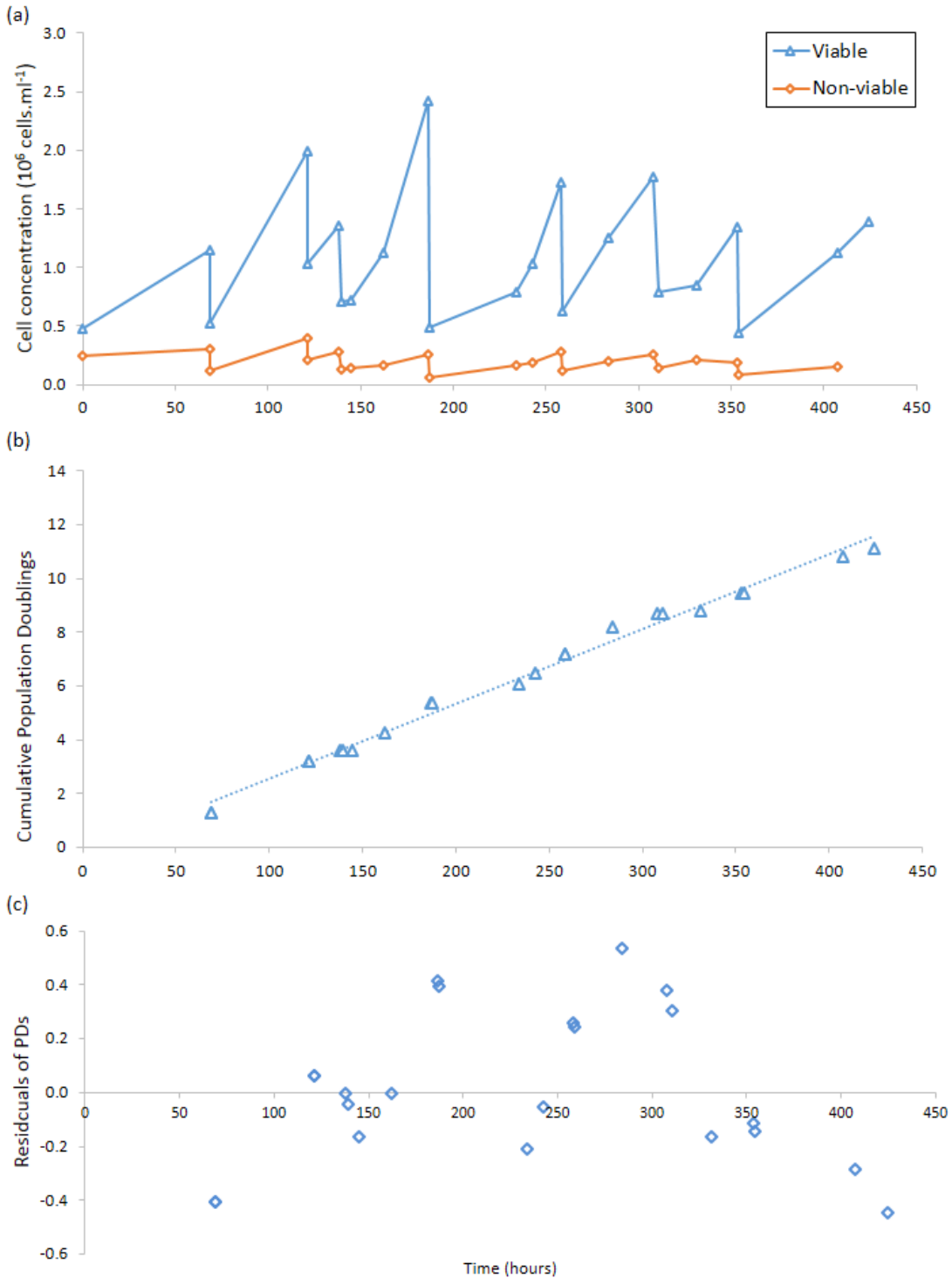

Figure 4-6: Culture volume was doubled by the addition of fresh medium once the concentration of viable cells exceeded 1 × 10^6 cells.mL^{-1}. (a) Cell concentration changes with time show maintenance of a high proportion of viable cells using the adjusted medium supply. (b) A linear relationship between cumulative population doublings and time shows a consistent growth rate of 0.019 h^{-1} from 50 to 420 hours. (c) Residuals of cumulative population doublings with time show a pattern of oscillating growth rate over the culture period, indicating that higher growth rates might be achievable with adjusted medium supply. Cell line used was BOB.

4.3.5. Changes in FOPMK phenotype across the culture period

Thus far, this work has been focused on FOPMK growth rate changes, however cell quality is a critical process output. As discussed in Section 3.2.1, cell phenotype is used here as a surrogate measure for cell quality. Figure 4-7 shows that FOPMK phenotype trended over a culture period of 35 days. Two competing hypothesises are that this trend was a function of medium supply, or the observed trends were inherent to FOPMKs. This trend was not investigated further using FOPMKs derived from the 1st generation forward programming process since the technology moved on to second generation inducible system. Section 5 describes how supply of specific components impacted cell phenotype.

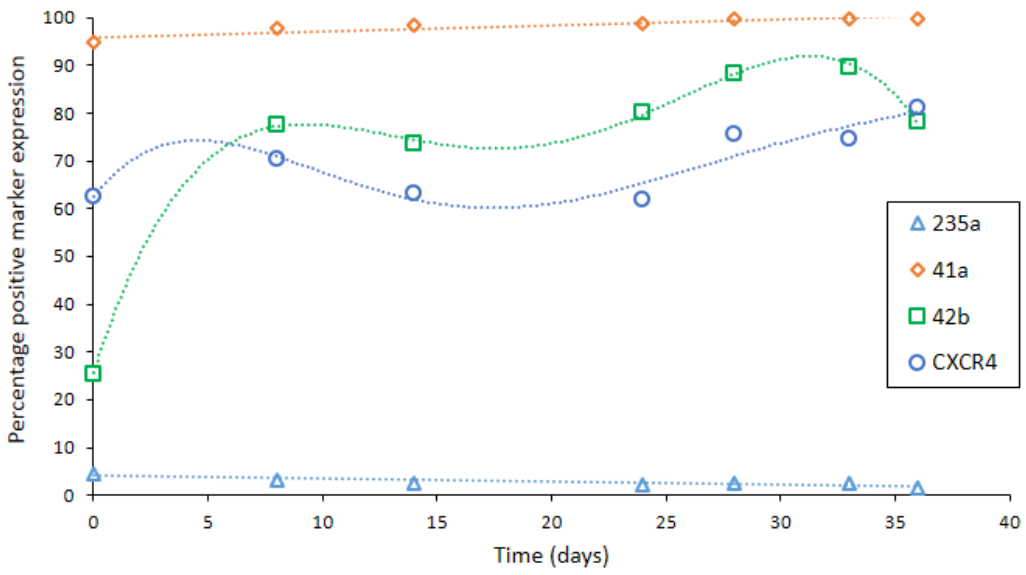

Figure 4-7: FOPMK phenotype trends over a month-long culture period. It is unclear whether this is related to medium supply or is inherent. Cell line used was BOB.

4.3.6. Qualitative culture dynamics summary

Qualitative culture dynamics summary:

- A stable doubling rate was achievable.
- Modification of the cell culture milieu by FOPMKs led to promotion of cell death, not purely cell density or medium decay with time.
- FOPMKs converted rapidly to non-viable cells as a response to medium exhaustion, rather than simple growth inhibition, which is a critical control window issue.
- Cells were also likely subject to growth inhibition related to medium exhaustion and cell density (complex and potentially multiple mechanisms, for example: mass transfer limitations or cell contact, and culture platform dependent).
- Growth rate after medium exchange appears to be related to density in a non-simple way – relatively minor effect.

Figure 4-8: Summary box of observed qualitative culture dynamics colour coded to show confidence, green being the points with the most certainty, and red being the points which are least certain.

A summary of the observed culture dynamics for the system is shown in Figure 4-8. The most critical aspect with respect to controlling an FOPMK manufacturing process was the rapid conversion of viable to non-viable cells which was an effect of cell.time mediated medium exhaustion. Since growth medium will contribute to a significant proportion of the COGs of large scale allogeneic cell therapies [73], the number of cells that a volume of medium can support over a given amount of time (i.e. medium productivity) will be a large determining factor of the end stage COGs. Therefore, there were two aspects to follow as part of developing an understanding of FOPMK proliferation to inform an FOPMK manufacturing strategy. The first was elucidating the factor causing rapid cell death, which could lead to medium modification to increase the productivity and therefore drive costs down. The second was to quantify the culture dynamics observed thus far and develop a control strategy based around medium supply.

This two pronged approach was critical because elucidating the factor causing FOPMK death is unlikely to be straight-forward: Previous work by our group has shown that traditional

bioprocess limitations such as glucose, lactate and ammonium are not primary inhibitors in the production of red blood cells [58] and since megakaryocytes are closely related in the hematopoietic linage it is not unreasonable to expect similar metabolic behaviour. Furthermore, the growth medium used for FOPMK production is a chemically defined, and although this is beneficial in terms of regulatory compliance and consistency [38], it means the proprietary medium is a black box system which limits possibilities of medium development.

Quantitatively defining the dynamics of the FOPMK culture system would allow for an improved production strategy based simply on medium supply and does not rely on identifying complex culture limitations and arbitrary values could be assigned to, for example, medium exhaustion factors, which can then be used to calculate relative sensitivities. This de-risks research into the manufacturing strategy because even if the limiting factor cannot be identified it can still be controlled.

The rest of this chapter forms the foundation of the assessment of culture limitations and quantitative assessments of culture dynamics using an in-house developed, novel mechanistic modelling platform.

4.4. Identifying culture limiting factors

4.4.1. Growth factor concentration

Growth factors SCF and TPO are required for FOPMK proliferation [5]. To determine whether the concentration of these cytokines impacted the FOPMK culture dynamics, varying combinations of growth factors were used with two difference cell seeding densities. Figure 4-9 shows that there was little difference in growth caused by different growth factor concentrations.

In the lower density cultures, as shown in Figure 4-9a, the lowest combination of both SCF and TPO deviated from the other cultures from 40 hours, this could be as a result of growth factor decay with time. This is less clear in the higher density cultures in Figure 4-9a, but normalising for seeding density variations and plotting the doubling times (Figure 4-9b) also showed that the lowest cytokine concentration combination underperformed in the high density cultures. However, the middle combination also underperformed. There is also a relatively high variation between biological repeats. It is unclear whether this was linked to mass transfer limitations as observed from Figure 4-5.

Since the effect of growth factor concentration was small (and not statistically significant), it was not prioritised for further assessment. However, to ensure it is not a limiting factor, the highest combination of growth factor concentrations was used in further work.

Here, these nutrients/metabolites were monitored over the cultures shown in Figure 4-3 and are displayed in Figure 4-10. Over the 150 hours, only 20% of the baseline glucose was depleted showing that glucose concentration was not limiting the cultures. Compared to limiting values assessed on a red blood cell system [58], neither lactate nor ammonium were likely to be causing rapid cell death, although they may be contributing to growth inhibition. Fresh medium contained a comparatively high concentration of ammonium (1.5 $mmol.L^{-1}$), which suggests that glutamine present in the medium is degrading overtime. The medium used was well within the manufacturing date of expiry, so might be indicative of other degradation occurring within the culture time frame. In order to define the effect of these metabolites on the FOPMK cultures, a dose response experiment could have been performed in future work, but was not included in this work, since the 2nd generation FOPMK system did not demonstrate the same medium exhaustion effects (see Section 5).

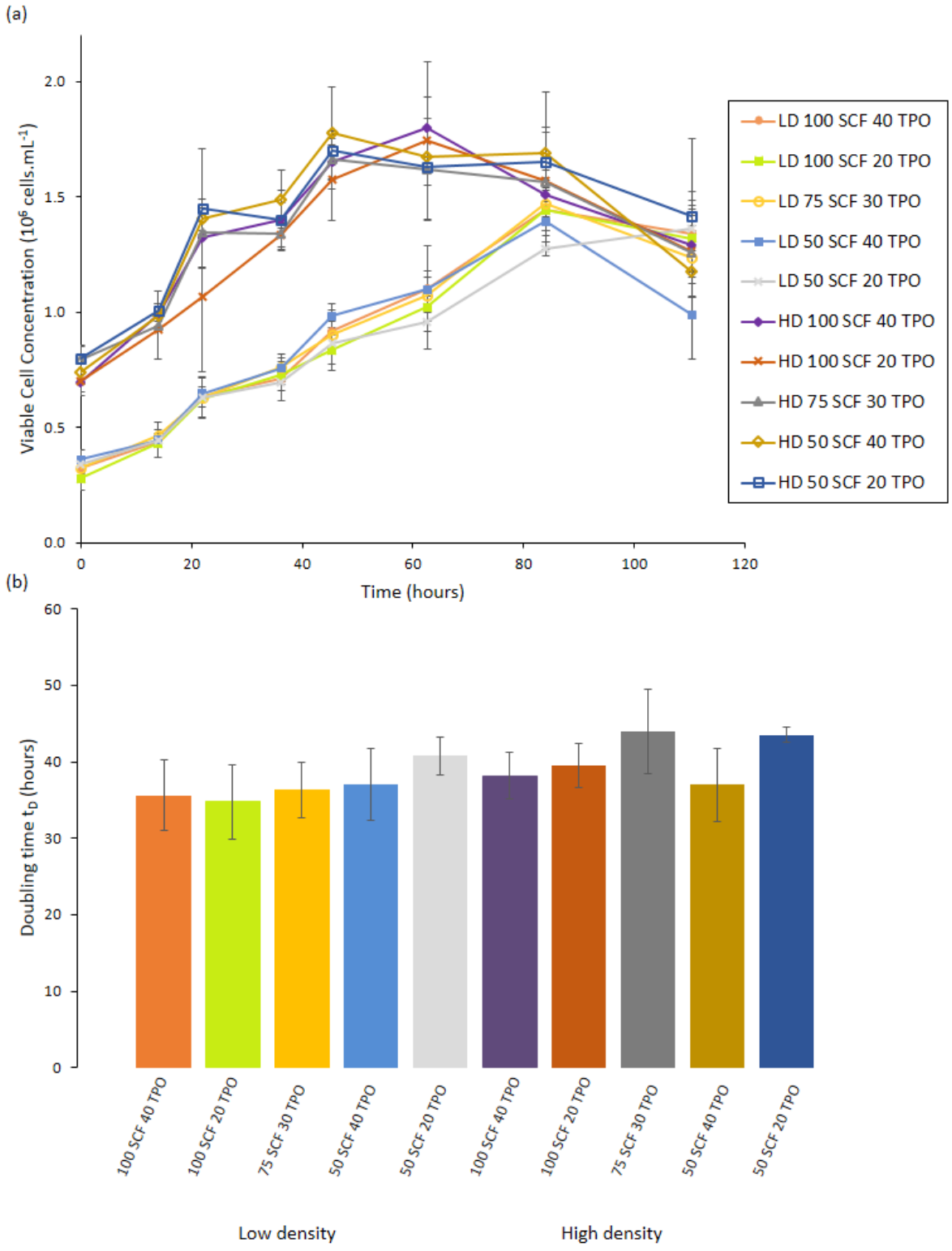

Figure 4-9: Concentration of SCF and TPO have a complex and interacting effect on FOPMK proliferation, but this is minimal compared to cell death effects. (a) Viable cell concentrations show the largest difference between the lowest concentrations of SCF and TPO and the highest concentration in the low density cultures, however the difference is minimal. (b) Doubling times over 60 hours for low density cultures and 40 hours for high density cultures normalise for deviations in culture seeding densities and show minimal difference between growth factor concentrations. Cell line used was FFDK, data shows N=3 ±STD. Legend key : LD – low seeding density, HD = high seeding density, 20, 30, 40 show concentration of TPO (ng.mL^{-1}), 50, 75, 100 show concentration of SCF (ng.mL^{-1}).

4.4.2. Common nutrient metabolite limitations

In different cell culture systems, such as MSCs, glucose, lactate and ammonium limitations are often limiting factors that inhibit growth [137].

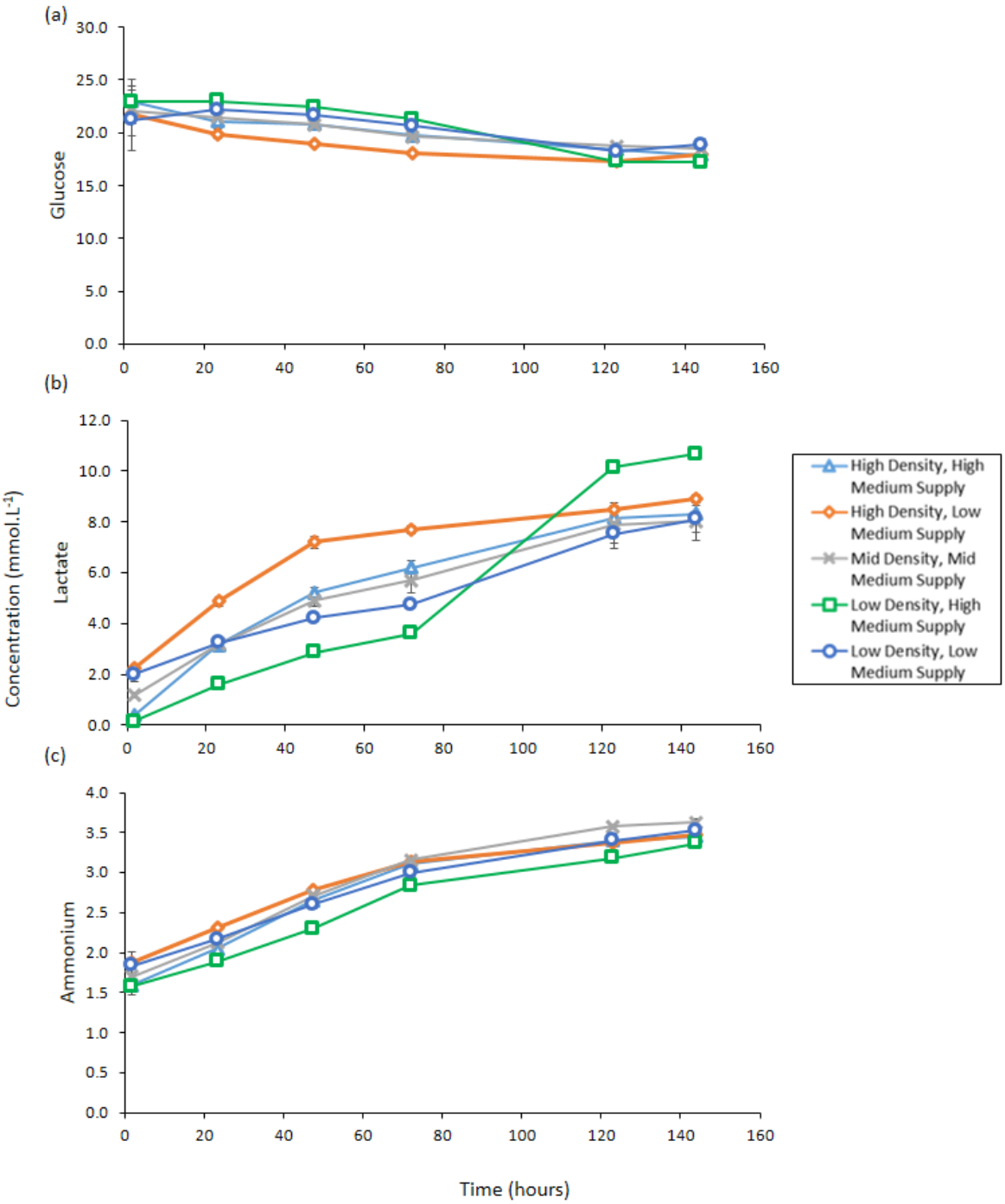

Figure 4-10: Concentration of (a) glucose, (b) lactate and (c) ammonium across the culture period of 150 hours. These were unlikely to be causing cell death at these concentrations. Cell line usd was BOB, Data shows N=2 ±STD.

4.4.3. Comparison of culture media

Since FOPMK death dynamics are linked to medium exhaustion, it was likely that different media compositions would have different effects on FOPMK growth and inhibition. A comparison is shown in Figure 4-11 between Cellgro-based medium and a supplemented Iscove's modified Dulbecco's medium (IMDM) based medium (see Section 4.2 for materials), used for the growth of red blood cells [138][58]. High growth factor supplemented Cellgro SCGM contained 100 $ng.mL^{-1}$ SCF and 40 $ng.mL^{-1}$, and the low growth factor supplemented Cellgro SCGM contained 50 $ng.mL^{-1}$ SCF and 20 $ng.mL^{-1}$.

From 20 hours onwards, the high growth factor (HGF) cultures (both Cellgro and SCGM) contained a higher number of viable cells compared to the low growth factor (LGF) cultures, supporting the differences shown in Figure 4-9, suggesting a promotion of a higher growth rate in response to cytokine availability.

However, HGF Cellgro cultures reached a peak in viable cell concentration at 50 hours, 20 hours prior to LGF Cellgro concentrations, suggesting HGF cultures promoted higher growth and either the presence of more cells, or possibly promotion of exhaustion as a result of a higher growth rate, limits the medium productivity.

The IMDM-based medium outperformed Cellgro cultures from 60 hours, and the same spike in non-viable cells was not observed in the IMDM-based cultures. The increased concentration of viable cells in IMDM-based cultures suggests that this system has a higher medium productivity. However, Figure 4-11b shows that non-viable cells decay in the IMDM-based system, which could mask possible death dynamics.

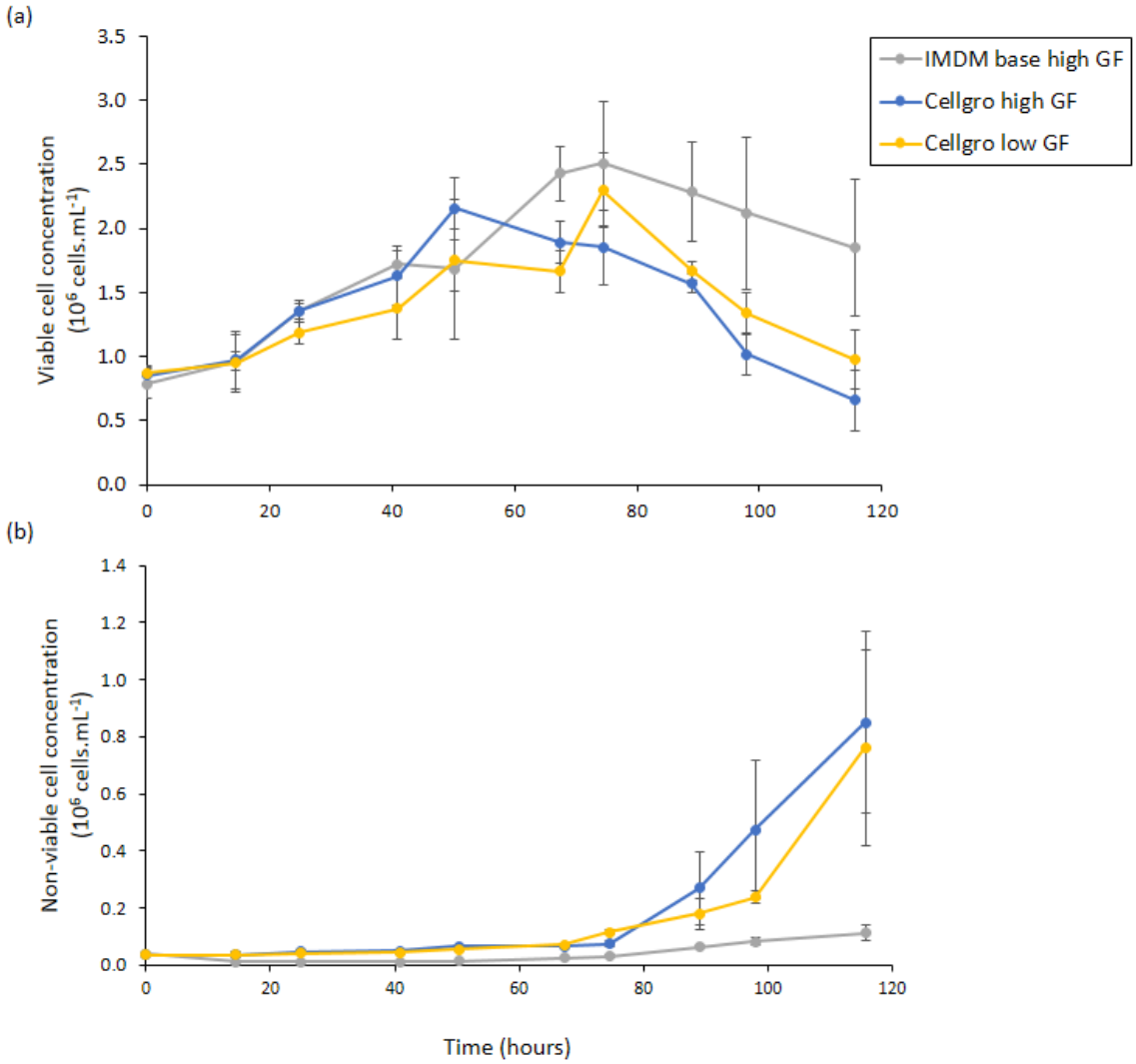

Figure 4-11: Comparison of cell culture media Cellgro SCGM (chemically defined) and an IMDM base medium supplemented with human serum. The IMDM-based supported cell growth for a longer period than Cellgro SCGM and cultures did not experience the same spike in non-viable cell concentrations. (a) Viable cell concentrations show same observed peaks in Cellgro-based cultures, and a higher concentration of viable cells was achieved with IMDM-based cultures. (b) A spike in non-viable cell concentrations was observed in Cellgro cultures but was less pronounced in IMDM-based cultures. Cell line used was FFDK, data shows average cell counts ±STD.

4.5. Developing mechanistic hypotheses underpinning FOPMK culture dynamics

There are many ways in which qualitative relationships between process parameters and process outcomes can be modelled. Structured approaches to process development applied to cell therapy manufacturing, such as Quality by Design approaches (QbD), have traditionally

focused on statistical, empirical methods to map the relationships between process parameters and process outcomes. By treating culture systems as “black-boxes” they provide limited process insight, and single-time points used for analysis can often result in the models failing over longer time courses due to the dynamic and complex nature of cell therapy systems. Mechanistic models are hypothesis-driven and the underlying mechanisms must be identified and mathematically expressed. As such they are more robust over the longer time courses and can offer enhanced process development capabilities through better sensitivity and risk analysis functions.

It was shown in Section 4.3 that FOPMK cell death is promoted by medium exhaustion. The chapter aims to quantify this relationship and suggest courses for improved medium supply, using a dynamic mechanistic modelling.

4.5.1. Cell death in response to medium exhaustion

The aim of developing mechanistic models is to describe behaviour with simplest mechanisms that adequately represent the FOPMK culture system in order to define a manufacturing process. Models with higher numbers of parameters risk over parameterisation. Over-parameterisation generally produces better fit models, but it is more requires more computational power, more resource to collect data to adequately parameterise variables, and potentially limits the extrapolation potential of the model (if the parameterisation of variables are only valid for the data set collected) [139].

In Section 4.3, it was observed that the highest priority culture dynamics identified were the cell growth and conversion of viable cells to non-viable cells (cell death) in response to a cell.time mediated medium exhaustion. Such a response is well documented in the literature; exhaustion could occur either through the release of toxic metabolites, such as lactate and

ammonium, or through depletion of essential nutrients [128]. Since growth inhibition was more challenging to "observe" when combined with the conversion of viable to non-viable cells, it was not included in the first instance.

The first model developed described is depicted in the Di-graph in Figure 4-12 (a). The underlying dynamic equations, concepts and data fitting methods are described by Stacey et al. [81] and also briefly in Section 2.9.

Whether the root cause of cell death is nutrient depletion or toxic metabolite build up, this model structure is still applicable to describe the phenomena – but as the inverse (as described by Stacey et al. [100]). In this case, a cell released factor was attributed to cell death – but the model would still apply if nutrient depletion occurred and optimised medium supply as an output from the model would still be applicable.

To parameterise the model, cell density data from short-term, high temporal resolution, high density cultures with a complete medium exchange was used, as shown in Figure 4-12. Therefore, no conditioning factor was present at time zero and possible effects due to low density effects are mitigated. It was assumed that there was no decay of non-viable cells, no decay of cell conditioning factor as short-term data was over a period of 150 hours and there was no growth inhibition present.

There were systematic deviations between the cell density experimental data and the parameterised model fit as shown in Figure 4-12 (b). The model predicted the number of non-viable cells well, however the viable cell density was much lower, since a lower growth rate was fitted, presumably to enable adequate fitting of the conversion rate of viable to non-viable cells to produce the non-viable cell fit.

The deviation of modelled cell density compared to experimental data suggests that maximum growth rate was likely to be higher than the parameterised growth rate obtained from the model fit in

Figure 4-12 (c). Furthermore, growth inhibition was observed as noted in Section **Error! Reference source not found.** and Figure 4-8 (however its effects were not easily observed) it was hypothesised that growth inhibition could account for the lack of fit. Therefore, growth inhibition was included in the next model iterations.

(a)

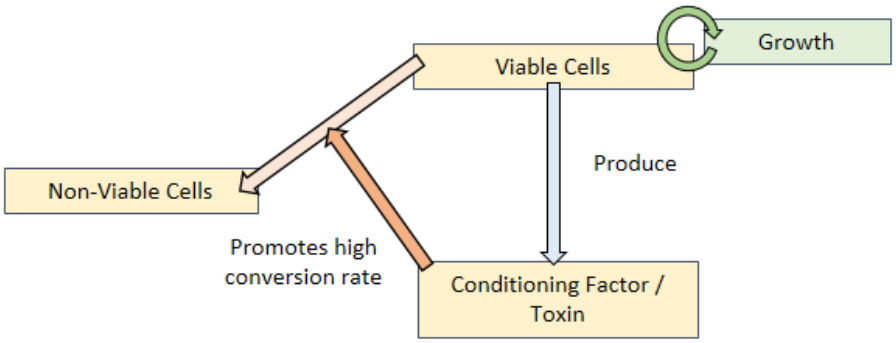

(b)

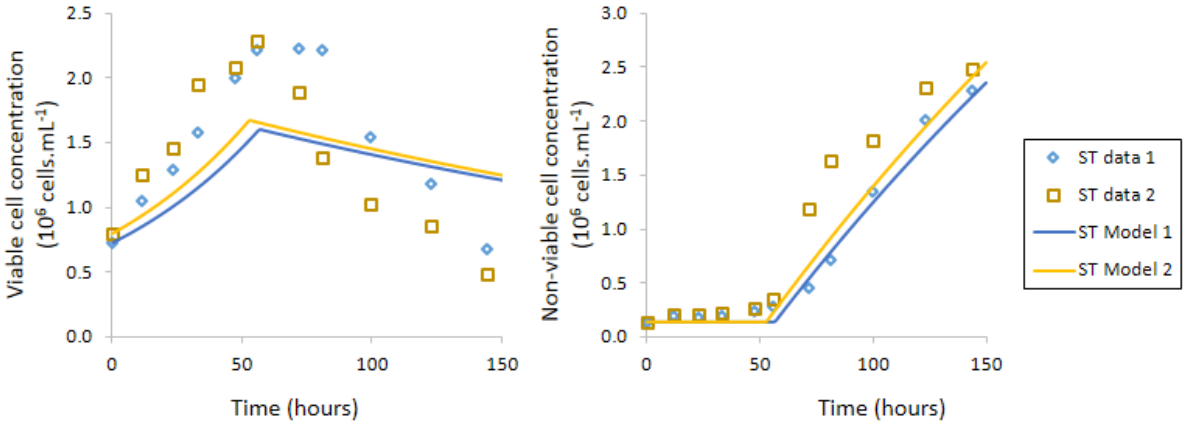

(c)

Max. growth rate (h^{-1})	Max. conversion rate (h^{-1})	Toxin conversion threshold ($U.mL^{-1}$)	Toxin conversion Sensitivity	Creation rate of toxin ($U.cell^{-1}.hr^{-1}$)	Response
0.014	0.017	5	150	8×10^{-8}	1.56×10^{11}

Figure 4-12: Model containing cell death in response to a medium exhaustion produced a systematic deviation from the viable cell concentration data. (a) Di-graph showing mechanistic hypothesis being tested using novel mechanistic modelling framework. (b) Model fit to experimental data shows deviations in the viable cell density over the culture period. The model under predicted viable cell concentration until 80 hours and then over predicted viable cell concentration. The non-viable cell concentration was accurately predicted. (c) Values of parameters fitted by StemCAD, where the response is the sum of the squared errors from the model and the data.

4.5.2. Cell death and growth inhibition in response to the same factor

It was assumed that both growth inhibition and conversion of viable to non-viable cells were driven by the same medium exhaustion parameter, which was a function of cell.time, as illustrated in the Di-graph (Figure 4-13 a). Using the same experimental data used to fit the model as in

Figure 4-12, the parametrised fit using the model adjusted to consider growth inhibition showed no systematic deviations of the pattern in the residual error between the experimental data and the model fit. Compared to

Figure 4-12, a faster growth rate of viable cells was fitted in Figure 4-13, with decreased threshold and sensitivity, giving a better fit of viable cells. Furthermore, the sum of the squared error (Response – noted in

Figure 4-12 and Figure 4-13 c) decreased through inclusion of growth inhibition from 1.56×10^{11},

to 3.33×10^{10}, demonstrating a better overall fit of the model to the experimental data.

(a)

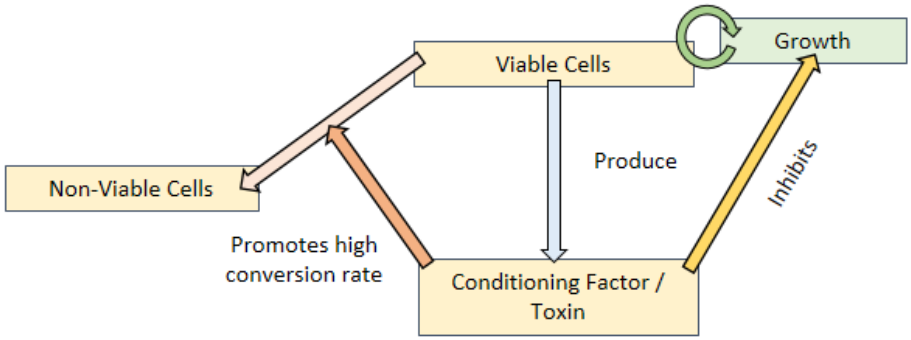

(b)

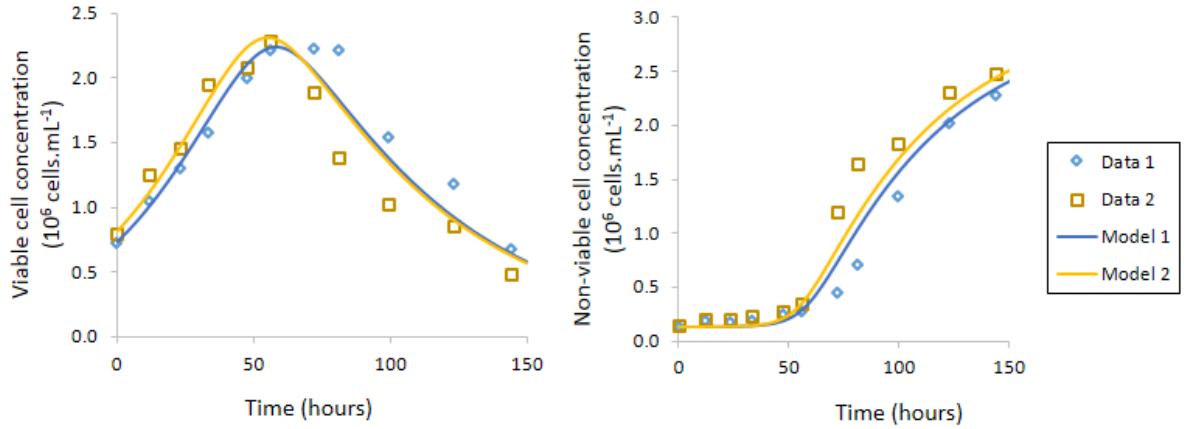

(c)

Max. growth rate (h^{-1})	Max. conversion rate (h^{-1})	Toxin conversion threshold ($U.mL^{-1}$)	Toxin conversion sensitivity	Creation rate of toxin ($U.cell^{-1}.hr^{-1}$)	Toxin growth inhibition threshold ($U.mL^{-1}$)	Toxin growth inhibition sensitivity	Response
0.034	0.018	3.9	1.5	4.5×10^{-8}	2.5	0.6	3.33×10^{10}

Figure 4-13: Model of short-term data based on hypothesis that a cell released factor inhibits growth and promotes conversion of viable to non-viable cells. (a) Di-graph depicting mechanistic hypothesis. (b) There is no systematic deviation between the model and the experimental data, showing model produced a good fit to experimental data. (c) Fitted parameters of model rates.

4.5.3. Model validation over longer culture periods

To validate the model and parameterisation of the short-term growth kinetics, the same model and parameterisation was applied to a longer culture period (350 vs. 150 hrs), which included a series of partial medium exchanges (experimental data used is shown in Figure 4-6). However, as shown in Figure 4-14 (a), the number of non-viable cells was systematically under-predicted by the parameterised model and the highest values of viable cells achieved in the experimental data were not predicted by the model.

In order to trouble shoot the discrepancies in behaviour between the long- and short-term culture dynamics, the model was parameterised using the long-term culture experimental data. The resulting model fit is shown in Figure 4-14 (b) and the parameterisation in Figure 4-14 (c). This re-parametrisation produced a better model fit (shown by the proximity of the experimental data to the model). However, it was parameterised differently, as shown in Table 4-2.

Table 4-2: Comparison of fitted parameters from the short-term and long-term experimental data

Parameter	Short-term culture	Long-term culture
Maximum growth rate (h^{-1})	0.034	0.028
Maximum conversion rate (h^{-1})	0.018	0.006
Toxin conversion threshold ($U.mL^{-1}$)	3.9	1.6
Toxin conversion sensitivity	1.5	1.6
Creation rate of toxin ($U.cell^{-1}.h^{-1}$)	4.5×10^{-8}	6×10^{-8}
Toxin growth inhibition threshold ($U.mL^{-1}$)	2.5	6
Toxin growth inhibition sensitivity	0.6	0.5

Compared to the short-term, the long-term parameterised model had a lower maximum growth rate, conversion rate and conversion rate threshold and a higher creation rate of toxin and toxin growth inhibition threshold. The parameters produced from the long-term culture

model fit were then overlaid on the short-term data as a validation step. The re-parameterisation produced a good fit until 50 hours, suggesting that the rapid death is not captured in the long-term model.

The short-term data set recorded cell numbers over 150 hours without a medium exchange, whereas a medium exchange was performed at 50 hours in the long-term data set. Therefore, it was possible that the response of viable cells to the higher level of medium exhaustion (which was produced in the short-term data) was not adequately captured by the long-term experimental data set.

(a)

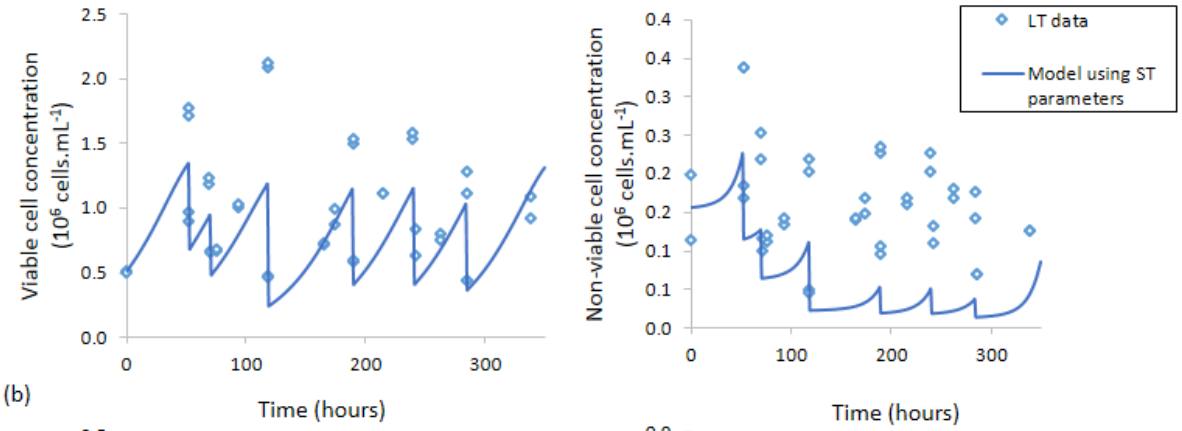

(b)

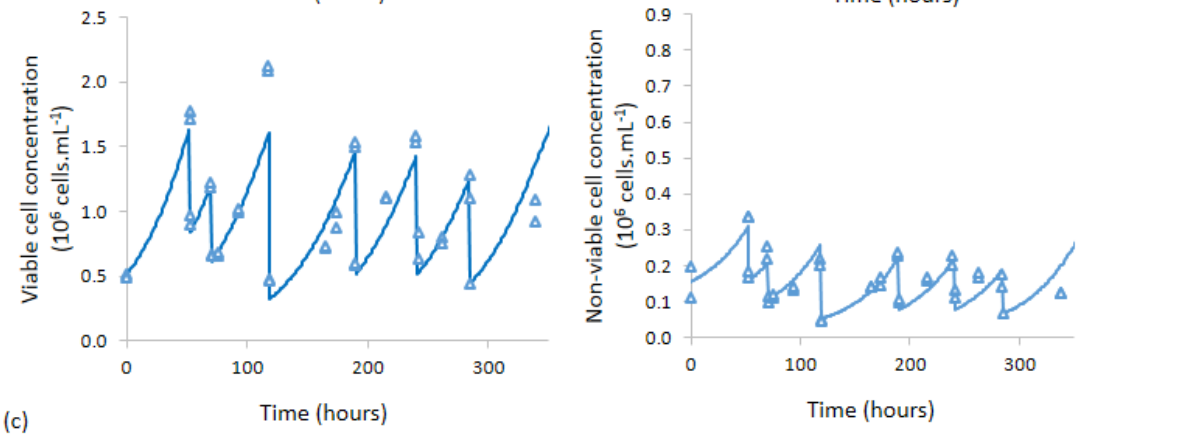

(c)

Max. growth rate (h^{-1})	Max. conversion rate (h^{-1})	Toxin conversion threshold ($U.mL^{-1}$)	Toxin conversion sensitivity	Creation rate of toxin ($U.cell^{-1}.hr^{-1}$)	Toxin growth inhibition threshold ($U.mL^{-1}$)	Toxin growth inhibition sensitivity	Response
0.028	0.006	1.6	1.6	6×10^{-8}	6	0.5	4.22×10^{10}

(d)

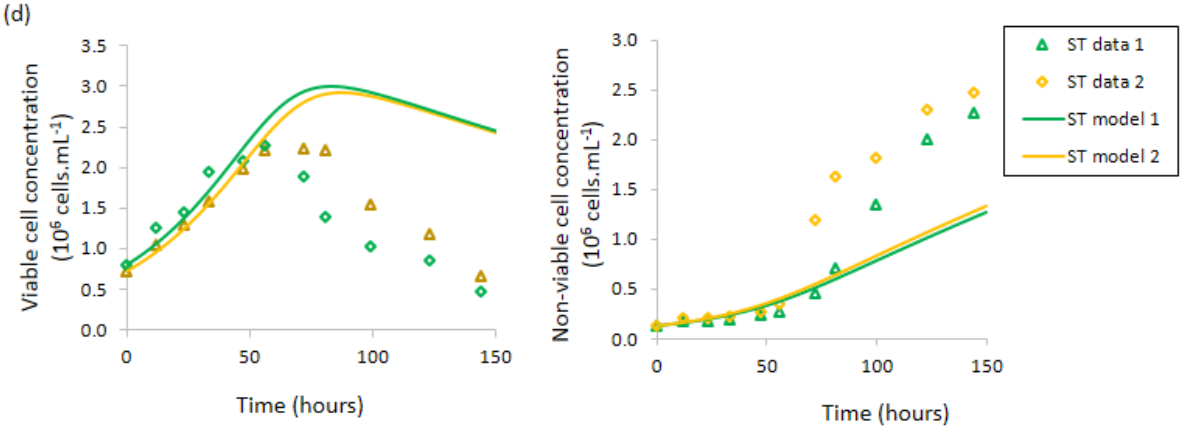

Figure 4-14: There is systematic deviations between the fitted models of short-term and long-term FOPMK data. (a) Parameters from the short-term model were used with the long-term data as an attempted validation step. The model under predicted the concentration of non-viable cells and viable cells. (b) Parameters were fit to the long-term model which removed systematic deviations. (c) Fitted values showed long-term data had a lower threshold compared to short-term models and a lower maximum conversion rate. (d) The long-term parameters were used with the short-term data producing a good fit for the first 50 hours, suggesting the rapid conversion is not accurately modelled in the long-term data.

4.5.4. Expanding model fit to include both long- and short-term culture data

To diagnose the differences in the short-term and long-term data, the model was expanded and re-parameterised using both data sets.

The parameterisation led to a good model fit for the long-term viable cell data closely as shown in Figure 4-15 (ai), however slightly under-predicted maximum cell concentrations (also demonstrated in Figure 4-14 d). As shown in Figure 4-15 (bi), the parameterisation led to a good model fit to viable cell densities in the short-term culture, prior to inhibition and conversion, suggesting that the same maximum growth rate was applicable to both the long-term and short-term data (also shown in Figure 4-14 d).

There was a systematic deviation between the non-viable cell density experimental data and fitted model as shown in in Figure 4-15 (aii and bii). Non-viable cell concentrations were over predicted in the long-term model, and were over, then under, predicted in the short-term model.

To determine whether the there was a decay of non-viable cells over the long-term data, a decay rate of non-viable cells was included as an addition model parameter. However, the fit drove the parameter to very low values ($<1\times10^{-15}$ h^{-1}) (data not shown). Furthermore, including a parameter to capture conditioning factor decay with time did not improve fit either. Again, because the parameter was driven to very low values ($<1\times10^{-15}$ h^{-1}) (data not shown). Therefore, it was unlikely that the decay of non-viable cells or the decay of toxin were causing the systematic deviations of the model fit to the experimental data as shown in Figure 4-15.

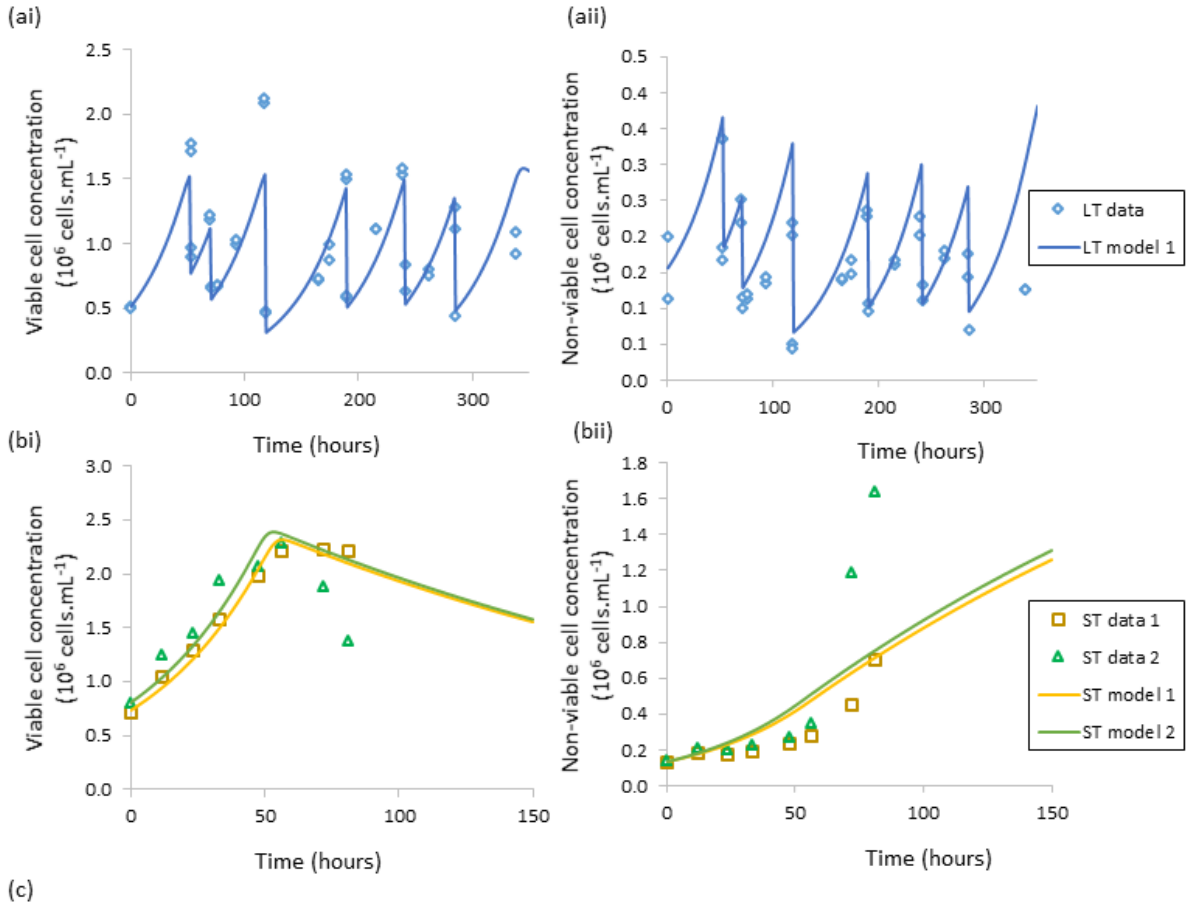

(c)

Max. growth rate (h^{-1})	Max. conversion rate (h^{-1})	Toxin conversion threshold ($U.mL^{-1}$)	Toxin conversion sensitivity	Creation rate of toxin ($U.cell^{-1}.hr^{-1}$)	Toxin growth inhibition threshold ($U.mL^{-1}$)	Toxin growth inhibition sensitivity	Response
0.026	0.01	52	0.006	4×10^{-8}	3	7.5	6.04×10^{4}

Figure 4-15: Fitting both the long-term (a) and short-term (b) data with the same model parameterisation produces systematic deviation with respect to non-viable cell concentrations. (c) Fitted toxin concentrations across the time frame. (d) Fitted parameters show a high conversion rate, high threshold with a low sensitivity and a low threshold for growth inhibition.

4.5.5. Fitting the model with a reduced short-term data set

It was hypothesised that the long-term and short-term data were more useful to parameterise different growth dynamics. There was a much higher concentration of conditioning factor in the short-term data set past 150 hours which was not present in the long-term data and so the model may not be complex enough to deal with the response of viable cells to the different range of toxin concentrations present in the short- and long-term

experimental data. As death rate rapidly increased in the short-term data set there could have been multiple failure modes which accelerated the cell death rate. Therefore, only the first 80 hours of the short-term data was included, and the model was parameterised again.

The re-parametrised model using the reduced short-term data set produced a better fit to long-term data and parameters were closer to the parameterised produced when using the long-term data only. This may have been influenced by the lack of short-term data to fit the

(a)

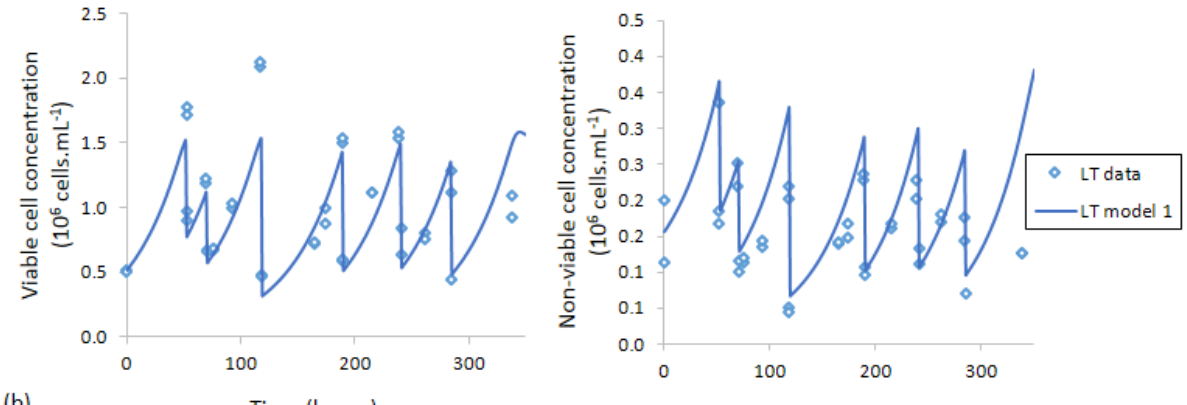

(b)

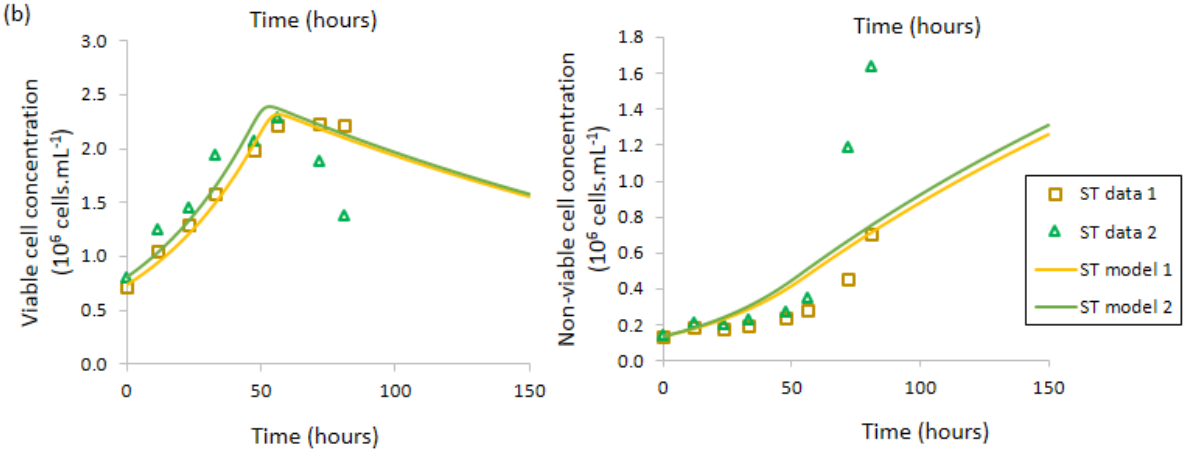

(c)

Max. growth rate (h^{-1})	Max. conversion rate (h^{-1})	Toxin conversion threshold ($U.mL^{-1}$)	Toxin conversion sensitivity	Creation rate of toxin ($U.cell^{-1}.hr^{-1}$)	Toxin growth inhibition threshold ($U.mL^{-1}$)	Toxin growth inhibition sensitivity	Response
0.026	0.01	52	0.006	4×10^{-8}	3	7.5	6.04×10^{4}

Figure 4-16: Short-term data only included up to 80 hours as after this point the mechanisms that govern cell conversion may not be applicable. Further experimental data will be needed to confirm this hypothesis. (a) Long-term data and fitted model shows good prediction of both viable and non-viable cells (b) Reduced short-term data and fitted model fits viable cells well, however still diverges from non-viable cell concentration data. (c) Fitted values are closer to values produced by long-term data fit alone.

model too – since the fitting is based on a least squares method, fewer data points would allow the model to skew towards the data set with the most points.

4.6. Model validation using scalable stirred suspension platform

It was hypothesised that static cultures could be used to parameterise models and these models could be applied to scalable, stirred suspension culture systems to identify similarities and differences between the mechanisms underpinning cell expansion in different culture platforms. A similar approach has been taken by Kiparissides et al. [80].

Experimental data from static cultures was used to parameterise the cell growth, death and inhibition model (depicted by Di-graph in Figure 4-13 a). The resulting parameters are shown in Figure 4-17 (a) and compared with the final combined short- and long- term data in Table 4-3.

Table 4-3: Comparison of finalised parameters for the short- and long- term model using cell line BOB and the static model parametrised using cell line FFDK.

Parameter	Short-and long-term combined model (cell line BOB)	Static culture model (cell line FFDK)
Maximum growth rate (h^{-1})	0.026	0.014
Maximum conversion rate (h^{-1})	0.01	0.05
Toxin conversion threshold ($U.mL^{-1}$)	52	13
Toxin conversion sensitivity	0.006	0.06
Creation rate of toxin ($U.cell^{-1}.h^{-1}$)	4×10^{-8}	1.1×10^{-7}
Toxin growth inhibition threshold ($U.mL^{-1}$)	3	11
Toxin growth inhibition sensitivity	7.5	16

In the FFDK data set there was a lower growth, higher maximum rate of conversion of viable to non-viable cells and a lower conversion threshold compared to the model parameterised using BOB. Whereas the growth inhibition threshold was higher in the FFDK model. This resulted in higher conversion rates of viable to non-viable cells in the FFDK culture system

whereas growth inhibition was more likely to occur the BOB culture system for equivalent concentration of toxin. It is unclear what the root cause of the parameterisation differences was but it was likely that multiple mechanisms were being represented as one medium exhaustion dynamic (for example, time decay of medium components, interacting nutrient / metabolic consumption / production kinetics) that could be dependent on cell line differences or variation in medium lots (and response of the medium to storage). To elucidate the differences in behaviour, additional measurements would be needed (for example glucose, amino acids, fatty acids, ammonium, lactate, growth factor concentrations) to determine whether the metabolic profile of the two cell lines was causing the difference, or whether it was a difference in medium lots. Furthermore, medium development work should be conducted on a non-proprietary-defined system (which is ideally comprised of recombinant components only to ensure batch-to-batch consistency), that can be deconstructed as the effect of each component on the system can be measured.

The model fit parameterised on the static system is shown in Figure 4-17 (b), and the parameters achieved from the static system are the fitted parameters were applied to a drip-fed batch stirred suspension culture Figure 4-17 (c) as a form of validation. There was a good fit to the viable cell data (i) as shown since there was a lack of systematic deviations between the experimental data and the model. In both the static and the drip-fed batch systems the number of non-viable cells were systematically under-predicted, suggesting that there was higher growth and death rates than the model was capturing. The toxin concentration for both systems remained similar (Figure 4-17 iii). Overall this preliminary model data set suggests the two platforms were comparable and there are no obvious detrimental factors caused by a stirred suspension system to FOPMKs.

(a)

Max. growth rate (h^{-1})	Max. conversion rate (h^{-1})	Toxin conversion threshold ($U.mL^{-1}$)	Toxin conversion sensitivity	Creation rate of toxin ($U.cell^{-1}.hr^{-1}$)	Toxin growth inhibition threshold ($U.mL^{-1}$)	Toxin growth inhibition sensitivity	Response
0.014	0.05	13	0.06	1.1×10^{-7}	11	1.6	2.41×10^{10}

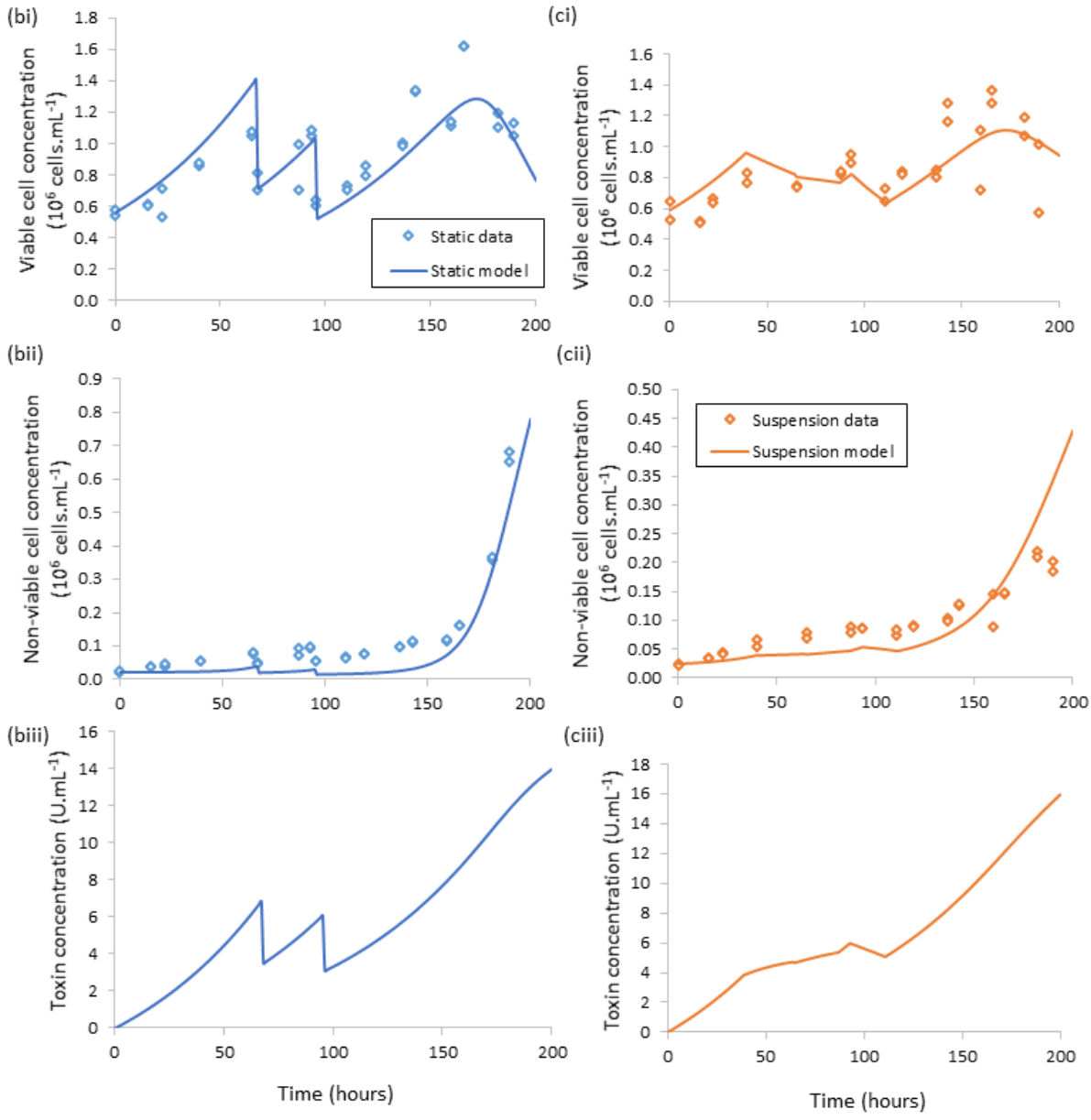

Figure 4-17: Model parameterised using data collected using (a) static culture platform and (b) applied to the suspension culture data showed that similar culture dynamics are found in both systems. Cell line used was FFDK, data shows N=2.

4.7. Conclusions and Future Work

This chapter aims to present a proof of concept study for a methodology to identify and quantify key process dynamics for a cell expansion system, using 1st generation FOPMKs as a clinically relevant case study.

The first section of this chapter identifies medium exhaustion, which was a function of cell.time, was causing a conversion of viable to non-viable cells as being the major culture limitation. The system productivity limit was 1.48 ± 0.28 × 10^6 viable cells.ml^{-1}. Growth inhibition, resulting from complex and multiple mechanisms such a mass-transfer limitations, cell contact or medium exhaustion, was also identified. From this a brief assessment of the possible factors that caused the critical processing issues (cell death) was conducted, which indicated that glucose lactate, ammonium or growth factor concentrations were unlikely to be limiting. Since the medium used consisted of proprietary base, a small study was undertaken with non-proprietary IMDM-based medium, which sustained growth longer than the proprietary medium. Furthermore, a small study was conducted using the Ambr-15 bioreactor system, which showed that the culture dynamics identified in static platforms (cell growth and conversion to non-viable cells) were broadly conserved.

A model using ODE equations were used to express the cell growth and death in response to medium exhaustion. Cell growth and death alone was not sufficient to explain fit adequately to the culture dynamics, therefore growth inhibition in response to the same exhaustion causing cell death. Short- and long- experimental data was used to parameterise the model. A second cell line was used, and the parameterisation of the models created with the two different cell lines were compared, and the model was validated using a fed-batch stirred suspension platform.

This chapter showed that by dynamic, mechanistic models could be used to adequately model cell expansion and culture limitations. Limited model validation and robustness tested was applied here. Goodness-of-fit metrics are widely debated and challenged in modelling fields [140]. Here, systematic deviations of experimental data from the model fit were informally analysed and used as the main goodness-of-fit metric. In published work using this platform [81] and in models developed in Section 6, residual error is plotted and R2 values are reported.

Further experimental work to define the components causing cell growth inhibition or refine and validate the culture dynamics model was not undertaken since the technology moved onto the 2nd generation FOPMK system. To gain further insights into the causes of cell death the following would have been completed:

- Assessment of the impact of lactate, ammonium and glutamine concentrations on FOPMK growth dynamics through the additions of known concentrations.
- Assessment of cytokine profiles across a culture period to identify possible limiting factors.
- Oxygen consumption evaluation as an assessment of the possible limitations in stirred-tank culture systems.

The culture dynamics described are complex and interacting, therefore qualitative assessments to provide improve production strategies are not straightforward but are essential. Here the foundation of a quantified models of FOPMK culture behaviour using the data are presented. To further develop the models presented in this chapter, the following questions would need to be addressed:

i. Was the difference between the short-term and long-term data caused by experimental specification in long-term data?

- The long-term data contained serial interventions. Small errors in each may have caused a build-up of errors resulting in significant deviations.
- Differences in static culture platforms (for example, T-flasks and well-plates), noted in Section 3.3, could be causing variation, for example in mass transfer coefficients, which are not described in the model.

ii. Was the difference caused by behaviours in the long-term data set that are not modelled currently?

- For example, the medium exchange is a partial exchange over 400 hours and it could be possible that other nutrient decay is affecting the culture system.

iii. Are cell populations being modelled are inherently different and therefore cannot be described by a common model?

- If no secondary short-term data sets matched the collected data set, this would be the most likely explanation for model deviations.

In order to answer these questions, further experimental work could have included:

1. Hypothesis driven experiments to allow in depth discussion of what changes dynamically in the culture FOPMKs and identify culture productivity limitations. This would include cytokine arrays and common nutrient / metabolite screening.
2. Monitoring phenotypic rate of change over the longer term to address whether phenotypic cycles are connected to feed regime or completely independent and whether this correlated to changes noted in (1).

This would culminate in the unification of the modelling and the measurement driven approaches into a single process which can be used for detailed manufacturing insight.

However, the forward programming technology that produced the cell types presented in this chapter evolved, making further iterations to the above data sets of limited value. To create the 1st generation FOPMKs, PSCs were transduced with 3 transcription factors, each contained within their own lentiviral vectors. This created a multi-clonal population that could proliferate for over 90 days. In the 2nd generation of forward programming iPSCs were targeted with an inducible genetic cassette therefore cells could be cultured as iPSCs and forward programming could be induced with the simple addition of Dox to the culture medium. This second generation of cells only expanded for around 30 days, and therefore the long-term, stable expansion was likely to be less critical. Also, the population of the 2nd generation FOPMKs were more homogeneous and so there may be different culture dynamics. Therefore, the subsequent chapters focus on the application of both statistical and dynamic modelling tools to the culture of inducible iPSCs and the forward programming using 2nd generation FOPMKs.

5. Application of Quality by Design to forward programming of doxycycline-inducible iPSCs to define system productivity limits

5.1. Introduction

In the original forward programming approach described by Moreau et al. [116] a cocktail of lentiviral vectors delivered three transcription factors – GATA1, FLI1 and TAL1 to PSCs to initiate "forward programming" which transformed iPSCs to FOPMKs (defined as CD41a+ cells) in around 15 days. These FOPMKs could be cultured for a period of around 90 days post transduction [116]. This process produced high yields of MKs per input PSC (2×10^5 MKs.PSC^{-1}), yields much higher than previously achieved using non-genetically engineered, directed differentiation methods (see Section 1.3.3 for a broader discussion). This system had manufacturing disadvantages in that population heterogeneity could arise from the individual expression (or 2 of 3) of the transcription factors, and once a population was transduced it was committed to terminally differentiation with a limited (if extended) proliferative capacity.

In the second generation of this process (currently unpublished), a TET-ON system was introduced, which incorporated a tetracycline-responsive promoter, GFP, GATA1, TAL1 and FLI1. Post transduction cells were cultured with the same method as non-programmed PSCs. The genetic cassette was activated by adding doxycycline hyclate (Dox – a tetracycline derivative) to the culture medium, which induced forward programming. Currently production of GMP lentiviral vectors is a bottleneck for the gene editing field. Therefore, including a Dox-inducible cassette forward programming method reduces reliance on repeated genetic modification processes, since the FOP-cassette can be present, but silent, in a phenotype that is indefinitely expandable, whereas genome modification in the first generation FOPMK needs to be repeatedly conducted as it immediately creates a system with limited proliferative capacity. The linked gene-expression also overcomes some of the issues of population heterogeneity.

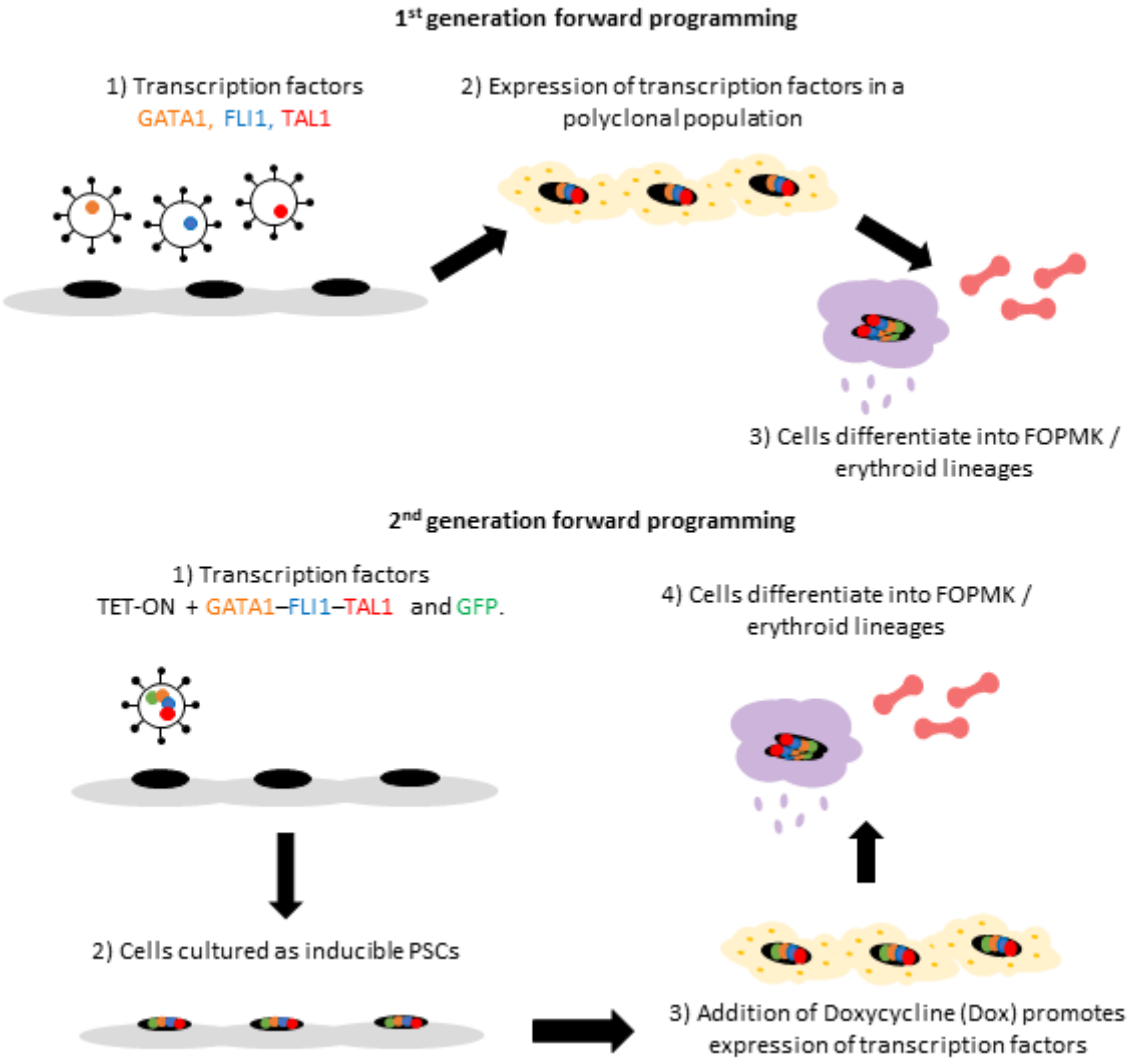

Figure 5-1: Graphic to represent the 1st and 2nd generation of forward programming approaches. The first generation produced polyclonal FOPMKs which proliferated for around 90 days. The second generation was derived using a single cassette which incorporated all 3 transcription factors with a TET-ON promoter and GFP. A single clone was selected to produce an inducible iPSC line.

The graphic shown in Figure 5-2 demonstrates the difference between the two programming methods. Section 4 focuses on defining the system productivity limit of the expandable, stable, MK line generated using the 1st generation process using a novel mechanistic modelling tool. In the 2nd generation process, developing a control strategy to produce megakaryocytes from pluripotent stem cells is more critical since this will be repeatable with the same cell line with reduced heterogeneity.

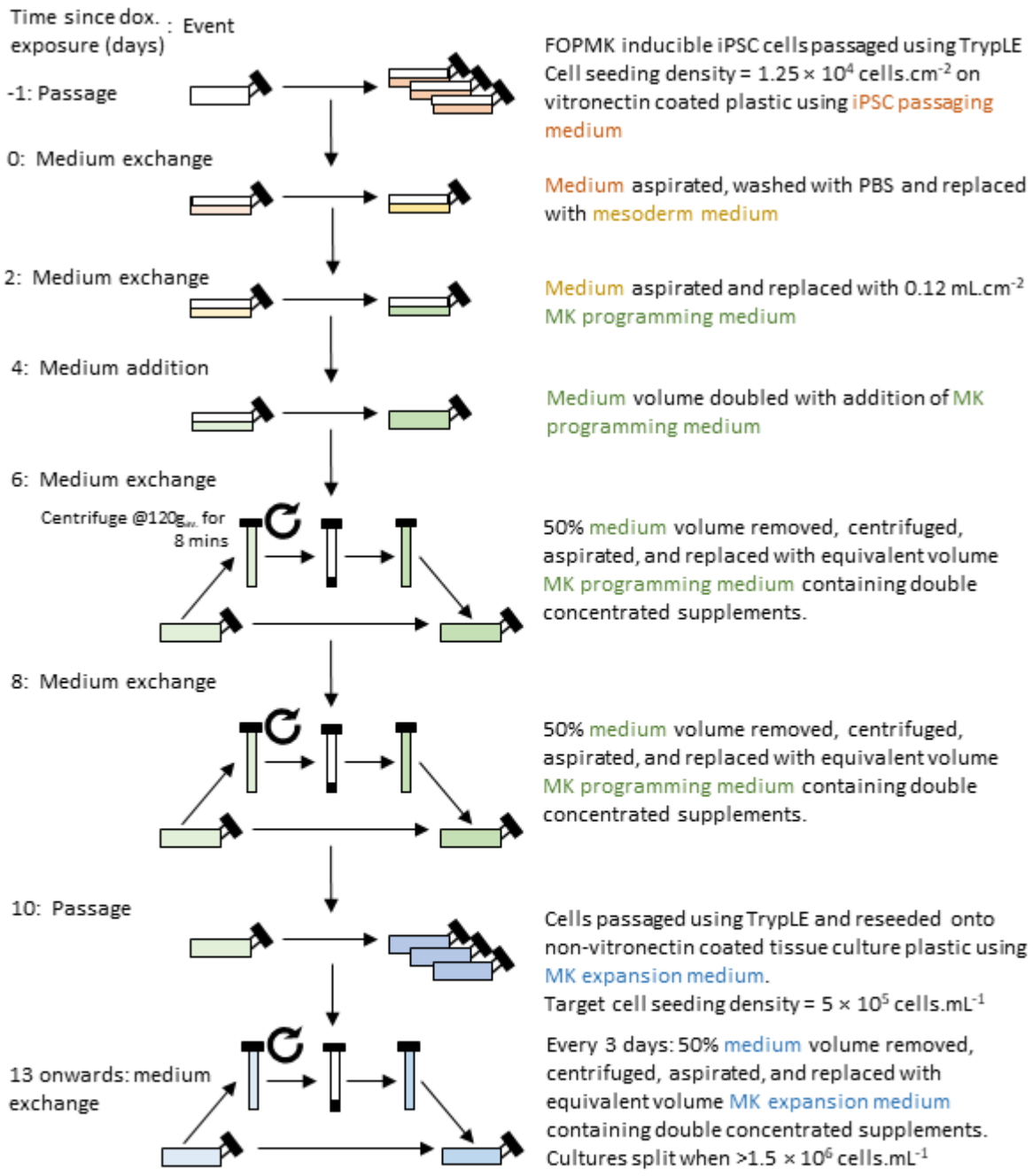

iPSC passaging medium	Mesoderm medium	MK programming medium	MK expansion medium
AE6 medium	AE6 medium	Cellgenix SCGM medium	Cellgenix SCGM
FGF2 (15 ng.mL^{-1})	FGF2 (20 ng.mL^{-1})	TPO (100 ng.mL^{-1})	TPO (20 ng.mL^{-1})
Activin-A (15 ng.mL^{-1})	BMP4 (10 ng.mL^{-1})	SCF (25 ng.mL^{-1})	SCF (25 ng.mL^{-1})
Y27632 (10 mM)	Dox (1 µg.mL^{-1})	Dox (1 µg.mL^{-1})	

Figure 5-2: Process flow diagram for SOP of FOPMK programming process of inducible iPSCs derived from Moreau et al. operating procedures (currently unpublished and described in more detail in Section 2.3.2). Four different media are required which contain several different supplements.

As described in Section 3, a quality by design approach is driven by system risk assessment. From the risk assessment exercise, the impact of the highest risk variables were selected for experimentation to quantify relationships between control variables and CQAs. Design of experiments (as discussed in Section 1.4.1) is a powerful methodology which can define simple linear or curvilinear relationships between experimental variables and responses in an experimentally efficient manner. The value of design of experiments is dependent on some understanding of variable ranges and key risks, hence the risk assessment is important to ensure the response is practically more modellable.

A key step in process development for manufacture is technology transfer between sites either due to contracting out of development stage or changes of scale or geography. Such tech transfer steps often give rise to significant problems due to, for example, unknown variables, differences in available processing equipment, operator variability, communication challenges, and accurate record keeping. However, technology transfer exercises are a valuable opportunity to gain insight in, and experience of, process risks and can therefore be used to inform subsequent targeted experimental design.

In this chapter the challenges in a Quality by Design approach to megakaryocyte precursor manufacture are evaluated. A technology transfer exercise of the second-generation FOPMK process from the originating laboratory to our development laboratory was undertaken. A series of transfer runs were conducted to provide the input to a structured risk assessment for initial DOE. This was the necessary first step towards a platelet manufacturing process, where the production of FOPMKs from inducible iPSCs must be acceptable for production, in terms of economic, quality and risk constraints.

5.1.1. Chapter Objectives

- To apply the CQAs and assays developed in Section 3 to a process transfer, risk assessment and DOE improvement exercise.
- To conduct a technology transfer exercise between laboratories.
- To collate information to inform a risk assessment of key manufacturing controls.
- Identify opportunities for process changes that would improve manufacturability, and related manufacturing controls.
- To apply the most valuable design of experiment approach that accounts for the known attributes and behaviours of the process.
- Provide process recommendations to the originator laboratories, as well as a reasoned requirement/methodology for further development.

5.2. Materials and Methods

Cell line derivation and culture was performed as described in Sections 2.3.1 & 2.3.2. Cell counting was performed using flow cytometry and described in Section 2.5.2. Flow cytometry sample preparation, equipment used, staining and acquisition is described in Sections 2.6.1-2.6.2 - 2.6.3. The flow cytometry assays and cell counting assays used are described in Section 3.3.1 and the assays used are identified in relevant sections and figure legends associated with flow cytometry data.

Design of experiments were conducted as detailed in Section 2.8.1. The number of factors, levels of factors, outputs and whether a centre point was included is detailed along with the results of the DOE outputs in relevant sections.

5.3. Rationale for analytical strategy in process transfer

Chapter 3 describes the surface markers and associated assays for monitoring megakaryocyte quality that will be applied to monitor process transfer. However, there are other process attributes that are critical to delivering the QTPP. In particular, the consistency of the number of cells produced per input iPSC and per unit volume of medium (or specific component amount added) impacts on product quality since the minimum dose must be achieved to satisfy release criteria at a sustainable cost. Furthermore, changes in growth rate or population doubling level may indicate the production of an off-target cell type or production of cells that are metabolically different, which in-turn could act as a surrogate measure for changing functionality. Variability in growth rates could also lead to changes in process state with knock on consequences for phenotype or yield. Therefore, in addition to the phenotypical markers identified above, growth rate and population doubling levels will be monitored.

5.4. Evaluation of transfer protocol to generate inputs to Risk Assessment

The technology originator provided an outline protocol for the culture of the 2nd generation FOPMK cells, which is detailed in Section 2.3.2, and outlined as a schematic diagram in Figure 5-2. Stable, Dox-inducible iPSC clones can, theoretically, be cultured indefinitely as PSCs. Section 4 addresses the culture of inducible PSCs, and this chapter focuses on seeding cells for, and then inducing, forward programming through addition of Dox to the culture medium. Firstly, the performance of the system during tech transfer is described in terms of growth rate, phenotype, and longevity of proliferation, and associated risks are identified. Secondly, the first 10 days of the differentiation process are assessed due to the specific challenges of controlling a process transitioning from adherent cells to suspension cells. Finally,

observations are made on the operational regime during transfer, in particular medium exchange and cryopreservation.

5.4.1. Growth rate

The cell number with time for two tech transfer experiments are shown in Figure 5-3. The net growth across the run were comparable with tech Transfer Experiment #1 produced an average net growth rate of 0.168 days-1 (A), compared to 0.166 $days^{-1}$ in Tech Transfer Experiment #2. This rate was also comparable to the reported growth rate of the 1^{st} generation programming method over a period of 90 days [116], but low compared to other stem cell systems – for example HSCs differentiating to red blood cells have a reported growth rate of 0.0462 hr^{-1}.

The pattern in residual errors between the recorded cell numbers and the exponential trend line, shown in Figure 5-3 (Aii) and to a lesser extent (Bii) until day 22, suggest that there were periods of higher and lower growth rates, rather than a constant lower growth rate, which would have produced a random residual value with time. If the periods of higher growth rates could be sustained without periods of lower growth, this could lead to a higher system productivity (cells produced per unit time) which would decrease facility costs in a manufacturing setting. This is important since facilities can contribute up to 40% of the costs of cell therapy manufacture [141]. However, this would have to be considered alongside the effect of growth rate on total production of desired cell type and the medium provision to the system.

In Tech Transfer Experiment #2, cells were cultured over 31 days is shown in Figure 5-3 (Bi). Cells expanded until Day 22 post Dox addition, after which time the growth rate slowed, as shown in (Bii) where the recorded cell numbers deviated from an exponential fit.

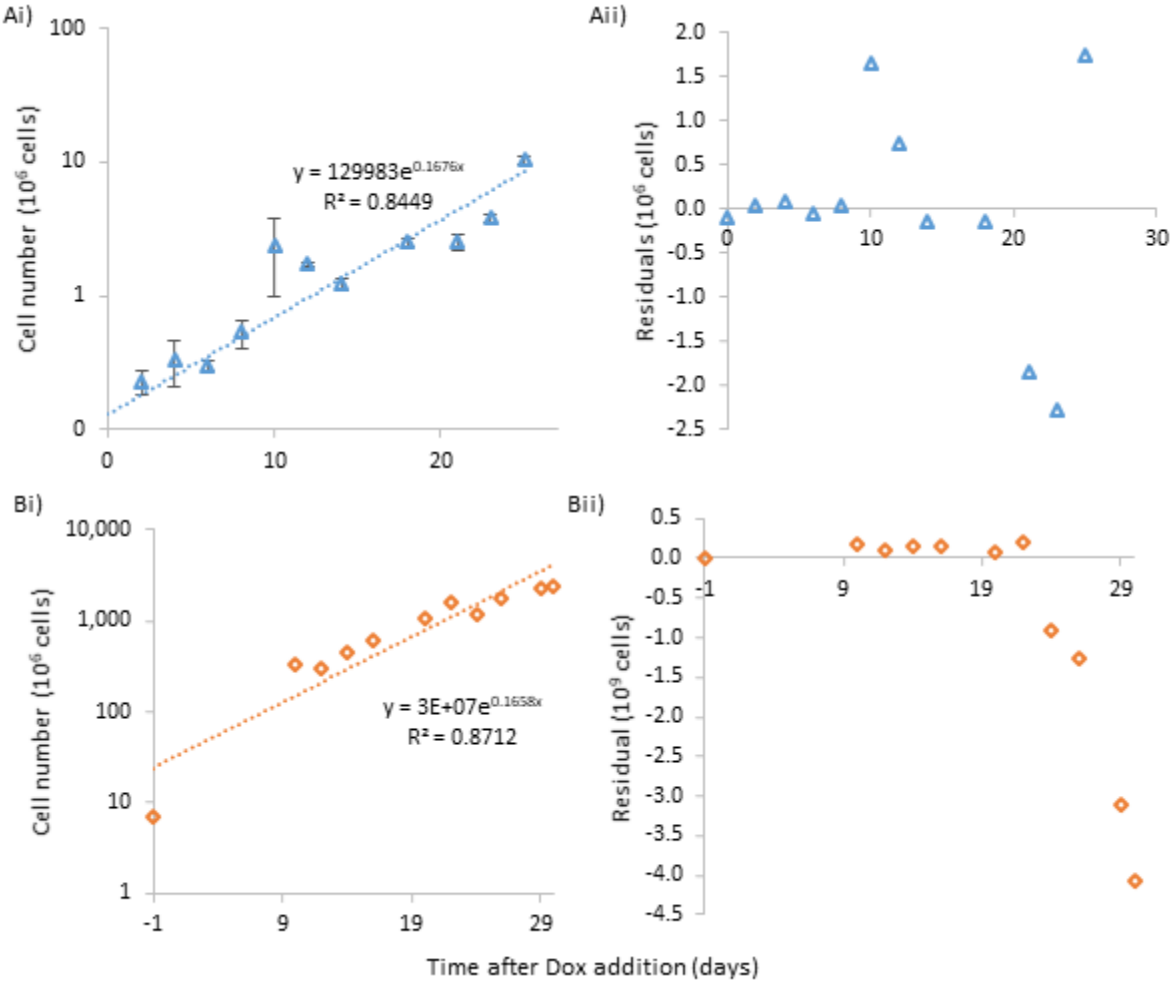

Figure 5-3: Cell densities recorded over the two tech transfer experiments following the transfer protocol produced a consistent net growth rate. Net growth rates were achieved by fitting exponential trend lines to cell density data in Tech Transfer Experiment #1 (Ai) and Tech Transfer Experiment #2 (Bi) show net growth rates of 0.168 day^{-1} (equivalent to t_D= 4.1 days) and 0.166 day^{-1} (equivalent to tD= 4.2 days) respectively. (Aii) Residual plots of the average cell count with respect to the exponential model show that in Tech Transfer Experiment #1 the model underestimated cell number at days 10, 12 and 25, but over-estimated cell number at days 21 and 23, therefore suggesting that the growth rate was not constant across the time-period. (Bii) Residual plots show cell growth rate was constant until day 22, after which time there was a rapid decrease in cell expansion. For (A) data show N=3 biological replicates originating from a single culture at Day -1, ±STD, and for (B) data show N=1.

Process Risk 1: The transfer identified that whilst total growth was comparable as seen by growth rates calculated over the full transfer period, growth rate at any given time was inconsistent with random residuals (to an exponential fit) in transfer 1 and an apparent systematic path of higher growth to lower growth in transfer 2. Such inconsistent growth would make it impossible to keep culture/manufacturing environment in a closely defined

optimal range with a fixed process (i.e. without the expense of online monitoring and control) and would therefore likely to lead to variable process outputs.

5.4.2. Phenotype

To understand the phenotype trajectory of the cells, CD235a, CD41a and CD42a were tracked through both tech transfer experiments, CD42b expression was additionally tracked in Tech Transfer Experiment #2 as shown in Figure 5-4. Data was obtained using optical capture settings in Table 3-12 (panel 5) for Tech Transfer Experiment #1 and Table 3-10 (panel 4) for Tech Transfer Experiment #2. Cells followed the literature established differentiation route [46], [47], with CD235a expression increasing first and then decreasing, followed by increasing CD41a expression and latterly by increasing CD42a expression showing that megakaryocytes had been produced from the inducible PSC line. A small proportion of cells expressing CD42a did not express CD42b (since the loss of CD42b has been associated with apoptosis [142] CD42b- populations should be minimised).

In Tech Transfer Experiment #1 (Figure 5-4 A), by Day 18 over 98% of cells were CD41a+ and by Day 25 over 90% of cells were double positive for CD41a and CD42a. Whereas in Tech Transfer Experiment #2 (Figure 5-4 B) only 62% of cells were positive for CD41a by day 20 post Dox addition, rising to 86% at day 26. The same parameters were used for both tech transfer experiments (as outlined in Figure 5-2), except for the freshness of the Dox. In Tech Transfer Experiment #2 the Dox has been stored in at 4^{o}C for 2 months. It was hypothesised that the reduction in the proportion of cells expressing the right target phenotype was due to decay of Dox leading to reduced efficacy as a promoter of the transcription factors.

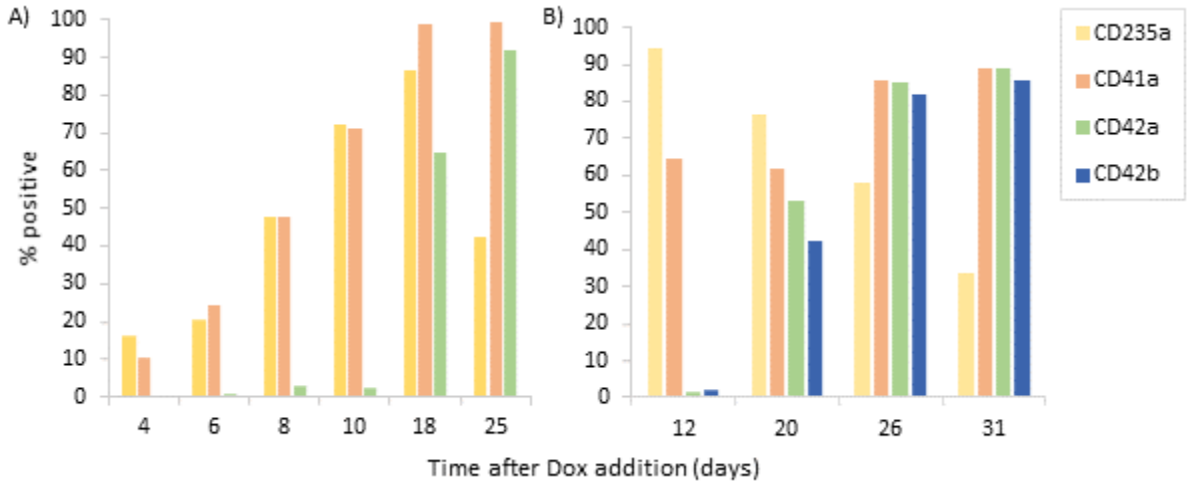

Figure 5-4: Cell phenotype changes over time showed that CD235a increased and decreased with time (indicating a transitioning progenitor population), CD41a expression reached a plateau, CD42a expression increased later than CD41a and a high proportion of CD42a+ cells were also CD42b+. (A) A higher proportion of cells expressed CD41a in Tech Transfer Experiment #1 at Day 18 compared to Day 20 in (B) Tech Transfer Experiment #2. Data show pooled phenotyping from 3 biological replicates originating from a single culture at Day -1 in (A) and N=1 in (B). Phenotype assays used were (A) Panel 5 and (B) Panel 4.

Process Risk 2: Similarly to the variable growth rate, a variable phenotypic output to the extent seen in the transfer runs would inevitably lead to out of specification clinical product. It is unclear from the transfer whether the phenotypic variability is driving growth rate variability or vice versa, or whether the two are entirely independent (although this seems unlikely as cells with different phenotypes are recognised to have different growth properties). An analysis of variation between the transfer runs identifies Dox control (storage and other factors effecting exposure concentrations) as a high priority experimental variable for impacting product purity.

To provide an in-depth comparison of tech transfers for a deeper understanding of the population shifts across time, and to discuss how these may be evaluated with respect to subsequent investigation of process control variables, flow cytometry plots are shown for each tech transfer experiment in more detail in the following sections.

5.4.2.1. Detailed phenotype of Tech Transfer Experiment #1

The cell population decreased in size with time as shown in Figure 5-5 A-Fi as the forward scatter profile decreased. The high side scatter – low forward scatter population also increased. This population stained positive for non-integral membrane dyes (data not shown here, see discussion in Section 3.4) had high granularity, measured by side scatter magnitude. This combination of positive staining for membrane integrity dyes, a shift to higher side scatter and a decrease in forward scatter is an indication of apoptosis [143], showing that there was an increase in the proportion of non-viable cells with increased time since Dox addition. This increased cell death could indicate that FOPMKs matured and produced proplatelets (since there was also a high amount of debris seen in the low forward scatter – side scatter range which could represent proplatelets) as apoptosis has been linked with maturity previously [144], [145] (although that has been disputed [146]). Regardless of whether apoptosis is linked to maturity of megakaryocytes, this process aims to expand the megakaryocytes prior to platelet production, so loss of cells in this stage, whether through apoptosis or proplatelet formation adds to process inefficiencies unless a continual product harvest system is envisaged. Such a continuous harvest system would add a great deal of complexity and is an ongoing challenge for existing simpler biologic products. Furthermore, apoptotic cells in culture can inhibit proliferation in otherwise healthy cells [147].

Process Risk 3: Cell debris are produced during the process that could be the consequence of death or premature maturation. This could also be a driver of inconsistent growth rates due to cyclical changes in populations. Process improvements should seek to minimise cell losses and debris creation where possible to target an efficient batch process, and the flow cytometry debris field could be a useful tool to monitor this.

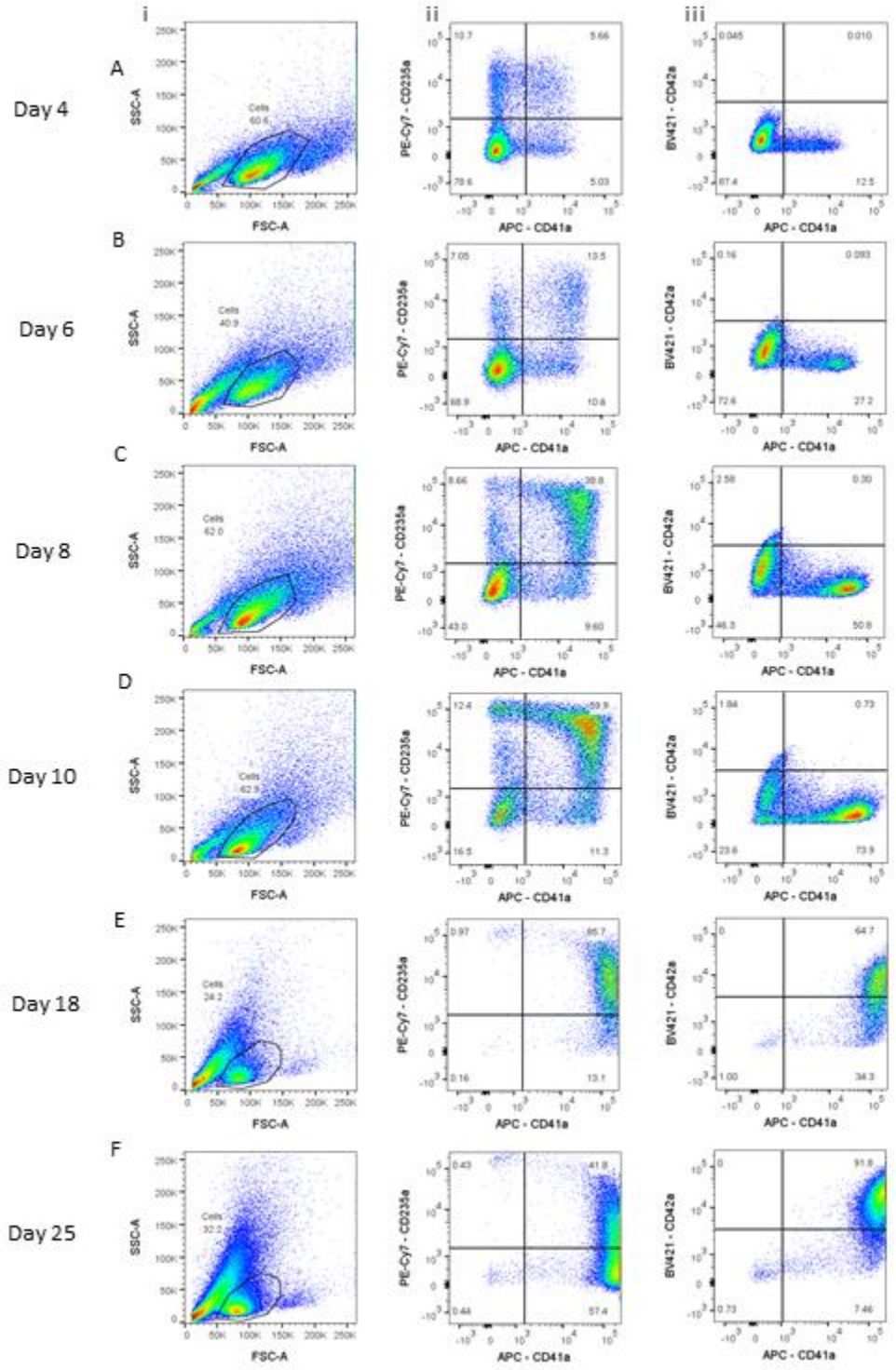

Figure 5-5: Flow cytometry plots for Tech Transfer Experiment #1 shown in Figure 5-4 (A). A-F show increasing time points; (i) Forward scatter – side scatter plots show decreased forward scatter (and therefore cell size) and an increased proportion of events which are low forward scatter and high side scatter (small size and high granularity) indicating the proportion of apoptotic cells and cell debris increased with time. (ii) Cells initially increased their expression of CD235a and CD41a, with a proportion of cells appearing to transition straight to CD41a expression without first expressing CD235a. Over time cells mature by increasing CD41a expression and initially increasing, then decreasing CD235a expression. (iii) CD42a does not increase until after day 10, however there was slight changes in the fluorescence in the BV421 channel in the double negative gate, which was present in the unstained sample (data not shown) showing that the auto-fluorescence of the populations increased. In E and F, a new antibody lot of…

[Figure 5-5 continued]…APC-CD41a was used which increased the MFI in the APC channel above the detectable range, demonstrating the importance of antibody titrations. The trend of CD41a expression is still conserved along with a small population of CD41a- cells showing that this data can still be used to determine %CD41a+. Optical Capture settings used was Panel 5 as detailed in Table 3-12.

At Day 4 (Aii) most cells were double negative for CD235a and CD41a, but some began to express CD235a and CD41a. It appears that some cells expressed CD235a and then gained CD41a expression, whereas others moved to expressing CD41a without first passing through CD235a. However, the exact transition path is unclear because the cells could have first expressed CD235a and lost this expression prior to Day 4. Since the first measurement was taken at Day 4 the changes in phenotype between Day -1 and Day 4 were not recorded.

Process Risk 4: There is uncertainty in the path that cells take to reach a given target phenotype, and the precise dynamics of marker expression. CD235a expression may be transient or not present at certain early stages. This uncertainty and potentially rapid change should be borne in mind if interpreting intermediate cell phenotypes as in process CQAs.

For the phenotype analysis at Day 18, a new antibody lot of APC-CD41a was used and, although used at the manufacturer's recommended concentration and the same concentration as the previous antibody lot, the fluorescence became higher than the detectable range. Since the two antibody lots were never used in parallel, it is not certain whether the shift was caused by the difference is antibody lot, or a genuine increase in CD41a expression. However, since a proportion of cells at Day 10 had a similar CD235a expression level, it is unlikely that the increase in APC fluorescence at Day 18 was linked to an increase in marker expression; the most probable cause was a difference in antibody lots. Furthermore, variability between antibody lots is a known issue [148].

Process Risk 5: Antibody lot variability may lead to differences in measured phenotypes between process batches that do not correspond to real differences. This is a broader issue relating to assay and analytical equipment control in development within and across sites. Within subsequent development experiments antibody lots were controlled.

5.4.2.2. Detailed Phenotype of Tech Transfer Experiment #2

As was seen in Tech Transfer Experiment #1, significant debris were also found in Tech Transfer Experiment #2 (Figure 5-6 i), which again demonstrated that the release of debris occurred during forward programming and confirmed *Process Risk 3*.

Compared to Tech Transfer Experiment #1 at day 10, Tech Transfer Experiment #2 produced a much higher proportion of CD235a+/CD41a- at day 12 as shown in Figure 5-6 (Aii). At day 18 a separate population which was high CD235a expression and CD41a/42a/42b- emerged. Furthermore, there was a red colouring to the cell pellet after centrifugation which indicated that these are contaminating erythroid cells rather than immature megakaryocytes (Figure 5-6 E).

Process Risk 6: CD235a appears to be expressed on megakaryocyte, "on-target" progenitor cells mid-differentiation, however expression reduces in the later stages of differentiation (Day 18 onwards) or on-target megakaryocytes but increased on "off-target" erythroid lineages. As with Process Risk 4, this must be considered when developing process CQAs.

Feedback from our collaborators suggested the large number of contaminating cells may be due to sensitivity to Dox exposure, since they had qualitatively found that using Dox which was made fresh and frozen led to better process outcomes. The product data sheet does not provide information on the shelf life of Dox dissolved in water stored in the fridge, therefore

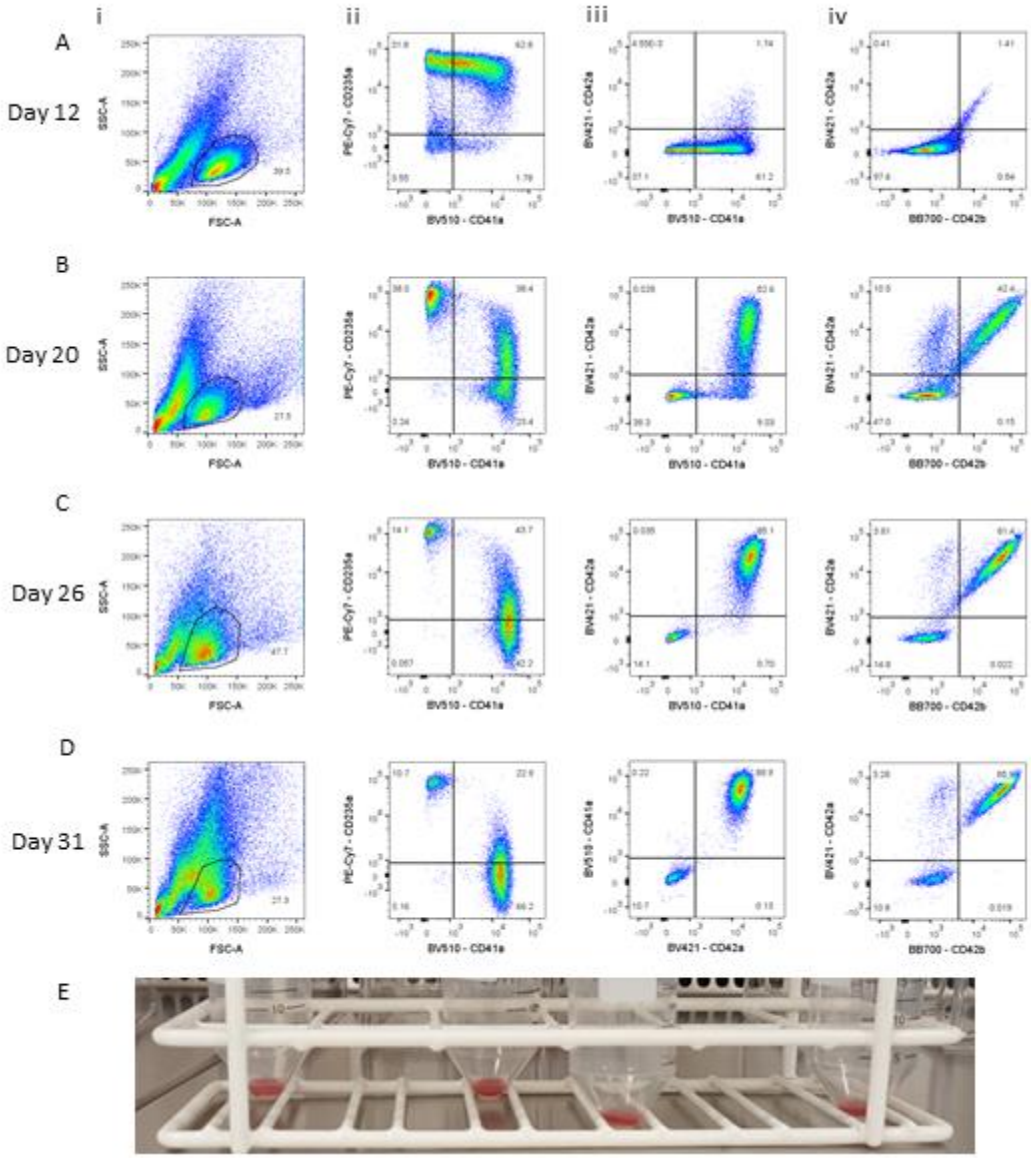

Figure 5-6: Phenotype changes in Tech Transfer Experiment #2 shown in Figure 5-4 (B). By Day 26 >85% of cells were double positive for CD41a and CD42a. (A-D) show detailed phenotype changes with increased time since Dox addition, (i) Forward scatter / side scatter profiles show target cell profiles along with a population with increased granularity - at Day 31 (Di) there was a shift into the higher granularity population which coincided with lower net expansion, indicating an increase in cell death. (ii) Expression of CD41a and CD235a changed with time. At Day 12 (Aii) most cells are positive for CD235a and are gaining expression of CD41a. From Day 20 (Bii) two populations were present, one of which was CD235a+/CD41a- and the second was CD41a+ with decreasing CD235a expression and the former population decreases with time and is not seen in Tech Transfer Experiment #1. (iii) Expression of CD41a and CD42a changed with time. At Day 12 cells expressed low levels of CD41a and CD42a, whereas from Day 20 (B, C, Diii) there were 2 separate populations, one which was CD41a+/CD42a+ and the other CD41a-/CD42a-, the latter of which decreased across time. (iv) The proportion of cells expressing CD42a and CD42b increased with time. A small proportion of cells were an off-target phenotype CD42a+/CD42b-. (E) Red pellets at Day 20 indicate that there was a significant contamination from erythroid lineage cells. Flow cytometry acquisition was performed with Panel 4 (Table 3-10).

the decay rate of Dox with time would need to be assessed or verified for a manufacturing process that utilised Dox. This re-emphasised the focus on Dox as a key control variable.

5.4.3. Proliferative longevity of cells

The proliferative longevity of the cells potentially varied between the tech transfer experiments. In Tech Transfer Experiment #1 the cells expanded until day 27 post-Dox addition (Figure 5-3 A), after which time they were cryopreserved. In Tech Transfer Experiment #2, the cell number growth began to slow systematically after 22 days, as shown by the deviating cell number from the exponential growth curve (Figure 5-3 B). It is possible this discrepancy in expansion potential was caused by cell phenotype divergence associated with the risks identified (Figure 5-4, Figure 5-5 and Figure 5-6).

Process Risk 7: Variable expansion per input iPSC increases process risk as the target number of FOPMKs required may not be reached. However, this is going to be a function of phenotype, so appropriate lineage and proliferation rate control would be expected to address variable longevity.

5.4.4. Identifying analytical and process challenges during the day 0 to day 10 phase transition from adherent to suspension culture of target cells

Cells began to lift from the culture plastic surfaces during the first 10 days of culture. To investigate the cell populations that were being released, the cells in the medium supernatant were collected and analysed as shown in Figure 5-7. Gating was applied on the forward scatter – side scatter flow cytometry profiles based on the target population identified in the attached cell cultures (Figure 5-7 A). However, even within these gates the target population was not visible until Day 8, instead there was a large population of debris. Figure 5-7B also shows that at Day 2 there were large numbers of small, very granular cells (yellow arrows

show examples) whereas at Day 10 cells were larger and less granular cells (blue arrows show examples). This suggests that early in the culture the cells released are apoptotic debris, but suspension cells later in the culture are part of the target population. Also, at day 2 there was evidence of structures with proplatelet-like morphology (small and elongated) but since they did not express the right phenotypic markers it was unlikely the structures were functional platelets.

The number of attached cells compared to suspended cells is shown in Figure 5-7 C. At Day 2, 26% of the total cells are suspension cells. However, this figure is obtained by placing the target cell gate on the suspension cells and at days 2-6 the target population was not discernible from the debris (since there was a large amount of debris and a small number of target cells). Therefore, the recorded number of suspension cells could be an increased value based on gating only (i.e. a measurement error) and not representative of the actual number of target cells.

Process Risk 8: Target cell counts prior to day 8 are difficult to distinguish from the high amount of debris, therefore quality indicators within this period may lead to inaccurate conclusions about process outputs and challenges interpreting the impact of control variables. Subsequent experimental work will space the phenotypic analysis at regular intervals to reduce risk of phenotypic misinterpretation at specific timepoints; also, although time-consuming, subsequent experiments will need to be conducted for a sufficient differentiation time course to validate that early stage effects translate to end of process.

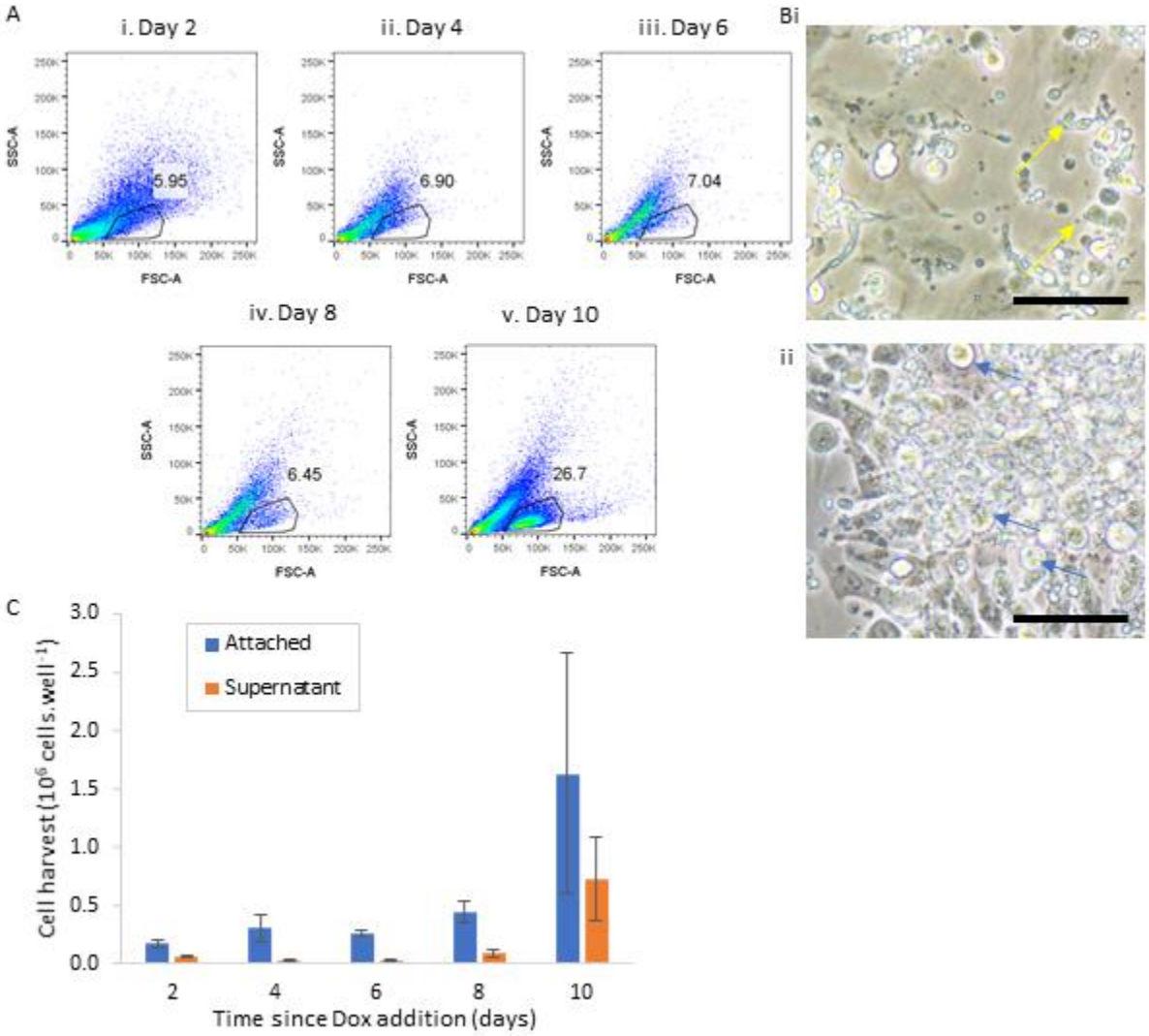

Figure 5-7: Medium supernatant from Day 2 – 10 post Dox addition showed a high proportion of debris (A) Graphs show flow cytometry forward scatter – side scatter profiles of medium supernatant for Day 2 (i), Day 4 (ii), Day 6 (iii), Day 8 (iv) and Day 10 (v), showing cultures had a high proportion of debris compared to target cells, but this improved at Day 10. (Data show N=3 ± STD) (B) Light microscopy images of cells at Day 2 (i) and Day 10 (ii); cells at Day 2 were smaller and granular (examples shown with yellow arrows) and cells at Day 10 were larger and less granular (examples shown with blue arrows). Scale bar shows 50 µm. (C) Graph shows number of cells in each well that were attached were greater than the number of cells suspended in the medium supernatant at each time point, but the difference is much smaller at Day 10.

Since similar debris was not seen in iPSC cultures (data not shown) it was likely that the debris was released in response to Dox addition. It is unclear whether this was caused by the activation of the forward programming transcription factors, or whether it was a response to Dox which can be toxic to cells [149]. However, since debris is present in FOPMK long term cultures (data not shown) and megakaryocytes shed their membranes to produce platelets or platelet like particles, it was probable that the release of debris was caused by activation of the forward programming transcription factors. The effect of debris on the culture is not known, but may be indicative of process inefficiencies, since the debris is lost biomass, as noted in Section 5.4.2.

The effect on the cultures of the large amount of released debris is unclear. It is uncertain whether small, granular cells become target cells, or whether these small cells decay and target cells are generated from a different progenitor cell source. The secretion of paracrine factors from the debris could have either a positive, negative or no effect on the cultures. This reflects a general problem when tracking cell populations vs. individual cells, and the disentangling of these effects must be considered in experimental design.

Process Risk 9: Particulates such as cell debris can affect cells in culture due to co-released intracellular factors or directly through membrane interactions. Retention of debris will be affected by the medium exchange operations, both volume and fluid handling methodology. Any approach should be evaluated for consistency and fraction of debris transfer.

5.4.5. Operational regime observations: Bulk medium supply

As noted in Section 2.3.2, a combination of partial and complete medium exchanges were performed. Where a complete medium exchange was performed all toxic metabolites and decayed medium components were removed and replaced with fresh. However, all released

target cells were also removed and any remaining “used” medium was also removed, reducing process efficiency. It should be noted that this point in the process the cell numbers and the volumes used were very low compared to the end of the process, since the number of cells (and therefore culture volume) increased exponentially with time, therefore focusing on the medium efficiency and the volumetric productivity at this point will have little impact on the overall process economics. For example, it is estimated that at least 10 population doublings are required for maturation, which would result in this part of the process contributing 0.1-0.5% to total process productivity (unweighted for length of process stage or specific productivity of stage).

Doubling the culture volume at Day 4 may lead to mass transfer limitations depending on the cell’s oxygen consumption rate and whether the higher volume depth creates a hypoxic environment for the cells [74]. To determine whether the higher volume would restrict the mass transfer rate of oxygen to the system, the oxygen transfer rate (kLa) of the bioreactor at relevant medium volumes and the oxygen consumption rates of the cells would also need to be determined.

Where a 50% medium exchange was performed (day 6 & 8), half the medium was removed, centrifuged and resuspended in fresh medium with double concentrated factors. This process intervention had a greater number of process steps, and since half the suspended cells were exposed to centrifugation this could increase the variability within the system. The advantage of this exchange was the retention of unexhausted medium and some cell debris was removed, whilst retaining target cell populations, but also retaining some apoptotic cells.

Process Risk 10: Doubling the culture volume at day 4 reduces the kLa in the current culture system (planar well plates / T-flask systems), which may lead to mass transfer limitations.

Process Risk 11: The medium exchange regime is currently relatively arbitrary. Complete medium exchange removes target cells and therefore potentially lowers process efficiency. It also wastes unused medium if conducted prematurely, and may remove beneficial factors, therefore lowering process efficiency. A partial medium exchange potentially increases process variation by exposing half the suspended cells to centrifugation and may retain detrimental or positive factors. In short, medium exchange controls are likely to be critical in reducing variation in process outcome, and optimisation of operational timings and volumes will drive process costs and quality.

5.4.6. Effect of cryopreservation

Cells from Tech Transfer Experiment #1 were cryopreserved at Day 27 post Dox addition. As shown in Figure 5-8, only 17% of cells were initially recovered on thaw and cell numbers did not recover in culture. It is unclear whether cells of this general lineage were intolerant to cryopreservation (which seems unlikely since the method was used previously for long term FOPMKs as described in Section 2.4.1), or whether it was an aspect of cell state largely orthogonal to lineage such as proliferative or metabolic state the cell state.

Process Risk 12: Given that a standard cryopreservation protocol was applied, this suggests that cells may have different sensitivities to cryopreservation at different process points, and would need to be considered if manufacturing logistics required a cryopreservation banking step at an intermediate point in product differentiation. This is yet to be determined and is an unknown process risk.

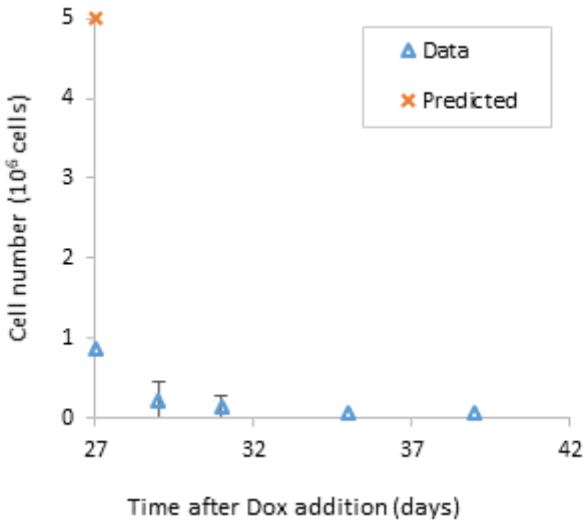

Figure 5-8: Seventeen percent of cells were recovered from cryopreservation and cell number did not recover.

5.5. Summary of Risk Assessment and selection of control variables for Design of Experiments

The process risks outlined in Section 5.4 can be grouped into two types, risks that relate to the effect of control variables on product quality and purity and risks that relate to the interpretation of characterisation assays. The risks can be summarised as follows:

<u>Operation and control risks that impact product quantity and quality</u>

- Medium exchange controls are likely to be critical in reducing variation in process outcome, and optimisation of operational timings and volumes will drive process costs and quality (*Process Risk 11*).
- Inconsistent growth rates across differentiation trajectory within process transfer experiments leading to variable outcomes (*Process Risk 1*).
- Differences in phenotype between differentiation runs leading to variable outputs most likely linked to Dox supply (*Process Risk 2*).

- Variable expansion potential per iPSC is likely to be a function of phenotype changes which is in-turn a function of medium and component supply (*Process Risk 7*).
- Debris creation and control through bulk medium supply has unknown effects (*Process Risk 3*, *Process Risk 9* and *Process Risk 11*).
- Mass transfer limitations of the systems are currently unknown (*Process Risk 10*).

Characterisation risks

- The utility of culture characteristics early in the differentiation process as surrogate measures for end of process outcomes (cell yield, purity) is currently challenging. Cell counts are difficult to achieve prior to day 8 (*Process Risk 8*). Also more investigation is required to enable the use of CD235a as a differentiation trajectory marker since it is expressed variably in early differentiation (*Process Risk 4*), on megakaryocyte on-target cells mid-differentiation (around day 10) and on off-target cells later in the differentiation process (around day 18) (*Process Risk 6*). Although time and resource consuming, late stage differentiation outputs are required to make meaningful conclusionse in a process development context.
- Assays within and across sites for process development and manufacturing must be kept as consistent as possible (*Process Risk 5*).

Characterisation risks relate to the interpretation of cell states at different part of the process. Following the risks identified in the technology transfer runs, assays were kept as consistent as possible within experiments (for example, the same antibody lots were used). Examining the biochemical pathways and mechanisms of action that drive megakaryocyte differentiation was beyond the scope of this work, therefore understanding the dynamic changes in early differentiation marker (CD235a) expression was not investigated but

continued to be monitored through further experiments. The rest of this section relates to understanding control variable impact on process outcome.

The driving force behind process control variable risks relate to medium utilisation, either specific cytokine / compounds or more generally bulk medium supply depletion, both of which depend on the number of cells present. The control variables identified as relating to medium supply and utilisation during the tech transfer process are listed in Table 5-1, along with their set points and potential risks of over and undersupply, in order to prioritise variables for further investigation.

Seeding density and provision of supporting milieu cannot be separated as the former determines specific cell activity. Dox was repeatedly highlighted as a high-risk system component in the process transfer. TPO and SCF were used for the duration of the process and have also been relatively arbitrarily altered in historic versions of the process, suggesting the potential for more serious process impact. These were therefore selected as next priorities, but a preliminary study was conducted (see Section 5.5.1) to determine whether they are investigated further. Activin A, FGFb, and BMP maybe influential but are considered lower priority for investigation due to literature base, briefer application, and application at a process stage that will require less intensification. Therefore, seeding density, bulk medium and Dox provision were prioritised for a DOE approach with SCF and TPO as potential candidate variables for inclusion depending on the outcome of the short study. A DOE approach was selected because of its efficiency for examining the effect of many variables, despite its limitations of defining effects empirically rather than mechanistically.

Table 5-1: Summary of process control variables and list of the potential effects of over and under supply.

Control variable	SOP set points for protocol transfer	Potential effects (relative to optimal)
Seeding density	12,500 cells.cm^{-2}	High densities – medium exhaustion, surface area limitations Low densities – wastage of growth factors (time decay), inefficient utilisation of facilities. These effects are not intendent to seeding density and are affected by the medium supply.
Bulk medium supply	Combination of partial and complete exchanges as listed in Section 2.2.2 and outlined in Figure 5-2.	High – Increased costs as bulk medium not fully utilised, dilution of released positive paracrine factors. Low- Toxic build-up of metabolites / nutrient exhaustion leading to growth inhibition and cell death which decreases process efficiency and increases cost. These effects are not intendent to bulk medium supply and are affected by the supply of cytokines and seeding density.
Dox concentration	0.25 µg.mL^{-1}	High – toxic to cells [149] Low – inefficient reprogramming
Dox exposure time	Until day 10	High – toxic to cells [149] Low – inefficient reprogramming
TPO concentration	100 ng.mL^{-1} until day 10 then reduced to 20 ng.mL^{-1}	High – increased cost, potential signal silencing or toxicity issues Low – sub-optimal cell growth and phenotype
SCF concentration	25 ng.mL^{-1}	
Activin-A concentration	10 ng.mL^{-1}	
FGF2 concentration	10 – 20 ng.mL^{-1}	
BMP4 concentration	10 ng.mL^{-1}	

5.5.1. Preliminary Screening of sensitivity of the culture to SCF and TPO

To examine the effect of growth factor concentrations, as previous data had suggested that the combination concentration of SCF and TPO may affect the growth of cultures (see Figure 4-9), various concentrations of SCF and TPO were used to test the impact on the growth and phenotype of late-stage FOPMKs shown in Figure 5-9. This was tested over 4 days at day 32 after Dox addition in Tech Transfer Experiment #2. Cells originated from the same culture at day 32 and underwent a complete medium exchange with Cellgenix SCGM supplemented with various concentrations of SCF (1, 15.5, 50.5, 85.5 and 100 $\mu g.mL^{-1}$) and TPO (0.4, 6.2, 20.2, 34.2 and 40 $\mu g.mL^{-1}$) making a total of 25 combinations of SCF and TPO. Conditions were performed with duplicate wells. Cell counts were performed at 70 and 91 hours post seeding and phenotype analysis (using Panel 4 was used, as described in Table 3-10) was performed at 91 hours post seeding on five conditions (combinations of highest and lowest concentrations as well as a centre point).

The cell densities across 91 hours for the lowest (1 $ng.mL^{-1}$) and highest (100 $ng.mL^{-1}$) SCF concentrations and all concentrations of TPO used are shown in Figure 5-9 A. The trend across all conditions was cell growth until 70 hours followed by cell death from 70 to 91 hours. Since it was across all conditions, there is no evidence that this trend was caused by changing growth factor conditions. As shown in Figure 5-3 (B), there was less expansion later in the cultures by day 32 so meaningful conclusions about the effect of growth factors on cell expansion cannot be determined from this experiment. It is possible that growth factor concentrations may have different impact on cell expansion at different points in the differentiation trajectory, but that was not tested here.

The detailed flow cytometry analysis shown in Figure 5-9 C-G shows forward scatter / side scatter profiles (i), viability of gated cells (ii), CD235a / CD41a expression (iv), CD41a / CD42a expression and (v) CD42a / CD42b expression for combinations of highest and lowest growth factor concentrations as well as the centre point.

Compared to the conditions with high and mid concentrations of TPO (Figure 5-9 B, D and E) the condition with low TPO concentrations (C and F) had:

- High side-scatter profiles (i) which were therefore more granular which is indicative of cell death.
- A lower proportion of viable cells (ii).
- A higher proportion of CD235a+/CD41a- cells (iii).
- A lower proportion of CD42a+/CD41a+ cells (iv).
- A higher proportion of CD42a+/CD42b- cells (v).

All the attributes listed above are non-desirable and an indication of low quality. This qualitative analysis did not show the same magnitude of effect of SCF. To quantify the effect of SCF and TPO exposure on phenotype, CD41a expression after 91 hours was input into a DOE analysis, the parameters for which are shown in Table 5-2. A two level, two factor design with a centre point was analysed with stepwise, backwards elimination (α>0.1 was used for removal).

Table 5-2: DOE inputs and observations for quantifying effect of SCF and TPO concentration on phenotype following exposure of 91 hours to a complete medium exchange with different concentrations of growth factors.

Parameter	**High level**	**Low level**
TPO concentration	40 ng.mL^{-1}	0.4 ng.mL^{-1}
SCF concentration	100 ng.mL^{-1}	1 ng.mL^{-1}
Output	Percentage of CD41a positive cells	

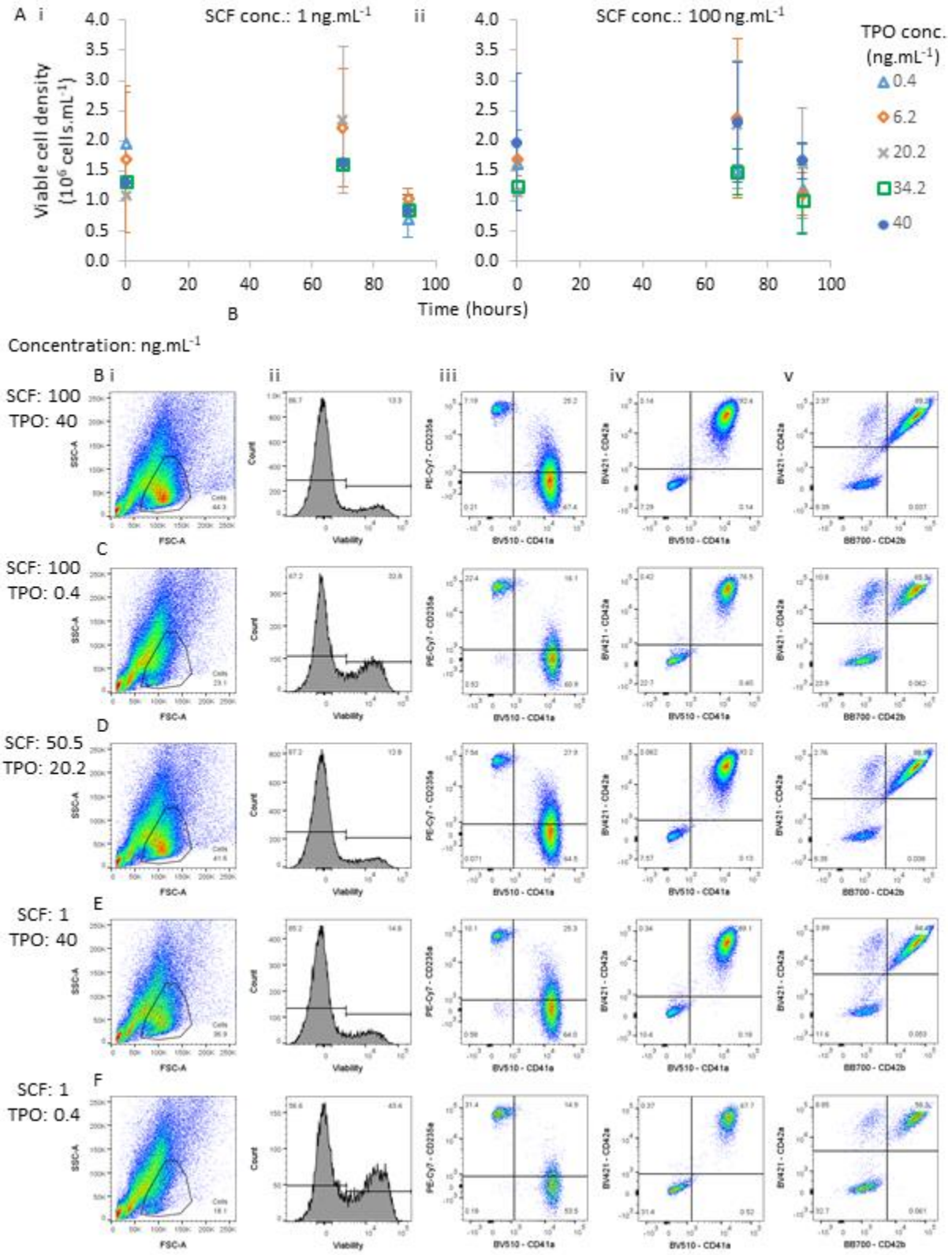
A i
SCF conc.: 1 ng.mL-1
ii
SCF conc.: 100 ng.mL-1
Viable cell density (10^6 cells.mL-1)
Time (hours)
TPO conc. (ng.mL-1)
0.4
6.2
20.2
34.2
40
B
Concentration: ng.mL-1
B i
ii
iii
iv
v
SCF: 100
TPO: 40
C
SCF: 100
TPO: 0.4
D
SCF: 50.5
TPO: 20.2
E
SCF: 1
TPO: 40
F
SCF: 1
TPO: 0.4
SSC-A
FSC-A
Count
Viability
PE-Cy7 - CD235a
BV510 - CD41a
BV421 - CD42a
BB700 - CD42b

Figure 5-9: Cells were grown for 26 days (as shown in Figure 5-3**Error! Reference source not found.**) and w ere then exposed to different combinations of SCF and TPO concentrations. (A) examples of various concentrations of TPO at two SCF concentrations (i) 1 ng.mL^{-1} and (ii) 100 ng.mL^{-1} (data show N=2, ±STD). There was little difference between treatments with respect to cell numbers.(B-F) Detailed flow cytometry analysis. (i) Forward scatter, side scatter plots show that lower concentrations of TPO (C, F) and to some extent the low SCF/high TPO (E), shows a decrease in the target cell phenotype. (ii) Cell viability was higher with high and mid-range TPO concentrations (B, D, F) as in (i). (iii) shows two distinct populations – CD235a+/CD41a- and CD41a+ (iv) The largest proportion of off target phenotype (CD42b-) was again produced using the lowest concentrations of TPO. Flow cytometry Panel 4 was used, as described in Table 3-10.

The main effects plot shown in Figure 5-10 (A) shows that increasing the concentration of both SCF and TPO increased the proportion of CD41a+ cells, however only TPO was statistically significant (P = 0.07). This quantified, statistically significant effect combined with the qualitative effects on cell size, granularity and viability led to TPO being prioritised for further investigation.

The R^2 (adj) value obtained from this model was 62.3% showing that approximately 37% of the variation in the expression of CD41a could not be explained by TPO concentration changes alone. A proportion of this variation could be due to changes in SCF concentration (which were not included in the model).

The lack of impact of SCF on cell phenotype from 1 – 100 ng.mL^{-1} suggests that a much lower SCF concentration may be tolerated in cell cultures at the later stage. This would decrease production costs. However, the effects of lower the SCF concentrations would need to be tested further, as lower concentrations over the long term may cause different effects. It could be, for example, that there was residual SCF present attached or absorbed into the cells and this takes longer than 4 days to decay. It is also possible that the more mature FOPMKs (CD41a+) do not respond to SCF, since cells may lose responsiveness to SCF as they mature

[150], so only a small, more progenitor population of cells are affected when SCF is removed, hence the small difference in expression. If this is the case, the removal of SCF may have

A

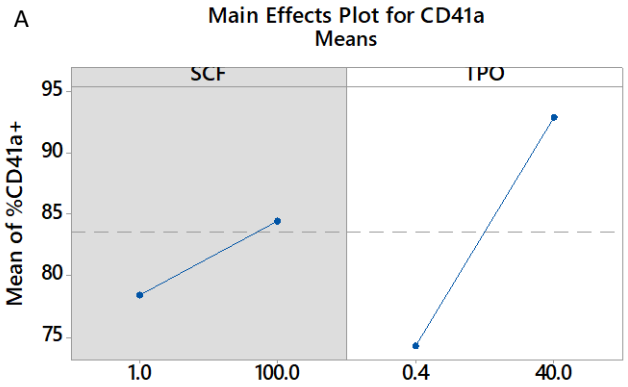

B

A gray background represents a term not in the model.

```
Backward Elimination of Terms

α to remove = 0.1


Analysis of Variance

Source          DF  Adj SS  Adj MS  F-Value  P-Value
Model            1  347.82  347.82     7.61    0.070
  Linear         1  347.82  347.82     7.61    0.070
    TPO          1  347.82  347.82     7.61    0.070
Error            3  137.05   45.68
  Curvature      1   92.88   92.88     4.21    0.177
  Lack-of-Fit    2   44.17   22.08        *        *
Total            4  484.87


Model Summary

      S    R-sq  R-sq(adj)  R-sq(pred)
6.75883  71.74%     62.31%      33.28%


Coded Coefficients

Term      Effect    Coef  SE Coef  T-Value  P-Value   VIF
Constant          83.58     3.02    27.65    0.000
TPO        18.65    9.32     3.38     2.76    0.070  1.00


Regression Equation in Uncoded Units

CD41a = 74.07 + 0.471 TPO
```

Figure 5-10: DOE analysis of exposure to different concentrations of SCF and TPO showed that only TPO had a statistically signicant (P<0.1) effet on CD41a expression. (A) main effects plot showed that both SCF and TPO concentrations increased CD41a expression (although SCF was eliminated from the model). (B) DOE output showed that TPO was statistically significant variable (P<0.1).

consequences for the long-term proliferation as the progenitor population may become exhausted at lower SCF concentrations and therefore would not repopulate the culture. Since

the protocol standard concentration of 25 ng.mL^{-1} was well within the concentration tested here, and statistically significant effects were not seen, SCF concentration was not deemed a priority for further study at this time. Given the indication of potential effects and the potential cost savings from reducing SCF it should be considered for future follow-on studies.

5.6. Using Design of Experiments to test the effects of process variables on forward programming outcomes

The risk assessment in Section 5.5 identified bulk medium and growth factor provision as high priorities for further assessment for understanding manufacturing constraints. Of those factors identified a subset of Dox, TPO and seeding density were selected as the highest priority for further investigation with a Design of Experiment approach (as justified in Section 5.5 and 5.5.1). Seeding density is a mechanistic indicator; if it is significant and interacts with cytokine concentration in a particular way, it would indicate whether density was affecting the system by consumption of the other control variables or an alternate undefined paracrine effect. Timing of Dox removal from the culture (Day 10 removal or continued supplementation) was included as a further DOE condition as it was hypothesised that retaining Dox past Day 10 might promote continued proliferation and on-target phenotype maintenance. Table 5-3 details the DOE experimental parameters and measured responses and XX details the DOE experimental conditions.

Table 5-3: High and low levels of DOE parameters and measured responses.

Parameter	High level	Low level
Seeding density	5,000 cells.cm^{-2}	20,000 cells.cm^{-2}
Dox concentration	0.25 µg.mL^{-1}	1 µg.mL^{-1}
Dox removal at day 10	Continued supplementation	Discontinued supplementation
TPO concentration	100 ng.mL^{-1}	25 ng.mL^{-1}
Output	Cumulative number of population doublings Net growth rate CD41a expression at day 18 CD41a expression at day 10 CD34 expression at day 4	

Table 5-4: Cells were cultured at various seeding density and reagent concentrations to better understand the cell proliferation and differentiation trajectory through forward programming. Table details different treatment conditions. The original 8 conditions were split at day 10, and cultures were treated by removing Dox or continuing supplementation from day 10 onwards.

Condition	Target seeding density at day -1 (cells.cm^{-2})	[Dox] Day 0-10 (µg.mL^{-1})	[TPO] Day 0-10 (ng.mL^{-1})	Dox Day 10+ (µg.mL^{-1})	[TPO] Day 10+ (ng.mL^{-1})
1	5×10^3	0.25	25	0.25	20
2	2×10^4	0.25	25	0.25	20
3	5×10^3	0.25	100	0.25	20
4	2×10^4	0.25	100	0.25	20
5	2×10^4	1	25	1	20
6	5×10^3	1	25	1	20
7	5×10^3	1	100	1	20
8	2×10^4	1	100	1	20
11	5×10^3	0.25	25	0	20
12	2×10^4	0.25	25	0	20
13	5×10^3	0.25	100	0	20
14	2×10^4	0.25	100	0	20
15	2×10^4	1	25	0	20
16	5×10^3	1	25	0	20
17	5×10^3	1	100	0	20
18	2×10^4	1	100	0	20

Growth and phenotypic responses were analysed and used as model outputs. Section 5.6.1 describes and discusses the growth response over the first full 19 days, as well as separately over day 3-19 (where the latter had a more reliable initial measured cell value to avoid any error of initial seeding.

5.6.1. DOE analysis of cell proliferation to Day 18

The effect of the control variables on cumulative number of population doublings by Day 18 as determined from the DOE output is shown in Figure 5-11. The main effects plot (Figure 5-11 A) shows that TPO and Dox concentrations had a positive correlation with the cumulative number of population doublings, whilst seeding density had a negative impact.

There was a statistically significant interaction between Dox and TPO concentrations (Figure 5-11 B), where the lower number of cumulative population doublings caused by using low Dox was offset by using the higher concentration of TPO. The pareto chart (Figure 5-11 C) shows that seeding density had the highest effect on the cumulative number of population doublings – its standardised effect was more than double the other model terms. In order of magnitude this was followed by Dox, TPO, and the interaction of Dox and TPO (Figure 5-11 C).

It was further hypothesised that a distinct effect of variables may be observed on growth between D10 and D18 compared to an analysis over the full experimental duration. To quantify these effects the number of cumulative population doublings from day 10-18 were analysed but no control variable reached the $\alpha \leq 0.1$ threshold. This suggests that legacy effects of treatments prior to Day 10 of culture had a minimal impact on the proliferation of cultures from Day 10 -18.

The effect of Dox on cumulative number of population doublings over the full-time course to D18 is shown for each individual condition in Figure 5-12. The removal of Dox at D10 was not significant (P>0.1 in DOE model), so wasn't included in the model and therefore is not shown on the main effects plot (Figure 5-11 A). However, a higher level of variability was observed in the Dox- conditions as shown by the larger error bars for the number of population doublings between day 10 and day 18 for the Dox- data (conditions 11-18) in Figure 5-13.

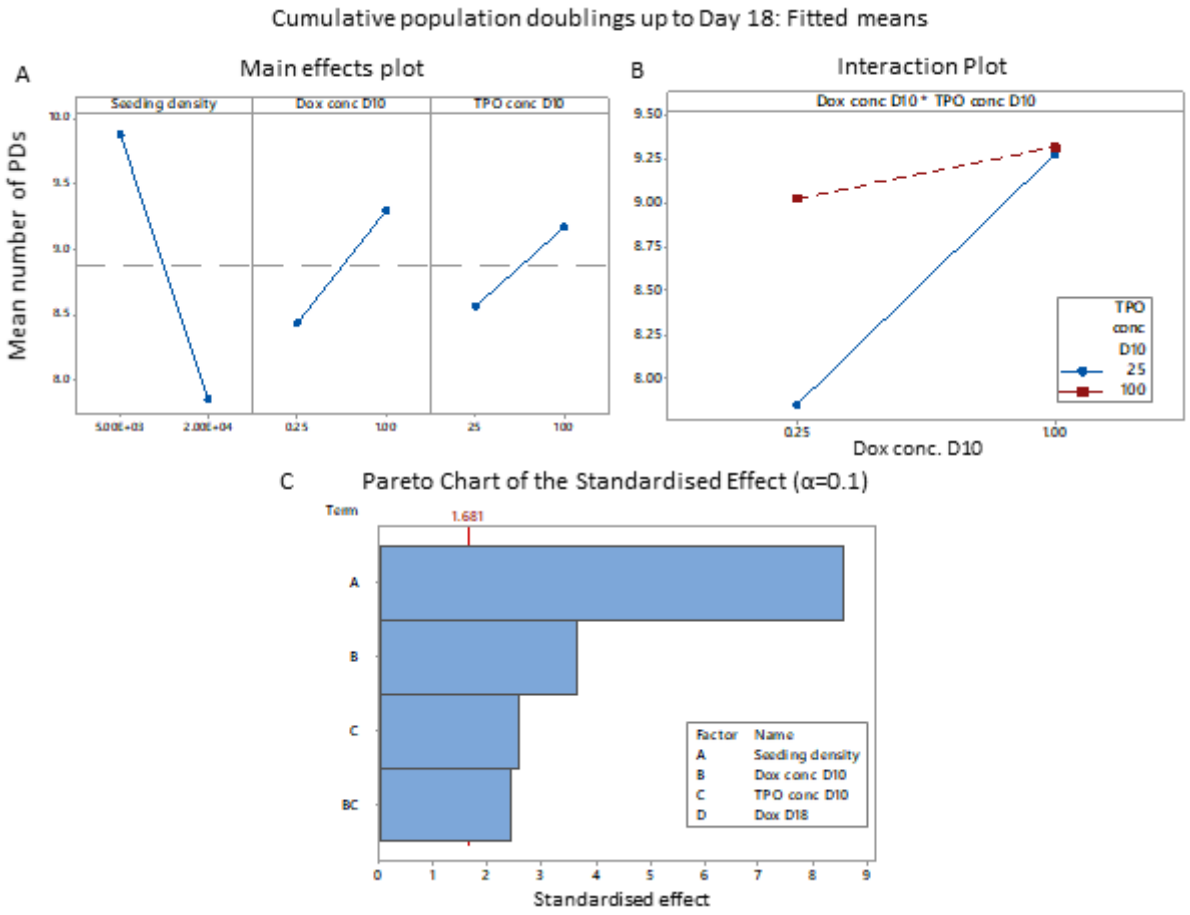

Figure 5-11: DOE output summary for cumulative population doublings until Day 18. DOE analysis was performed using statistical software package Minitab with stepwise backwards elimination (a=0.1) applied for a 2-level, 4-factor, factorial design (A) Main effects plot shows mean cumulative population doublings was decreased with increasing seeding density, increased with increased Dox concentration between Day 0 -10, and increased TPO concentration between Day 0-10. (B) Interaction plot shows that TPO concentration had a larger increase on the cumulative population doublings at lower Dox concentrations. (C) Pareto chart shows that the seeding density had the greatest impact on the number of cumulative population doublings. Removal of Dox at Day 18 was included in the analysis but did not reach the α=0.1 threshold and is therefore not shown in the outputs.

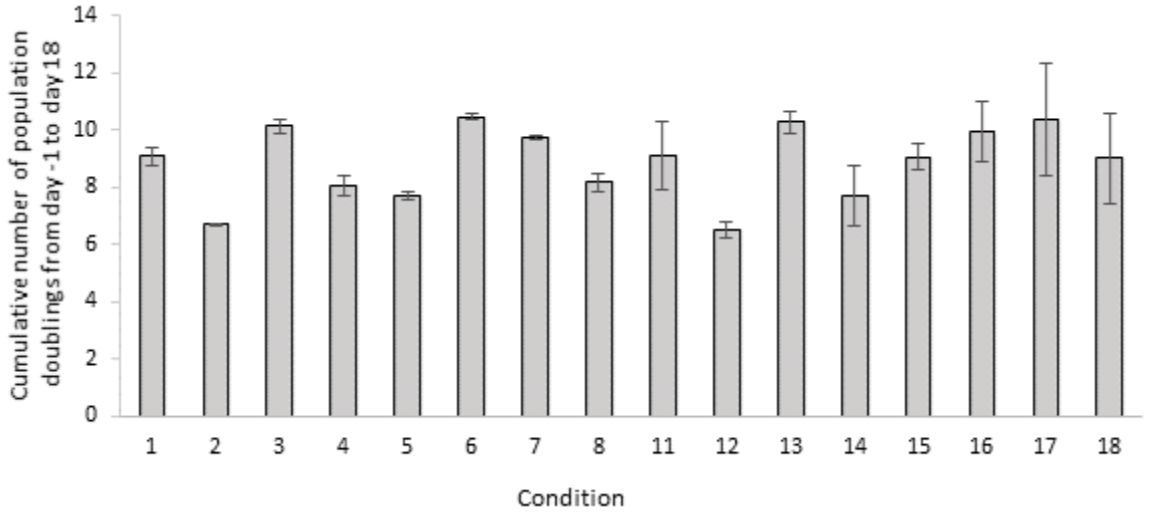

Figure 5-12: The average cumulative number of population doublings from day -1 to 18 show Dox concentration increased cumulative PDs. The impact was higher in low TPO cultures (conditions 1 & 6, 2 & 5), than when comparing high TPO conditions (3 & 7, 4 & 8).

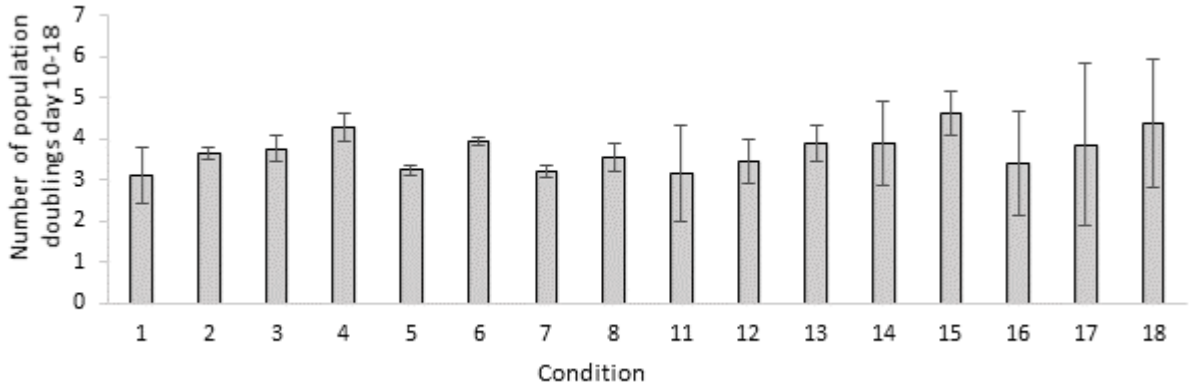

Figure 5-13: The average number of population doublings from Day 10 – 18 were similar or slightly higher in cultures which had Dox removed (11-18) compared to those which retained their original Dox treatment concentrations, however the removal of Dox caused an increase in variation, as shown by the relative size of the error bars (data shows N=3, ±STD).

Furthermore, the average CV for Dox- conditions was 10.8% compared to 2.2% for Dox+ conditions. The variation of a process is important in a manufacturing setting as a higher variation increases the risk of not meeting the QTPP specification and so increases costs. It was therefore hypothesized that if only the Dox+ data was analysed the noise would be reduced and new statistically significant effects could be observed within the remaining half of the experiment design space. Further, due to concern about the dependence of cumulative population doublings on the initial seeded cell value, a different method of growth assessment using multiple data points to calculate net growth rate was evaluated.

5.6.1.1. DOE analysis of cell proliferation to Day 18 using Dox+ only data and net growth rate response

Comparing the proliferation of the cultures by considering the cumulative number of population doublings over the 18 days (Figure 5-12) shows that culture condition 6, followed by 7, proliferated the most. However, this was significantly influenced by large differences in the number of population doublings from Days -1 to 2 across conditions. This difference could be caused by incorrect cell counts at Day -1, since here a single cell count for each condition was obtained by measuring the cells that were remaining in the pooled solution used to fill each vessel and were not taken from the wells directly. In section 3.4.1, it was shown that cell counts using this method can be inaccurate. Furthermore, there was large proportional variation observed between the number of cells recorded biological replicates (maximum CV was 18.8%) by day 18 suggesting evolving noise over the experimental time course. Rather than using the cumulative number of population doublings based on seeded and terminal values, the gradient of the graph of cumulative number of population doublings against time was used, since this uses multiple data points and reduces the influence of error in any individual data point.

Table 5-5: Dox+ conditions used for to calculate net growth rate

Condition	Target seeding density at day -1 (cells.cm^{-2})	[Dox] Day 0-10 (µg.mL^{-1})	[TPO] Day 0-10 (ng.mL^{-1})	Dox Day 10+ (µg.mL^{-1})	[TPO] Day 10+ (ng.mL^{-1})
1	5×10^3	0.25	25	0.25	20
2	2×10^4	0.25	25	0.25	20
3	5×10^3	0.25	100	0.25	20
4	2×10^4	0.25	100	0.25	20
5	2×10^4	1	25	1	20
6	5×10^3	1	25	1	20
7	5×10^3	1	100	1	20
8	2×10^4	1	100	1	20

Cumulative population doublings across time are shown in Figure 5-14 for each condition individually detailed in Table 5-5, along with linear trend lines and the residual error of the data points from the trend lines. The gradient of the trend lines were used to calculate net growth rate (shown in Figure 5-15). For all conditions, except 2 and 4 (Figure 5-14 Bi and Di respectively), the R^2 value was greater than 0.9, indicating that greater than 90% of the variance of the data from its mean can is accounted for by the linear trend line. In general there is no evidence on the pattern of residuals in the conditions with high R^2 values, except that the growth was slower from day 10 to 14 where the residuals show that the number of population doublings were underestimated at Day 14 in all conditions. At Day 10 cells were passaged and transferred to ULA tissue culture plastic and so the lower growth rate may have been caused by the cells going through a transition phase and adapting to suspension culture, which has been reported in ESC cultures [151]. Additionally, enzymatic passage has been noted to cause low levels of cell damage [152], which may have contributed to the inhibited

growth between Day 10 and Day 14. Jager et al. [152] noted that using TrypLE to passage (as used here) was the least harmful method, obtaining the highest post-passage cell viability and low apoptotic cells compared to mechanical methods. Therefore if the cells need to be removed from tissue culture plastic for expansion, lag may be inherent to this part of the process and cells did recover after this time point, as seen by rising residuals aat Day 18 (Figure 5-14 A-H ii). This may be overcome by using suspension cultures to produce FOPMK cultures. Furthermore, condition 7 (G) deviated least from a constant growth rate model. This indicates that consistent growth may be achieved if the input variables are optimal.

However, in conditions 2 and 4 the lower R^2 values appear to be caused by an additional systematic deviation from the model seen as trends in the residuals (Figure 5-14 Bii and Dii) where there was no expansion of cells between day 2 and 14.

The summary of the calculated growth rates is shown in Figure 5-15 (A) , and the equivalent doubling times shown in (B). The graphs used for these calculations are also shown in Figure 5-14. This shows that conditions 3, 6, and 7 had very similar net growth rates (0.011 hr^{-1}). All three of these cultures were seeded at low density and had high concentrations of either TPO, Dox or both. This indicates that there was a cell mediated decay rate of TPO and Dox (since higher density cultures had lower net growth rates, which suggests inhibition) and that by using higher levels or either Dox of TPO the potential growth inhibition due to a lower concentration of the other was offset. Since this growth rate was so similar, this was likely to be the highest growth rate of this system and is equivalent to a doubling time of 3.82 days. This is still low for mammalian cell cultures, possibly because the cells were transitioning into more mature cell types and the net growth rate was likely to be offset by some levels of cell death, seen by the debris in the flow cytometer in the high side scatter region.

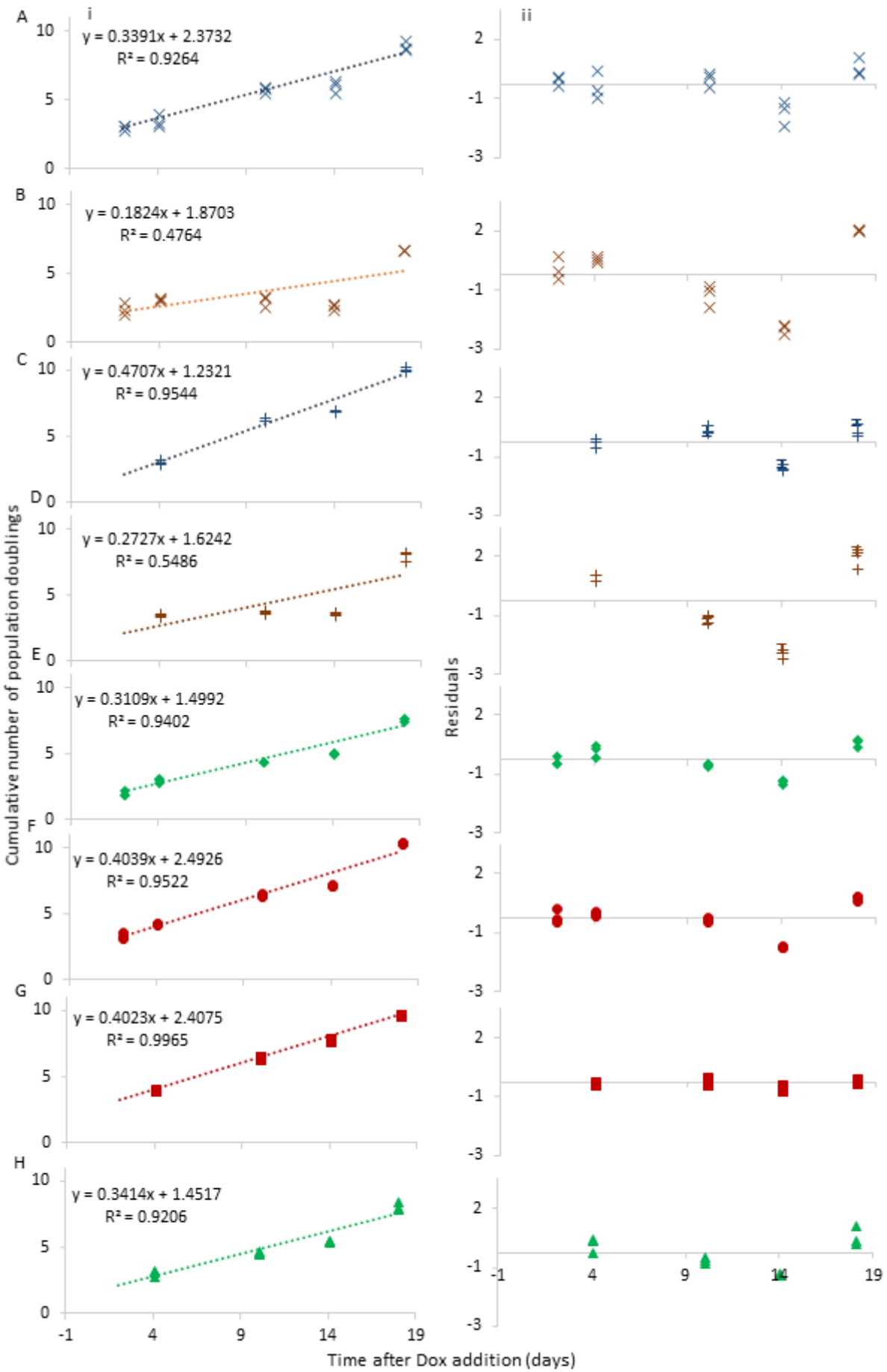
A
i
y = 0.3391x + 2.3732
R² = 0.9264
ii
B
y = 0.1824x + 1.8703
R² = 0.4764
C
y = 0.4707x + 1.2321
R² = 0.9544
D
y = 0.2727x + 1.6242
R² = 0.5486
E
y = 0.3109x + 1.4992
R² = 0.9402
F
y = 0.4039x + 2.4926
R² = 0.9522
G
y = 0.4023x + 2.4075
R² = 0.9965
H
y = 0.3414x + 1.4517
R² = 0.9206
Cumulative number of population doublings
Residuals
Time after Dox addition (days)

Figure 5-14: Cumulative number of population doublings against time for individual conditions (i) and residuals of data from model (ii). (A-H) show conditions 1-8. In all cases the number of population doublings was less than the linear model at Day 14, possibly due to the required passaging at Day 10. Conditions 2 and 4 (B and D) did not grow between Days 4-14, but recovered from Day 14 onwards, suggesting that if growth is prevented it could be recovered in latter stages. Condition 7 (G) produced the most consistent growth rate across the culture period.

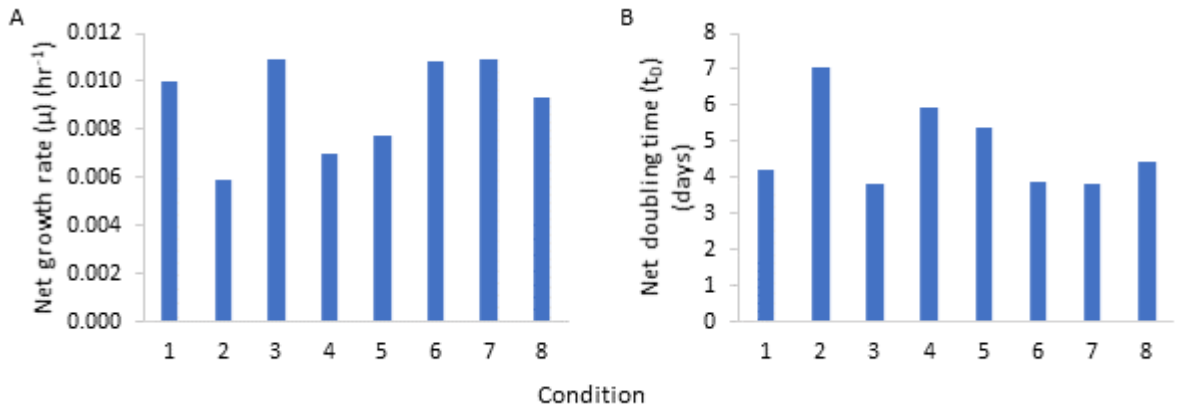

Figure 5-15: Summary of the net growth rates achieved calculated using a trend line of cumulative population doublings with time (shown in Fig. Figure 5-14) (A) Net growth rates achieved over the culture period show similar growth rates for conditions 3, 6 and 7, suggesting this is possibly the highest achievable net growth rate. (B) Equivalent doubling times for growth rates shown in (A) show that cultures varied between a net doubling rate of 7 to 3.8 days.

5.6.1.2. Quantifying the effect of Dox concentrations, TPO concentration and seeding density on net growth rate for Dox+ conditions

The effect of input variables (Dox and TPO concentrations and seeding density) were quantified using DOE software, Minitab, as shown in Figure 5-16. (A) shows the main effects of each variable when the others were set at a constant (mean) value. This shows that TPO and Dox concentrations had a positive correlation with net growth rate, whilst seeding density has a negative impact on growth rate. Furthermore, the seeding density had a higher magnitude of impact (across the experiment range) on the net growth rate compared to TPO and Dox concentrations.

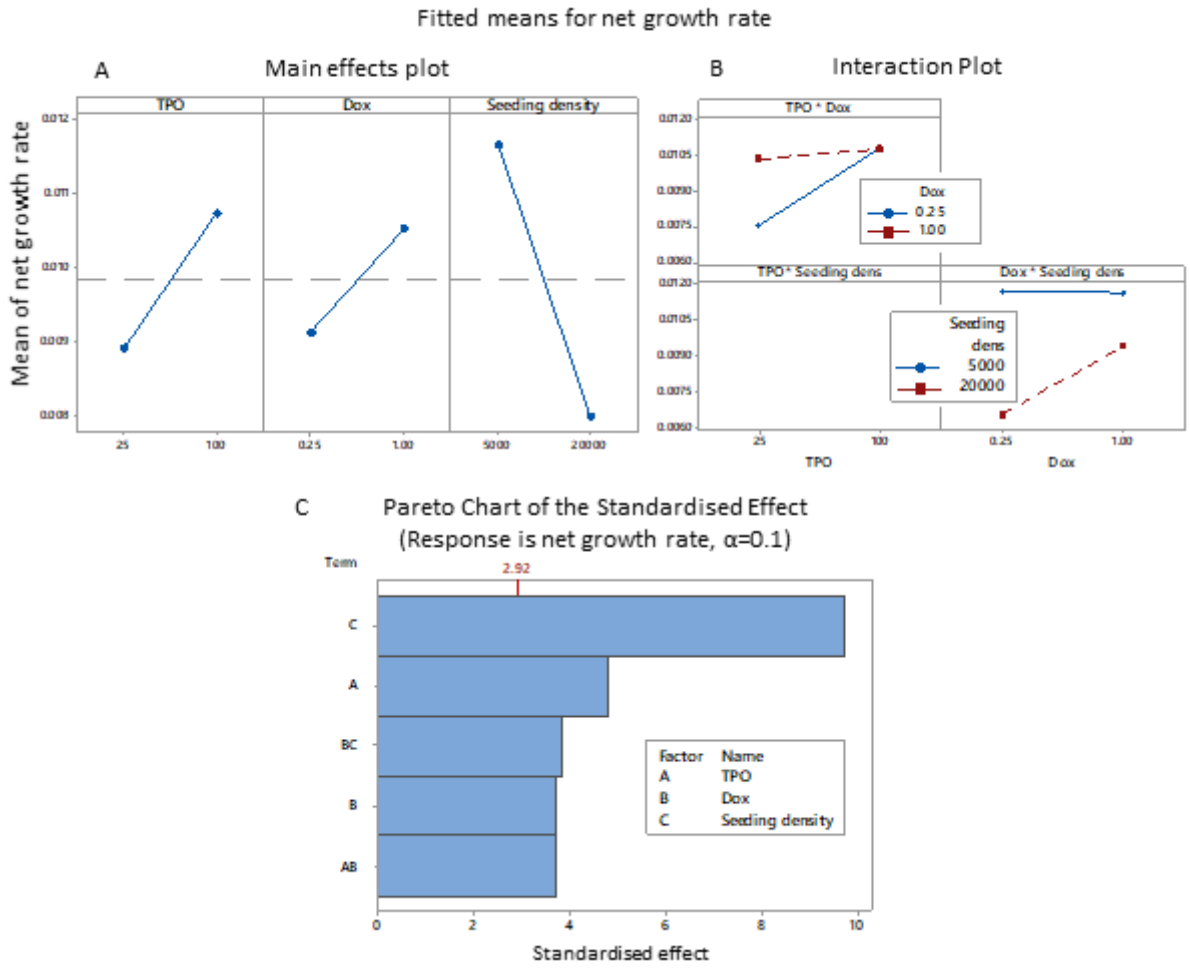

Figure 5-16: DOE output summary for cumulative population doublings until day 18 with Dox+ conditions. DOE analysis was performed using statistical software package Minitab with stepwise backwards elimination (a=0.1) applied for a 2-level, 3-factor, factorial design (R^2 adj. = 95.7%). (A) Main effects plot shows mean of net growth rate was increased with higher concentrations of TPO and Dox but lowered with increased seeding density. (B) Interaction plots show that TPO had a greater effect on the net growth rate when lower Dox concentrations were present and increased Dox concentrations only increased proliferation at higher cell concentrations. (C) Pareto chart shows all parameters included in the statistical model for which $\alpha \geq 0.1$; out of these parameters seeding density had the greatest impact on proliferation.

Interactions between the variables were also statistically significant. The interaction plots (B) demonstrate that when low TPO concentrations were used, higher Dox concentrations increased growth rate. However, there was little effect of increasing TPO concentrations at high Dox concentrations. Therefore, it is hypothesised that the response of the cells to Dox and TPO (with respect to growth rate) are linked through either the same biochemical pathways or independent biochemical pathways that produced the same growth rate effect.

There was also a significant interaction between seeding density and Dox concentrations, which showed that at lower seeding densities, the concentration of Dox did not affect the proliferation, yet at higher seeding densities an increased Dox concentration increased the net growth rate, indicating that Dox degradation was cell-mediated, leading to the cultures with more cells experiencing a lower Dox concentration which decreased net growth rate. This presumes there was a dose-dependent net growth rate response to Dox; evidence for this dose-dependent relationship is indicated by the main effects plot in Figure 5-16 (A), where Dox concentration correlated to increased growth rate (as discussed above). The effect of the interaction of TPO and seeding density was not included in the model, since this effect did not reach the α threshold of 0.1, suggesting that there was a lower rate of (or no) cell mediated TPO degradation.

The Pareto Chart in Figure 5-16 (C) shows the standardised effects of the model terms. The alpha value to remove was set at 0.1, hence any terms with greater than 10% risk that an association between the term and net growth rate exists when there is no association were removed. Of these effects, only seeding density and TPO concentration were statistically significant at the traditional threshold of $P < 0.05$. However, there is still a greater than 90% chance that there was an association between each of the model terms Dox, Dox*seeding density, and TPO*Dox and removing them for the model may lead to overlooking inputs that have a true effect on net growth rate.

The R^2 adjusted value for this model is 95.7%, meaning that, when adjusting for the number of model terms, this model explains all but 4.3% of the variance of net growth rate with respect to the model variables. However, the noise in this data set is underestimated due to the method of fitting the net growth rate. As shown in Figure 5-14, the cumulative number of

population doublings from triplicate biological replicates were used to plot a linear model (calculated as shown in Figure 5-14), the gradient of which was used to derive the net growth rate for each condition. This method has averaged measurement system error and growth rate variation to calculate one input value into the model and, as described above, the growth rate was not consistent across the experiment. This means that the variability in the data is likely to be higher than reported here, which would also impact on the significance level of the model terms. However, if more data were input (i.e. three biological repeats for each growth rate) the DOE model would have more information input and so the significance values may be increased.

5.6.1.3. Comparison between using cumulative population doublings and net growth rate the to assess the impact of control variables on proliferation

Here, two analyses were used to understand the effect of control variables (Dox removal, Dox concentration, TPO concentration and seeding density) on proliferation of cells during forward programming. The first analysis used the number of cumulative population doublings (Figure 5-11) as an output and the second used net growth rate (Figure 5-16) . In both cases seeding density had the highest impact on proliferation. Seeding density could either have limited proliferation through bulk medium or surface area limitations. Bulk medium limitations might have either been a build-up of toxic metabolites such as lactate and ammonium [153], [154] or lack of nutrients such as glucose or amino acids [155]. Since there was a difference caused by seeding density, it is unlikely that the time-decay of reagents in the bulk medium caused these differences as the conditions would have been exposed to the medium for the same time.

In this system, assessing the impact of surface area limitations is complex, since the cells were adherent until Day 10, at which point they were enzymatically treated and cultured as suspension cells (see Figure 5-2). However, the Dox high density cultures achieved harvest densities of between 4 and 5×10^5 cells.cm^{-2} whereas the low Dox cultures achieved densities of only 1 & 3×10^5 cells.cm^{-2} as shown in Figure 5-17. Therefore, either surface area limitations did not occur (because if surface area had caused these limitations, the same harvest densities would have been achieved) or Dox allowed the cultures to achieve higher local cell densities.

The order of magnitude of standardised effect for the significant variables was different when comparing the two methods of assessing proliferation. The variable with the second highest impact on cumulative number of population doublings was Dox concentration (Figure 5-11 C), whereas the variable with the second highest impact on growth rate was TPO (Figure 5-16 C).

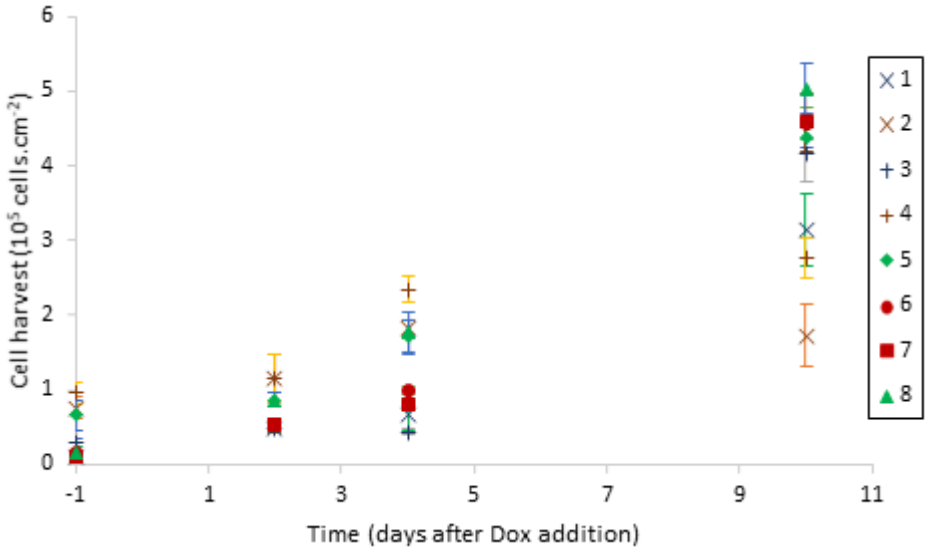

Figure 5-17: Cell harvest density from day -1 to day 10 shows that cultures were not limited by surface area since the higher cell densities cultures (2, 4, 5 & 8) achieved very different final harvest densities at day 10.

Both methods for measuring proliferation showed an interaction between Dox and TPO concentrations, where higher Dox conditions with low TPO concentration proliferated at a similar rate to conditions treated with high TPO concentrations. The cost per unit volume of high TPO medium was approximately 73% higher (based on approximate costs of research grade reagents) compared to the low TPO medium, whereas the cost of Dox was very low so there was no difference between the low and high Dox medium. If higher growth rates can be achieved by lowering TPO concentration but using higher Dox then this could have a large impact on process economics (assuming there is no significant effect on cell phenotype / quality).

When measuring proliferation by comparing growth rates, the interaction between seeding density and Dox is statistically significant. At low seeding densities the Dox concentration did not impact the growth rate of cells, whereas (as shown in Figure 5-16 B), whereas at higher seeding densities higher concentrations of Dox increased growth rate (as discussed in section 5.6.1.2) which also supports the hypothesis that Dox decay is cell-mediated. This effect was not statistically significant when comparing proliferation using the number of cumulative population doublings and was therefore removed from the model since stepwise, backwards elimination was applied. The lack of statistical significance was either due to the large noise associated with the biological repeats in the Dox- conditions or differences in cell loses between day -1 and 2 were less impacted by this interaction meaning the total number of cumulative population doublings changed less.

5.6.2. Assessing the impact of control variables on phenotype

To understand the correlation between of proliferation and phenotype, a scatter diagram was plotted using all conditions to Day 18 of the cumulative population doublings vs. the

proportion of on-target (CD41a+) and off-target (CD41a-/CD235a+) cells. As shown in Figure 5-18, there was a positive correlation between proliferation and on-target (CD41a+) phenotype and a negative correlation between proliferation and off-target phenotype (CD235a+, CD41a- at day 18), which suggests that the conditions that support the best growth also support on-target phenotype, demonstrating that growth factors are tailored to target populations.

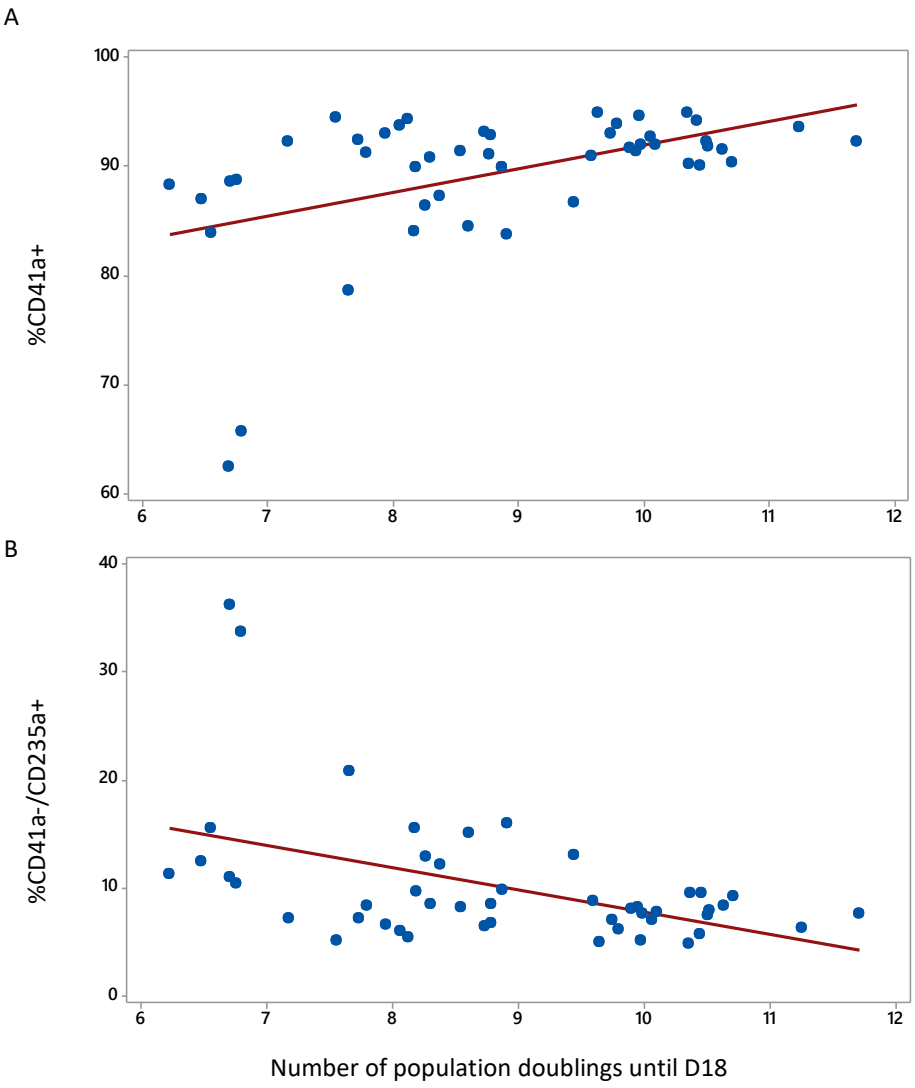

Figure 5-18: Correlations of population doublings with phenotype. An increase in the number of population doublings correlated with increased in the proportion of cells with target phenotype (A) and a decrease in the number of cells correlated with off-target phenotype (B). Flow cytometry Panel 6 was used, as described in Table 3-14.

5.6.2.1. Qualitative impact on cell maturity markers

The phenotype of all conditions at Day 18 is shown in Figure 5-19. Figure 5-19 (A) shows qualitatively that the high Dox cultures (conditions 5-8) had a higher proportion of CD41a+ cells. Compared to the cultures which had Dox removed at Day 10 (Dox-) (11-18), the Dox+ equivalent cultures had a lower proportion of CD41a+ cells.

Mature megakaryocytes do not express CD235a in vivo [156], therefore CD235a expression, inferred by median fluorescence intensity (MFI) in the PE channel for CD41a+ cells, was monitored to compare maturity, where it's assumed that lower MFIs signify more mature cells. Only CD41a+ cells were monitored for PE-CD235a intensity since this would capture cells that were MK rather than erythroid-lineage committed. Maturity using this measure was similar across Dox+ cultures, except for conditions 7 and 8 (high Dox, high TPO and low and high density respectively) which had a lower average PE-MFI values. This suggests that high Dox and high TPO concentration promoted cell maturity. The MFI values for conditions 12 and 13 (Dox-, low Dox, high and low density, low and high TPO respectively) had the highest MFI expression, indicating that maturity was inhibited in cultures which had Dox removed at day 10 and were treated with low Dox concentrations.

The relative expression levels of CD34 for all conditions are shown in Figure 5-19 (C). Here cells treated with high concentrations of Dox (conditions 5-8) expressed the highest levels of CD34 expression and the Dox- cultures (conditions 11-18) expressed the lowest CD34 levels. CD34 expression is linked to progenitor cells in vivo [157] which could indicate that FOPMKs with higher CD34 levels have a higher proliferative capacity. However, CD34 expression on megakaryocytes from patients has been linked to higher levels of myelodysplasia (where

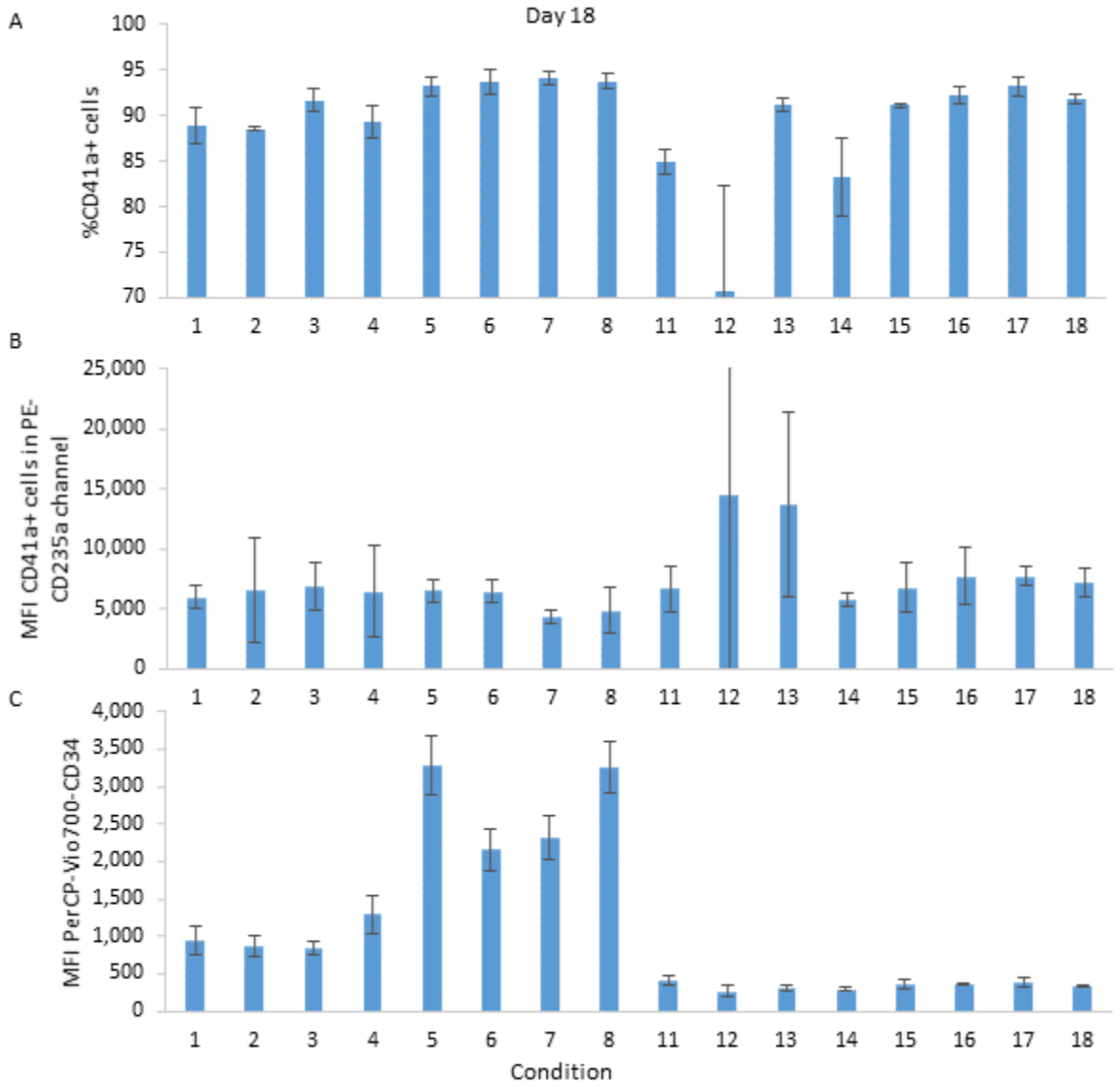

Figure 5-19: Phenotype of conditions at Day 18 of culture. (A) All conditions achieved at least an average of 70% of cell as CD41a+, with higher Dox treatment producing the highest and most consistent proportion of CD41a+ cells (conditions 5-8). Of the lower Dox treatment conditions, higher CD41a expression was achieved with higher TPO concentrations (Condition 3). The most variable outcomes were achieved when Dox was removed at Day 10 in the conditions with a lower amount of Dox initially (11, 12, 14), however, again this could be compensated for by using higher TPO concentrations as 3 and 13 both had 91% of cells which were CD41a+. (B) The median fluorescence intensity (MFI) of CD41a+ cells in the PE-CD235a channel gives an indication of maturity (with a lower expression of CD235a indicating a more mature phenotype). Qualitatively, conditions which produced lower proportion of CD41a+ cells also produced higher expression of CD235a in those cells, indicating an immature phenotype. Condition 7 produced the most mature phenotype, comparing this to condition 17, where Dox was removed at Day10, shows that continuing to supplement with Dox increased maturity. (C) CD34 expression shows higher levels of Dox maintained CD34 expression, and removal of Dox produced the lowest expression at Day 18. High density cultures (conditions 5 and 8) showed the highest expression levels, but had comparably lower number of population doublings at this point (see Figure 5-12), indicating that CD34 might be a measure of growth potential. Flow cytometry Panel 6 was used, as described in Figure 3-13.

blood cells do not mature correctly) [158]. Therefore, it is not clear whether the differences in CD34 expression levels lead to a positive or negative outcome for maturity of FOPMK cultures and resulting platelet production. Since CD41a expression is directly linked to platelet functionality it was decided that effect of control variables on CD41a expression would be investigated further using a DOE analysis.

5.6.2.2. DOE analysis of CD41a expression at day 18

To more robustly determine the impact of control variables on CD41a expression a DOE analysis was performed using statistical software Minitab (parameters as described in Table 5-3). The results of the DOE analysis are shown in Figure 5-20. The main effects plot (Figure 5-20 A) shows that low seeding densities, high Dox, high TPO and Dox retention at Day 10 all increased the proportion of cells which were CD41a+. The statistically significant interactions ($P<0.05$) are shown in Figure 5-20 (B). The effects of low Dox concentration and Dox removal were mitigated at low densities and at high TPO concentrations.

Furthermore, the effect of Dox removal was mitigated by using a higher concentration of Dox between D0 - D10 and a higher concentration of TPO. This suggested that TPO and Dox had a similar effect on the biochemical pathways that promote CD41a expression and that they were degraded at a rate proportional to the concentration of cells. The higher expression of the three transcription factors GATA1-FLI1-TAL1 have also been linked to MK lineage markers, whereas GATA1-TAL1 expression (without FLI1) have been linked to off target erythroid lineage [134], so it may be possible that low Dox / TPO concentrations do no promote high enough FLI1 expression for megakaryocyte lineage commitment.

The Pareto Chart (Figure 5-20 C) shows that the main effects had the greatest impact on CD41a expression, and of the main effects, Dox concentration was the highest. Most

secondary, and one tertiary, effect were statistically significant (Dox concentration Day 0-10*TPO concentration*Dox removal / BCD is shown since 0.1>P>0.05 and is therefore not statistically significant using the traditional metric of P<0.05) showing that the impact of the factors on CD41a expression is high complex and interacting. Furthermore, since the lack of fit error P value is 0.53 (P>0.05) no lack of fit was detected by the analysis.

Compared to the outputs from the DOEs measuring proliferation (Figure 5-11 and Figure 5-16), more terms were shown to be statistically significant when using %CD41a+ as an output. This indicates that there was more noise as a ratio of experimental effect associated with methods used to measure proliferation.

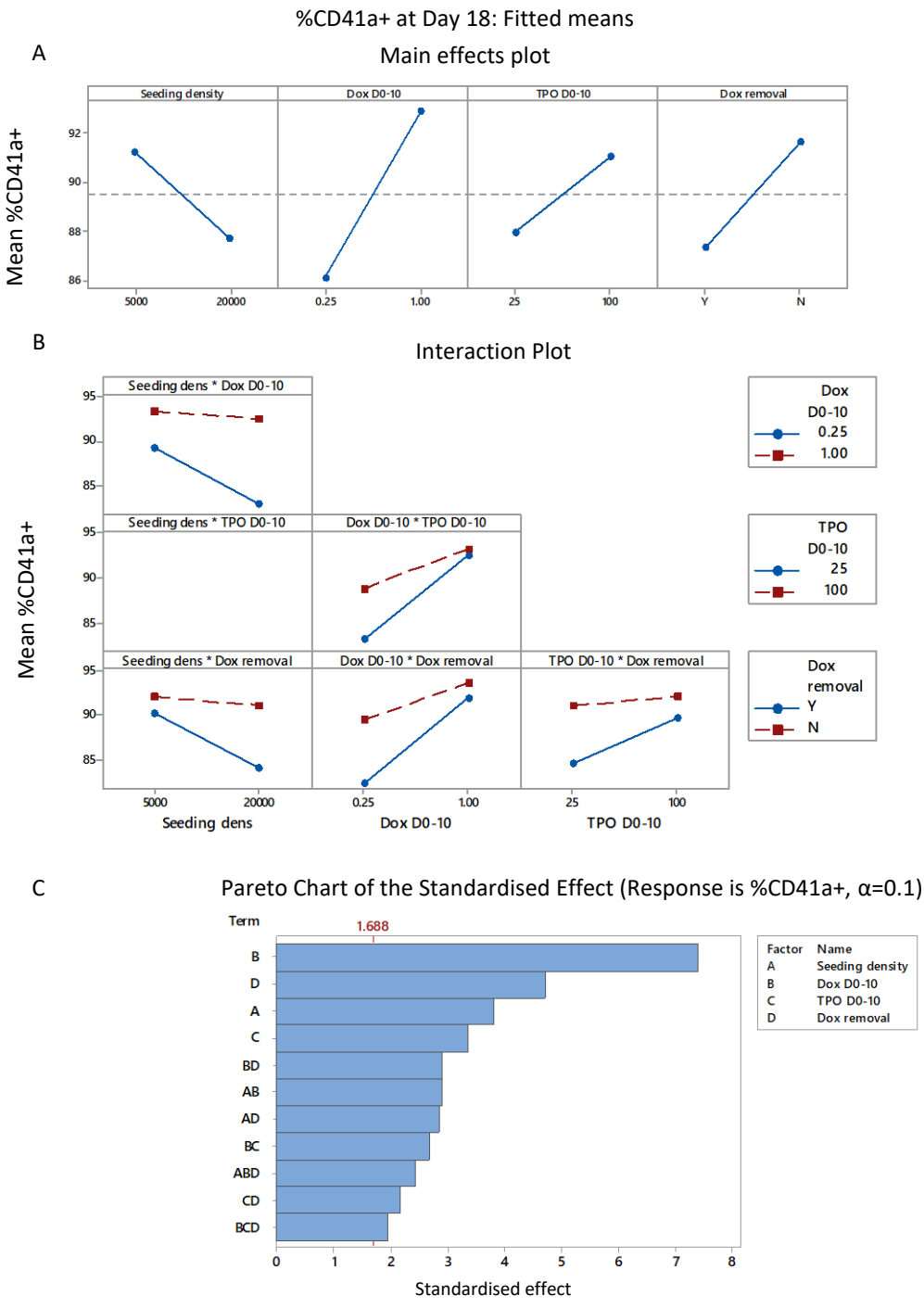

Figure 5-20: DOE output summary for %CD41a+ cells at Day 18. DOE analysis was performed using statistical software package Minitab with stepwise backwards elimination (a=0.1) applied for a 2-level, 4-factor, factorial design. The R^2 (adj) fit of this model was 74.6%. (A) Main effects plot shows Dox concentration Day 0-10 had the greatest impact on mean %CD41a+ expression, with high Dox increasing the proportion of CD41a+ cells at Day 18. Seeding density at D-1 decreased the proportion of CD41a+ cells whereas TPO concentration Day 2-10 increased the CD41a+ proportion and Dox removal at Day 10 decreased the mean proportion of CD41a+ cells (B) Interaction plots show that there were 5 statistically significant interactions affecting %CD41a+ proportion. (C) Pareto chart showed that the main effects had the highest impact on phenotype; Dox concentration Day 0-10 had the greatest effect followed by Dox removal and seeding density. Some secondary and tertiary interactions were also statistically significant. Flow cytometry Panel 6 was used, as described in Figure 3-13.

5.6.3. Expansion and phenotype trajectory of cultures past day 18

The impact of control variables on cultures to mid-stage differentiation has so far been examined. Day 18 was chosen because it was apparent from the technology transfer runs that by this time point cells were likely to be committed to either MK or erythroid linages (as denoted by the expression of CD41 and CD235a). However, the impact on late stage differentiation (remaining expansion of cells and expression of mature phenotype markers CD42a/b) was unknown. It was experimentally impractical to continue all cultures past day 18, and since seeding density was the variable with the highest standardised effect on proliferation (as measured by both cumulative number of population doublings and net growth rate) it was decided that one low and one high seeding density culture would be continued to be maintained past day 18. It was also decided that high TPO and high Dox conditions should be used since this combination of variables had proliferated most and produced the highest proportion of CD41a+ cells. Therefore condition 7 and 8 were selected for expansion to terminal differentiation or as close to this point as possible. Cultures were monitored for differences in expansion and phenotype trajectory, to determine whether growth rate and phenotype differences caused by seeding density converged or diverged.

5.6.3.1. Proliferation of conditions 7 and 8 past day 18

Figure 5-21 (A) showed cultures had similar net average growth rates until Day 26 (0.0118 and 0.0120 hr^{-1} for conditions 7 and 8 respectively), although condition 7 underwent an average of 1.29 PDs extra that condition 7 over the 28 day period (Day -1 – 27). This suggests that either the cell counts at Day 0 were offset, impacting the cumulative number of PDs, or the growth inhibition that occurred between D-1 – 2 was not recovered later. At day 18 the net growth rate of the cultures was 0.0116 and 0.0099 for conditions 7 and 8 respectively (Figure

5-15) which also suggests that condition 8 regained some of the lost expansion from Day -1 – 18.

At day 14 the residuals show that condition 8 had a slower growth rate, but this was recovered later, suggesting this growth inhibition can be recovered later in the process, so avoiding growth inhibition is this stage (day 10 – 14) was less critical for process control than in the early stage (day -1 – 2), assuming that the early stage growth loss was a real effect rather than an cell count measurement effect.

There was a systematic deviation of the data from the trend line representing exponential growth with a constant growth rate occurred from Day 27 onwards as shown in Figure 5-21 (B). Cell growth did not occur in either Condition 7 or Condition 8 after day 27. The cause of this inhibition point is not known. As mentioned above, either the conditions had the same number of cumulative doublings which is not seen due to an offset in the cell counts at day -1, or the cells only proliferate for a finite period post Dox addition. Since both these conditions had the same concentrations of TPO and Dox, it is unknown whether these variables would affect the maximum number of population doublings achievable or the maximum proliferation time post Dox addition. Some cell growth may have been returning at Day 37, however because culture volume was being used for sample analysis and the cells were not expanding, there were too few cells to continue the experiment.

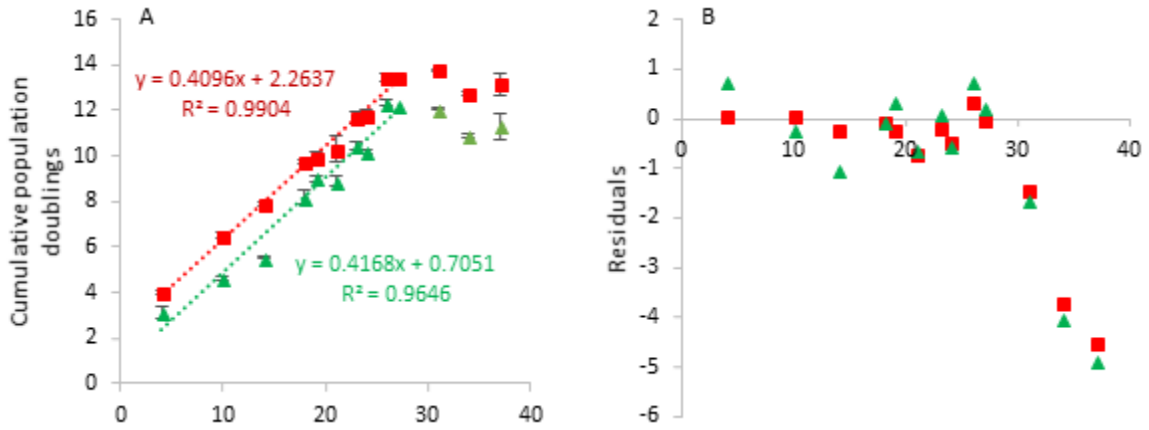

Figure 5-21: Condition 7 and 8 were cultured to Day 37 after Dox addition. The linear increase in cumulative number of population doublings over time shows a maintained net growth rate from day 2 until day 27 followed by a period of no net increase in viable cell number. (A) shows the rate of change in population doublings (trend line gradient) with time for condition 7 and 8 were similar, (0.4096 and 0.4168 PDs.day^{-1} respectively) however the total number of population doublings were lower for condition 8 due fewer population doublings between day -1 and 2. This could either be an artefact of cell counting measurement (i.e. the recorded number of cells counted initially was higher than actually seeded, giving a lower number of population doublings), or the initial growth inhibition decreased the total reachable number of population doublings. (B) Plotting the residuals showing the difference between the constant growth rate trend line and the data shows the growth of cells was not maintained past day 27 of culture. Residuals for condition 8 show lower growth rate until day 14 then increasing growth rate until a growth inhibition at day 27.

5.6.3.2. Phenotype of long-term expanded cultures

Between Day 32 and Day 37 the number of on-target cells decreased by 7% in Condition 7 and by 9% in Condition 8 (Figure 5-22 A & B), showing that the lack of growth was concurrent with a decline in cell quality and cells also become smaller and more granular as shown in Figure 5-22 (iv), suggesting they were undergoing apoptosis. The MFI of fluorescence in the CD41a and CD42a channels also decreased and a double negative population was beginning to emerge (v, vi). This again shows that the quality of the cells was declining.

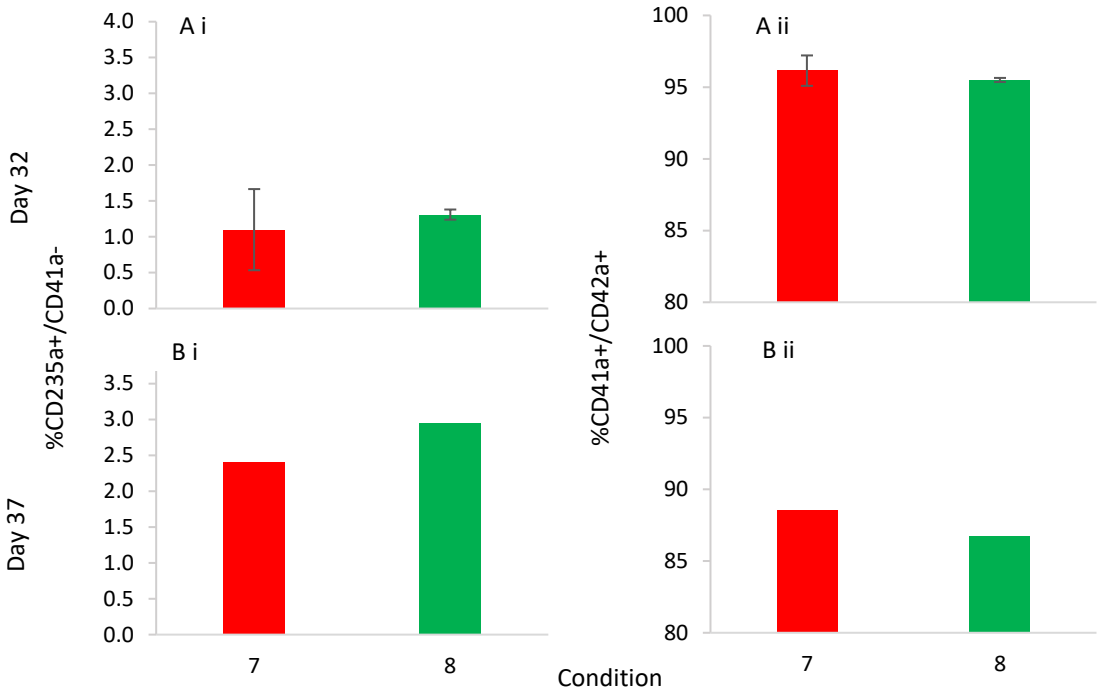
A i
A ii
B i
B ii
Day 32
Day 37
%CD235a+/CD41a-
%CD41a+/CD42a+
Condition
7
8

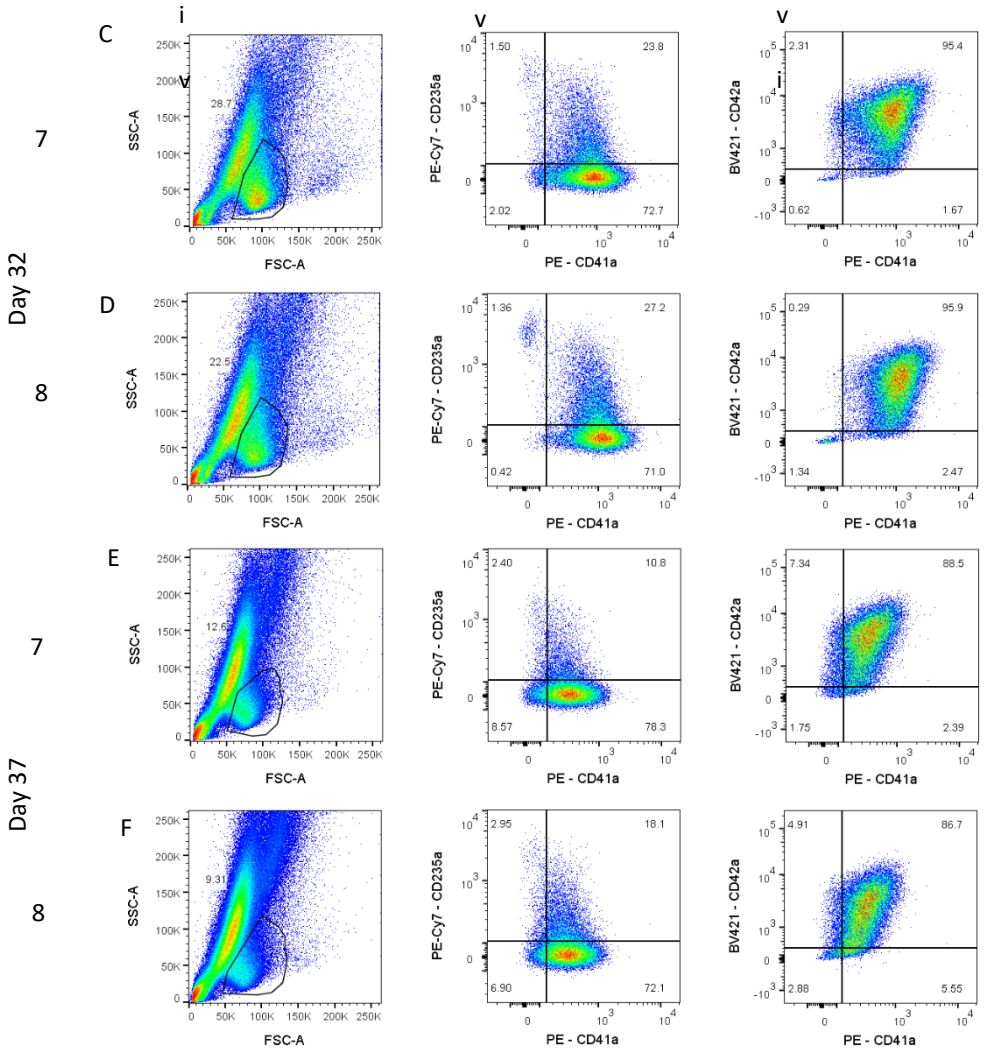
C
D
E
F
Day 32
Day 37
7
8
SSC-A
FSC-A
PE-Cy7 - CD235a
PE - CD41a
BV421 - CD42a

Figure 5-22: Cell phenotype at Day 32 and 37. Bar charts shows average proportion of off target CD235a+/CD41a- cells (i) and proportion of target CD41a+/CD42a+ cells (ii) at Day 32 (A) (data shows average N=2 ±STD) and Day 37 (data shows polled analysis) (B). Across both cultures, the proportion of off-target cells increased, and the proportion of on-target cells decreased across between Day 32 and 37, coinciding with a decrease in growth (see Figure 5-21). Exemplar flow cytometry plots show forward scatter – side scatter plots (iv), CD235a and CD41a expression (v), and CD42a and CD41a expression (vi) for conditions 7 (C,E) and 8 (D, F) at Day 32 (C, D) and Day 37 (E, F). Forward scatter – side scatter plots (iv) show a decrease in the proportion of target cells from Day 32 to Day 37, and target cells that remained were smaller in size. This decrease in size could also be attributed to lower expression levels of CD41a and CD42a, since it is possible that the smaller cells had the same receptor density (receptors per unit cell surface area) but a decreased size decreased the absolute expression. However, at Day 37 there appeared to be a lower expressing CD42a population emerging (Evi and Fvi), it's unclear whether this was caused by decreasing cell size, is a signal of failing cell health or even whether a maturity even has occurred and caused the megakaryocytes to shed platelets. The increase in apparent CD235a+/CD41a- cells could be caused by the small sized cells shifting into the negative CD41a gate and not a true reflection of reduced receptor density (Ev and Fv). Flow cytometry Panel 6 was used for acquisition, as described in Table 3-14.

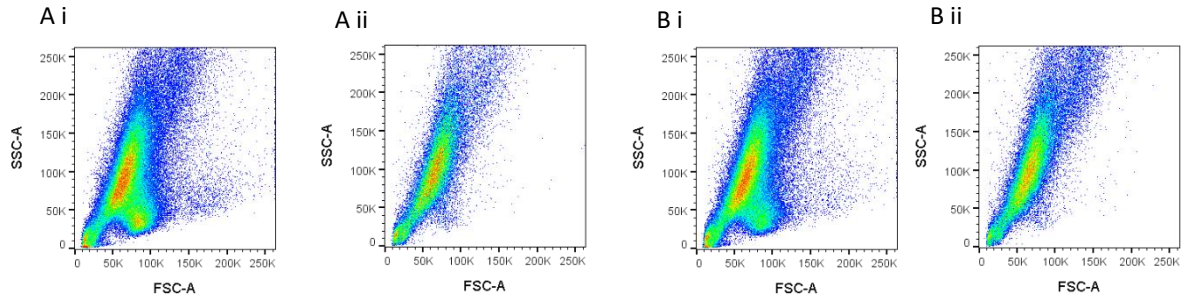

Figure 5-23: To reduce the concentration of dead cells (high side scatter region) a ficoll procedure was performed at Day 34 to conditions 7 and 8. A and B show conditions 7 and 8 respectively; i and ii show forward scatter – side scatter profiles of cells before and after ficoll processing. In this case, the ficoll procedure did not select for the target cell population.

The large number of small and granular cells, which were likely apoptotic bodies, could have released factors that promoted cell death and loss of on-target phenotype in other cells. Therefore, a Ficoll protocol was performed to separate the live cells based on an established protocol from our collaborators. However, I was unable to replicate it. Figure 5-23 shows that the Ficoll protocol failed to purify the target phenotype.

5.7. Early culture dynamics as an indicator of forward programming trajectory

Monitoring early differentiation trajectory attributed (markers and / or proliferation) and using those attributes to predict end stage programming outcomes– or better - enhance process control to ensure products achieve the required specification would be a powerful process development tool. Understanding how control variables influence process parameters at different time points through the process may also lead to improved understanding of the mechanisms which drive growth and phenotypic changes, which also could enable the implementation of better processes and enhanced control.

As noted in the technology transfer exercise (Section 5.4.4), currently the marker expression and transition during forward programming are not fully understood . To gain insight into early stage growth and phenotypic changes, high temporal resolution cell counts and phenotype assays were performed during the DOE experiment outlined in Table 5-3. Cell counts using flow cytometry, and Panel 6 as described in Table 3-14 was used for phenotypic analysis. Both cell counts and phenotype analysis was performed at day 2, 4 and 10. At day 2 there were only 4 conditions (rather than 8) because TPO was supplemented from day 2 onwards, according to the transfer protocol (see Figure 5-2 and Section 2.3.2)

The proliferation and phenotype changes from day -1 until day 10 are shown in Figure 5-24. Highest proliferation was achieved between day -1 and 2 and in low density cultures (as shown in A). At this stage Dox concentration did not appear to affect the proliferation. This might be because the cell numbers were relatively low and, assuming a cell-mediated degradation of Dox, small cell densities may have produced slow rate of Dox degradation leading to similar growth responses in high Dox treated cultures (5,6) and low Dox treated cultures (1,2).

The comparatively high growth rate between Day -1 and 2, which was reduced in higher density cultures, likely contributed to the identification of seeding density as the variable that had the highest effect on the number of cumulative population doublings at D18 (Figure 5-11). Furthermore seeding density was also the term with the biggest standardised effect when using net growth rate as a measure of proliferation (Figure 5-15 C), suggesting that seeding density has a negative effect across the culture period.

Growth rate from day 2 – 4 is approximately half that of day -1 – 2. Condition 3 (low density, low Dox, high TPO) proliferated less during this period, but recovered from Day 4 – 10. From Day 4 – 10 differences in proliferation due to cell density were observed; for equivalent TPO/Dox conditions (1 & 2, 3 & 4, 6 & 5, 7 & 8) the lower density cultures had a greater number of population doublings per day. This may have been caused by cell mediated degradation of nutrients / supplements or contact inhibition. The cultures with high Dox concentrations also outperformed low Dox conditions, except for 3 (low density, low Dox, high TPO), again supporting the hypothesis that TPO supported growth in the presence of low Dox.

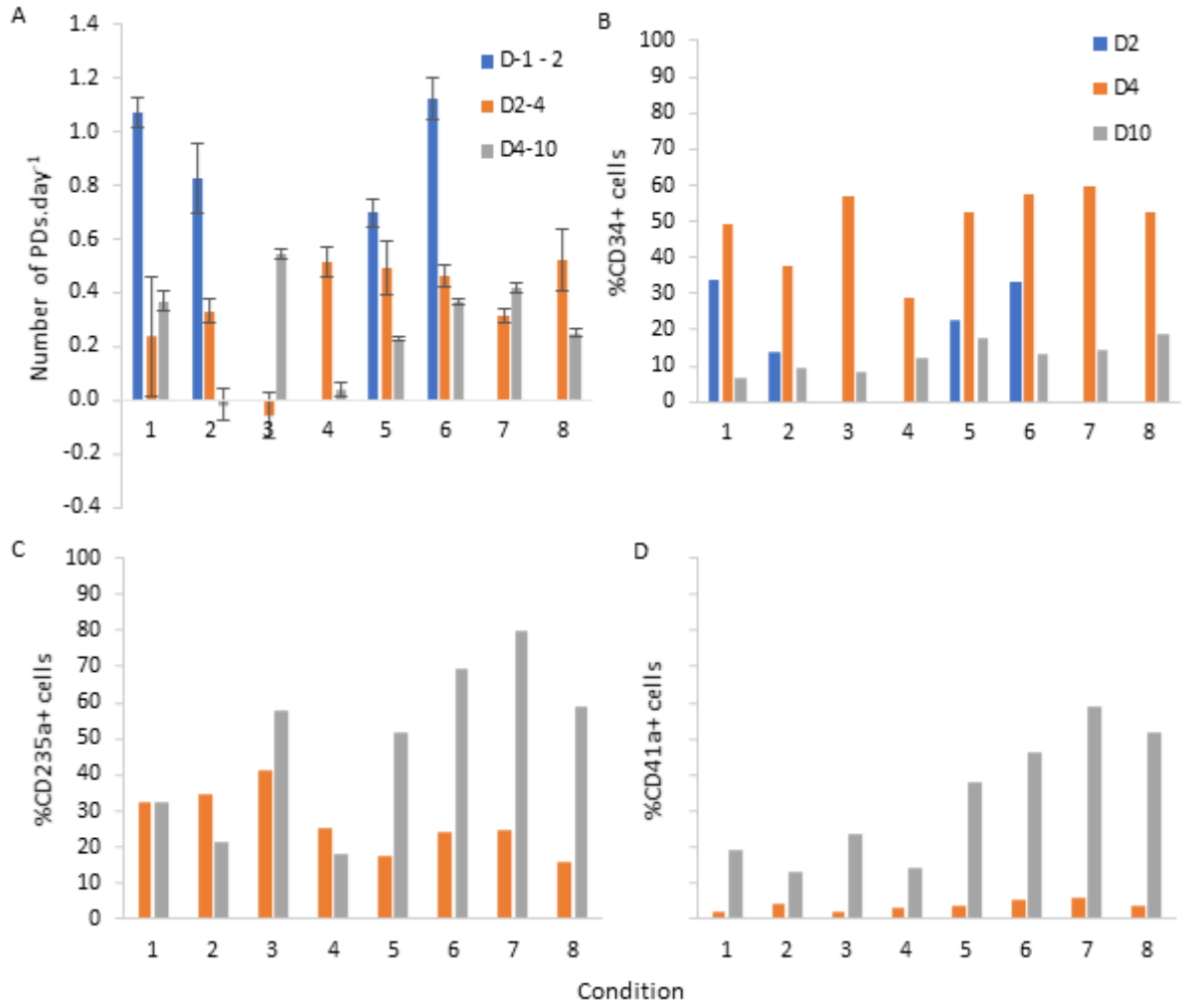

Figure 5-24: Summary of cell culture until Day 10. (A) Number of population doublings per day at various time points show highest growth rates were achieved between Day -1 and 2, with lower density cultures reaching higher growth rates (data shows N=3, ±STD) (B) The proportion of CD34+ cells peaked at Day 4, at which point lower density cultures showed higher expression that high density cultures (conditions 1, 3, 6 and 7). By Day 10 this trend was reversed as higher density cultures (conditions 2, 4, 5 and 8) had higher proportion of cells which were CD34+, suggesting that the higher density cultures are delayed in maturing rather than the higher densities preventing maturity. (C) The proportion of CD235a+ cells increased from Day 4 to 10. At Day 4 the cultures treated with the lower concentrations of Dox had a higher proportion of CD235a+ cells, however at Day 10 this trend switched since the cultures with the highest expression were low density, high Dox and high TPO treated (7) followed by low density, high Dox and low TPO (condition 6) and low density, low Dox and high TPO. (D) A low proportion of cells are CD41a+ at Day 4. At Day 10 the high Dox treated cultures (conditions 5, 6, 7, 8) had a higher proportion of CD41a+ cells compared to low Dox cultures (conditions 1, 2, 3, 4). Again, the highest the condition with the highest proportion of CD41a+ cells was low density, high Dox and high TPO treated (7). Flow cytometry Panel 6 was used for acquisition, as described in Table 3-14.

The proportion of cells that were CD34+ peaked at Day 4 (Figure 5-24 B) and then decreased again, suggesting cells were differentiating along the haematopoietic lineage. Cultures which had highest expression were low seeding density, and either high Dox concentration (Condition 6), high TPO concentrations (3) or both (7). CD235a expression peaked at Day 10 (Figure 5-24 C), and the highest expression was seen in low seeding density, high Dox, high TPO concentrations (7). It should be noted that the data is a snapshot of the cells in time as they are passing through lineage trajectories, so other cultures may have reached peak levels at different time points, which limits the conclusions which can be drawn. Greater insight would be gained by considering the transition rates between populations and the growth rate of each population in response to different media or media supplementation and the degradation of each media component.

CD41a expression also increased from Day 4 to Day 10 (Figure 5-24 D). All high Dox treated conditions (5, 6, 7, 8) had a higher proportion of CD41a+ cells compared to the counterpart low Dox concentration conditions (2, 1, 3, 4). Of the high Dox concentration cultures, high TPO and low seeding density (7) had the highest CD41a expression, which indicates that high Dox concentrations promoted cell maturity.

From the outputs measured early in the differentiation and presented above, CD41a expression at day 10 and CD34 expression at day 4 were prioritised for further analysis. CD41a expression is a key marker required for functionality of platelets (See Section 3.2.1), and therefore measuring expression differences between different conditions is likely to inform differentiation trajectory. CD34 expression was selected because this is a key haematopoietic progenitor marker, and therefore would possibly be useful when measuring markers early in the differentiation process. Measuring proliferation was not selected because cell counts can

be variable in early differentiation (as noted by *Process Risk 8*) and CD235a expression was not selected because of uncertainty of expression in off-target (erythrocyte lineage) as well as on-target (MK lineage) cells.

5.7.1.1. DOE analysis of CD41a expression at day 10

At day 10, all control variables were found to have a statistically significant effect on CD41a expression as shown in Figure 5-25 (A). Seeding density had a negative correlation with CD41a expression whereas Dox and TPO concentrations had a positive correlation with CD41a expression. The interaction plot Figure 5-25 (B) shows that the interaction between Dox and TPO was the only statistically significant interaction, where higher TPO concentrations increased only increased CD41a expression (relative to low concentrations of TPO) at high concentrations of Dox. The pareto chart Figure 5-25 (C) shows Dox was the variable with the highest impact on CD41a expression, followed by TPO and seeding density (which had similar standardised effects).

Aside from Dox removal (which is not considered here, as it only occurred after day 10) compared to the effect of control variables at day 18 (Figure 5-20) all main effects have the same trend of effect (positive or negative correlation with expression) of effect on CD41a expression and Dox concentration still has the overall highest standardised effect.

However, the interaction between Dox and TPO is reversed. It is hypothesised that:

- At day 10 Dox was driving differentiation and therefore at higher concentrations of Dox more cells were at a differentiation stage where they are responsive to TPO.

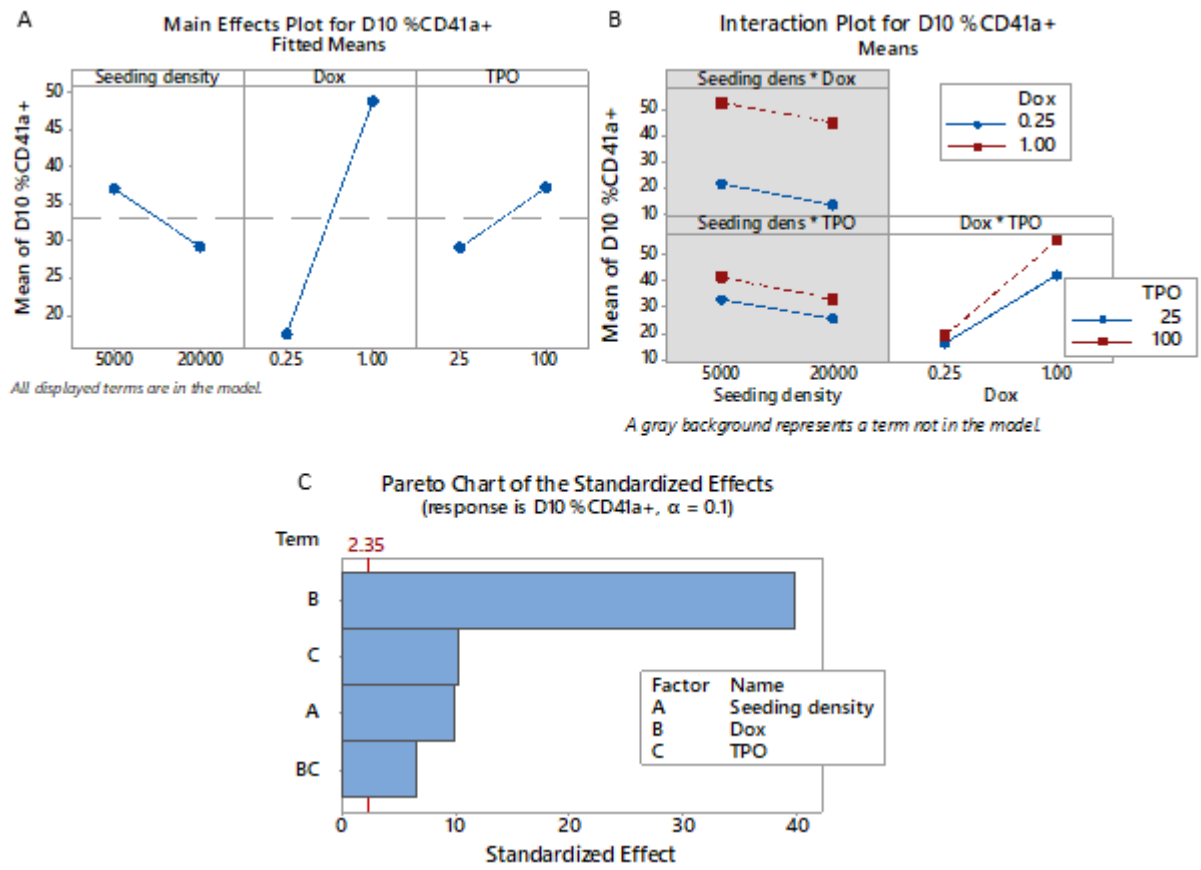

Figure 5-25: DOE analysis of the effect of control variables on CD41a expression at day 10. (A) Main effects plot shows seeding density had a negative correlation with CD41a expression, whereas Dox and TPO had a positive correlation with CD41a expression. (B) The only statistically significant interaction was Dox*TPO which showed that at lower concentrations of Dox the concentration of TPO did not correlate with a change in CD41a expression, whereas at higher concentrations of Dox, increasing TPO concentrations correlated with higher CD41a expression. (C) Pareto chart showed that Dox concentration was the variable with the highest effect on CD41a expression.

- By day 18 most cells were responsive to TPO, and if Dox triggers the same biochemical pathways as TPO in this differentiation stage, at higher concentrations of Dox supplementation of extra TPO would not improve phenotype since the pathway is already saturated (i.e. is at the top of the sigmodal dose response curve).

Seeding density had a significant ($P<0.05$) effect at both day 10 and day 18. As discussed in Section 5.6.1, it is unlikely that local cell density effects were driving this effect, rather was a function of the effects of bulk medium and supplement supply per unit cell density. and time

as confirmed by the differences in achieved local density (Figure 5-17) and interactions between seeding density and supplements (Figure 5-20 B). As shown in Figure 5-21, when conditions 7 and 8 were expanded past day 18, differences in phenotype converged, as did net growth rate. At day -1 cells were seeded at a set number of cells per surface area and the bulk medium supply was the same volume (meaning different cell density conditions had both different cell densities per surface area and per volume of media), whereas at day 10 all conditions were set to the same cell density per volume (as they were forced into suspension – see Figure 5-14). Therefore, all conditions had the same bulk medium supply per unit cell.time Since in conditions 7 and 8 the phenotype and net growth rate converged by day 27, .this indicates that the detrimental effects of medium undersupply in early stages can be "recovered" if the supply of bulk medium is adjusted later. This means that bulk medium supply is a lower priority from a control perspective as it can be corrected; however, a detailed study of the impact on COGs of over- or under-supply is not covered in this work. This style of DOE analysis does not identify what the optimal bulk medium supply rate should be; a modelling approach including dynamic culture environment changes would be more suited to determining improved medium supply regimes [81].

5.7.1.2. DOE analysis of CD34 expression at day 4

CD34 expression was monitored as a surrogate measurement for cells that were progressing from a pluripotent to a haematopoietic linage. Day 4 was the earliest time point where CD34 expression was measured in addition to TPO being supplemented. The main effects plot Figure 5-26 (a) shows that seeding density had a negative correlation with CD34 expression whilst Dox had a positive correlation with CD34 expression. TPO did not have a significant effect. This suggests that the cells were not were not at a point in the differentiation trajectory where they responded to TPO. If this is the case, future studies could be targeted to finding

the point at which TPO supplementation is required, since COGs could be decreased by initiating TPO supplement at a later point in the differentiation trajectory.

The only statistically significant effect was seeding density and Dox, where at higher seeding densities, higher Dox concentration promoted a higher CD34 expression, whereas at lower seeding densities, higher Dox concentrations did not improve CD34 expression to the same extent. The seeding density * Dox interaction was a significant effect on CD41a expression at day 18 (Figure 5-20 B) but not at day 10 (Figure 5-25 B) Therefore, the following mechanisms are hypothesised:

Day 4

- Cultures which had been seeded at a higher seeding density still had higher recorded cell counts compared to lower density (Figure 5-17), therefore cell seeding density could be used as an accurate surrogate measure for cell number present at day 4.
- The cells did not respond to TPO (and future work may consider supplementing TPO at later stages of culture), Dox drove differentiation.
- Cell mediated decay of Dox was higher at higher seeding densities, so lower concentrations of Dox had lower CD34 expression at higher cell seeding densities.

Day 10

- Cultures which had been seeded at a higher seeding density did not have higher recorded cell counts compared to lower density, so cell seeding density could not be used as an accurate surrogate measure for cell number present at day 10 (Figure 5-17). Therefore, it is more challenging to make accurate assumptions about cell-mediated decay effects based on cell numbers. This is limitation of DOE analysis with dynamic data sets.

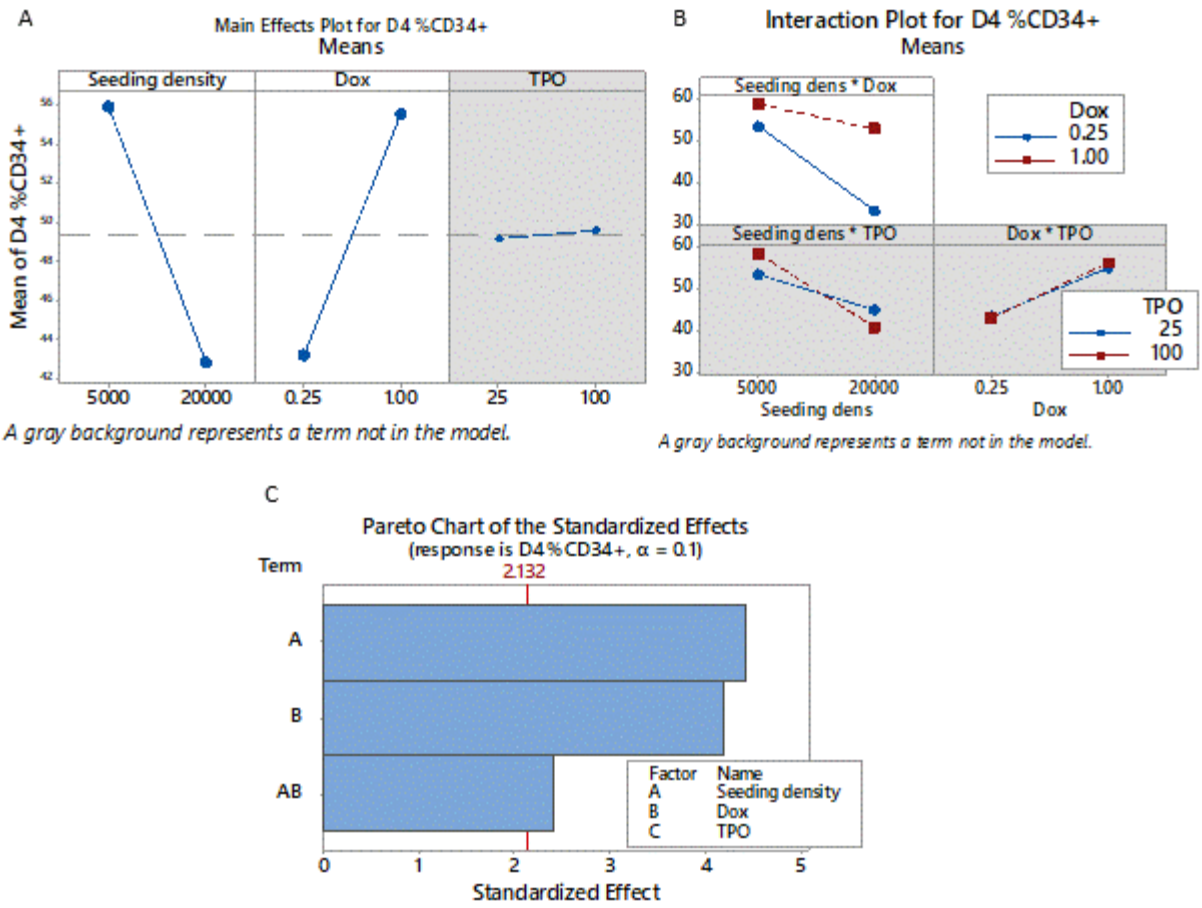

Figure 5-26: DOE analysis showing the effect of control variables on CD34 expression at day 4. (A) main effects plots indicates that was a negative correlation with seeding density and CD34 expression, the was a positive correlation between Dox and CD34 expression and there was little impact of TPO on CD34 expression. (B) The interaction between seeding density and Dox concentration was the only statistically significant interaction, where Dox mitigated the negative effect of higher seeding densities compared to lower Dox concentrations. (C) Pareto chart showed the standardised effect of seeding density and Dox concentrations were similar.

- Therefore, the interaction between Dox and seeding density was not statistically significant due to changing relative cell numbers between conditions confounded cell-mediated effects.
- TPO concentration was a statistically significant effect since at day 10 a higher proportion of cells responded to TPO in addition to Dox as cultures were progressing towards a MK phenotype.

5.8. DOE model validation

To check the validity of the DOE model effects, an experiment was conducted which replicated a smaller number of conditions the low TPO / low Dox, low TPO / high Dox and high TPO / high Dox, and concentrations, at low seeding density and retaining Dox supplementation throughout culture (conditions 1, 6 and 7 respectively as listed in Table 5-4). These conditions were selected as Dox and TPO concentrations were found to have complex and interacting effects on both cell growth (Figure 5-11) and phenotype (Figure 5-20). A low cell density was selected as it was likely that medium exhaustion effects were likely to be confounding cell output (as shown by the interactions between Dox / TPO concentrations and since a higher input cell number resulted in lower cell growth - Figure 5-11). Dox supplementation was continued post-day 10 since the was no benefit to its withdrawal on cell proliferation (Figure 5-11) and lead to a decrease in CD41a expression (Figure 5-20). A further change was made from the original experimental conditions where the high TPO supplementation was retained past day 10 at 100 $ng.mL^{-1}$ (previously TPO supplementation had been decreased to 25 $ng.mL^{-1}$ after day 10), to test the effect of continued higher supplementation.

Here, the individual effects of Dox and TPO are more clearly demonstrated. Figure 5-27 (a) shows that both low TPO conditions had virtually identical average cell expansion rates, whereas the high TPO condition had an average of one extra cumulative population doubling levels at day 26 (although this was not a statistically significant effect). Whereas the low Dox conditions produced average CD41a expression of 70% compared to 97% for both high Dox conditions.

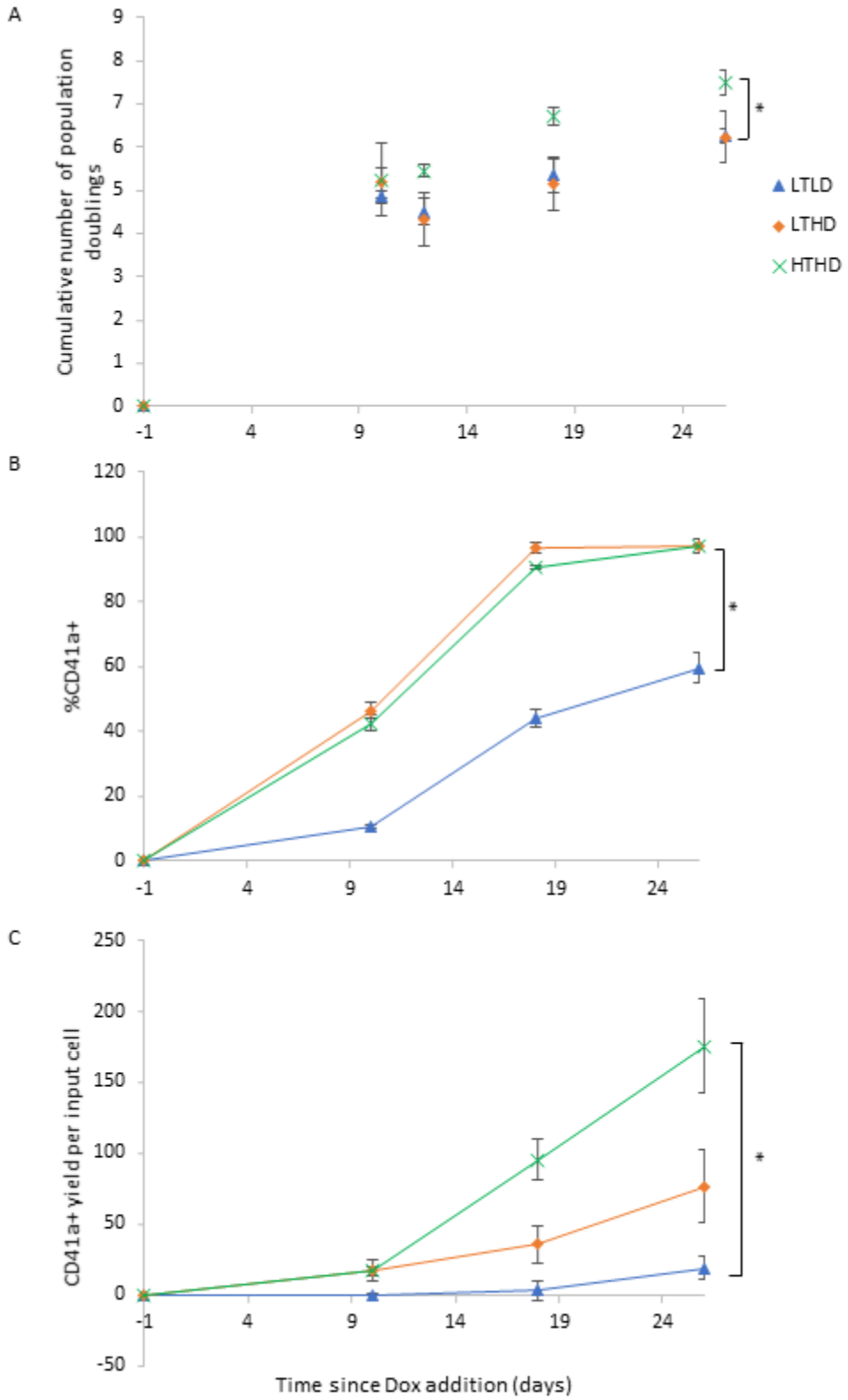

Figure 5-27: Confirmatory runs showed that (a) higher TPO supplementation increased cell expansion (although there was not statistically significant effect on the number of population doublings) and (b) increased Dox supplementation increased CD41a expression with (c) over 9x greater on-target cell yield was achieved from high TPO/Dox compared to low Dox/TPO supplementation. and (*) denotes statistical significance ($P<0.05$) using ANOVA. Legend key: LTLD = low TPO & low Dox, LTHD = low TPO & high Dox, HTHD = high TPO & high Dox.

Qualitatively, these results confirm the relationships established with the DOE models for proliferation and phenotype (Dox and TPO having positive effects on both). However, when using the DOE model to predict the cell expansion (shown in Table 5-6) only one of the confirmatory runs form the LTLD and HTHD conditions and none of the runs from LTHD condition achieved within the 95% confidence interval predictions. All the runs from the high Dox conditions achieved CD41a expression within the 95% confidence interval predictions but the LTLD condition underperformed in terms of phenotype. Therefore, expansion is more variable across experiments than within experiments, indicating that there is an unknown variable within the system that has not been controlled. Phenotype is more stable at high Dox concentrations between experiments but not at low Dox concentrations – another indication that high Dox concentrations should be used in future work.

Table 5-6: DOE model predicted expansion and phenotype and confirmatory run results. Yellow highlights indicate runs within 95% confidence predictions.

Condition	**Cumulative number of population doublings**		**CD41a expression**	
	Predicted (95% PI)	Confirmatory runs (1, 2, 3)	Predicted (95% PI)	Confirmatory run
LTLD	4.92 (4.78, 5.06)	5.35, 4.86, 5.86	89.4 (82.1,96.7)	42.3, 42.1, 48
LTHD	6.73 (6.60, 6.87)	4.45, 5.61, 5.31	93.7 (86.5, 101.5)	98.2, 95.0, 97.4
HTHD	7.03 (6.89, 7.17)	6.52, 6.93, 6.66	94.2 (86.9, 101.5)	90.1, 90.6, 90.9

5.9. Proposed mechanistic model framework describing forward programming

This work has shown that DOE can be applied to assess the general impacts of control variables on CQAs for FOPMKs and to narrow down routes for further investigation (for example, Dox supplementation should continue past day 10 of culture). However, DOE is limited in utility since the relationships between variables and outcomes are complex and non-linear and therefore applying DOE to define optimal process are challenging, since DOE does not directly test the nature of the underlying mechanism.

Based on the data presented in this chapter and relevant literature [46], [55], [134], [159], Figure 5-28 shows a schematic diagram for a proposed mechanistic model for FOP. Here, cell populations are divided into discrete units which assume consistent growth and rate conversion behaviours within each population unit. Different variables (growth factor concentration, Dox concentration, medium exhaustion, positive cell released conditioning factors) may have different impacts on the growth and conversion rates of associated populations. It would be assumed that rates have a sigmodal dose response to variables [100].

The challenge with developing models that are usable for manufacturing outcomes is to develop a model which has the minimum level of complexity to achieve desired manufacturing outputs. More complex models may more accurately describe behaviour, but they require much more resource to parameterise. A first iteration of this model could utilise a single growth rate modulated by TPO and medium exhaustion could be applied to all

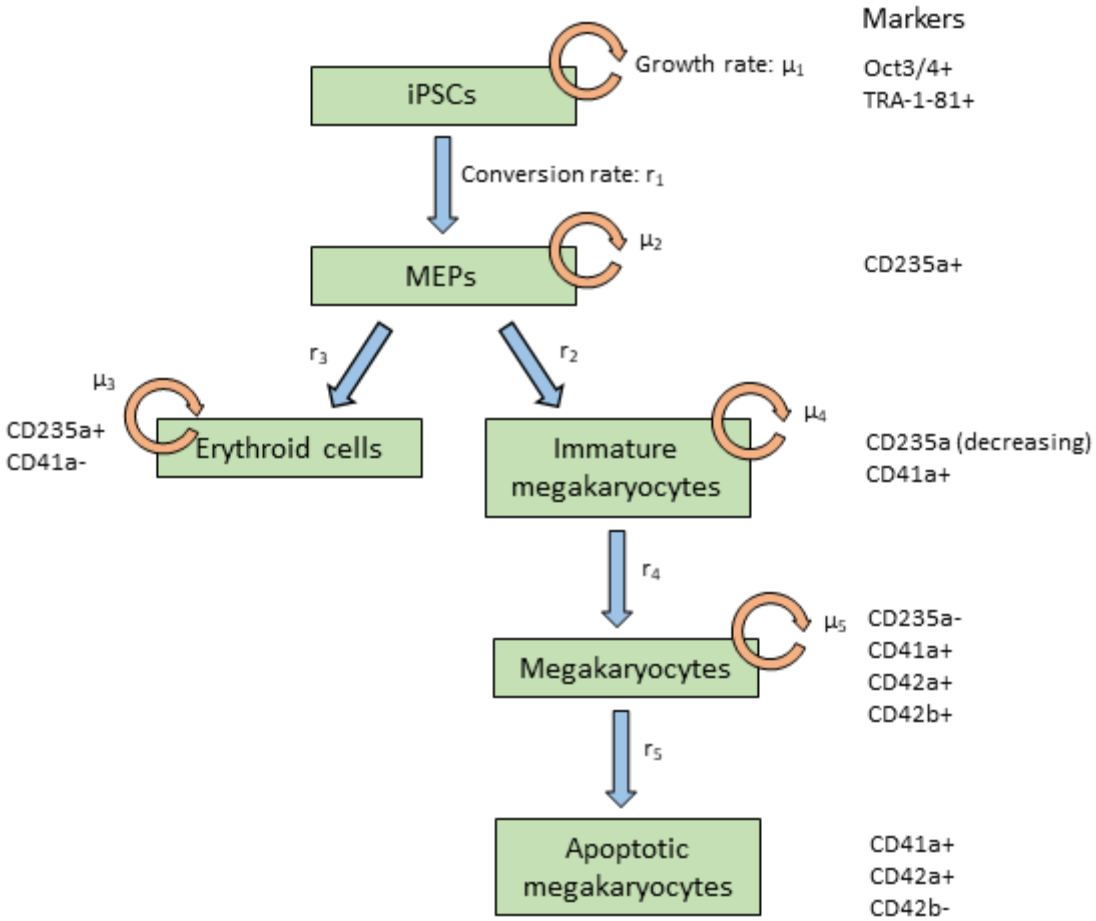

Figure 5-28: Proposed mechanistic model structure for FOP. The model would separate cell populations into discrete populations (green boxes) with associated growth rates (μ_x) and conversion rates (r_x), utilising the smallest number of populations to create a model with process optimisation utility. It hypothesised that there is a sigmodal dose response of Dox on r_2, r_3 and μ_2, and a sigmodal dose response of TPO on μ_x. It is also hypothesised that a cell-mediated factor (medium exhaustion through either nutrient depletion or metabolite excretion) would impact μ_x and r_x.

populations with r_2 and r_3 modulated by a Dox and TPO relationship. To parameterise this model the following relationships would need to be established:

- The maximum growth rate of populations when growth factors, Dox and medium exhaustion isn't limiting.
- Whether there is a changing trajectory of dose response to supplement concentrations across forward programming.
- Whether the time-dependent decay rate of medium components, growth factors and Dox were significantly impacting rates.

This type of mechanistic model would be challenging to parameterise, but it would have advantages over established DOE methods, since the outcomes of different components would be traceable through the differentiation and proliferation of cultures. It would account for non-linear, dynamic relationships that aren't currently described in this work and thus allow more precise optimisation of processes and has huge potential to reduce medium costs and therefore COGs for clinical cell therapies.

5.10. Conclusions

In the first part of this work a technology transfer exercise was completed with two runs of the protocol from the originating lab. During the tech transfer process, the cultures were analysed using the rationale outlined in Section 5.3 and process risks were identified (Section 5.4) for input into a Risk Assessment (Section 5.5). The following factors were identified as a high priority for further study: Seeding density, bulk medium supply, Dox, SCF and TPO concentrations and Dox exposure time. Since effects of medium exhaustion could not be separated from seeding density effects bulk medium supply (volume per unit time) was kept consistent, but volume per cell was adjusted through seeding density changes. A preliminary study was conducted to test concentration ranges of TPO and SCF and from this TPO was selected for use in DOE analysis.

A DOE was conducted with seeding density, Dox and TPO concentrations and Dox exposure times as control variables. Effects on proliferation and phenotype were measured for 19 days post seeding. Two conditions (high Dox, high TPO, continued Dox supplementation past day 10 and both high and low densities) were continued to day 34 post Dox-exposure. DOE analysis was also performed on CD41a expression at day 10 and CD34 expression at day 4 to

identify whether culture dynamics present early in FOP were similar to dynamics observed at day 18.

It was repeatedly shown that Dox (concentration and continued supplementation), TPO concentration and low seeding densities improved cell expansion and increased the proportion of phenotypically on-target cells; whereas seeding density had a negative impact on both proliferation and phenotype. Therefore, it is likely that both Dox and TPO are degraded at a rate which is cell density dependent. Although the removal of Dox from cultures at day 10 did not have a statistically significant impact on cell proliferation, removal had a negative impact on CD41a expression. Since Dox costs are insignificant compared to the rest of the bulk medium (<0.1% of cost per unit volume) Dox supplementation should be maintained throughout culture. Furthermore, the interaction between Dox and TPO (where a higher concentration of one overcame the negative effects of lower concentration on the other) could be investigated further. Since Dox costs a fraction of the cost of TPO small concentrations of TPO combined with higher concentrations of Dox may have the potential to reduce COGs for FOPMK derived platelet transfusion products.

When cultures were continued past 18 days, over 95% CD41/2a+ cells were achieved, but cultures stopped proliferating at Day 26 post Dox addition despite having different recorded levels of cumulative population doublings. It is unclear whether changing TPO or Dox supply would affect the total period of proliferation and the total number of achievable on-target FOPMKs.

In this system, Dox activates a genetic cassette containing GATA1, FLI1 and TLA1 – transcription factors that were shown to be essential in megakaryocyte differentiation and maturity [160], [161], hence their inclusion for forward programming [116]. The necessity of

TPO for megakaryocyte differentiation is widely reported [162]–[165] and its signalling pathway has been linked to endogenous GATA-1 expression [166]. Therefore, if there was Dox dose-dependent expression of the inserted transcription factors, at lower Dox concentrations higher TPO supplementation may stimulate the expression of endogenous GATA-1, which compensates for the lower expression of inserted GATA-1. Furthermore, if the degradation of TPO and Dox was cell-mediated, higher cell seeding densities would exacerbate the negative effects of low TPO / Dox concentrations, which is demonstrated in these data.

5.10.1. Further work

Further work characterising Dox inducible iPSCs should focus on determining whether the effect of seeding density on proliferation between Day -1 and 2 is a true effect or whether it was caused by an error in cell counting, and whether the TPO and Dox supply affect the overall proliferation capacity of the cells and the number of achievable CD41/2a+ cells. Further increases in TPO and Dox may produce added benefit, however this should be balanced against the extra cost of supplying these to the cultures and higher concentrations of Dox may be toxic to cells. Lower seeding densities may improve also improve quality of final product and lower concentrations of SCF may be tolerated.

The Cellgro SCGM medium is a proprietary medium formulation, and so work to modify this medium would be limited. Therefore, changing the basal medium to a system which the components are known and can be changed during optimisation work should also be considered. Potential benefits on an IMDM base medium is shown in Figure 4-11, but this medium contains supplements that are not chemically defined and are derived from humans.

Recombinant versions of these components are now available and should be used in future systems since these components would be most relevant to clinical applications.

The current differentiation process is undertaken as adherent cultures from Day -1 to Day 10 in planar vessels (well plates or T-flasks). Suspension cultures would allow for more precise control of the cell culture environment, cell density, medium exhaustion and supplementation which, as the data presented in this chapter demonstrates, can have a significant impact on culture trajectory and economics. Maintaining pluripotency and initiating differentiation in suspension cultures of PSCs is well established [167]–[169]. Investigating the potential to conduct forward programming in suspension platforms is a high priority for future work.

A mechanistic modelling framework is proposed in Section 5.9. Parameterising this model, in the current adherent or suspension format would facilitate process improvement and enhanced control. The work should also be repeated with clinically relevant cell lines as it is expected that the relationship between the variables will still be maintained (since the genetic engineering is the same), however it may be parameterised slightly differently.

6. The application of Design of Experiments and mechanistic modelling to identify and quantify iPSC culture phases and assess their potential impact on manufacturing of in vitro platelet transfusion units.

6.1. Introduction

In a manufacturing process that produces platelets from FOPMKs, the expansion of genetically engineered iPSCs is an important step. The economics and risk of this process will impact on the supply chain of FOPMKs and therefore the end platelet product. Determining the process productivity and understanding the factors which limit it allow process economics to be determined and focus improvement strategies. Aside from the production of platelets, iPSCs have wide-ranging applications due to their theoretical unlimited ability to produce functional human tissue, either for clinical application or drug discovery purposes [170]. So far, iPSCs have been used in clinical trials to treat age-related macular degeneration [171], clinical trials for Parkinson's disease are currently recruiting following successful primate disease models [172]. Other future clinical applications include hepatocyte replacement for liver failure and pancreatic β-cells for treatment of diabetes, for which it is estimated that 1-10 × 10^9 functional cells will be required per patient [173].

Pluripotent stem cells are adherent cells and are most commonly cultured using static flat plastic systems, and protocols usually dictate that cells are passaged once a certain confluency is reached as determined by observation using light microscopy [174]–[177]. For re-seeding, rather than obtaining cell counts, "split ratios" (where a proportion of cells are added to new flasks, e.g. 1:3 where cells harvested from one well are split into three wells) are sometimes used and are decided based on the observed confluency of cultures [176]–[178].

The passaging of adherent cells is often accompanied by a cell loss and/or lag phase of culture. The mechanisms underpinning lag and losses for pluripotent cells are not widely discussed in the literature. Instead, empirical comparisons are drawn between the length of lag phases and certain conditions, assuming that attachment is the primary driver of length of lag phase

[179], [180]. Lag phase studies in bacterial cultures are ubiquitous. Reported parameters that affect the length of the lag phase include absolute values of time, changes in temperature, pH, medium components and seeding density [181], [182]. Despite the breadth of studies, the lag phases of bacterial cultures are poorly understood due the impact and interactions of large numbers of variable.

It is a generally accepted that pluripotent cultures must not be allowed to become over confluent as this can lead to growth inhibition. As noted by Stacey et al. [100], the growth inhibition of a culture is a function of time, cells and/or the product of cells and time. In non-adherent culture, growth inhibition which is governed by cell density (cell number per unit volume) is a function of oxygen/nutrient demands of the cells and mass transfer properties of the system. Density limitation in adherent systems (cell number per unit volume and/or surface area) could be caused by contact inhibition, such as cell-cell interactions [183] (seems unlikely for PSCs, since cells grow in densely packed colonies), or a phenomena that behaves similarly to contact inhibition (for example concentration of paracrine factors over high density monolayer due to lack of mixing, or within multi-layered cells that grow on top of each other; similar factors could lead to mass transfer constraints for gasses). Growth inhibition governed by time can be caused by the decay of factors (either supplied through medium or produced by cells) and growth inhibition controlled by a function of cell × time is caused through medium utilisation (consumption of essential nutrients and growth factors or production of toxic metabolites). During passaging of pluripotent stem cells a ROCK inhibitor (RI, also referred to RhoK inhibitor in the literature) is also commonly included to reduce the occurrence of apoptosis within a population [184].

All mechanisms of culture growth inhibitions are dynamic; thus characterisation of these mechanisms will benefit from a framework which accounts for the dynamic changes. Previously, a mechanistic modelling framework has been successfully applied to suspension cultures [81], but its utility for describing adherent cultures and generating manufacturing outputs has yet to be demonstrated. Sections 4 and 5 describe suspension cultures which are limited by medium exhaustion using both tradition statistical and mechanistic modelling tools. Due to the added complexity of potential surface area limitations with adhered iPSCs we aim to investigate the primary growth dynamics and inhibition of iPSC cultures over the course of a passage in order to define the productivity limits of this culture system. Development of a complete system model (for example, one that treats each cell as an individual unit) is beyond the scope of this work; rather its aim is to produce a reasonably simple model (in terms of computation power required) but is still accurate enough to characterise the system to be useful for manufacturing process development.

6.1.1. Chapter Aims

- Identify the mechanisms of iPSC growth inhibition and cell loss upon seeding in flat plastic culture format.
- Identify the control variables that determine whether growth inhibition and cell loss upon seeding will occur.
- Quantify the operational boundaries of a system that will not incur significant growth inhibition or cell losses.
- Quantify the productivity of the system in terms of key resources given operational boundaries.
- Determine the likely requirement for system productivity improvement, given cell demand per product, and the strategies likely to deliver this.

6.2. Materials and methods

Cell line derivation and culture was performed as described in Section 2.3. Cell counting was performed using flow cytometry and described in Section 2.5.2. Flow cytometry sample preparation, equipment used, staining and acquisition is described in Sections 2.6.1-2.6.3. The flow cytometry assay used is described in Section 3.3.2.5, and the assays used are identified in relevant sections and figure legends associated with flow cytometry data.

Design of experiments were conducted as detailed in Section 2.8.1. The number of factors, levels of factors, outputs and whether a centre point was included is detailed along with the results of the DOE outputs in relevant sections.

6.3. Identifying the mechanisms of iPSC growth inhibition in flat plastic

The primary task of the first section of work was to qualitatively identify whether the primary mechanism of growth inhibition for iPSC cultures was a function of cells (cell density), time (medium factor decay) or cell × time (medium exhaustion). To determine which of these inhibitory factors was the primary limitation in the standard protocol, an experiment was designed where cultures were treated with the standard medium supply regime (a daily complete exchange, as described in 2.3) and twice daily exchanges of the same volume (therefore double the medium volume was supplied per day to those conditions). The medium exchanges are detailed in Figure 6-1. High temporal resolution cell counts were obtained from sacrificial wells to monitor the proliferation of cultures. The rationale for this experimental design is that the absolute cell density inhibition should occur at the same point irrespective of the medium exchange frequency. If this terminal inhibition is comparable across both experiments the absolute density limitation is therefore identified with reasonable confidence. If, however, the terminal inhibition occurs at a higher density in the

high frequency medium exchange this indicates that the medium supply is limiting under standard operating conditions.

The results of this experiment are shown in Figure 6-2. All conditions achieved a similar cell yield over 96 hours, proliferated at a similar rate and produced a good fit for an exponential growth curve, shown by high R^2 values. However, the average number of population doublings per hour achieved between each cell count measurement (Figure 6-2 C) decreased over the course of the experiment, which indicates that the growth rate decreased with time.

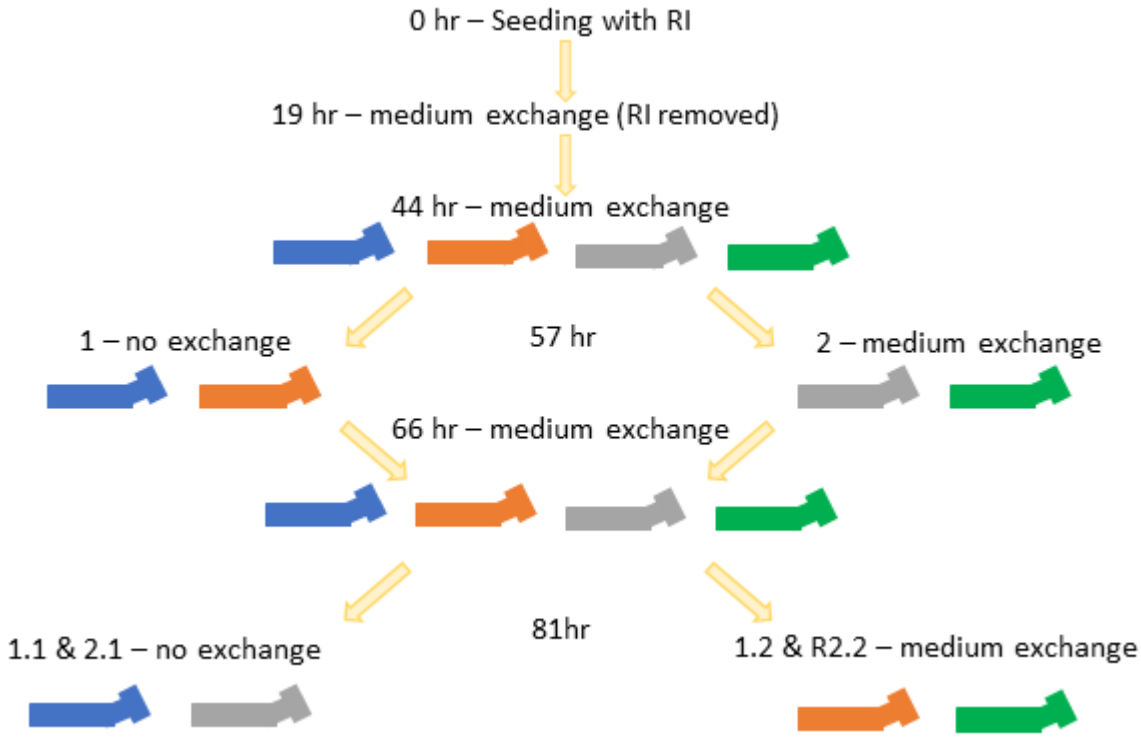

Figure 6-1: Schematic diagram representing experimental conditions to determine whether medium exhaustion was limiting cultures. All cultures were treated equally until 57 hours when a medium exchange was performed in for condition 2 but not in condition 1. A medium exchange was performed on all cultures at 66 hours. Conditions were split again at 81 hours where Conditions 1.2 and 2.2 underwent a medium exchange whereas conditions 1.1 and 2.1 did not. Cells were harvested at 96 hours. Medium supernatant was taken for nutrient and metabolite analysis and daily sacrificial wells were used for cell counts.

(A)

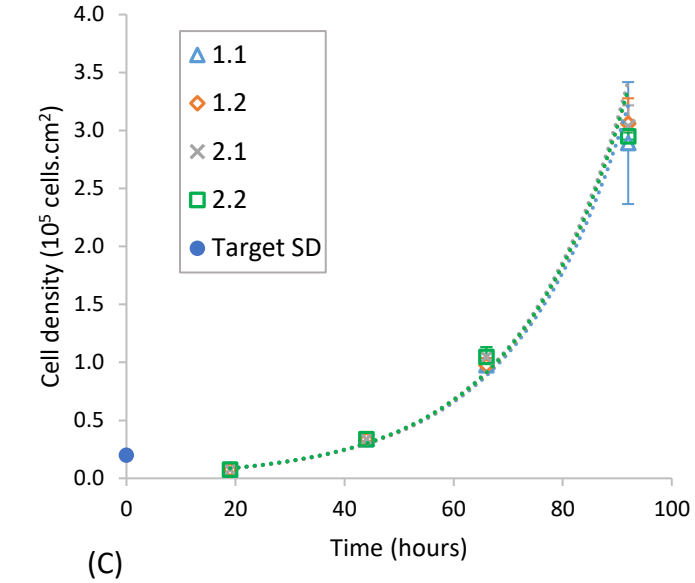

(B)

Condition	Net μ	R^2
1.1	0.0496	0.9929
1.2	0.0503	0.9946
2.1	0.0505	0.9925
2.2	0.0501	0.9912

(C)

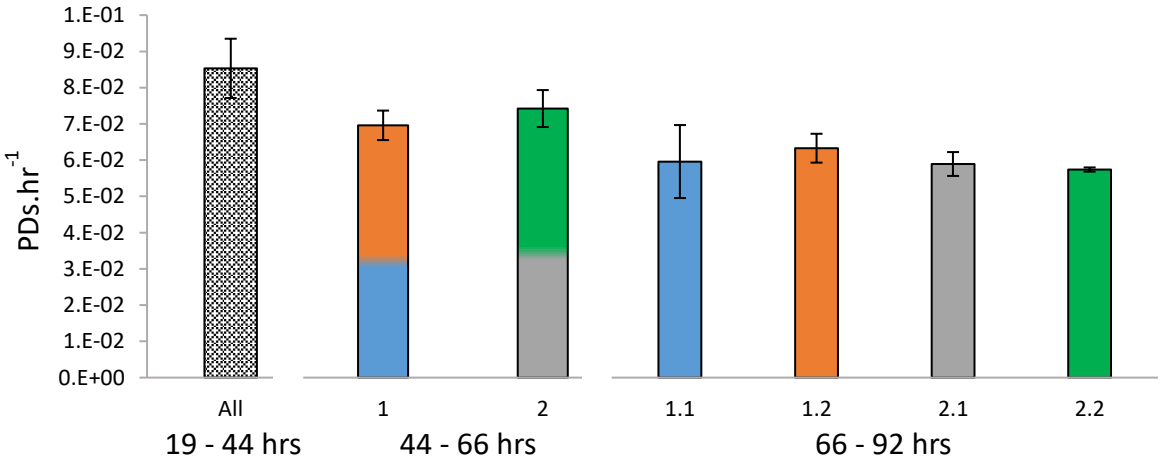

(D) One way ANOVA report summary

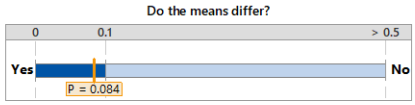

Differences among the means are significant (p < 0.1).

Which means differ?

#	Sample	Differs from
1	2.2	7
2	2.1	7
3	1	7
4	2	
5	1.2	
6	1.1	
7	All	1 2 3

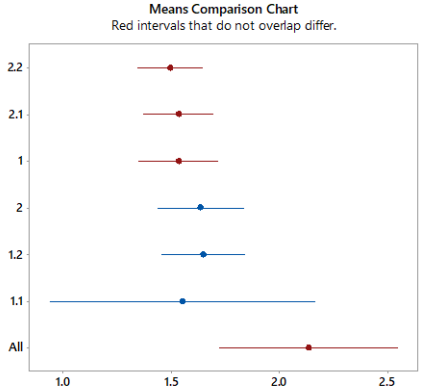

Comments

- Test: You can conclude that there are differences among the means at the 0.1 level of significance.
- Comparison Chart: Look for red comparison intervals that do not overlap to identify means that differ from each other. Consider the size of the differences to determine if they have practical implications.

Figure 6-2: Growth rate of all conditions were similar across a single passage. (A) Cell count data across time showed a similar expansion rate and end cell yield for all conditions. (B) Net growth rate calculated by applying an exponential model to cell count data varied by <2% and models for all conditions showed R^2 values > 99% indicating that this model was a good fit for the data. (C) Normalised number of population doubling between each cell count shows that mean growth rate decreased with increasing time since passage. However, there was no statistical significance between conditions or time periods. (D) ANOVA report summary from statistical software package Minitab showing that there was a statistical difference between the proliferation rate of all conditions at 19-44 and 66-92 hours (P = 0.084). Since P>0.05, significance is not noted on (C). Graphs show mean ± STD (N=3).

Since this reduction in growth rate was equivalent with time across all conditions, it was likely that the growth inhibition was linked to surface area (i.e. a local density limitation), rather than medium provision. It should be noted that the differences in the means of the growth rate were not statistically different from each other as determined using ANOVA (since P>0.05) but there was a difference between the growth rate means at P<0.1 level between the growth rate at 24 hours and condition 2.1 and 2.2 (66 – 92 hours) and condition 1 (48-66 hours) shown in Figure 6-2 D. Between 66 -92 hours the cultures which had received a higher supply of medium had a lower standard deviation, indicating that a higher supply of medium may have led to more consistent growth.

There was little difference between the growth rate of cultures when twice the medium provision was provided daily; therefore the assumption can be made that the lowest supply at the point where the cell density was highest (conditions 1.1 and 2.1, Figure 6-2 and Figure 6-3) was not limiting cultures; so the medium provision for the product of cell and time was sufficient at that point.

Since the cell density at time *T* (N_{T2}) (cells.mL^{-1}) is a function of the starting cell number N_{T1}, time (t) and growth rate (hr^{-1}) as in Equation 6-1:

$$N_t = f(t) = N_0 e^{\mu t} dt \qquad 6\text{-}1$$

Then the product of cell density time is the integral of Equation 6-2 between time T1 and T2:

$$\int_{T1}^{T2} N_t \, dt = \frac{N_{T1}}{\mu}(e^{\mu T2} - e^{\mu T1}) \qquad 6\text{-}2$$

Using Equation 6-2 to calculate the cell.time at the end of the culture period, the minimum medium capacity is 2.4×10^7 cell.hrs.mL^{-1}. Therefore, there are huge inefficiencies of medium usage in the first 72 hours of culture where cell numbers are low. In flat plastic systems is difficult to reduce medium volumes as a minimum volume of medium is required to cover the surface of the vessel. It could be possible that a lower frequency exchange regime could be employed, however supplementation of growth factors may be required since FGF2 is known to be unstable in culture [185], [186]. A detailed cost model would be required to evaluate the economic impact of adjusting feeding regimes and supplementation of FGF2, which is beyond the scope of this work since medium exhaustion is not the primary system limitation.

There was cell loss of 62% between seeding and the first 19 hours of culture compared to the target seeding density (Figure 6-2 A). As cell counts were not taken upon seeding and so it is not clear whether the loss of cells was caused as an effect of seeding or whether they were lost during the passaging process. For this reason, the growth rate of cells and nutrient consumption / metabolite production was not considered during this time period.

6.3.1. Medium consumption

To understand the medium utilisation, and identify potential inhibitory concentrations, lactate, ammonium and glucose production/consumption was monitored across the passage, as shown in Figure 6-3. Of these, lactate may have reached inhibitory concentrations at 92 hours in conditions 1.1 and 2.1 based on reported literature values [151]. However, since the

cell yields were very similar across all conditions (Figure 6-2 A), with different levels of lactate dilution, it is unlikely that the lactate concentrations were causing growth inhibition.

Across the passage the specific production rate of lactate decreased. As shown in Figure 6-3 (Aii), there was a statistically significant difference between the measured production rate of lactate across time compared to the previous period, but not between conditions within a time-period. The production rate of ammonium also decreased across the passage. However, there was not a statistically significant difference between the production rate during the first and second periods (19-44 hours and 44-66 hours). Although the mean ammonium concentrations were lower in the second period, the lower ammonium concentrations are towards the limits of the detection range of the analytical measurement technique, which leads to a larger proportion of variation compared to the mean. Ammonium and lactate production rates are linked to the supply of glucose and glutamate, where a higher supply leads to higher consumption [154], which in turn relates to a higher production rate of lactate and ammonium. The link between nutrient concentration and metabolite production may have caused the decreasing consumption rates across the passage; since more cells were present, more nutrients were consumed per unit time, which lowered the concentration of nutrients and so decreased the production rate of metabolites. The decrease in lactate and ammonium production also qualitatively correlate with decreased growth rate trends.

The measured glucose concentrations and consumption rates (Figure 6-3 Ci and Cii respectively) were more variable across the culture period compared to the lactate and ammonium production rates. The changes in glucose concentrations at the start of the cultures were low and so were likely to be outside the precision of detection of the measurement instrument.

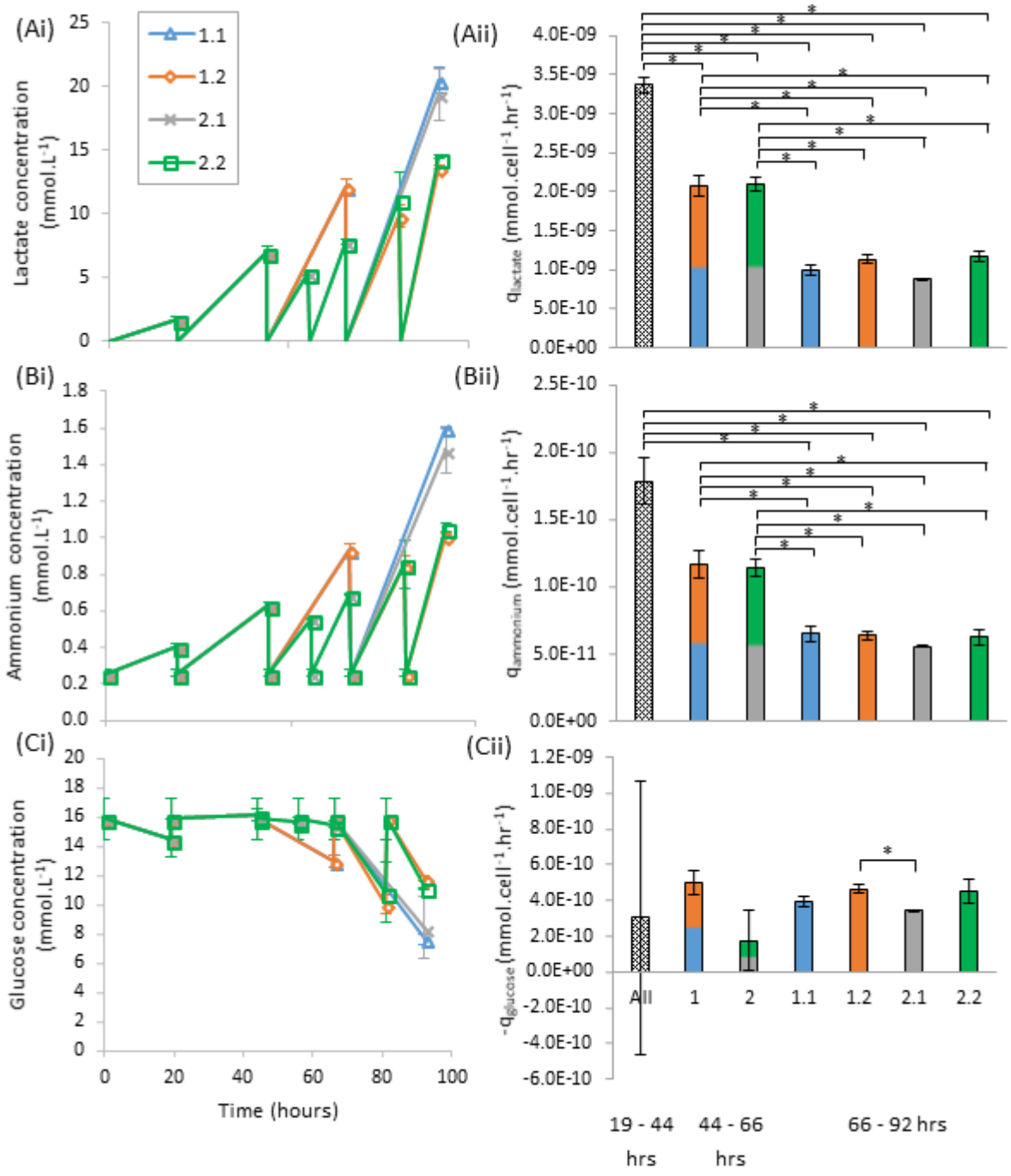

Figure 6-3: Consumption and production of glucose, lactate and ammonium reduced as time from passage increased. Changes in lactate (A), ammonium (B) and glucose (C) concentrations increased (i) and specific production rates decreased (ii) with increasing time since passage. Data show mean ± STD (N=3) and (*) denotes statistical significance (P<0.05) using ANOVA.

However, unlike the ammonium and lactate production rates there was a statistically significant difference between the consumption of glucose for conditions 1.2 and 2.1. This suggests that relatively high- and then low-supply of glucose compared to the baseline supply (and vice versa) caused larger differences in consumption rates. A lower supply of glucose has been linked previously to higher growth rates and lower lactate production in mammalian cell cultures [95], [187]. Furthermore, nutrient restriction has been shown to switch metabolic pathways [188] which could account for the differences in consumption rates observed here.

6.4. Qualitative identification of control variables which impact growth inhibition and cell loss / lag phase

In the previous section, cell surface area was the most likely primary limiting factor for system productivity and cell losses of 62% were observed upon passage. Therefore, understanding the effects of control variables on these two bottleneck areas is key to developing targeted strategies for improving system productivity. Furthermore, since the medium supplied at the beginning of the process was in excess for the first 24 hours (and probably the first 48 hours - as discussed previously in Section 6.3) the volume of medium used upon seeding was reduced by half across all conditions. It was hypothesised that the use of less medium would lead to reduced system costs.

It was hypothesised that increasing cell seeding density would reduce cell losses on seeding due to the release of beneficial paracrine factors [189] and the use of RI would promote cell survival therefore decreasing cell losses [190]. To test this hypothesis, a range of seeding densities were tested with and without the use of RI, as shown in Table 6-1.

Table 6-1: Summary of conditions to test the effect of seeding density and RI on culture phases.

Condition	Target seeding density (cells.cm^{-2})	RI present
1	1000	Y
2	5000	Y
3	9000	Y
4	1000	N
5	5000	N
6	9000	N

Sacrificial harvests were performed to obtain cell density data in Figure 6-4 (B). The cell density data at 0 hours were based on cell counts taken from the vessel that contained the cells prior to seeding. The data at 19 hours post seeding was measured from enzymatically removing the cells attached to the surface and sampling the suspended cells. The medium supernatant was also analysed to see if viable cells were suspended and not attached, however only debris was observed (data not shown).

Again, a cell loss phase was observed as all cultures observed a loss of cells from 0 - 19 hours which was followed by a period of growth and then inhibition at the end of the passage. In this case, all conditions had greater than 80% losses compared to the post-seeding count (Figure 6-4 C), with lower density conditions (1 and 4) having the highest losses. This was higher than observed previously, and it was therefore hypothesised that the low seeding volume contributed to the increased losses. Lag phases are commonly reported for pluripotent stem cell cultures and are mostly attributed to cell attachment; however, the mechanisms of the lag phase are largely unknown. For example, the effect of parameters on cell death, proliferation or attachment are often considered as a single phenomenon and referred to as the “lag-phase” [191]–[193].

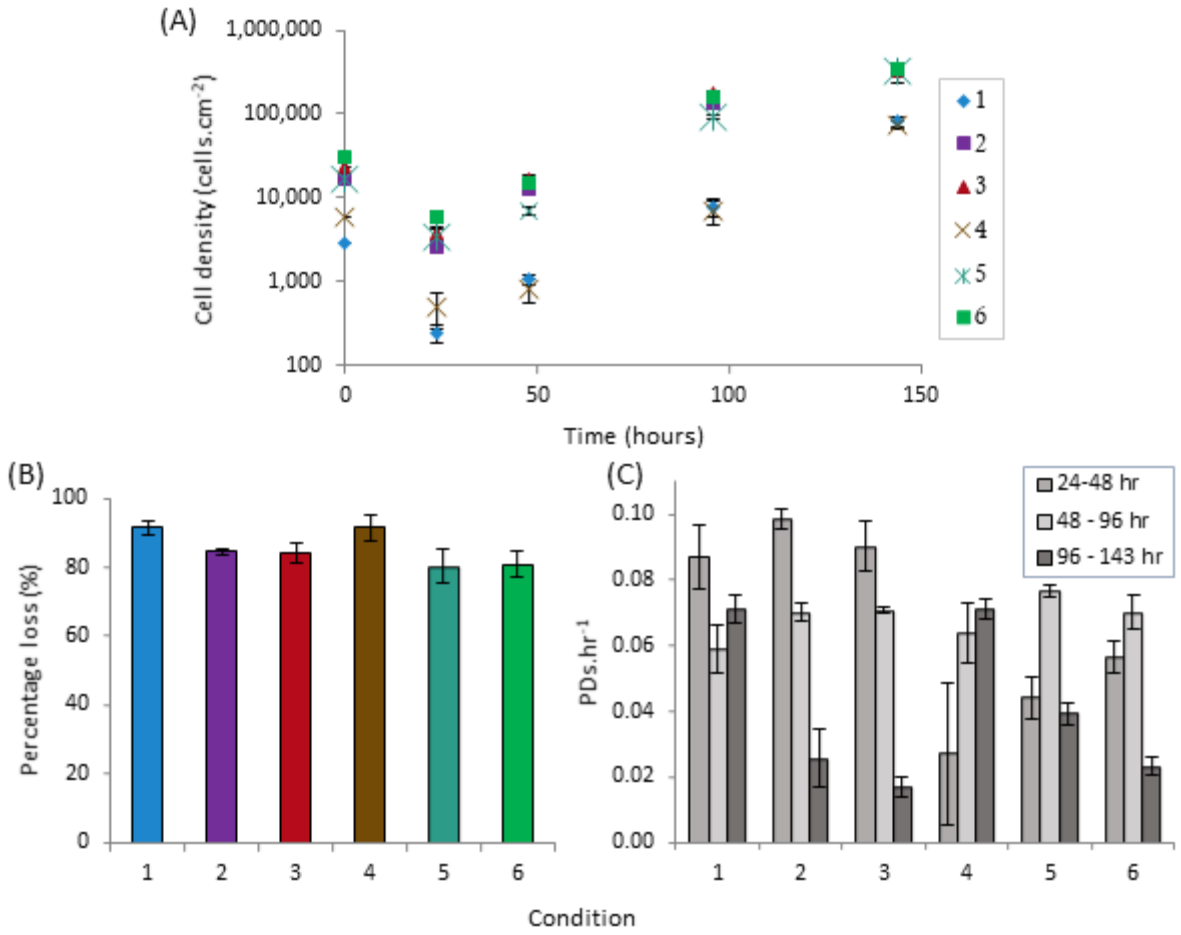

Figure 6-4: Cell density data for a single passage testing effects of different seeding densities and the presence of RI showed three culture phases; cell loss after seeding, exponential growth and growth inhibition. (A) Cell density data showed that cell loss occurred in the first 24 hours, followed by a period of exponential growth, which slowed in the latter hours for higher density cultures, indicating growth inhibition occurred. Graphs show mean ± STD (N=3). (B) There was >80% losses of cells 24 hours after seeding across all cultures and lower cell density cultures had higher proportional loss. (C) Population doublings per unit time show that cultures did not have a consistent growth rate across the experiment. Higher density cultures proliferated less at the end of the experiment, likely to be caused by density surface area limitations.

Figure 6-4 (D) shows the average population doublings per hour at different periods in the passage. Cultures that were treated with RI (RI+, 1,2 and 3) proliferated less from 24-48 hours compared to conditions without RI in the first 24 hours (RI-, 4,5 and 6). This was either caused by lower growth, or more cell death, leading to a lower average growth rate. It was hypothesised that the presence of RI would decrease cell losses since RIs are noted for aiding cell survival post-passage [184] and higher cell seeding densities would also decrease cell

losses since it has been noted that paracrine factors enhance cell survival and inhibit ROCK pathways [194], so the observation that the presence of a RI for the first 24 hours contradicted this hypothesis.

From 48 - 96 hours all conditions had a similar average growth rate, and from 96 – 143 hours, cultures with higher seeding densities proliferated less than medium densities, which in turn proliferated less than lower seeding densities. This indicates that cultures approached a surface area density limitation leading to growth inhibition. In a flat plastic system is it challenging to deliver higher surface area without providing extra volume (as discussed in Section 6.3). To overcome the issue of surface area limitations an alternative system may be considered for scale-up, such as a packed-bed culture platform or adaptation to suspension culture.

6.5. Quantitative methods for determining effect of control variables on culture phases

6.5.1. Cell loss upon seeding / lag phase

Since the mechanisms which govern cell culture lag phases are complex and largely undefined, non-dynamic statistical modelling (DOE) was selected to quantify the effects on input variables on lag phase in the culture format being used (6 well plates). This type of model could help to form mechanistic hypothesises that could be tested in future work with dynamic models that may be applicable across multiple culture platforms and scales.

6.5.2. Growth and inhibition phases

Considering the cell lag phase separately, it was hypothesised that the growth and inhibition dynamics observed from 24 hours onwards can be modelled using an mechanistic ODE framework [100] that predicts cell density (ρ, cells.cm^{-2}) at a given time where growth rate is

a function of a maximum growth rate and sensitivity to a critical cell density value determining growth inhibition as in Equation 6-3:

$$\frac{d\rho}{dt} = r_g \rho \left(1 + e^{i_s(\rho - i_c)}\right)^{-1} \qquad 6\text{-}3$$

Where t is time (hrs), r_g is maximum growth rate (hr^{-1}), i_s is inhibition sensitivity ($cm^2.mL^{-1}$) and i_c is the inhibition critical value ($cells.cm^{-2}$). It is frequently noted in the literature that the growth of pluripotent cells is dependent on the surface area available for adherence [195], [196].

To test this hypothesis, model formulation and parameter fitting was undertaken as described previously [81], [100] where least squares deviation was minimised. Modelling cell behaviour dynamics in this way gives enhanced insight to the process compared to statistical methods such as DOE which often fail to produce predictive models over longer time courses,

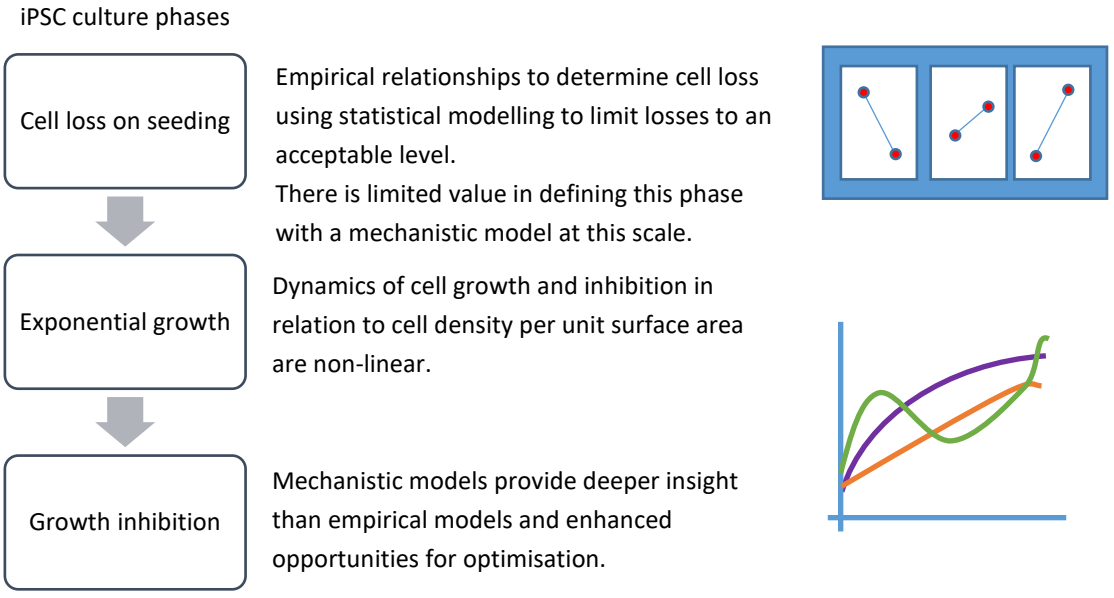

Figure 6-5: Summary of culture phases and the ways in which they were modelled.

since the behaviour is highly non-linear. The culture phases and how they were modelled are summarised in Figure 6-5.

6.6. Quantifying effects of system control variables on cell losses following seeding

6.6.1. Effect of seeding density and RI

To quantify the effect of seeding density and RI presence on proportional cell losses, shown in Figure 6-4 (C), were analysed using a 2 factor, 2 level DOE design using statistical software, Minitab. Backwards elimination was applied ($\alpha = 0.1$). Parameters are described in Table 6-2.

Table 6-2: DOE parameters to quantify effects of seeding density and RI on cell losses.

Parameter	High level	Low level	Midpoint(s)
Seeding density (cells.cm^{-2})	9000	1000	5000
RI presence for first 24hrs	Y	N	Y & N
Output	% cell loss after 24 hours compared to seeding count		

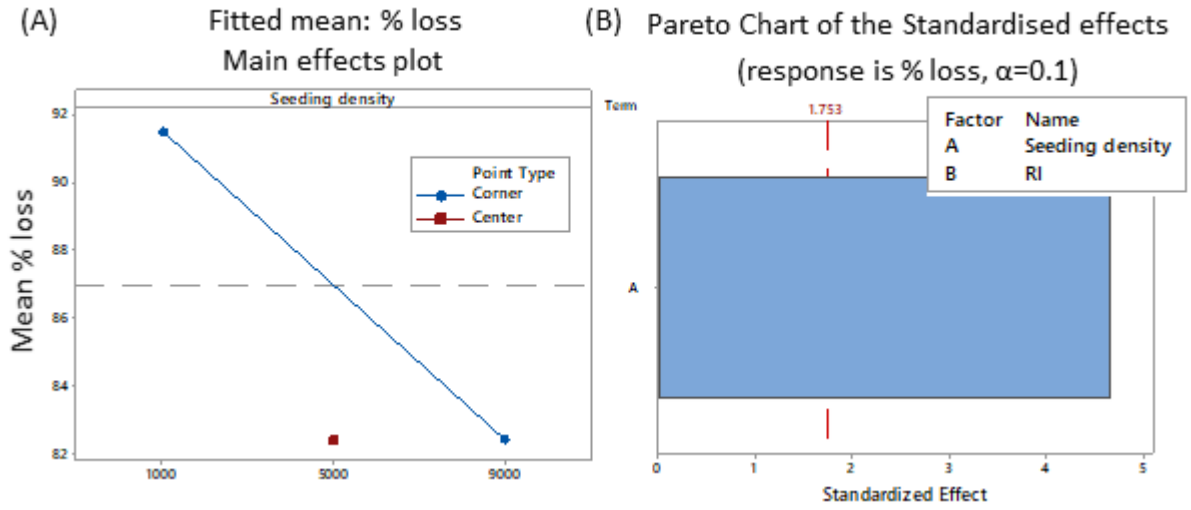

Figure 6-6: DOE analysis summary showed relationship between seeding density and cell loss upon seeding. DOE analysis was performed using statistical software package Minitab with stepwise backwards elimination (a=0.1) applied for a 2-level, 2-factor, factorial design. The R^2 (adj) fit of this model was 61.3 %. (A) Main effects lot showed a negative correlation between seeding density and cell loss. Centre point position suggested that the relationship was nonlinear. (B) Pareto chart showed that seeding density was the only parameter with P>0.05 effect on proportional loss.

As shown in Figure 6-6, only seeding density had a statistically significant effect ($P<0.05$) where increased seeding densities, decreased cell losses. The model was highly non-linear as shown by the position of the mid-point in the main effects plot (Figure 6-6 A) and the R^2 (adj) was 61%, meaning that nearly 40% of the variation in the proportional losses was not accounted for by this model, indicating high levels of noise. The non-linearity of the model contributed to the lack of fit also.

As mentioned in Section 6.4, the proportional losses were higher than those observed in Figure 6-2. Here, a lower volume was used to seed the cultures, as it was shown in Figure 6-3 that medium was supplied in excess. It was hypothesised that this change may have caused higher cell losses (due to independent effects of medium volume on initial adherence and survival vs subsequent growth) and therefore the effect of medium volume during seeding was investigated and the results are discussed below in Section 6.6.2.

6.6.2. Effects of seeding volume, seeding density and RI treatment

Since larger cell losses were shown in Figure 6-4 (A) compared to Figure 6-2 (A), it was hypothesised that the reduction in volume at seeding may have caused higher cell losses. Therefore, volume was tested along with seeding density and RI treatment. Furthermore, higher temporal resolution cell counts were taken at the beginning of the passage to further understand the nature of the cell losses post-seeding. A summary of the conditions used and the cell densities over the culture period are shown in Table 6-3.

Table 6-3: Summary of conditions to test the effect of seeding density, seeding volume and RI on culture phases.

Condition	Target seeding density (cells.cm^{-2})	RI present	Seeding volume (mL in a 12 well plate)
1	1000	Y	0.38
2	9000	Y	0.38
3	1000	Y	1.14
4	9000	Y	1.14
5	1000	N	0.38
6	9000	N	0.38
7	1000	N	1.14
8	9000	N	1.14
9	5000	Y	0.76
10	5000	N	0.76

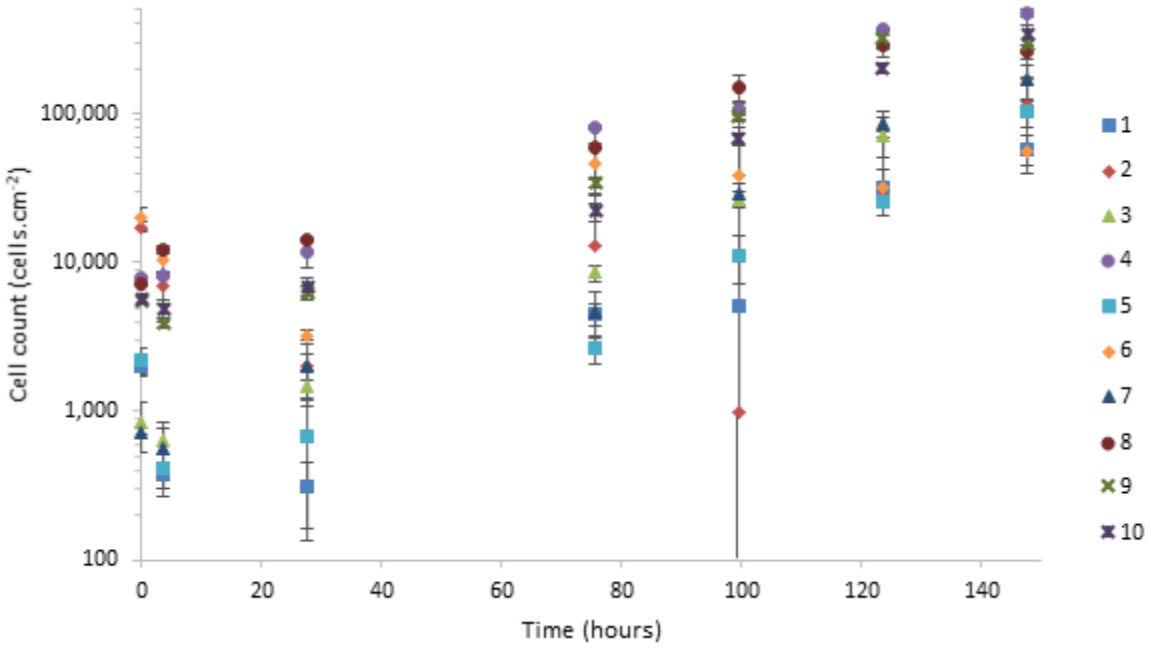

Figure 6-7: Cell densities across a single passage with various seeding densities, medium volume at seeding and treatment with RI conserved the three culture phases identified in Figure 6-5. (A) Details of different culture treatments. (B) Cell density data shows cell loss phase was followed by exponential growth and inhibition. Data shows mean (N≥2) ±STD.

Again, the three culture phases were present; cell loss, growth and growth inhibition; as shown in Figure 6-7. There was high variation in the high seeding density, low volume conditions (2 and 6) as shown by the large standard deviation error bars relative to the other conditions. It is unclear whether the source of the variation was a product of a variable growth rate or variations in detachment and processing or a combination of these effects. Despite the cause being unknown, the added variation from these conditions would be detrimental to a manufacturing process since it increases the risk of failure to meet required product yields.

The proportion of cell loss compared to the cell count at seeding is shown in Figure 6-8 (a). There was a range of losses across the culture conditions with the impact of the variables were analysed using a 3 factor, 2 level DOE design using statistical software, Minitab. Backwards elimination was applied ($\alpha = 0.1$). Parameters are described in Table 6-4.

The pareto chart (Figure 6-8 B) DOE analysis showed that seeding volume had the greatest impact on proportion of cell losses followed by the target seeding density, and the RI treatment. The main effects plot shows that increased target seeding density decreased the proportion of losses, the addition of RI increased losses and increased seeding volume decreased cell loss. The interaction plots (Figure 6-8 C) show that at low seeding densities the addition of RI did not impact the proportion of losses, whereas at higher cell densities the inclusion of RI increased proportion losses. The interaction plots also indicate that higher medium volumes at seeding led to lower proportional losses at higher seeding densities.

Table 6-4: DOE parameters to quantify effects of seeding density, RI and seeding volume on cell losses.

Parameter	High level	Low level	Midpoint(s)
Seeding density (cells.cm^{-2})	9000	1000	5000
RI presence for first 24hrs	Y	N	Y & N
Seeding volume (mL)	1.14	0.38	0.76
Output	% cell loss after 24 hours compared to seeding count		

The impact of medium volume on cell loss was unlikely to have been caused by lower provision of nutrients since, as shown in Figure 6-3, these are supplied in excess during the first 24 hours. Since seeding losses are relevant only in the first 24 hours the volume of medium used after this point does not impact losses, but after this point all conditions are provided with the same volume of medium.

Further, the conversion rate of suspended to attached cells was not likely to have caused the variation in cell losses. At 4 hours post seeding, cell counts were performed on the medium supernatant to check the number of cells suspended in the medium that had not attached. The expected number of suspended cells were calculated by subtracting the attached number of cells from the cell count at seeding. The number of counted cells in the medium supernatant at 4 hours was only 3% of the expected number (data not shown), and therefore it was concluded that the cell loss was caused by a physical effect due to the low medium volume. The mechanism underpinning this loss and whether it will affect different scales of culture is unknown. It is hypothesised that it is a physical effect of the meniscus, related to how cells interact between the surface boundary between air and medium. If this is the case, it will be highly dependent on culture vessel surface area, and may be irrelevant in other

systems, where gas-liquid surface area to volume ratio will be much lower than in flat plastic culture systems.

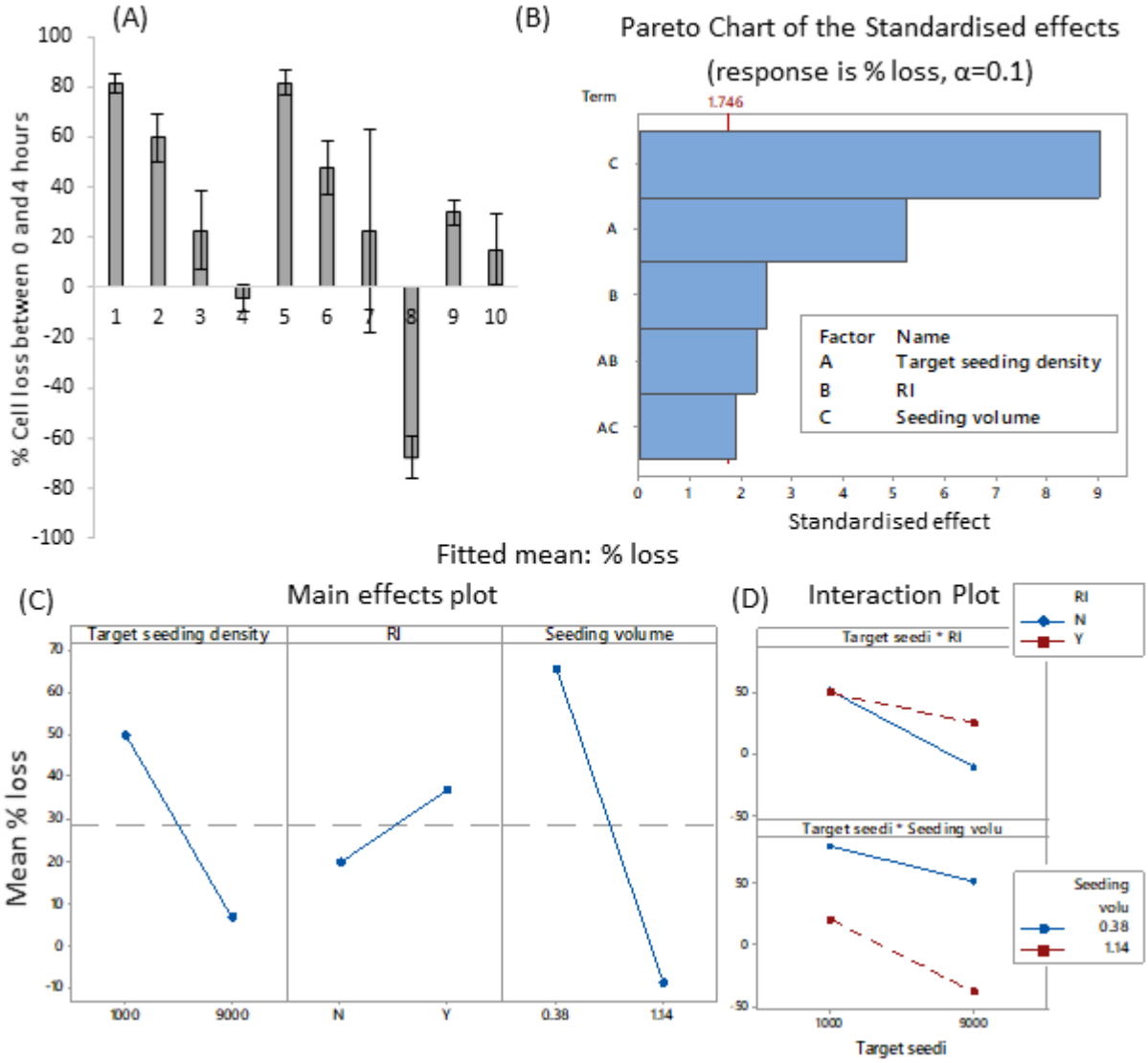

Figure 6-8: Cell loss after seeding was dependant on main effects target seeding density, RI treatment and seeding volume. (A) Proportional loss based on seeding counts. Data shows mean (N≥2) ±STD. (B) Pareto chart shows all significant main effects and interactions (P<0.05, except AC, where P=0.077 and therefore was not statistically significant). (C) Main effects plots show increased seeding density decreased proportional losses, RI treatment increased proportional losses and increased medium volume at seeding decreased proportional losses. (D) Interaction plots show RI treatment did not impact losses at low cell seeding densities, but at high cell seeding densities RI treatment increased proportion cell losses and increased seeding medium volume further decreased losses at high cell densities. DOE analysis summary showed relationship between seeding density and cell loss upon seeding. DOE analysis was performed using statistical software package Minitab with stepwise backwards elimination (a=0.1) applied for a 2-level, 3-factor, factorial design. The R^2 (adj) fit of this model was 85.0 %.

The presence of high cell loss in low seeding volumes in other systems would determine the value of further investigating the mechanisms underpinning cell loss due to low culture seeding volume. Despite not understanding these mechanisms, the simplest way to reduce cell losses is to use a higher volume of medium during seeding in this system. For example, comparing conditions 1 (low seeding density, +RI, low volume) and 3 (low seeding density, +RI, high volume) shows a reduction in average proportional losses from 83% to 23%.

An increase in cell seeding density was shown to decrease losses. This has been demonstrated by other groups [197] It is hypothesised that the mechanisms underpinning this are caused by the release of protective paracrine factors or cell-cell contact effects through cell adhesion molecules [184], [198]. Although higher seeding densities reduce cell losses, they also lead to cultures reaching confluency faster. This would lead to shorter passage times, meaning more frequent exposure of cells to dissociation reagents, which may impact cell quality (pluripotent phenotype or forward programming efficiency). This may be mitigated by using scalable-suspension aggregate systems, where higher cell densities per unit volume could be achieved. Suspension aggregate cultures have not been applied to FOP-inducible iPSCs yet.

The use of RI for pluripotent stem cell cultures is widely reported in the literature. The first reports of use was to enhance the survival of dissociated cells [184], and has been used as enhancing cell survival through the duration of a passage [199]. However, other reports show that the Rho-signal is critical to long-term survival and expansion of human embryonic stem cells [200]. The data presented here contradict this, since use of RI either had no effect at low densities; as demonstrated by comparing low density, low volume conditions 1 (+RI) and 5 (-RI) in Figure 6-8 (A); or promoted cell loss; as demonstrated by comparing the high density, high volume conditions 4 (+RI) and 8 (-RI) and the mid-point conditions 9 (+RI) and 10 (-RI). As

explained previously, these effects are quantified as shown in the DOE analysis Figure 6-8 (C and D).

6.7. Quantifying effects of control variables on growth inhibition

6.7.1. Effect of seeding density and RI

The fitted parameters for Equation 6-3 and the resulting model are shown in Figure 6-9. The data are split into +RI and -RI treatments for ease of comparison, but the same parameters were fitted to all conditions. There was an observable pattern in the residuals (Figure 6-9 ii) where the model under predicts cell counts in the latter stages of the passage for +RI cultures and over predicts cell count for -RI conditions. This suggests that the presence of RI during the first 24 hours affected either the growth rate or inhibition critical value (i_c) of the culture.

The R^2 value for each condition is shown in Figure 6-9 (D) which is high for all conditions except condition 4 with an R^2 of 73%. Further, for condition 4 the residuals show that the model systematically over predicted the cell count data (Figure 6-9 Bi and ii).

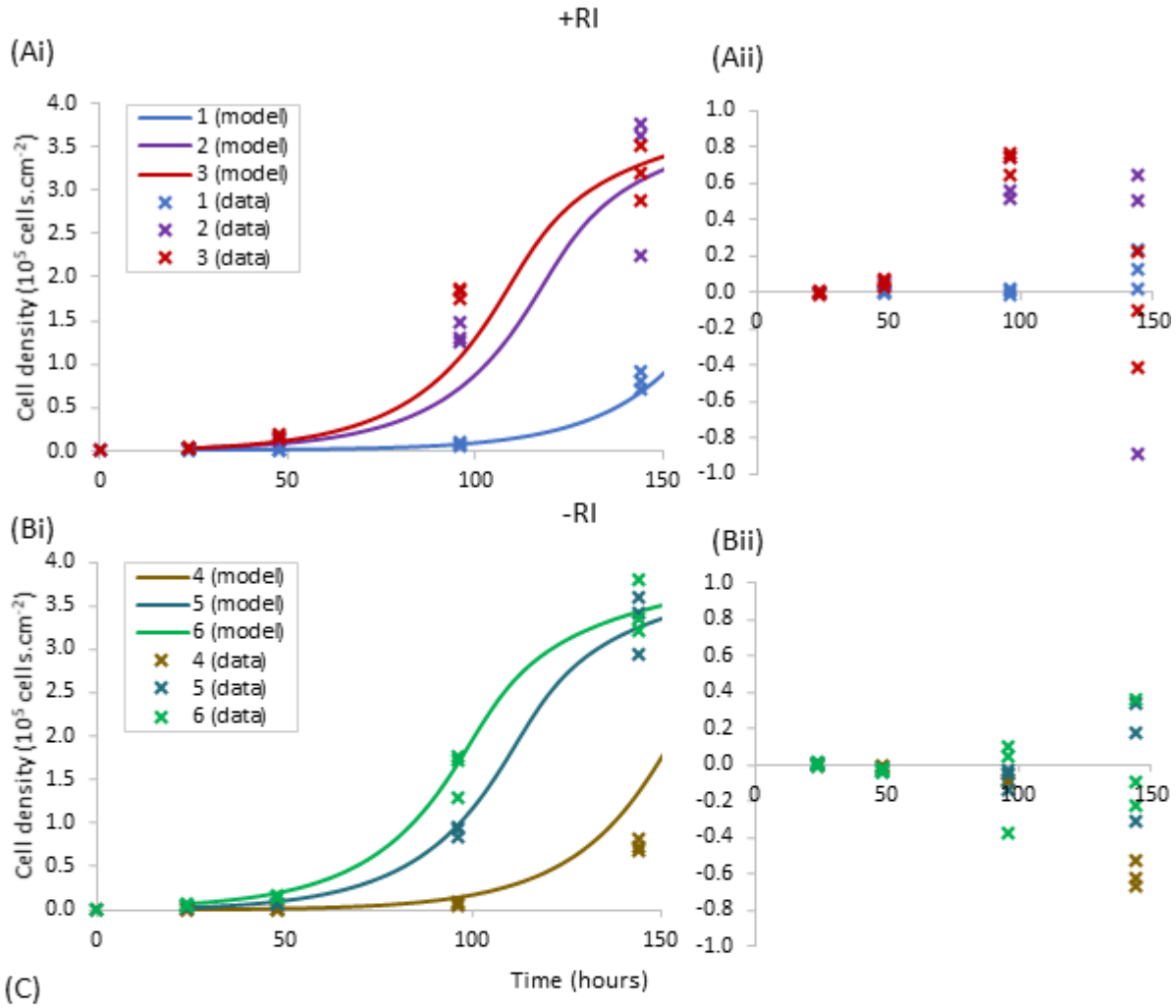

(C)

Maximum growth rate (hr^{-1}) (r_g)	Inhibition critical value ($cells.cm^{-2}$) (i_c)	Inhibition sensitivity ($cm^2.cell^{-1}$) (i_s)
0.047	2.45×10^5	2.5×10^{-5}

(D)

Condition	R^2	Condition	R^2
1	92.4	4	73.1
2	86.5	5	98.7
3	91.4	6	98.5

Figure 6-9: Mechanistic modelling output for fitting 24hr+ data to equation 6-3 using a least squares fit method. (i) shows observed cell counts and model predictions and (ii) shows residual error between observed cell counts and predictions for (A) +RI cultures and (B) -RI cultures. Model under predicted cell density in +RI conditions and over predicted cell density in -RI cultures. (C) Fitted parameters for equation 6-3 (D) R^2 values for each condition.

6.7.2. Effects of seeding volume, seeding density and RI treatment

The cell growth limited by density model (described in Equation 6-3) was parameterised using the observed cell densities from 24 hours after seeding. The low volumes cultures were excluded from this model since there was large variations in the data (presumed to be caused by the low volume treatment since this was not observed in the high volume cultures) and, as described in Section 6.6.2, it is likely that this detrimental effect was specific to the culture vessel (a 6 well plate). Therefore, the detrimental effect of low volume is unlikely to be relevant in a manufacturing setting and easily overcome by adding more volume for 24 hours post seeding. However, this again highlights the that medium engineering in a flat plastic system will make a low impact on system productivity, since a minimum volume must be supplied to prevent cell losses on seeding.

The fitted model and data are shown in Figure 6-9 (Ai) +RI and (Bi) -RI. The same model was fitted to each data set but are split in the figure to for ease of comparison. The residual error between the data and the fitted model are shown in (ii). There was a pattern in the residual error, where the model under predicted the cell densities in the latter stages of the culture for the RI+ cultures (Aii), whereas the model over predicted cell densities in the RI- cultures (Bii). The maximum growth rate (r_g) fitted in Figure 6-10 was 20% lower than in the first data set (shown in Figure 6-9), the inhibition critical value (i_c) was 18% higher and the inhibition sensitivity (i_s) was 4 orders of magnitude higher. The average of the R^2 values were also lower in Figure 6-10 compared to Figure 6-9.

Since there was a systematic pattern in the residual which was split on +RI / -RI conditions a separate model was fitted to these conditions, shown in Figure 6-11. In the RI+ cultures (Figure 6-11 A) the refit removed the pattern in the residuals shown Figure 6-10 Aii. As shown

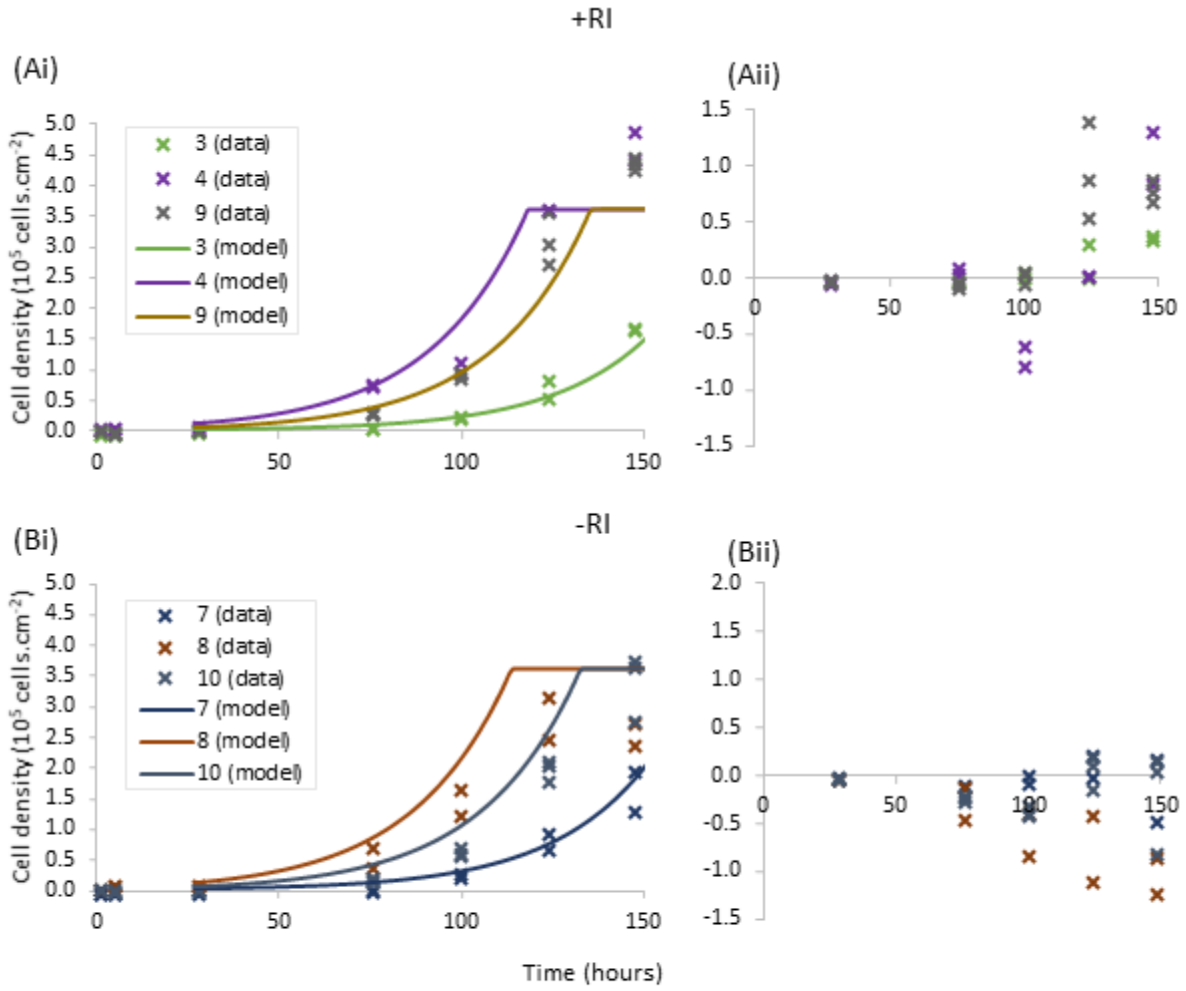

(C)

μ (hr^{-1}) (r_g)	Inhibition critical value (cells.cm^{-2}) (i_c)	Inhibition sensitivity (cm^2.$cell^{-1}$) (i_s)
0.0375	3.6×10^5	0.19

(D)

Condition	R^2	Condition	R^2
3	89.7	7	92.6
4	89.0	8	63.3
9	88.3	10	95.1

Figure 6-10: Mechanistic modelling output for fitting 24hr+ data to Equation 6-3 using the same parameters for each condition and a least squares fit method. Low volume cultures (1, 2, 5 and 6) were not included in model due to variation show in Figure 6-7 and large cell losses shown in Figure 6-8. (i) shows observed cell counts and model predictions and (ii) shows residual error between observed cell counts and predictions for (A) +RI cultures and (B) -RI cultures. Model under predicted cell density in +RI conditions and over predicted cell density in -RI cultures. (C) Fitted parameters for Equation 6-3. (D) R^2 values for each condition.

(Ai)

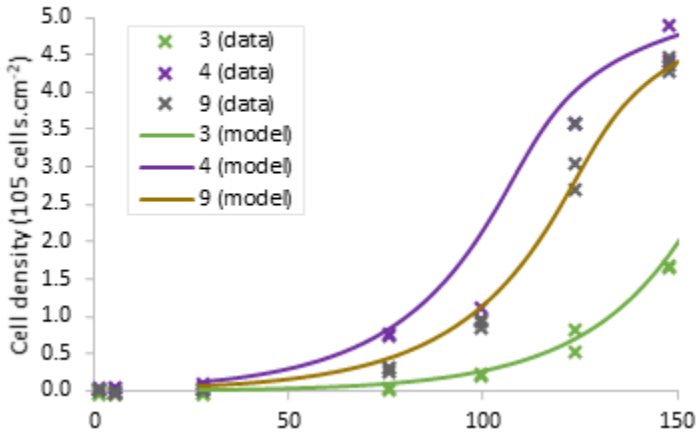

(Aii)

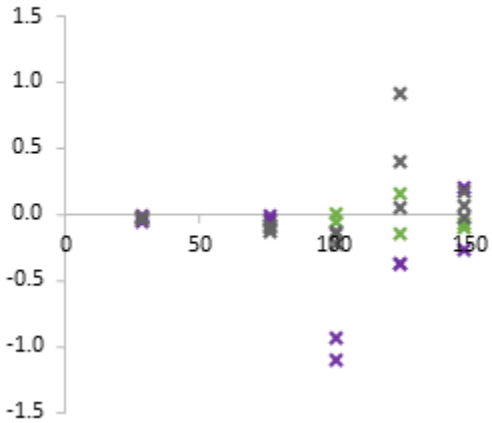

(Aiii)

μ (hr^{-1}) (r_g)	Inhibition critical value ($cells.cm^{-2}$) (i_c)	Inhibition sensitivity ($cm^2.cell^{-1}$) (i_s)
0.04	3.6×10^5	2×10^{-5}

-RI

(Bi)

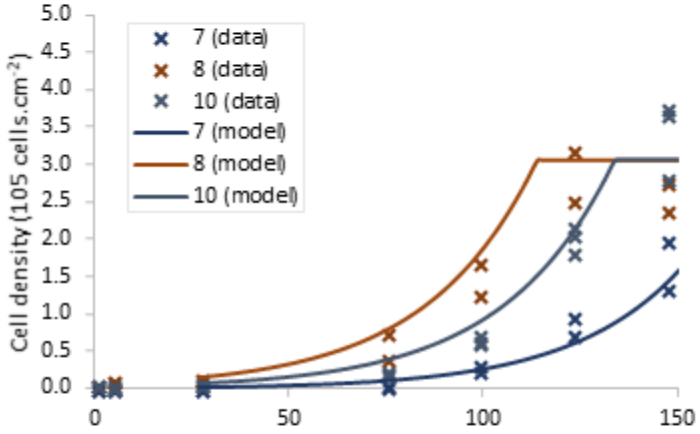

(Bii)

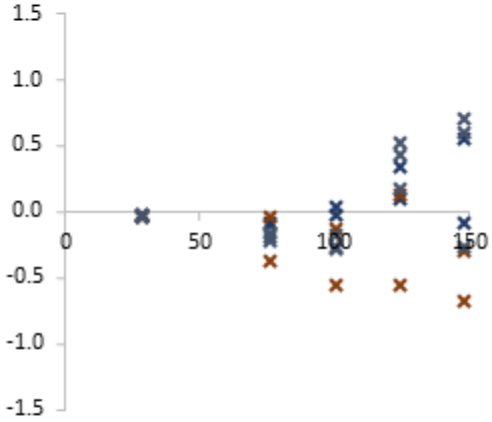

(Biii)

μ (hr^{-1}) (r_g)	Inhibition critical value ($cells.cm^{-2}$) (i_c)	Inhibition sensitivity ($cm^2.cell^{-1}$) (i_s)
0.0355	3.05×10^5	0.17

(C)

Condition	R^2	Condition	R^2
3	98.6	7	87.7
4	92.7	8	90.0
9	97.2	10	93.0

Figure 6-11: Mechanistic modelling output for fitting 24hr+ data to Equation 6-3 using different parameters for each RI treatment and a least squares fit method.(i) shows observed cell counts and model predictions, (ii) shows residual error between observed cell counts and predictions and (iii) shows fitted parameters for Equation 6-3 for (A) +RI cultures and (B) -RI cultures. Conditions treated with RI had higher growth rates and inhibition critical values. (D) R^2 values for each condition were improved for conditions treated with RI.

by Table 6-5, the maximum growth rate (r_g) increased relative to the fit in Figure 6-10, but was 15% lower than the initial data set shown in Figure 6-9; i_c was identical and the inhibition sensitivity was decreased by 4 orders of magnitude. For the RI- conditions 9 (Figure 6-11 B), r_g decreased, i_c decreased and i_s increased. This suggests that removing RI decreased the maximum achievable growth rate of the cells, or increased cell death which was not measured or accounted for in this model structure. Removal of RI also lowered the inhibition critical value, i.e. lower maximum cell capacity per unit surface area prior to growth inhibition and increased the sensitivity to this maximum, so when the critical value was reached, the rate of change of r_g was greater. RI has been previously empirically shown to "kick-start" growth of PSCs and increase colony sizes, and the effect of RI was reversable upon removal of RI from the culture [201]. However, here we see a lasting effect of RI on growth rate since it was used in the first 24 hours of a passage only. As discussed in Section Figure 6-4, the mechanism of action for RI is hypothesised to prevent apoptosis upon dissociation of PSCs [199], but in this work the use of RI increased losses on passage but increased growth rate from 24 hours onwards. Perhaps this is linked to the hypothesis presented by Ohgushi et al. [200] that Rho mediated signalling is required for long term survival and expansion of pluripotent stem cells and by providing RI in the first 24 hours only, the pathway is triggered, promoting higher survival and bulk growth rates.

The parametrisation applied for the RI- conditions appeared to systematically over predicted cell densities in conditions 7 and 10, but underpredicted cell densities for condition 8 in the later stages of the passage. Condition 8 was a high seeding density, high volume, no RI condition. It is unclear why this condition was an outlier. One reason may be related to the low cell loss upon passage – perhaps the cells that are lost are the slower growing less "healthy" cells which leads to a lower growth rate. This selection pressure could also explain

why there was a higher maximum achievable growth rate demonstrated in the initial data (see Figure 6-9 and Table 6-5) since greater than 80% of cells were lost in the first 24 hours.

Table 6-5: Comparison of the parameters fitted to equation 6-1 across all model fitted data sets.

	Figure 6-9	Figure 6-10	Figure 6-11 A (+RI)	Figure 6-11 B (-RI)
r_g	0.047	0.0375	0.040	0.355
i_c	2.45×10^{5}	3.60×10^{5}	3.60×10^{5}	3.05×10^{5}
i_s	2.45×10^{-5}	0.19	2.00×10^{-5}	0.17

6.8. Cell quality: qualitative effect of control variables on cell phenotype

The median fluorescence intensity for three common pluripotency markers at Day 3 and Day 6, during the passage from the experiment shown in Figure 6-4 , are shown in Figure 6-12. Lower density cultures had higher expression (higher MFI) for TRA-1-81 and NANOG than the higher density cultures and higher expression at Day 3 than Day 6. This suggests that there is an effect of density or of growth inhibition on expression of some pluripotent markers. The expression of Oct 3/4 increased in some conditions with time. However, the expression data were obtained from a pooled sample of three biological replicates so the variation within a condition is not known, so the magnitude of change of effect against background variation is unknown. This data was collected as first screen to check changes in common pluripotent marker expression. Further work should encompass a detailed literature search for pluripotent markers, since recent studies have focused on the use of flow cytometry to identify different pluripotent “states” i.e. naive vs. primed [202], [203] and include the use of differentiation markers (such as SSEA-2) to track early stages of loss of pluripotency.

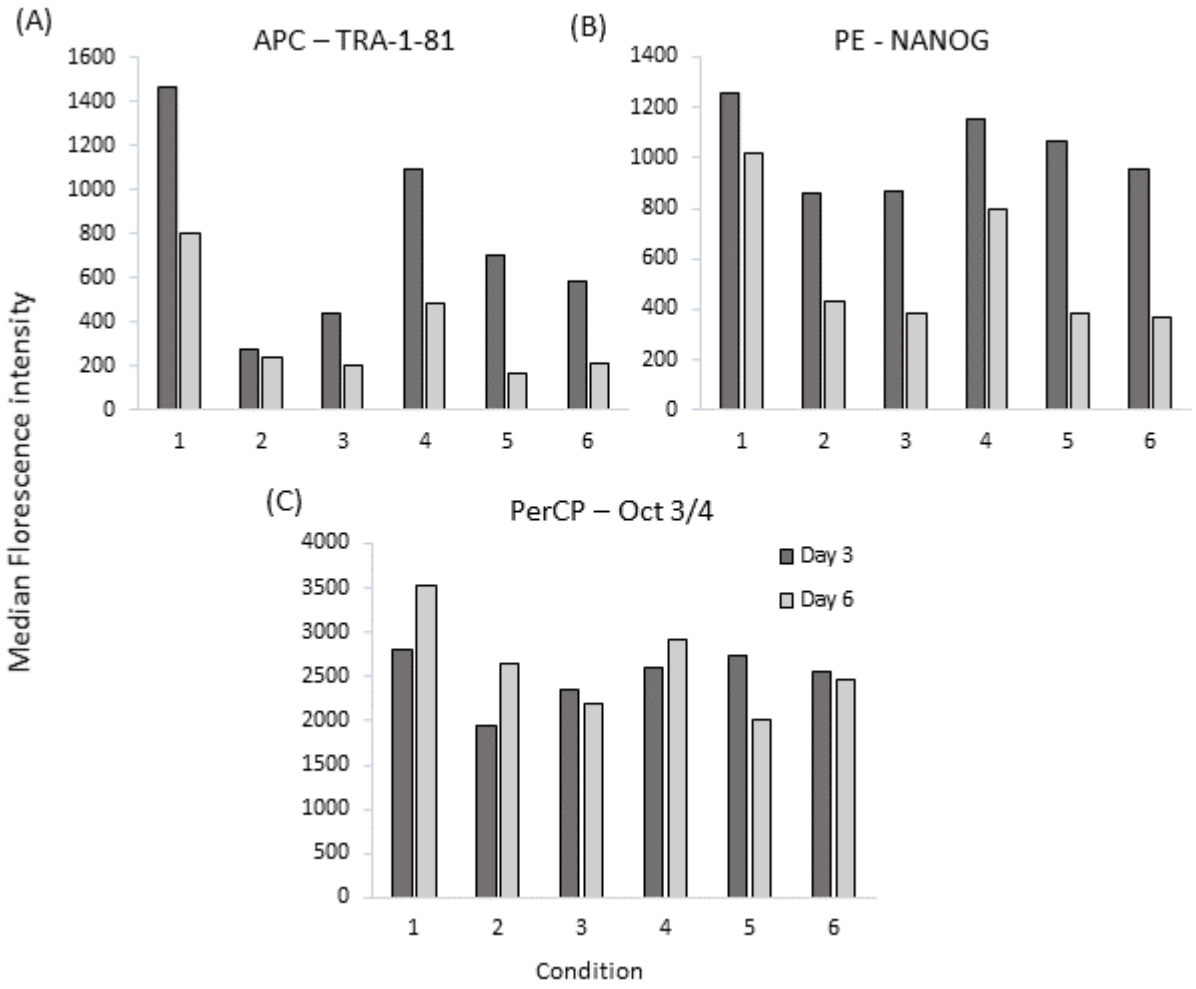

Figure 6-12: iPSC phenotype changes over a passage. MFI values show a decrease in TRA-1-81 (A) and NANOG expression (B). Oct 3/4 expression increased for conditions 1-4 but decreased for conditions 5 and 6. Data shows flow cytometry data acquisition results from three pooled cultures.

6.9. iPSC demand for in-vitro derived platelet transfusion product

The aim of this work is to understand the impact of iPSC culture dynamics as part of a production process for platelet transfusion units. Figure 6-13 shows the required input iPSCs to produce enough platelets for one transfusion unit (3×10^{11} platelets per transfusion unit), is determined by the expansion during forward programming post-Dox addition and the number of platelets produced per mature megakaryocyte. As the population doublings in

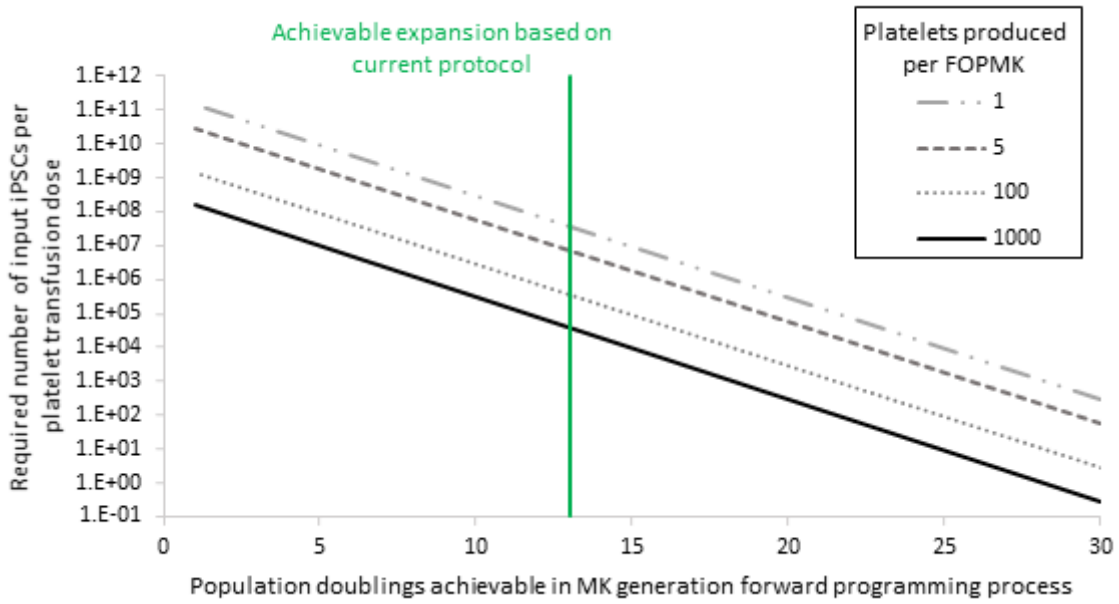

Figure 6-13: The required number of input iPSCs to produce a platelet transfusion unit is dependent on the expansion of cells post Dox-induction to maturity and the number of platelets that can be harvested and stored from each FOPMK. Based on data discussed in Section 5, approximately 13 population doublings can be achieved post Dox induction (shown here in green). In vivo, mature MKs produce around 1000 platelets per cell, whereas in vitro methods have produced between 5 platelets per MK, which could result in much lower productivity once losses from processing are considered.

forward programming decrease, the requirement of input iPSCs increases exponentially. Based on the data shown in Section 5, the achievable number of population doublings during forward programming was approximately 13, shown on Figure 6-13 as a green solid line. However, this expansion may be changed by altering the concentration of Dox, TPO and / or other factors such as bulk medium supply. The number of platelets produced in vitro is also variable, with studies reporting between 3-20 platelets.MK^{-1} [204], [205]. Ultimately, the relative cost of each process - iPSC culture vs. forward programming expansion vs. platelet generation – will determine the expansion / production in each phase to produce the adequate number and quality of platelets for clinical transfusion units.

6.10. Conclusions and future work

This chapter applies a combination of statistical and mechanistic modelling tools to understand culture dynamics within an iPSC passage. Three culture phases are identified: cell lag / loss phase, exponential growth and growth inhibition caused by surface area limitations. In mammalian cell culture and microbiology, the lag phase is complex and with ill-defined mechanisms and therefore a traditional statistical modelling tool (DOE) was selected to empirically define relationships between variables and cell losses. The DOE linked decreased cell losses in the first 24 hours with increased cell seeding density, not using RI in the first 24 hours and increasing the volume of medium used for the first 24 hours.

From 24 hours of culture onwards, the cell growth and inhibition was modelled using a mechanistic model that related culture growth to the availability of surface area. Cultures that were treated with RI in the first 24 hours achieved higher maximum growth rates compared to those that were not exposed to RI and had a higher critical sensitivity values.

It is hypothesised that the differences in maximum growth rates between conditions was caused by the selection of faster growing or advanatged cells surviving upon passage through loss of “fragile” cells. This hypothesis could be tested further through multiple passages, and clone colonies. There are examples in the literature where extended passaging increased differentiation capacity [206] and reduces the genetic abnormalities in iPSCs [207]. It is possible that the selection events observed in this data set could contribute to these phenomena, and further investigation would be needed to confirm this.

This work was conducted on FOP Dox-inducible iPSCs. To gain insight into the broader applicability of this work, it would be useful to see how the relationships defined here are conserved across other iPSCs. Regardless of parameterisation, the model frameworks and

approaches to model development, both for DOE and mechanistic modelling, are applicable to any adherent cell line.

The effect of variables on pluripotency was measured using flow cytometry markers. Both TRA-1-81 and NANOG appeared to decrease across a passage, whereas Oct 3/4 increased. Unlike haematopoietic cells which are highly characterised by cell surface markers, pluripotency markers are not well established, and measuring the "quality" of pluripotent stem cells is debated [208]. Gene expression monitoring methods have been developed [209] but flow cytometry had advantages over PCR methods, as it is rapid and allows for individual cell analysis. Future work focusing on the culture dynamics of pluripotent stem cells should consider developing a wider marker panel compatible with flow cytometry for the rapid measurement of the effect of pluripotency.

The outcomes of the modelling approaches (both DOE and mechanistic models) must be validated to confirm outcomes mentioned here. The effect of passage time with respect to growth rate trajectory (i.e the difference in performance in onward passage when cells are passaged at varying levels of growth inhibition) would be an important extension of this work to inform a longer scale expansion that would likely be required for clinically relevant manufacturing processes.

Finally, pluripotent cell passaging has been demonstrated in scalable, suspension aggregate cultures [167]–[169]. In this case, surface area limitations may not be relevant. However, as shown in Section 4 and relevant literature [81], [100], the mechanistic modelling approach used here can be readily applied to medium exhaustion dynamics. The need to drive towards this type of expansion will depend on the process economics required for expansion for each phase of platelet generation (iPSC expansion, forward programming or platelet biogenesis).

7. Conclusions

7.1. Introduction

Since the first scoping of this project in 2015 the cell therapy industry has matured significantly with the first regulatory approvals of CAR-T therapies in 2017. This work shows that in order to accelerate process development of complex cell therapy products, modelling approaches can be applied to define system productivity, thereby allowing targeted medium supply to ensure product quality and increase efficiency of input consumables. Here FOPMKs were used as a case study.

7.2. Identification and measuring CQAs

Quality by Design is an established methodology applied to the manufacture of small molecule pharmaceuticals which first identifies a product QTPP. In Section 3, standards used for clinical platelet transfusion units were used as the basis of the QTPP for a platelet product derived from forward programmed megakaryocytes. From the QTPP, CQAs were selected to be used to ensure quality in process development that were biologically relevant and measurable using currently available process analytical technologies. Markers were selected that represented different stages in maturity of cells (from pluripotent to mature MKs). Flow cytometry was the selected process analytical technology for marker measurement and robust assays were developed to measure selected markers. Cell counting assays were also developed as the number of cells present in culture is fundamental to build models based on the utilisation of culture medium by cells.

There is growing interest in standardisation in the cell therapy community [210]–[212]. Here, the first QTPP has been developed for a in vitro platelet derived product and a novel assay was developed to track the differentiation state of FOPMKs from pluripotent to mature MKs .

This flow cytometry assay has the ability to be standardised across multiple sites with the use of Application Settings.

7.3. Identifying the productivity limits of 1st generation FOPMKS

The first generation of FOPMKs displayed similar characteristics to a cell line, as cell expansion took place over 90 days and was relatively phenotypically stable. By conducting high-temporal resolution growth curves in Section 4, it was found that the system productivity of the first generation FOPMKs was $1.48 \pm 0.28 \times 10^6$ viable cells.ml^{-1}. The system productivity was a function of the product of cells present and time, which was linked to conversion of viable to non-viable cells. This medium exhaustion dynamic was quantified using a novel mechanistic modelling approach, which showed that growth inhibition in addition to cell death dynamics were present in cell culture systems.

There was a discrepancy between culture behaviour of short-term (days) and long term (weeks) cultures, where short-term cultures had higher maximum growth rate and lower creation rate of toxin (surrogate for medium exhaustion). It was hypothesised that this discrepancy was caused by different exhaustion kinetics being present over the long-term cultures (for example, medium component decay present through partial medium exchanges) and the short-term cultures being exposed to higher concentration of medium exhaustion since no medium exchange were performed, therefore creating a more “toxic” environment to cells than present in the long term environment.

The root cause of the medium exhaustion was not identified, since part way through this process the forward programming technology moved on and so further work on this system was no longer considered high value. However, it was unlikely to be glucose, lactate nor

ammonium as, compared to other systems described in the literature, the concentrations of these components were unlikely to be causing the cell death seen in this system.

Unlike other approaches which build models of cultures based on responses to specific factors [76], [79], [80], [95], [213], the model framework used here characterises cultures based on broad limitations – either a product of time, cell density or the product or cells and time. The model is a flexible framework that has a low barrier to entry for users who have little knowledge of ODEs.

7.4. Application of QbD to 2nd generation FOPMKs

The 2nd generation FOPMK process had different challenges associated with expansion, since the inducible nature of the cell line shifted cell expansion to a phase where cells were phenotypically maturing and cell growth ceased after approximately 30 day post-Dox induction, as shown in Section 5. Through a Technology Transfer exercise, it was found that the end stage number and quality (where quality was defined as phenotypic marker expression CQAs identified in Section 3) were dependent on input variables. Using DOE as a statistical modelling tool (as typical in QbD approaches), there was positive correlation between higher cell yields and CD41a expression and main effects TPO and Dox concentrations and a negative correlation for cell seeding density and the removal of Dox from culture. There were also multiple statistically significant variable interactions, for example at higher concentrations of Dox lower concentrations of TPO were required to produce the same effect on cell number and yield – suggesting that the same biochemical pathways may be triggered in response to both Dox and TPO. Dox costs are insignificant compared to TPO, therefore, investigating further the response of cells to Dox with lower TPO concentrations may lead to significant cost savings.

Statistical models should be driven by a mechanistic hypothesis, but they are empirical models which treat the system as a “black-box”. This can lead to little process insight. However, DOE is an efficient methodology which can help to form mechanistic hypothesis which could help to narrow down parameters for investigation using mechanistic modelling which is more resource intensive. Future investigations leading from this work should focus on enhanced productivity and control of FOPMK cultures by developing dynamics models of the effects of Dox and TPO concentrations on cell expansion and phenotype.

7.5. Application of DOE and mechanistic modelling to iPSC culture

Adherent culture of iPSCs would be the first phase of production for a platelet transfusion product derived from the 2nd generation FOPMK process, therefore the productivity limits of iPSC culture was investigated. iPSC culture was shown to have three distinct culture phases; lag/loss followed by exponential growth and eventual growth inhibition. Using an DOE approach, the lag phase was shown to be a function of seeding volume, RI treatment and cell seeding density. It was hypothesised that there was an interaction between the meniscus of the culture vessel and the cells which increased losses in the first 24 hours of culture. Since it was likely that the mechanisms of this loss would dependent on the culture vessel (a 6 well-plate is not a scalable platform for production) and losses may be easily overcome by using a higher culture volume, this was not investigated further. Mechanistic models were developed to quantify the growth and growth inhibition phases of iPSC cell growth and growth inhibition, which shown to be a function of cell density and the presence of RI (which facilitated higher cell densities to be achieved).

Since this work has identified a cell density limitation, future work should focus on identifying medium productivity limits, either in suspension iPSC cultures or prior to cultures reaching

their cell density limit. Since this system already utilises fully defined medium, component screening should be undertaken and, through understanding the medium exhaustion dynamics, a targeted medium supplement developed.

Finally, the required number of input iPSCs to create one platelet transfusion unit was shown to be driven by the expansion of FOPMK expansion post-Dox addition and the number of platelets produced per FOPMK. Based on the current protocol, and assuming 5 platelets were generated per FOPMK, approximately 7×10^6 iPSCs would be required per platelet transfusion unit – the equivalent to 20 cm^2 of confluent cells.

7.6. Future work

7.6.1. Improving system productivity of FOPMKs

The root cause of the medium productivity limit for the first generation FOPMK process was not established in this work, although it was unlikely to be due to "standard" bioprocess limits, such as glucose, lactate or ammonium. Future work should focus on a medium which is not a black box system and contains recombinant components only. From this, medium can be "reverse engineered" to determine what is limiting the culture system. Furthermore, scalable expansion systems should be employed, such as suspension culture of iPSCs rather than adherent cultures.

7.6.2. Application of modelling tools to cell therapy processes

This work has shown that dynamic, mechanistic models can deliver powerful insights into cell therapy expansion processes. However, the processes are complex and dynamic models can be resource intensive to build and validate. In order to characterise processes and obtain meaningful manufacturing insight, "simple" dynamic models were built here using a maximum of 7 parameters, but higher numbers of parameters may would be required to

characterise a system that was phenotypically unstable, as in the 2nd generation FOPMK expansion process.

8. References

[1] M. J. Jenkins and S. S. Farid, “Cost-effective bioprocess design for the manufacture of allogeneic CAR-T cell therapies using a decisional tool with multi-attribute decision-making analysis,” *Biochem. Eng. J.*, vol. 137, pp. 192–204, 2018.

[2] J. Carmen, S. R. Burger, M. McCaman, and J. a Rowley, “Developing assays to address identity, potency, purity and safety: cell characterization in cell therapy process development,” *Regen. Med.*, vol. 7, no. 1, pp. 85–100, 2012.

[3] P. D. Weinberg *et al.*, “Legal, Financial, and Public Health Consequences of HIV Contamination of Blood and Blood Products in the 1980s and 1990s,” *Ann Intern Med.*, vol. 136, no. 4, 2002.

[4] D. Stainsby *et al.*, “Serious Hazards of Transfusion: A Decade of Hemovigilance in the UK,” *Transfus. Med. Rev.*, vol. 20, no. 4, pp. 273–282, 2006.

[5] T. Moreau *et al.*, “Large scale production of platelet forming megakaryocytes from human pluripotent stem cells by a chemically defined forward programming approach,” *Nat. Commun.*, vol. 7, no. 11208, pp. 1–35, 2016.

[6] C. Mason and P. Dunnill, “A brief definition of regenerative medicine,” *Regen. Med.*, vol. 3, pp. 1–5, 2008.

[7] C. Mason, D. A. Brindley, E. J. Culme-Seymour, and N. L. Davie, “Cell therapy industry: billion dollar global business with unlimited potential,” *Regen. Med.*, vol. 6, no. 3, pp. 265–272, 2011.

[8] A. for R. Medicine, “Q1 2019: Quaterly Regenerative Medicine Global Data Report,”

2019. [Online]. Available: https://alliancerm.org/publication/q1-2019-data-report/. [Accessed: 20-Jun-2019].

[9] R. Brandenberger, S. Burger, A. Campbell, T. Fong, E. Lapinska, and J. a Rowley, “Cell therapy bioprocessing,” *Bioprocess Int.*, vol. 9, pp. 30–37, 2011.

[10] T. Bart *et al.*, “Impact of selection of cord blood units from the united states and swiss registries on the cost of banking operations,” *Transfus. Med. Hemotherapy*, vol. 40, no. 1, pp. 14–20, 2013.

[11] T. G. Fernandes, C. a. V. Rodrigues, M. M. Diogo, and J. M. S. Cabral, “Stem cell bioprocessing for regenerative medicine,” *J. Chem. Technol. Biotechnol.*, vol. 89, no. 1, pp. 34–47, Jan. 2014.

[12] E. Ratcliffe, R. J. Thomas, and D. J. Williams, “Current understanding and challenges in bioprocessing of stem cell-based therapies for regenerative medicine,” *Br. Med. Bull.*, vol. 100, no. 1, pp. 137–155, 2011.

[13] P. D. Mitchell, E. Ratcliffe, P. Hourd, D. J. Williams, and R. J. Thomas, “A Quality by Design approach to risk reduction & optimisation for human embryonic stem cell cryopreservation processes,” *Tissue Eng. Part C Methods*, vol. 20, no. 12, pp. 1–32, 2014.

[14] E. Gunsilius, G. Gastl, and A. . Petzer, “Hematopoietic stem cells,” *Biomed. Pharmacother.*, vol. 55, no. 4, pp. 186–194, 2001.

[15] J. Antonchuk, G. Sauvageau, and R. K. Humphries, “HOXB4-induced expansion of adult hematopoietic stem cells ex vivo,” *Cell*, vol. 109, no. 1, pp. 39–45, 2002.

[16] H. E. Broxmeyer *et al.*, “Growth characteristics and expansion of human umbilical cord

blood and estimation of its potential for transplantation in adults.," *Proc. Natl. Acad. Sci. U. S. A.*, vol. 89, no. 9, pp. 4109–13, 1992.

[17] M. Körbling, P. Anderlini, and M. Ko, "Peripheral blood stem cell versus bone marrow allotransplantation : does the source of hematopoietic stem cells matter ? Review article Peripheral blood stem cell versus bone marrow allotransplantation : does the source of hematopoietic stem cells matter," *Blood*, vol. 98, no. 10, pp. 2900–2908, 2008.

[18] T. R. J. Heathman, W. Nienow, M. J. Mccall, K. Coopman, B. Kara, and C. J. Hewitt, "The translation of cell-based therapies : clinical landscape and manufacturing challenges," *Regen. Med.*, vol. 10, pp. 49–64, 2015.

[19] J. A. Thurman-Newell, J. O. N. N. Petzing, and D. J. Williams, "A meta-analysis of biological variation in blood-based therapy as a precursor to bio-manufacturing," *Cytotherapy*, vol. 18, no. 5, pp. 686–694, 2016.

[20] S. Frauenschuh, E. Reichmann, Y. Ibold, P. M. Goetz, M. Sittinger, and J. Ringe, "A microcarrier-based cultivation system for expansion of primary mesenchymal stem cells.," *Biotechnol. Prog.*, vol. 23, no. 1, pp. 187–93, 2007.

[21] Y. Yuan, M. S. Kallos, C. Hunter, and A. Sen, "Improved expansion of human bone marrow-derived mesenchymal stem cells in microcarrier-based suspension culture," *J. Tissue Eng. Regen. Med.*, vol. 8, pp. 210–225, 2014.

[22] Q. A. Rafiq, K. M. Brosnan, K. Coopman, A. W. Nienow, and C. J. Hewitt, "Culture of human mesenchymal stem cells on microcarriers in a 5 l stirred-tank bioreactor.," *Biotechnol. Lett.*, vol. 35, no. 8, pp. 1233–45, Aug. 2013.

[23] J. Rowley, E. Abraham, A. Campbell, H. Brandwein, and S. Oh, "Meeting Lot-Size

Challenges of Manufacturing Adherent Cells for Therapy," *Bioprocess Int.*, vol. 10, no. 3, pp. 16–22, 2013.

[24] J. E. Italiano, P. Lecine, R. A. Shivdasani, and J. H. Hartwig, "Blood platelets are assembled principally at the ends of proplatelet processes produced by differentiated megakaryocytes," *J. Cell Biol.*, vol. 147, no. 6, pp. 1299–1312, 1999.

[25] D. Ross, L. Ayscue, J. Watson, and S. Bentley, "Stability of Hematologic Parameters in Healthy Subjects," *Am. J. Clin. Pathol.*, vol. 90, no. 3, pp. 262–267, 1987.

[26] K. R. Machlus and J. E. Italiano, "The incredible journey: From megakaryocyte development to platelet formation," *J. Cell Biol.*, vol. 201, no. 6, pp. 785–796, 2013.

[27] M. F. Murphy *et al.*, "Guidelines for the use of platelet transfusions," *Br.J.Haematol.*, vol. 122, no. 1, pp. 10–23, 2003.

[28] L. M. Williamson and D. V. Devine, "Challenges in the management of the blood supply," *Lancet*, vol. 381, no. 9880, pp. 1866–1875, 2013.

[29] B. I. Whitaker, R. a. Henry, and S. Hinkins, "Report of the US Department of Health and Human Services. The 2011 national blood collection and utilization survey report.," *… Hum. Serv. Off. …*, 2013.

[30] E. Massey, "Use of platelets in hospitals: Factors that are driving up demand," 2012.

[31] J. Cid, S. K. Harm, and M. H. Yazer, "Platelet transfusion - The art and science of compromise," *Transfus. Med. Hemotherapy*, vol. 40, no. 3, pp. 160–171, 2013.

[32] M. P. Lambert, S. K. Sullivan, R. Fuentes, D. L. French, M. Poncz, and W. Dc, "Challenges and promises for the development of donor-independent platelet transfusions Review Article Challenges and promises for the development of donor-independent platelet

transfusions," vol. 121, no. 17, pp. 3319–3324, 2013.

[33] J. R. Hess and J. B. Holcomb, "Transfusion practice in military trauma," *Transfus. Med.*, vol. 18, no. 3, pp. 143–150, 2008.

[34] D. F. Stroncek and P. Rebulla, "Platelet transfusions," *Lancet*, vol. 370, no. 9585, pp. 427–438, 2007.

[35] M. Gaur, T. Kamata, S. Wang, B. Moran, S. J. Shattil, and A. D. Leavitt, "Megakaryocytes derived from human embryonic stem cells: A genetically tractable system to study megakaryocytopoiesis and integrin function," *J. Thromb. Haemost.*, vol. 4, no. 2, pp. 436–442, 2006.

[36] D. G. Halme and D. A. Kessler, "FDA Regulation of Stem-Cell-Based Therapies," *N. Engl. J. Med.*, vol. 355, no. 16, pp. 409–415, 2006.

[37] K. V Honn, J. A. Singley, and W. Chavin, "Fetal Bovine Serum : A Multivariate Standard1 (38804) defined environment for cells and tissue in tories , Grand Island Biological Company followed the protocol of Endocrine Services .," vol. 347, pp. 344–347, 1975.

[38] D. A. Brindley, N. L. Davie, E. J. Culme-Seymour, C. Mason, D. W. Smith, and J. A. Rowley, "Peak serum: implications of serum supply for cell therapy manufacturing.," *Regen. Med.*, vol. 7, no. 1, pp. 7–13, Jan. 2012.

[39] T. R. J. Heathman *et al.*, "Scalability and process transfer of mesenchymal stromal cell production from monolayer to microcarrier culture using human platelet lysate," *Cytotherapy*, vol. 18, no. 4, pp. 523–535, 2016.

[40] N. Fekete *et al.*, "Platelet lysate from whole blood-derived pooled platelet concentrates and apheresis-derived platelet concentrates for the isolation and

expansion of human bone marrow mesenchymal stromal cells: production process, content and identification of active comp," *Cytotherapy*, vol. 14, no. 5, pp. 540–54, 2012.

[41] C. Capelli *et al.*, "Human platelet lysate allows expansion and clinical grade production of mesenchymal stromal cells from small samples of bone marrow aspirates or marrow filter washouts.," *Bone Marrow Transplant.*, vol. 40, no. 8, pp. 785–91, 2007.

[42] K. Schallmoser *et al.*, "Human platelet lysate can replace fetal bovine serum for clinical-scale expansion of functional mesenchymal stromal cells," *Transfusion*, vol. 47, no. 8, pp. 1436–1446, 2007.

[43] P. Karagiannis and K. Eto, "Manipulating megakaryocytes to manufacture platelets *ex vivo*," *J. Thromb. Haemost.*, vol. 13, pp. S47–S53, 2015.

[44] F. Notta *et al.*, "Distinct routes of lineage development reshape the human blood hierarchy across ontogeny," *Science (80-.).*, vol. 351, no. 6269, pp. 1–16, 2015.

[45] J. A. Reems, N. Pineault, and S. Sun, "In Vitro Megakaryocyte Production and Platelet Biogenesis: State of the Art," *Transfus. Med. Rev.*, vol. 24, no. 1, pp. 33–43, 2010.

[46] N. Pineault and G. J. Boisjoli, "Megakaryopoiesis and ex vivo differentiation of stem cells into megakaryocytes and platelets," *ISBT Sci. Ser.*, vol. 10, no. S1, pp. 154–162, 2015.

[47] V. R. Deutsch and A. Tomer, "Megakaryocyte development and platelet production," *Br. J. Haematol.*, vol. 134, no. 5, pp. 453–466, 2006.

[48] O. Garraud and F. Cognasse, "Are platelets cells? And if yes, are they immune cells?," *Front. Immunol.*, vol. 6, no. FEB, pp. 1–8, 2015.

[49] J. N. Thon and J. E. Italiano, “Platelet formation,” *Semin. Hematol.*, vol. 47, no. 3, pp. 220–226, 2011.

[50] D. Zucker-Franklin and C. S. Philipp, “Platelet Production in the Pulmonary Capillary Bed: New Ultrasound Evidence for an Old Concept,” *Am. J. Pathol.*, vol. 157, no. 1, pp. 69–74, 2000.

[51] S. S. Mostafa, E. T. Papoutsakis, and W. M. Miller, “Oxygen tension modulates the expression of cytokine receptors, transcription factors, and lineage-specific markers in cultured human megakaryocytes.,” *Exp. Hematol.*, vol. 29, no. 7, pp. 873–83, 2001.

[52] Y. Y. Lipsitz, N. E. Timmins, and P. W. Zandstra, “Quality cell therapy manufacturing by design,” *Nat Biotechnol*, vol. 34, no. 4, pp. 393–400, 2016.

[53] M. P. Avanzi and W. B. Mitchell, “Ex Vivo production of platelets from stem cells,” *Br. J. Haematol.*, vol. 165, no. 2, pp. 237–247, 2014.

[54] N. Takayama *et al.*, “Generation of functional platelets from human embryonic stem cells in vitro via ES-sacs, VEGF-promoted structures that concentrate hematopoietic progenitors,” vol. 111, no. 11, pp. 5298–5306, 2013.

[55] Q. Feng *et al.*, “Scalable generation of universal platelets from human induced pluripotent stem cells,” *Stem Cell Reports*, vol. 3, no. 5, pp. 817–831, 2014.

[56] K. Okita, T. Ichisaka, and S. Yamanaka, “Generation of germline-competent induced pluripotent stem cells.,” *Nature*, vol. 448, no. 7151, pp. 313–317, 2007.

[57] J. Thomson *et al.*, “Embryonic stem cell lines derived from human blastocysts.,” *Science*, vol. 282, no. 5391, pp. 1145–1147, 1998.

[58] R. Bayley, F. Ahmed, K. Glen, M. McCall, A. Stacey, and R. Thomas, “The productivity

limit of manufacturing blood cell therapy in scalable stirred bioreactors," *J. Tissue Eng. Regen. Med.*, vol. 12, no. 1, pp. e368–e378, 2018.

[59] I. Pallotta, M. Lovett, D. L. Kaplan, and A. Balduini, "Study of Megakaryocytes and Functional Platelet Production Using Silk-Based Vascular Tubes," *Tissue Eng. Part C Methods*, vol. 17, no. 12, pp. 1223–1232, 2011.

[60] J. N. Thon, "Platelet Biogenesis," 2016. [Online]. Available: http://www.plateletbiogenesis.com/. [Accessed: 20-Jul-2016].

[61] Y. Mayshar *et al.*, "Identification and classification of chromosomal aberrations in human induced pluripotent stem cells.," *Cell Stem Cell*, vol. 7, no. 4, pp. 521–531, 2010.

[62] N. Salomonis *et al.*, "Integrated Genomic Analysis of Diverse Induced Pluripotent Stem Cell from the Progenitor Cell Biology Consortium," *Stem Cell Reports*, vol. 7, 2016.

[63] U. Ben-David and N. Benvenisty, "The tumorigenicity of human embryonic and induced pluripotent stem cells.," *Nat. Rev. Cancer*, vol. 11, no. 4, pp. 268–77, 2011.

[64] D. Paull *et al.*, "Automated, high-throughput derivation, characterization and differentiation of induced pluripotent stem cells.," *Nat. Methods*, vol. 12, no. august, pp. 1–13, 2015.

[65] R. C. Mulligan, "The Basic Science of Gene Therapy," *Science (80-.).*, vol. 260, no. 5110, pp. 926–932, 1993.

[66] C. Sheridan, "Gene therapy finds its niche.," *Nat. Biotechnol.*, vol. 29, no. 2, pp. 121–128, 2011.

[67] S. E. Raper *et al.*, "Fatal systemic inflammatory response syndrome in a ornithine transcarbamylase deficient patient following adenoviral gene transfer," *Mol. Genet.*

Metab., vol. 80, no. 1–2, pp. 148–158, 2003.

[68] M. Calero-Garcia and H. B. Gaspar, “Gene Therapy for SCID,” *Curr. Pediatr. Rep.*, vol. 3, pp. 11–21, 2014.

[69] G. Bauer *et al.*, “In vivo biosafety model to assess the risk of adverse events from retroviral and lentiviral vectors.,” *Mol. Ther.*, vol. 16, no. 7, pp. 1308–15, 2008.

[70] D. Escors and K. Breckpot, “Lentiviral vectors in gene therapy: Their current status and future potential,” *Arch. Immunol. Ther. Exp. (Warsz).*, vol. 58, no. 2, pp. 107–119, 2010.

[71] M. Themeli, I. Rivière, and M. Sadelain, “New Cell Sources for T Cell Engineering and Adoptive Immunotherapy,” *Cell Stem Cell*, vol. 16, no. 4, pp. 357–366, 2015.

[72] T. Maetzig *et al.*, “Polyclonal fluctuation of lentiviral vector-transduced and expanded murine hematopoietic stem cells Polyclonal fluctuation of lentiviral vector-transduced and expanded murine hematopoietic stem cells,” *Blood*, vol. 117, no. 11, pp. 3053–3065, 2011.

[73] N. L. Davie, D. a Brindley, E. J. Culme-seymour, and C. Mason, “Streamlining Cell Therapy Manufacture,” *Bioprocess Int.*, vol. 10, pp. 24–49, 2012.

[74] Q. A. Rafiq, K. Coopman, A. W. Nienow, and C. J. Hewitt, “A quantitative approach for understanding small-scale human mesenchymal stem cell culture - implications for large-scale bioprocess development.,” *Biotechnol. J.*, vol. 8, no. 4, pp. 459–71, Apr. 2013.

[75] L. K. Nielsen, E. T. Papoutsakis, and W. M. Miller, “Modeling ex vivo hematopoiesis using chemical engineering metaphors,” *Chem. Eng. Sci.*, vol. 53, no. 10, pp. 1913–1925, 1998.

[76] P. Singh, S. S. Shera, J. Banik, and R. M. Banik, “Optimization of cultural conditions using response surface methodology versus artificial neural network and modeling of l-glutaminase production by Bacillus cereus MTCC 1305,” *Bioresour. Technol.*, vol. 137, pp. 261–269, 2013.

[77] G. Zhang and D. E. Block, “Using highly efficient nonlinear experimental design methods for optimization of Lactococcus lactis fermentation in chemically defined media,” *Biotechnol. Prog.*, vol. 25, no. 6, pp. 1587–1597, 2009.

[78] L. Simon, M. N. Karim, and A. Schreiweis, “Prediction and classification of different phases in a fermentation using neural networks,” *Biotechnol. Tech.*, vol. 12, no. 4, pp. 301–304, 1998.

[79] M. L. Acosta, A. Sánchez, F. García, A. Contreras, and E. Molina, “Analysis of kinetic, stoichiometry and regulation of glucose and glutamine metabolism in hybridoma batch cultures using logistic equations.,” *Cytotechnology*, vol. 54, no. 3, pp. 189–200, Jul. 2007.

[80] A. Kiparissides, E. N. Pistikopoulos, and A. Mantalaris, “On the model-based optimization of secreting mammalian cell (GS-NS0) cultures,” *Biotechnol. Bioeng.*, vol. 112, no. 3, pp. 536–548, 2015.

[81] K. E. Glen, E. A. Cheeseman, A. J. Stacey, and R. J. Thomas, “A mechanistic model of erythroblast growth inhibition providing a framework for optimisation of cell therapy manufacturing,” *Biochem. Eng. J.*, vol. 133, pp. 28–38, 2018.

[82] D. Yeo *et al.*, “Improving embryonic stem cell expansion through the combination of perfusion and bioprocess model design,” *PLoS One*, vol. 8, no. 12, pp. 1–14, 2013.

[83] N. V. Mantzaris, J. J. Liou, P. Daoutidis, and F. Srienc, “Numerical solution of a mass structured cell population balance model in an environment of changing substrate concentration,” *J. Biotechnol.*, vol. 71, no. 1–3, pp. 157–174, 1999.

[84] B. Ben Yahia, B. Gourevitch, L. Malphettes, and E. Heinzle, “Segmented linear modeling of CHO fed-batch culture and its application to large scale production,” *Biotechnol. Bioeng.*, vol. 114, no. 4, pp. 785–797, 2017.

[85] B. Ben Yahia, L. Malphettes, and E. Heinzle, “Macroscopic modeling of mammalian cell growth and metabolism,” *Applied Microbiology and Biotechnology*, vol. 99, no. 17. 2015.

[86] F. J. Bruggeman and H. V. Westerhoff, “The nature of systems biology,” *Trends Microbiol.*, vol. 15, no. 1, pp. 45–50, 2007.

[87] N. A. W. van Riel, “Dynamic modelling and analysis of biochemical networks: Mechanism-based models and model-based experiments,” *Brief. Bioinform.*, vol. 7, no. 4, pp. 364–374, 2006.

[88] D. Ramkrishna and M. R. Singh, “Population Balance Modeling: Current Status and Future Prospects,” *Annu. Rev. Chem. Biomol. Eng.*, vol. 5, no. 1, pp. 123–146, 2014.

[89] M. Fuentes-Garí *et al.*, “A mathematical model of subpopulation kinetics for the deconvolution of leukaemia heterogeneity.,” *J. R. Soc. Interface*, vol. 12, no. 108, pp. 20150276-, 2015.

[90] P. Domingos, “The role of Occam’s Razor in knowledge discovery,” *Data Min. Knowl. Discov.*, vol. 3, pp. 409–425, 1999.

[91] L. X. Yu *et al.*, “Understanding Pharmaceutical Quality by Design,” *AAPS J.*, vol. 16, no.

4, pp. 771–783, 2014.

[92] FDA, “Guidence for Industry Q8(R2) Pharmaceutical Development,” 2009.

[93] G. Amidon *et al.*, “Understanding Pharmaceutical Quality by Design,” *AAPS J.*, vol. 16, no. 4, pp. 771–783, 2014.

[94] D. C. Montgomery, *Design and Analysis of Experiments*, 6th ed. Hoboken, New Jersey: Wiley, 2005.

[95] V. Konakovsky *et al.*, “Metabolic Control in Mammalian Fed-Batch Cell Cultures for Reduced Lactic Acid Accumulation and Improved Process Robustness,” *Bioengineering*, vol. 3, no. 1, p. 5, 2016.

[96] P. W. Zandstra, A. L. Petzer, C. J. Eaves, and J. M. Piret, “Cellular determinants affecting the rate of cytokine depletion in cultures of human hematopoietic cells,” *Biotechnol. Bioeng.*, vol. 54, no. 1, pp. 58–66, 1997.

[97] J. A. Selekman, A. Das, N. J. Grundl, and S. P. Palecek, “Improving efficiency of human pluripotent stem cell differentiation platforms using an integrated experimental and computational approach,” *Biotechnol. Bioeng.*, vol. 110, no. 11, pp. 3024–3037, 2013.

[98] E. Bartolini *et al.*, “Population balance modelling of stem cell culture in 3D suspension bioreactors,” *Chem. Eng. Res. Des.*, vol. 101, pp. 125–134, 2015.

[99] M. T. A. P. Kresnowati, G. M. Forde, and X. D. Chen, “Model-based analysis and optimization of bioreactor for hematopoietic stem cell cultivation,” *Bioprocess Biosyst. Eng.*, vol. 34, no. 1, pp. 81–93, 2011.

[100] A. J. Stacey, E. A. Cheeseman, K. E. Glen, R. L. L. Moore, and R. J. Thomas, “Experimentally integrated dynamic modelling for intuitive optimisation of cell based

processes and manufacture," *Biochem. Eng. J.*, vol. 132, pp. 130–138, 2018.

[101] S. T. Rashid *et al.*, "Modeling inherited metabolic disorders of the liver using human induced pluripotent stem cells," *Tech. Adv.*, vol. 120, no. 9, pp. 3127–3136, 2010.

[102] D. Herbenick *et al.*, "Targeted gene correction of α1-antitrypsin deficiency in induced pluripotent stem cells," *Nature*, vol. 3, no. 7369, pp. 1–8, Jul. 2011.

[103] HipSci, "HPSI0813i-ffdk_1," 2013. [Online]. Available: http://www.hipsci.org/lines/#/lines/HPSI0813i-ffdk_1. [Accessed: 20-May-2017].

[104] B. S. Cummings, L. P. Wills, and R. G. Schnellmann, "Measurement of Cell Death in Mammalian Cells," *Curr Protoc Pharmacol*, vol. 25, no. 1, pp. 12.8.1-12.8.22, 2004.

[105] Becton Dickinson, "BD FACSCanto II Flow Cytometer Reference Manual," 2006.

[106] H.-U. Bergmeyer, *Methods of Enzymatic Analysis*. Academic Press, 1965.

[107] N. Blumberg, J. M. Heal, and G. L. Phillips, "Platelet transfusions: trigger, dose, benefits, and risks," *F1000 Med. Rep.*, vol. 5, no. January, pp. 1–5, 2010.

[108] L. Estcourt *et al.*, "Prophylactic platelet transfusion for prevention of bleeding in patients with haematological disorders after chemotherapy and stem cell transplantation," *Cochrane Database Syst. Rev.*, no. 5, 2012.

[109] W. A. L. Heaton, S. Holme, and T. Keegan, "Development of a combined storage medium for 7-day storage of platelet concentrates and 42-day storage of red cell concentrates," *Br. J. Haematol.*, vol. 75, no. 3, pp. 400–407, 1990.

[110] R. L. Sparrow, "Red blood cell storage and transfusion-related immunomodulation," *Blood Transfus.*, vol. 8, no. SUPPL. 3, pp. 1–6, 2010.

[111] M. S. Y. Ng, J. P. Tung, and J. F. Fraser, "Platelet Storage Lesions: What More Do We

Know Now?," *Transfus. Med. Rev.*, vol. 32, no. 3, pp. 144–154, 2018.

[112] E. Maurer-Spurej and K. Chipperfield, "Past and Future Approaches to Assess the Quality of Platelets for Transfusion," *Transfus. Med. Rev.*, vol. 21, no. 4, pp. 295–306, 2007.

[113] X. Du, L. Beutler, C. Ruan, P. A. Castaldi, and M. C. Berndt, "Glycoprotein lb and Glycoprotein IX Are Fully Complexed in the Intact Platelet Membrane," *Blood*, vol. 69, no. 5, pp. 1835–1837, 1987.

[114] J.-L. Choi, S. Li, and J.-Y. Han, "Platelet Function Tests: A Review of Progresses in Clinical Application," *Biomed Res. Int.*, vol. 2014, pp. 1–7, 2014.

[115] F. Bertolini and S. Murphy, "A multicenter inspection of the swirling phenomenon in platelet concentrates prepared in routine practice," *Transfusion*, vol. 36, no. 2, pp. 128–132, 1996.

[116] T. Moreau *et al.*, "Large-scale production of megakaryocytes from human pluripotent stem cells by chemically defined forward programming," *Nat. Commun.*, vol. 7, no. 11208, pp. 1–15, 2016.

[117] A. Campbell *et al.*, "Concise Review : A Safety Assessment of Adipose- Derived Cell Therapy in Clinical Trials : A Systematic Review of Reported Adverse Events," *Stem Cells Transl. Med.*, vol. 4, pp. 1786–1794, 2015.

[118] I. Rivière and K. Roy, "Perspectives on Manufacturing of High-Quality Cell Therapies," *Mol. Ther.*, vol. 25, no. 5, pp. 1067–1068, 2017.

[119] F. Peyvandi, I. Garagiola, and L. Baronciani, "Role of the von Willebrand factor in atherogenesis," *Blood Transfus.*, vol. 9, no. Suppl. 2, pp. s3–s8, 2011.

[120] H. Maecker and J. Trotter, “Flow Cytometry Controls, Instrument Setup, and the Determination of Positivity,” *Cytometry. A*, vol. 69, no. 1, pp. 1037–1042, 2006.

[121] BD Biosciences, “Robust Statistics in BD FACSDiva ™ Software,” 2012.

[122] E. Meinelt, M. Reunanen, M. Edinger, and M. Jaimes, “Standardizing Application Setup Across Multiple Flow Cytometers Using BD FACSDiva™ Version 6 Software,” 2012.

[123] W. G. Telford, S. A. Babin, S. V. Khorev, and S. H. Rowe, “Green fiber lasers: An alternative to traditional DPSS green lasers for flow cytometry,” *Cytom. Part A*, vol. 75, no. 12, pp. 1031–1039, 2009.

[124] J. A. Cook and J. B. Mitchell, “Viability measurements in mammalian cell systems,” *Anal. Biochem.*, vol. 179, no. 1, pp. 1–7, 1989.

[125] N. Arden and M. J. Betenbaugh, “Life and death in mammalian cell culture: Strategies for apoptosis inhibition,” *Trends Biotechnol.*, vol. 22, no. 4, pp. 174–180, 2004.

[126] J. F. R. Kerr, A. H. Wyllie, and A. R. Currie, “Apoptosis: a Basic Biological Phenomenon With Wide- Ranging Implications in Tissue Kinetics,” *J. Intern. Med.*, vol. 258, no. 6, pp. 479–517, 1972.

[127] G. Manzini, M. L. Barcellona, M. Avitabile, and F. Quadrifoglio, “Interaction of diamindino-2-phenylindole (DAPI) with natural and synthetic nucleic acids,” *Nucleic Acids Res.*, vol. 11, no. 24, pp. 8861–8876, 1983.

[128] S. Mercille and B. Massie, “Induction of apoptosis in nutrient-deprived cultures of hybridoma and myeloma cells,” *Biotechnol. Bioeng.*, vol. 44, no. 9, pp. 1140–1154, 1994.

[129] NIST, “Biosystems and biomaterials division,” *Cell Counting Overview*, 2015. [Online].

Available: https://www.nist.gov/mml/bbd/cell-counting-overview. [Accessed: 30-Jul-2017].

[130] H. Murasiewicz, A. W. Nienow, M. P. Hanga, K. Coopman, C. J. Hewitt, and A. W. Pacek, "Engineering considerations on the use of liquid/liquid two-phase systems as a cell culture platform," *J. Chem. Technol. Biotechnol.*, vol. 92, no. 7, pp. 1690–1698, 2017.

[131] A. C. Schlinker, M. T. Duncan, T. A. DeLuca, D. C. Whitehead, and W. M. Miller, "Megakaryocyte Polyploidization and Proplatelet Formation in Low-Attachment Conditions," *Biochem. Eng. J.*, vol. 15, no. 111, pp. 24–33, 2016.

[132] T. L. Simon, "The Collection of Platelets by Apheresis Procedures," *Transfus. Med. Rev.*, vol. 8, no. 2, pp. 132–145, 1994.

[133] L. Wang and R. A. Hoffman, "Standardization, Calibration, and Control in Flow Cytometry," *Curr. Protoc. Cytom.*, vol. 2017, no. January, pp. 1.3.1-1.3.27, 2017.

[134] A. Dalby *et al.*, "Transcription Factor Levels after Forward Programming of Human Pluripotent Stem Cells with GATA1, FLI1, and TAL1 Determine Megakaryocyte versus Erythroid Cell Fate Decision," *Stem Cell Reports*, vol. 11, pp. 1–17, 2018.

[135] R. E. Spier and J. B. Griffiths, *Animal Cell Biotechnology*, 2nd editio., vol. 1. Totowa, New Jersey: Human Press, 2007.

[136] S. S. Ozturk and B. Palsson, "Chemical decomposition of glutamine in cell culture media: Effect of media type, and serum concentration," *Biotechnol. Prog.*, vol. 6, pp. 121–128, 1990.

[137] D. Schop *et al.*, "Growth, Metbolism, and Growth Inhibitors of Mesenchymal Stem Cells," *Tissue Eng. Part A*, vol. 15, no. 8, pp. 1877–1886, 2009.

[138] K. E. Glen, V. L. Workman, F. Ahmed, E. Ratcliffe, A. J. Stacey, and R. J. Thomas, “Production of erythrocytes from directly isolated or Delta1 Notch ligand expanded CD34+ hematopoietic progenitor cells: Process characterization, monitoring and implications for manufacture,” *Cytotherapy*, vol. 15, no. 9, pp. 1106–1117, 2013.

[139] J. Baranyi, T. Ross, T. A. McMeekin, and T. A. Roberts, “Effects of parameterization on the performance of empirical models used in ‘predictive microbiology,’” *Food Microbiol.*, 1996.

[140] D. Sorbom and E. E. Rigdon, “Evaluating Goodness-of-Fit Indexes for Testing Measurement Invariance,” vol. 9, no. 2, pp. 233–255, 2009.

[141] A. G. Lopes, A. Sinclair, and B. Frohlich, “Cost Analysis of Cell Therapy Manufacture Autologous Cell Tharapies, Part 2,” *Bioprocess Int.*, no. 16(4), 2018.

[142] X. Sim *et al.*, “Identifying and enriching platelet-producing human stem cell – derived megakaryocytes using factor V uptake,” *Blood*, vol. 130, no. 2, pp. 192–204, 2017.

[143] A. L. Bertho, M. a Santiago, and S. G. Coutinho, “Flow cytometry in the study of cell death.,” *Mem. Inst. Oswaldo Cruz*, vol. 95, no. 3, pp. 429–33, 2000.

[144] H. Yang, W. . Miller, and E. . Papoutsakis, “Higher pH Promotes Megakaryocyte Maturation and Apoptosis,” *Stem Cells*, vol. 20, pp. 320–328, 2002.

[145] M. P. Avanzi, M. Izak, O. E. Oluwadara, and W. B. Mitchell, “Actin inhibition increases megakaryocyte proplatelet formation through an apoptosis-dependent mechanism,” *PLoS One*, vol. 10, no. 4, 2015.

[146] E. C. Josefsson *et al.*, “Platelet production proceeds independently of the intrinsic and extrinsic apoptosis pathways.,” *Nat. Commun.*, vol. 5, pp. 3455–3469, 2014.

[147] C. D. Gregory, J. D. Pound, A. Devitt, M. Wilson-Jones, P. Ray, and R. J. Murray, “Inhibitory effects of persistent apoptotic cells on monoclonal antibody production in vitro,” *MAbs*, vol. 1, no. 4, pp. 370–376, 2014.

[148] R. Hoffman, C. Chauret, J. Standridge, and L. Peterson, “Evaluation of four commercial antibodies,” *J. / Am. Water Work. Assoc.*, vol. 91, no. 9, pp. 69–78, 1999.

[149] J. Xie, A. Nair, and T. W. Hermiston, “A comparative study examining the cytotoxicity of inducible gene expression system ligands in different cell types,” *Toxicol. Vitr.*, vol. 22, no. 1, pp. 261–266, 2008.

[150] J. Lennartsson and L. Ronnstrand, “Stem Cell Factor Receptor/c-Kit: From Basic Science to Clinical Implications,” *Physiol. Rev.*, vol. 92, no. 4, pp. 1619–1649, 2012.

[151] M. Serra *et al.*, “Improving expansion of pluripotent human embryonic stem cells in perfused bioreactors through oxygen control,” *J. Biotechnol.*, vol. 148, no. 4, pp. 208–215, 2010.

[152] L. D. Jager *et al.*, “Effect of enzymatic and mechanical methods of dissociation on neural progenitor cells derived from induced pluripotent stem cells,” *Adv Med Sci.*, vol. 61, no. 1, pp. 78–84, 2016.

[153] S. D. Patel, E. T. Papoutsakis, J. N. Winter, and W. M. Miller, “The lactate issue revisited: Novel feeding protocols to examine inhibition of cell proliferation and glucose metabolism in hematopoietic cell cultures,” *Biotechnol. Prog.*, vol. 16, no. 5, pp. 885–892, 2000.

[154] M. W. Glacken, R. J. Fleischaker, and A. J. Sinskey, “Reduction of waste product excretion via nutrient control: Possible strategies for maximizing product and cell yields

on serum in cultures of mammalian cells," *Biotechnol. Bioeng.*, vol. 28, no. 9, pp. 1376–1389, 1986.

[155] D. Duval, K. Demangel, S. Munier-Jolain, S. Miossec, and I. Geahel, "Factors Controlling Cell Proliferation and Antibody Production in Mouse Hybridoma Cells: I. Influence of the Amino Acid Supply," *Biotechnol. Bioeng.*, vol. 50, pp. 6–15, 1996.

[156] I. C. Macaulay *et al.*, "Comparative gene expression profiling of in vitro differentiated megakaryocytes and erythroblasts identifies novel activatory and inhibitory platelet membrane proteins," vol. 109, no. 8, pp. 3260–3269, 2012.

[157] L. E. Sidney, M. J. Branch, S. E. Dunphy, H. S. Dua, and A. Hopkinson, "Concise review: Evidence for CD34 as a common marker for diverse progenitors," *Stem Cells*, vol. 32, no. 6, pp. 1380–1389, 2014.

[158] G. Tang, S. A. Wang, M. Menon, K. Dresser, B. A. Woda, and S. Hao, "High-level CD34 expression on megakaryocytes independently predicts an adverse outcome in patients with myelodysplastic syndromes," *Leuk. Res.*, vol. 35, no. 6, pp. 766–770, 2011.

[159] K. Miyawaki *et al.*, "Identification of unipotent megakaryocyte progenitors in human hematopoiesis," *Blood*, vol. 129, no. 25, pp. 3332–3343, 2017.

[160] M. Eisbacher *et al.*, "Protein-Protein Interaction between Fli-1 and GATA-1 Mediates Synergistic Expression of Megakaryocyte-Specific Genes through Cooperative DNA Binding," vol. 23, no. 10, pp. 3427–3441, 2006.

[161] M. R. Tijssen and C. Ghevaert, "Transcription factors in late megakaryopoiesis and related platelet disorders," *J. Thromb. Haemost.*, vol. 11, no. 4, pp. 593–604, 2013.

[162] F. Wendling *et al.*, "C-Mpl ligand is a humoral regulator of megakaryocytopoiesis,"

Nature, vol. 369, no. 6481, pp. 571–574, 1994.

[163] K. Kaushansky *et al.*, "Promotion of megakaryocyte progenitor expansion and differentiation by the c-Mpl ligand thrombopoietin," *Nature*, vol. 369, no. 6481, pp. 568–571, 1994.

[164] S. Lok *et al.*, "Cloning and expression of murine thrombopoietin cDNA and stimulation of platelet production in vivo," *Nature*, vol. 369, no. 6481, pp. 565–568, 1994.

[165] F. de Sauvage *et al.*, "Stimulation of megakaryocytopoiesis and thrombopoiesis by the c-Mpl ligand," *Nature*, vol. 367, p. 19, 1994.

[166] Y. Nagata and K. Todokoro, "Thrombopoietin induces activation of at least two distinct signaling pathways.," *FEBS Lett.*, vol. 377, no. 3, pp. 497–501, 1995.

[167] R. Krawetz *et al.*, "Large-Scale Expansion of Pluripotent Human Embryonic Stem Cells in Stirred-Suspension Bioreactors," *Tissue Eng. Part C Methods*, vol. 16, no. 4, pp. 573–582, 2009.

[168] U. Martin *et al.*, "Suspension Culture of Human Pluripotent Stem Cells in Controlled, Stirred Bioreactors," *Tissue Eng. Part C Methods*, vol. 18, no. 10, pp. 772–784, 2012.

[169] H. Kempf *et al.*, "Controlling Expansion and Cardiomyogenic Differentiation of Human Pluripotent Stem Cells in Scalable Suspension Culture," *Stem Cell Reports*, vol. 3, no. 5, pp. 876–891, 2014.

[170] D. A. Robinton and G. Q. Daley, "The promise of induced pluripotent stem cells in research and therapy," *Nature*, vol. 481, no. 7381, pp. 295–305, 2013.

[171] M. Mandai *et al.*, "Autologous Induced Stem-Cell–Derived Retinal Cells for Macular Degeneration," *N. Engl. J. Med.*, vol. 376, no. 11, pp. 1038–1046, 2017.

[172] T. Kikuchi *et al.*, “Human iPS cell-derived dopaminergic neurons function in a primate Parkinson’s disease model,” *Nature*, vol. 548, no. 7669, pp. 592–596, 2017.

[173] C. Kropp, D. Massai, and R. Zweigerdt, “Progress and challenges in large-scale expansion of human pluripotent stem cells,” *Process Biochem.*, vol. 59, pp. 244–254, 2017.

[174] V. Akopian *et al.*, “Comparison of defined culture systems for feeder cell free propagation of human embryonic stem cells,” *Vitr. Cell. Dev. Biol. - Anim.*, vol. 46, no. 3–4, pp. 247–258, 2010.

[175] B. Valamehr *et al.*, “Platform for induction and maintenance of transgene-free hiPSCs resembling ground state pluripotent stem cells,” *Stem Cell Reports*, vol. 2, no. 3, pp. 366–381, 2014.

[176] J. Beers *et al.*, “Passaging and colony expansion of human pluripotent stem cells by enzyme-free dissociation in chemically defines culture condictions.,” *Nat. Protoc.*, vol. 7, no. 11, pp. 2029–2040, 2012.

[177] P. H. Schwarz, D. J. Brick, H. E. Nethercott, and A. Stover, “Traditional Human Embryonic Stem Cell Culture Philip,” *Methods Mol. Biol.*, vol. 767, pp. 107–123, 2011.

[178] S. Rodin *et al.*, “Long-term self-renewal of human pluripotent stem cells on human recombinant laminin-511,” *Nat. Biotechnol.*, vol. 28, no. 6, pp. 611–615, 2010.

[179] Y. C. Ng, J. M. Berry, and M. Butler, “Optimization of physical parameters for cell attachment and growth on macroporous microcarriers,” *Biotechnol. Bioeng.*, vol. 50, no. 6, pp. 627–635, 1996.

[180] B. W. Phillips, R. Horne, T. S. Lay, W. L. Rust, T. T. Teck, and J. M. Crook, “Attachment

and growth of human embryonic stem cells on microcarriers," *J. Biotechnol.*, vol. 138, no. 1–2, pp. 24–32, 2008.

[181] I. A. M. Swinnen, K. Bernaerts, E. J. J. Dens, A. H. Geeraerd, and J. F. Van Impe, "Predictive modelling of the microbial lag phase: A review," *Int. J. Food Microbiol.*, vol. 94, no. 2, pp. 137–159, 2004.

[182] M. D. Rolfe *et al.*, "Lag phase is a distinct growth phase that prepares bacteria for exponential growth and involves transient metal accumulation," *J. Bacteriol.*, vol. 194, no. 3, pp. 686–701, 2012.

[183] R. J. Wieser *et al.*, "Growth control in mammalian cells by cell-cell contacts," *Environ. Health Perspect.*, vol. 88, pp. 251–253, 1990.

[184] K. Watanabe *et al.*, "A ROCK inhibitor permits survival of dissociated human embryonic stem cells," *Nat. Biotechnol.*, vol. 25, no. 6, pp. 681–686, 2007.

[185] G. Chen, D. R. Gulbranon, P. Yu, Z. Hou, and J. A. Thomson, "Thermal Stability of Fibroblast Growth Factor Protein Is a Determinant Factor in Regulating Self-Renewal, Differentiation, and Reprogramming in Human Pluripotent Stem Cells," *Stem Cells*, vol. 30, pp. 623–630, 2012.

[186] S. Lotz *et al.*, "Sustained Levels of FGF2 Maintain Undifferentiated Stem Cell Cultures with Biweekly Feeding," *PLoS One*, vol. 8, no. 2, pp. 1–10, 2013.

[187] S. Takuma, C. Hirashima, and J. M. Piret, "Dependence on glucose limitation of the pCO2 influences on CHO cell growth, metabolism and IgG production," *Biotechnol. Bioeng.*, vol. 97, no. 6, pp. 1479–1488, 2007.

[188] J. D. Young, "Metabolic flux rewiring in mammalian cell cultures," *Curr. Opin.*

Biotechnol., vol. 24, no. 6, pp. 1108–1115, 2013.

[189] Y. Zhang *et al.*, "Potent Paracrine Effects of human induced Pluripotent Stem Cell-derived Mesenchymal Stem Cells Attenuate Doxorubicin-induced Cardiomyopathy," *Sci. Rep.*, vol. 5, no. April, pp. 1–17, 2015.

[190] K. Gauthaman, C. Y. Fong, and A. Bongso, "Effect of ROCK inhibitor Y-27632 on normal and variant human embryonic stem cells (hESCs) in vitro: Its benefits in hESC expansion," *Stem Cell Rev. Reports*, vol. 6, no. 1, pp. 86–95, 2010.

[191] D. A. Fluri *et al.*, "Derivation, expansion and differentiation of induced pluripotent stem cells in continuous suspension cultures.," *Nat Methods*, vol. 9, no. 5, pp. 509–516, 2012.

[192] A. M. Fernandes, T. G. Fernandes, M. M. Diogo, C. L. da Silva, D. Henrique, and J. M. S. Cabral, "Mouse embryonic stem cell expansion in a microcarrier-based stirred culture system," *J. Biotechnol.*, vol. 132, no. 2, pp. 227–236, 2007.

[193] M. P. Storm, C. B. Orchard, H. K. Bone, J. B. Chaudhuri, and M. J. Welham, "Three-dimensional culture systems for the expansion of pluripotent embryonic stem cells," *Biotechnol. Bioeng.*, vol. 107, no. 4, pp. 683–695, 2010.

[194] Y. Xu *et al.*, "Revealing a core signaling regulatory mechanism for pluripotent stem cell survival and self-renewal by small molecules," *Proc. Natl. Acad. Sci.*, vol. 107, no. 18, pp. 8129–8134, 2010.

[195] E. Abranches, E. Bekman, D. Henrique, and J. M. S. Cabral, "Expansion of Mouse Embryonic Stem Cells on Microcarriers," *Biotechnol. Bioeng.*, vol. 96, no. 1221–1221, pp. 503–505, 2006.

[196] K. G. Chen, B. S. Mallon, R. D. G. Mckay, and P. G. Robey, "Human Pluripotent Stem Cell

Culture: Considerations for Maintenance, Expansion, and Therapeutics," *Cell Stem Cell*, vol. 6, no. 9, pp. 2166–2171, 2015.

[197] G. Chen, Z. Hou, D. R. Gulbranson, and J. A. Thomson, "Actin-myosin contractility is responsible for the reduced viability of dissociated human embryonic stem cells," *Cell Stem Cell*, vol. 7, no. 2, pp. 240–248, 2010.

[198] L. Li, S. A. L. Bennett, and L. Wang, "Role of E-cadherin and other cell adhesion molecules in survival and differentiation of human pluripotent stem cells," *Cell Adhes. Migr.*, vol. 6, no. 1, pp. 59–70, 2012.

[199] H. Kurosawa, "Application of Rho-associated protein kinase (ROCK) inhibitor to human pluripotent stem cells," *J. Biosci. Bioeng.*, vol. 114, no. 6, pp. 577–581, 2012.

[200] M. Ohgushi, M. Minaguchi, and Y. Sasai, "Rho-Signaling-Directed YAP/TAZ Activity Underlies the Long-Term Survival and Expansion of Human Embryonic Stem Cells," *Cell Stem Cell*, vol. 17, no. 4, pp. 448–461, 2015.

[201] D. a. Claassen, M. M. Desler, and A. Rizzino, "ROCK Inhibition Enhances the Recovery and Growth of Cryopreserved Human Embryonic Stem Cells and Human Induced Pluripotent Stem Cells," *Mol Reprod Dev.*, vol. 76, no. 8, pp. 722–732, 2009.

[202] O. Trusler, Z. Huang, J. Goodwin, and A. L. Laslett, "Cell surface markers for the identification and study of human naive pluripotent stem cells," *Stem Cell Res.*, vol. 26, pp. 36–43, 2018.

[203] A. J. Collier *et al.*, "Comprehensive Cell Surface Protein Profiling Identifies Specific Markers of Human Naive and Primed Pluripotent States," *Cell Stem Cell*, vol. 20, no. 6, pp. 874-890.e7, 2017.

[204] S. Nakamura *et al.*, “Expandable megakaryocyte cell lines enable clinically applicable generation of platelets from human induced pluripotent stem cells,” *Cell Stem Cell*, vol. 14, no. 4, pp. 535–548, 2014.

[205] C. A. Di Buduo *et al.*, “Programmable 3D silk bone marrow niche for platelet generation ex vivo and modeling of megakaryopoiesis pathologies,” *Blood*, vol. 125, no. 14, pp. 2254–2264, 2015.

[206] E. Hashino *et al.*, “Extended passaging increases the efficiency of neural differentiation from induced pluripotent stem cells,” *BMC Neurosci.*, vol. 12, no. 1, p. 82, 2011.

[207] R. Autio *et al.*, “Copy number variation and selection during reprogramming to pluripotency,” *Nature*, vol. 471, no. 7336, pp. 58–62, 2011.

[208] K. P. Smith, M. X. Luong, and G. S. Stein, “Pluripotency: Toward a gold standard for human ES and iPS cells,” *J. Cell. Physiol.*, vol. 220, no. 1, pp. 21–29, 2009.

[209] F. Müller, B. M. Schuldt, R. Williams, D. Mason, and G. Altun, “A bioinformatic assay for pluripotency in human cells,” *Nat Methods*, vol. 8, no. 4, pp. 315–317, 2012.

[210] NIST, “NIST Workshop: Strategies to Achieve Measurement Assurance for Cell Therapy Products,” in *BIOMATERIALS GROUP*, 2015.

[211] J. F. S. D. Lana *et al.*, “Contributions for classification of platelet rich plasma - Proposal of a new classification: MARSPILL,” *Regen. Med.*, vol. 12, no. 5, pp. 565–574, 2017.

[212] I. A. Jones, X. B. Chen, D. Evseenko, C. Vangsness, and J. Thomas, “Nomenclature Inconsistency and Selective Outcome Reporting Hinder Understanding of Stem Cell Therapy for the Knee,” *JBJS*, vol. 101, no. 2, pp. 186–195, 2019.

[213] J. Caldwell, W. Wang, and P. W. Zandstra, “Proportional-Integral-Derivative (PID)

control of secreted factors for blood stem cell culture," *PLoS One*, vol. 10, no. 9, pp. 1–20, 2015.